The immunopeptidomic landscape of clear cell renal cell carcinoma: identification and characterization of T-cell epitopes for immunotherapeutic approaches

Das Immunpeptidom vom klarzelligen Nierenzellkarzinom: Identifizierung und Charakterisierung von T-Zell-Epitopen für immuntherapeutische Ansätze

Dissertation

der Mathematisch-Naturwissenschaftlichen Fakultät

der Eberhard Karls Universität Tübingen

zur Erlangung des Grades eines

Doktors der Naturwissenschaften

(Dr. rer. nat.)

vorgelegt von

Dipl. Biochem. Moreno Di Marco

aus Tübingen

Tübingen

2017

Gedruckt mit Genehmigung der Mathematisch-Naturwissenschaftlichen Fakultät der Eberhard Karls Universität Tübingen.

Tag der mündlichen Prüfung:	26.10.2017
Dekan:	Prof. Dr. Wolfgang Rosenstiel
1. Berichterstatter:	Prof. Dr. Stefan Stevanović
2. Berichterstatter:	Prof. Dr. Hans-Georg Rammensee

Contents

1. Introduction

1.1. The Immune System

The immune system is composed of a variety of cells and molecular mechanisms to defend the organism against a plethora of pathogens and transformed cells of the organism itself. It can be classified into two subgroups: the innate immune system and the adaptive immune system.

The innate immune system is composed of several cellular components, such as dendritic cells (DCs), macrophages, mast cells, granulocytes and natural killer cells (NK cells) and non-cellular (humoral) components such as the complement system [**Figure 1**]. Defense mechanisms of the innate immunity are phagocytosis, recruitment of further immune cells, direct killing and opsonization of pathogens.

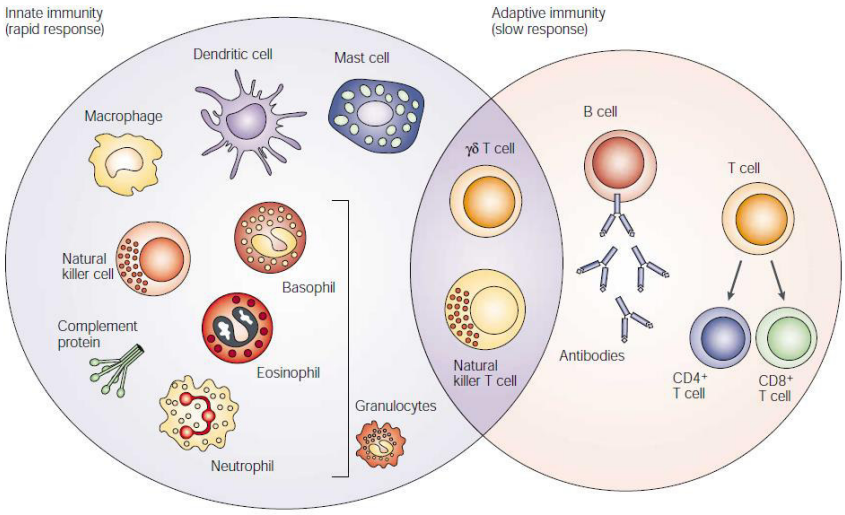

Figure 1: Components of the innate and adaptive immune system. Left) Cellular and humoral components of the innate immune system. Right) Cellular and humoral components of the adaptive immune system.[1]

DCs, macrophages and neutrophilic granulocytes are specialized in phagocytosis through binding of common foreign structures, the so called pathogen-associated patterns (PAMPs) or cell compounds which are released during cell damage and death, named damage-associated molecular patterns (DAMPs) with their pattern recognition receptors (PRRs).[2,3] Apart from endocytosis, phagocytes may act as antigen presenting cells (APCs) presenting protein fragments of digested pathogens on their cell surface on major histocompatibility complex (MHC) molecules and thereby bridging the innate with the adaptive immune system. Depending on the presentation ability one may distinguish between professional and atypical APCs.[4] Yet, DCs are the most specialized APCs. Recruitment and activation of further immune cells is a second mechanism achieved by cytokines, such as interferons, interleukins and chemokines, produced by cells of the innate immune system. NK cells are able to directly kill infected or malignant transformed host cells through MHC-dependent ("non-self" and "missing-self")[5], antibody-dependent (antibody-dependent cellular cytotoxicity, ADCC)[6] or

death-receptor-dependent mechanisms[7]. The first two mechanisms conduct killing through secretion of cytotoxic molecules, such as perforin and granzymes, whereas the third mechanism induces directly the apoptosis pathway. The complement system opsonizes pathogens for phagocytes, recruits immune cells through the chemokine function of some complement proteins and may directly kill via membrane perforation.[8] In general, the innate immune system is limited in diversity and specificity of the immune response and is focused on fast distinction between harmful and harmless antigens.[9]

The adaptive immune system emerged in jawed vertebrates (fishes) and was accompanied by the development of lymphocytes, MHC molecules, immunoglobulins (Ig), T-cell receptors (TCRs) and recombinase activating genes (RAG).[10] An adaptive immune system is often required for an effective defense due to its specific reaction against antigens. The cellular components are lymphocytes, namely T cells and B cells. T cells can be subdivided into the main subsets $CD8^+$ cytotoxic T lymphocytes (CTLs), $CD4^+$ T helper cells (T_H cells) and regulatory T cells (T_{reg} cells). T cells are antigen-specific and are preselected in the thymus to avoid reactivity against self-antigens (central tolerance).[11] Activation of naïve T cells take place through interaction with APCs presenting their antigen of choice.[12] Three signals are required for an activation of T cells [**Figure 2**]. First, binding of the TCR to the appropriate MHC-peptide complex (pMHC), which is stabilized by the co-receptors CD8 on CTLs, binding onto the α_3-domain of the MHC class I molecules, or CD4 on T_H cells, binding to the β_2-domain of MHC class II molecules. Second, a costimulatory signal between T cell and APC, such as the interaction of the T-cell costimulatory protein CD28 and the CD80/CD86 (B7.1/B7.2) complex on APCs. Lack of the costimulatory signal leads to T cell anergy and/or tolerance (peripheral tolerance) and functions as a second mechanism in preventing an immune response against self-peptides. Last, cytokines produced by the APC and the T cell itself have to bind to their respective cell surface receptors.[12-14] The cytokine milieu decides the polarization of the T cell towards an effector phenotype. B cells produce antigen-specific antibodies. Antibodies are able to neutralize antigenic structures, activate the complement system and subsequently induce the complement dependent cytolysis (CDC) or opsonize pathogens for phagocytosis or direct killing by cells of the innate immunity.[15] While T cells recognize linear antigens, B cells may direct antibodies against non-linear antigenic structures. Antibodies therefore act in back-bridging the adaptive to the innate immunity. In addition, the interplay of innate and adaptive immunity is tightly regulated by cytokines produced by either cells of the innate or adaptive immune system. The response of the adaptive immune system is highly antigen-specific and diverse. The specific response against antigens has to be acquired by recombining and specifying TCRs[16] or immunoglobulins[17] and starts with a delay of a few days. A further distinction is the ability of the adaptive immune system to

memorize antigens which were already combated by the generation of memory B and T cells which can be quickly reactivated.[18,19]

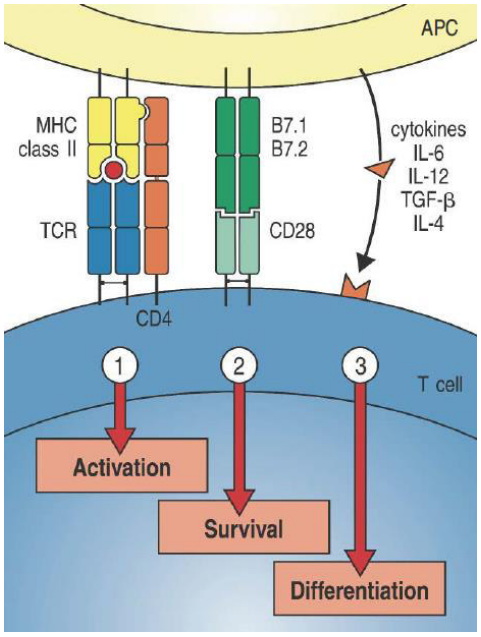

Figure 2: T cell activation by APC involves three kinds of signals. Naïve T cells get their first activation signal by recognition of foreign pMHC complexes. A costimulatory signal received from the same APC is required for T cell survival and for the proliferation ability. The lack of signal 2 leads to T cell anergy and/or tolerance. The cytokines produced by the APC determine the differentiation of the naïve T cell into an effector T cell subtype.[20]

1.2. Human leukocyte antigen

MHC molecules provide the junction for the activation of the adaptive immune system. In humans they are also referred to as human leukocyte antigen (HLA) molecules. Two classes of HLA molecules can be distinguished: HLA class I and HLA class II. Both classes are glycosylated membrane proteins with differences existing in their respective structure, their source of proteins and their cell type-dependent expression.[21]

HLA class I molecules are expressed on all nucleated cells and present mainly peptides of intracellular antigens to $CD8^+$ T cells. They are constituted of an approximately 43 kDa heavy α-chain with their domains α_1-α_3 and the invariant 12 kDa light β_2-microglobulin (β_2m) which is non-covalently linked to the heavy chain [**Figure 3**]. The α-domains α_1 and α_2 constitute the peptide binding groove formed by two α-helices and an antiparallel β-strand.[22] Peptides loaded onto the HLA class I are 8 to 12 amino acids (aa) in length. The bended α-helices and large aromatic residues enclose the binding groove constraining the length of ligands.[23] Peptides with 9 aa are usually preferred while longer sequences bulge out of the groove. The HLA molecule interacts with the peptide through sequence-independent interactions with the peptide termini and sequence-dependent interactions with amino acid residues located in the groove.[24-26] Six pockets A-F can be refined contacting specific residues of the located peptide. The accommodation of a peptide is especially restricted by two pockets, usually pocket B (interacts with the peptide residue at position 2) and F (interacts with the C-terminal peptide

residue), which allows only particular residues to bind. Peptide positions which are especially restricted by the binding pockets are defined as anchor positions.[27] Additionally, residues binding to less restricted pockets can be referred to as auxiliary anchors. In total, about 50 amino acid positions within the binding groove may interact with the peptide, many of which are highly polymorphic and therefore individualize the peptide repertoire of each MHC molecule.[28,29]

HLA class II molecules are expressed in particular on APCs and present mainly peptides from extracellular antigens to $CD4^+$ T cells. They are constituted of two chains, the α- and the β-chain with two domains each (α_1 and α_2, and β_1 and β_2, respectively) [**Figure 3**]. The α_1- and β_1-domains form the binding groove which is opened on both ends rendering binding of longer peptides feasible. Peptides are usually 12-20 aa in length. Due to the ability to bind peptides with extended ends, length variants of the same core sequence (anchors usually at position 1, 4, 6, 9) can be presented without bulging out of the peptide (which is required for presentation of length variants in HLA class I). In addition, the same peptide may bind to different HLA class II molecules by shifting the core. Finally, anchor positions are less defined compared to HLA class I leading to a high promiscuity between allotypes.

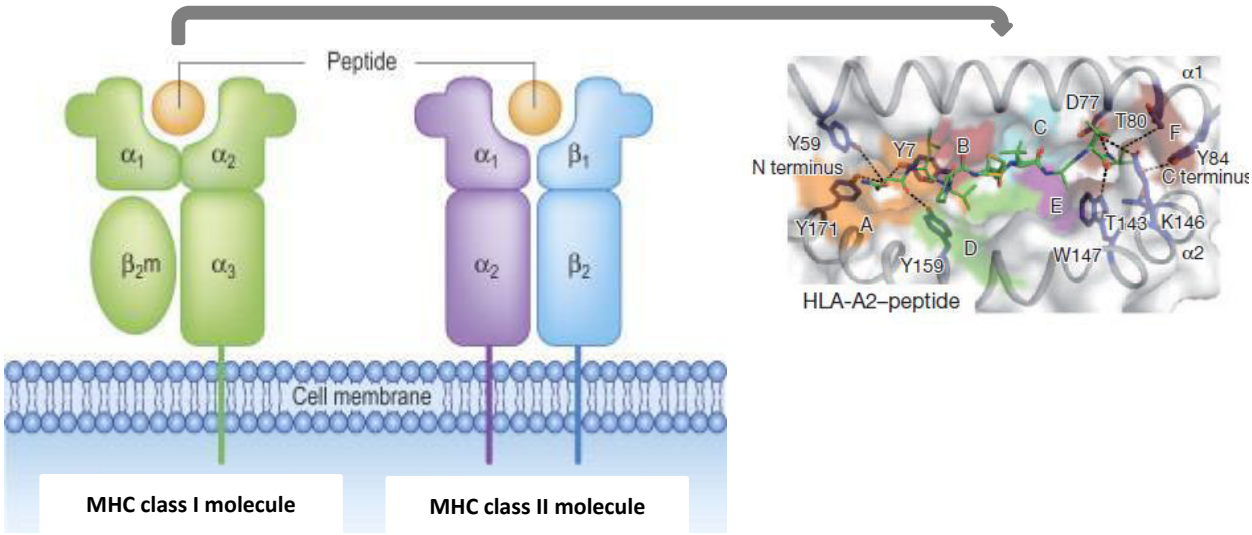

Figure 3: Schematic structure of HLA class I and HLA class II molecules. The ligand is bound in the binding groove. Pockets A-F of HLA class I molecules are illustrated on the right for an exemplary HLA-A*02 peptide.[30,31]

The HLA molecules are encoded in the HLA region on the short arm of chromosome 6.[32] Besides HLA molecules, the HLA gene complex comprises several genes with immunological relevance like complement factors, cytokines and proteins of the antigen processing pathway.[33] Three classical HLA class I molecules (HLA-A, -B and -C) and three classical HLA class II molecules (HLA-DP, -DQ, -DR) are encoded in the HLA gene complex. The classical HLA alleles are highly polymorphic and codominantly expressed. Further, non-classical HLA molecules like the class I HLA-E, -F, and -G and the class II

HLA-DM and HLA-DO are encoded in this gene region. The number of known alleles is 12,351 for HLA class I and 4,404 for HLA class II (www.ebi.ac.uk/ipd/imgt/hla/stats.html, 2017-04).

1.3. HLA class I antigen processing

HLA molecules present linear fragments of antigens which are prior degraded within the cell. Cytosolic proteins originating from self or non-self antigens are the source of HLA class I molecules [**Figure 4**]. In addition, extracellular antigens can be presented on HLA class I by cross presentation.[34,35] Apart from proper folded and functional proteins, substantial amounts of peptides arise from misfolded proteins, the so called defective ribosomal products (DRiPs). DRiPs represent about 30% of all proteasome degraded proteins.[36,37]

The first step in antigen processing is the tagging of proteins for proteasomal degradation by the addition of three to four ubiquitin molecules.[38] The degradation is carried out in the 26S proteasome, a macromolecular assembly of one 20S subunit (core) and two 19S subunits (caps). Four rings with seven subunits each ($\alpha_7\beta_7\beta_7\alpha_7$) provide a cavity in which the unfolded protein is proteolytically degraded. The subunits β_1, β_2 and β_5 (contained in both ring structures of the core) possess proteolytic activity with different cleavage specificity each. C-terminal acidic residues are preferred by the subunit β_1. Tryptic-like specificity, cleaving sequences after basic residues, is displayed by the β_2-subunit and cleavage after C-terminal hydrophobic residues is exhibited by subunit β_5 with their chymotryptic-like specificity. The average length of emerging protein fragments is 7 to 9 aa with a range from 4 to 25 aa.[39] The caps have two major roles which are accomplished by two protein groups. The Rpn proteins recognize ubiquitin-tagged proteins which are subsequently unfolding ATP-dependent by Rpt proteins.[40] The constitutively expressed proteolytic subunits β_1, β_2 and β_5 can be exchanged by the subunits β_1i (also called LMP2), β_2i (also called MECL1) and β_5i (also called LMP7) forming the immunoproteasome.[40] All three subunits are induced by interferon-γ (IFN-γ) which is mainly produced by NK cells, NKT cells, effector CTLs and T_H1 cells.[41] The substitution of one up to all six subunits leads to a change in the proteolytic activity with structural rearrangements of the proteasome. Enhanced tryptic-like and chymotryptic-like activity of the immunoproteasome facilitates the generation of HLA ligands with hydrophobic and basic C-terminal residues.[42,43] Additionally, the IFN-γ-induced PA28 subunit enhances the peptide production.[44,45] Produced peptides can be further cleaved by peptidases in the cytosol or the endoplasmic reticulum (ER). This is in particular important for the N-terminal trimming of peptides.[21] The N-terminal trimming can be prevented by the binding to the chaperonin TRiC.[46]

Loading of peptides onto HLA molecules takes place in the ER. The heterodimeric TAP1/TAP2 complex (transporter associated with antigen processing) transports cytosolic peptides, preferentially with hydrophobic or basic C-terminal residues and a length of 9 to 12 aa, ATP-dependent into the ER. The ER contains additional proteases for further trimming of peptides.[21] Peptides are loaded onto HLA molecules assisted by the peptide loading complex (PLC) consisting of HLA class I-stabilizing proteins calreticulin, Erp57 and tapasin. The HLA class I molecule is assembled in the ER aided by the chaperon calnexin which is then replaced by the PLC. pHLA complexes are subsequently transported via the secretory pathway onto the plasma membrane.

The production of too short peptides by the proteasome, proteases in the cytosol and ER, TAP complex constraints in peptide C-terminal amino acids and length, and sequence restrictions of the expressed HLA lead to a rate of about one presented peptide out of 1000 produced peptides.[47-49]

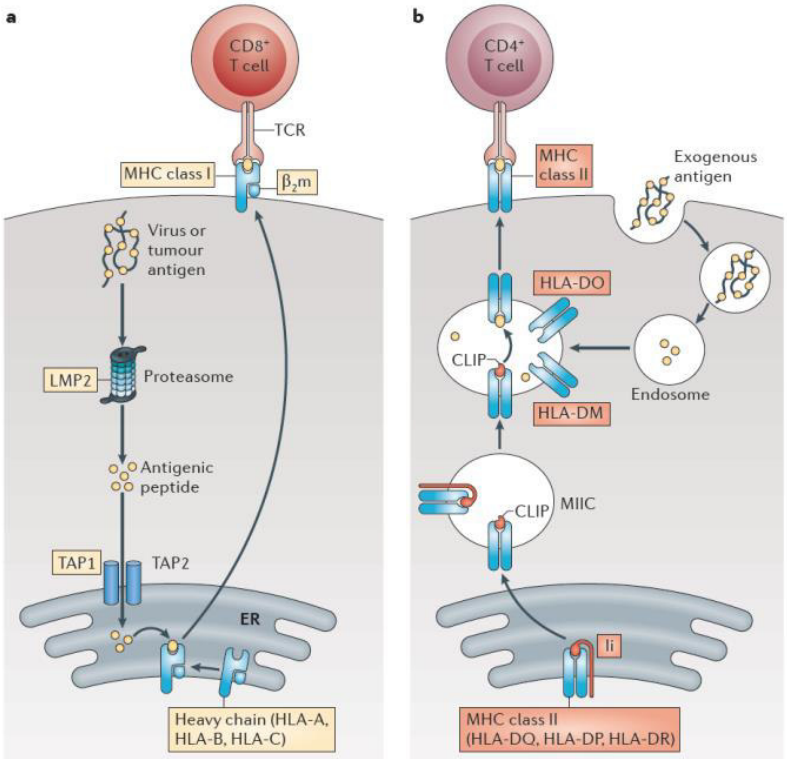

Figure 4: Antigen processing pathways for HLA class I and HLA class II. a) Intracellular antigens are processed by the proteasome and proteases into peptides which are transported into the ER by TAP and loaded onto chaperone-stabilized HLA class I molecules. pHLA complexes are transported onto the cell surface via the secretory pathway. b) Extracellular antigens are processed by endosomal enzymes and loaded onto HLA class II molecules in the MIIC compartment. Prior, HLA class II is stabilized by the invariant chain which is degraded to the CLIP fragment by proteases. HLA-DM and HLA-DO catalyze the exchange of the CLIP fragment against the peptide.[50]

1.4. HLA class II antigen processing

Peptides descending from endocytosed antigens as well as endogenous proteins entering lysosomal degradation, e.g. via autophagy[51,52], are presented by HLA class II molecules [**Figure 4**]. HLA class II molecules are folded in the ER like HLA class I. However, HLA class II molecules enter the secretory pathway without loaded peptide, but stabilized with the invariant chain. The proteolysis of antigens by proteases and cathepsins and the subsequent peptide loading takes place in the acidic MHC class

II compartment (MIIC).[21] The Ii is degraded to a short leftover called CLIP fragment (class II invariant chain-associated peptide) which remains in the binding groove. The CLIP fragment is replaced by an appropriate peptide with the aid of the chaperones HLA-DM and HLA-DO.[53] HLA-DM facilitates the dissociation of peptides binding with low affinity enabling the replacement against peptides with high affinity.[54]

1.5. The HLA ligandome

The HLA ligandome, also referred to as the immunopeptidome, is the collection of peptides presented by HLA molecules at the cell surface and is in perpetual communication with T cells. The HLA ligand repertoire of a cell depends on the expressed HLA allotypes as well as different physiological, intrinsic as well as pathogenic factors which may influence HLA expression or the ligand repertoire itself.[55] Around 100,000 HLA molecules are presented on a cell presenting peptides with copy numbers varying from one to up to 10,000 copies per cell.[47] Especially in tumor cells the HLA ligandome undergoes substantial changes following mutations in one or several oncogenes which affect cellular transcription, pathways or the metabolism.

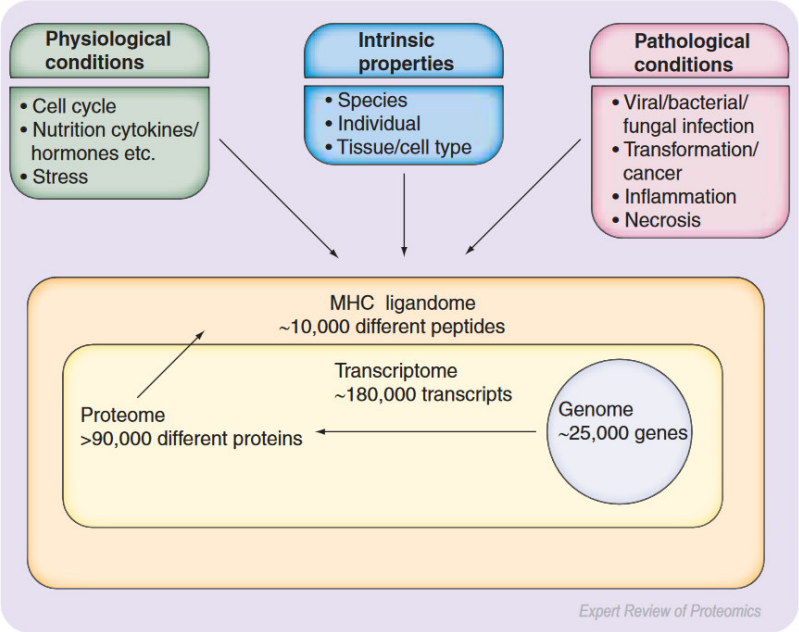

Figure 5: Factors influencing the HLA ligandome. Each HLA allotype has its specific binding repertoire which is further influenced by physiological, intrinsic and pathological factors.[55]

1.6. Peptide motifs and binding prediction

The high polymorphism of HLA molecules, especially of residues within the peptide binding groove, leads to unique peptide binding specificities which in turn mean unique ligand repertoires. Peptide binding specificities can be illustrated in so called peptide motifs providing information about the

importance of a position (bits) as well as the amino acid preferences at a specific position (size of amino acid).

Three main approaches are commonly used to disclose binding specificities of HLA class I allotypes. The first approach is based on *in vitro* binding experiments using extended libraries of synthetic peptides or already known ligands from publically available databases such as SYFPEITHI or IEDB. The second approach is the liquid chromatographic tandem mass spectrometry (LC-MS/MS)-based identification of naturally presented ligands from tissue or cell lines. Therefore, the monoallelic transfection of HLA-negative (or low-expressing) cells, used in the definition of HLA-C and HLA-G peptide motifs in the results and discussion part II of this thesis, is a convenient approach.[56-60] The third approach is based on the *in silico* prediction of the structural surrounding within the binding pocket.

The information can be used to establish binding prediction tools. Commonly used tools are NetMHC, NetMHCpan and SYFPEITHI. The methods differ in the strategy used to establish binding prediction (described in section **3.3.8**). NetMHCpan is the only method integrating binding specificities from related and uncovered HLA class I allotypes for the prediction of unknown HLA. Yet, all methods are suited for *in silico* binding prediction of peptides to HLA class I alleles. However, for HLA class II no tool meets the need.

1.7. Interplay of cancer and the immune system

The first part of the thesis examines the HLA ligandome of clear cell renal cell carcinoma (ccRCC). Therefore, the interplay of cancer with the immune system as well as generally applied immunotherapeutic approaches will be highlighted in the following sections before a more detailed focus will be placed onto ccRCC in the introductory section of the results and discussion part.

Tumor cell development is caused by genetic alterations sequentially acquired over time. The transformation of a normal cell into a tumor cell is a gradual processing including critical mutations in suppressor genes, oncogenes and genes involved in DNA repair. Consequences of these mutations are the unregulated proliferation of tumor cells losing the ability to appropriately respond to signals which control normal cell behavior. Benign tumors, such as skin warts, remain confined, whereas malignant tumors (cancer) are capable to invade the surrounding tissue and to spread into distant locations using the circulatory or lymphatic system and thereby generating metastasis.[61,62] Besides the above mentioned hallmarks, further characteristics of cancer cells are known.[63] Genetic alterations usually come along with the immortality of these cells preventing telomere loss by

upregulating the telomerase as well as telomere-interacting proteins.[64] Cancer cells are further resistant to apoptosis, a controlled suicide-mechanism induced by other cells like immune cells (extrinsic pathway) or by intracellular processes which sense cellular stress (intrinsic pathway).[65-67] The induction of angiogenesis, the mechanism to form new blood vessels, is particularly important for tumor growth in that nutrients as well as oxygen can be delivered to the tumor.[68-70] In addition, tumor cells may reprogram their energy metabolism to persist, a hallmark already described by Warburg in 1930.[71,72]

The transformation of cancerous cells engenders changes in the peptide repertoire presented at the cell surface with the appearance of tumor-specific antigens (TSAs) and tumor-associated antigens (TAAs). Mutated antigens, also referred to as neoantigens, are tumor-specific. TAAs can be categorized into cancer-testis antigens, oncofetal antigens, viral antigens, differentiation antigens, differential post-translational modified antigens[73-75] or overexpressed self-antigens[76]. The presentation of TSAs or TAAs implicates the recruitment of the immune system which eliminates transformed cells [**Figure 6**].

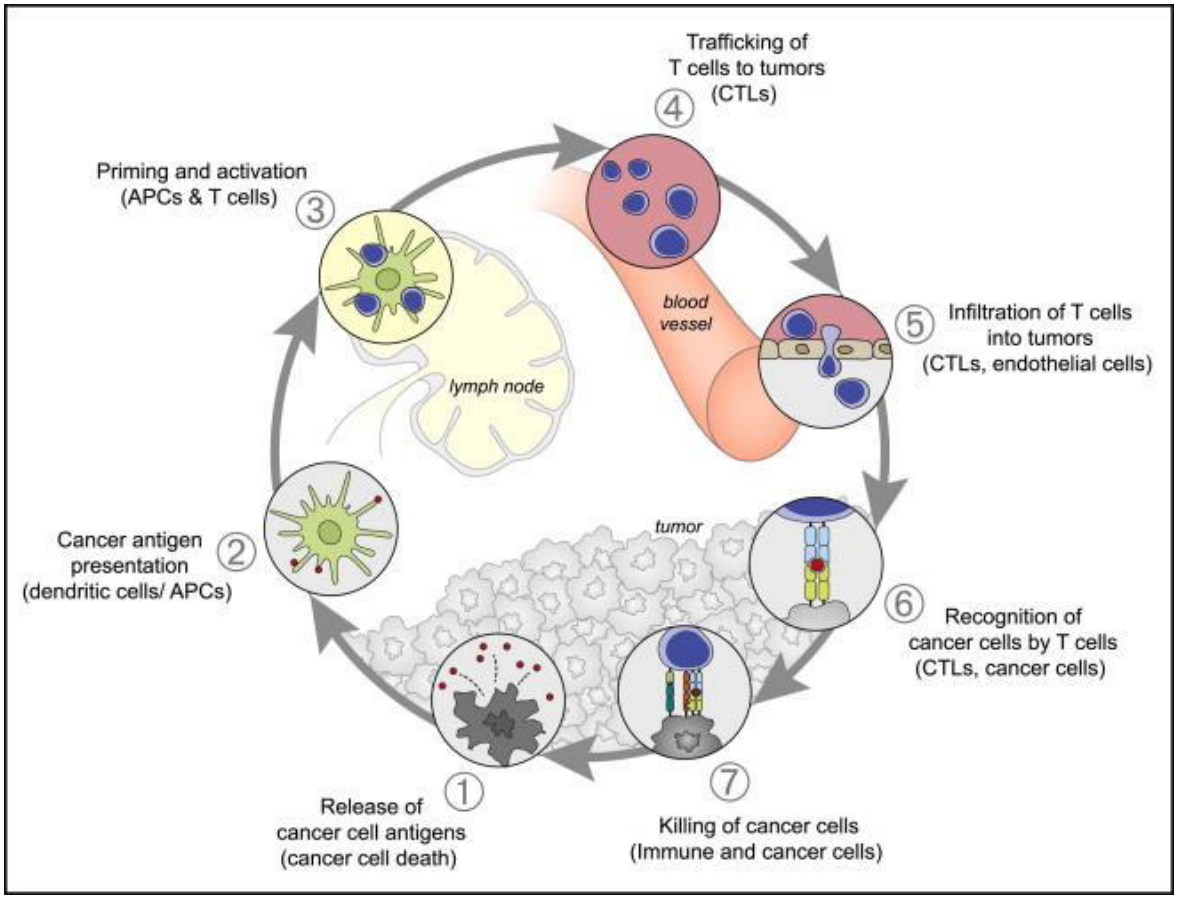

Figure 6: The Cancer-Immunity cycle. The death of cancer cells leads to the release of antigens. APCs ingest, process and present the antigen to T cells. The priming of T cells in nearby lymph nodes lead to the activation and subsequent trafficking to the tumor site. T cells infiltrate into the tumor and recognize cancer cells presenting the antigen for which T cells were primed. The recognition of the antigen leads to the subsequent killing of the cancer cells.[77]

The first step in the so called cancer-immunity cycle is the release of antigens by dying cells. For the activation of T cells, which takes place in nearby lymph nodes, antigens have to be ingested by APCs. Additional signals which are necessary for APC activation and trafficking to the lymph nodes include pro-inflammatory cytokines such as IFN-α or TNF-α, TLR agonists or products from dying tumor cells [**Table 1**].[77,78] APC activation is inhibited by cytokines such as interleukin-4 (IL-4), IL-10 or IL-13. Costimulatory receptors and cytokines (see section **1.1**) are necessary for successful T-cell activation and differentiation. T-cell migration from the lymph node to the tumor site across the blood vessels is directed by chemokines binding to their corresponding chemokine receptor such as CXCR3 (ligands CXCL9/10/11) or CCR5 (ligands CCL3/4/5/8).[79-81] Subsequent infiltration into the tissue is dependent on integrins, such as the LFA-1 receptor (Lymphocyte function-associated antigen 1) on leukocytes binding to ICAM-1 (intercellular adhesion molecule 1) on endothelial cells, and selectins (L-selectin on lymphocytes and E- or P-selectins on endothelial cells).[82-84] Effector T cells recognize and kill tumor cells which present the antigen.

Table 1: Overview of regulatory mechanism for each step of the cancer-immunity cycle.[77]

Steps	(+) Stimulators	(–) Inhibitors	Other Considerations
1. Release of cancer antigens	Immunogenic or necrotic cell death	**Tolerogenic or apoptotic cell death**	Tumor-associated neoantigens and cancer testis antigens
2. Cancer antigen presentation	● Proinflammatory cytokines (e.g., TNF-α, IL1, IFN-α) ● Immune cell factors: CD40L/CD40 ● Endogenous adjuvants released from dying tumors: CDN (STING ligand), ATP, HMGB1 ● Gut microbiome products: TLR ligands	IL-10, IL-4, IL-13	Dendritic cell maturity
3. Priming and activation	CD28:B7.1, CD137 (4-1BB)/ CD137L, OX40:OX40L, CD27:CD70, HVEM, GITR, IL-2, IL-12	CTLA4:B7.1, PD-L1:PD-1, PD-L1:B7.1, prostaglandins	Central tolerance, T cell repertoire, T regulatory cells
4. Trafficking of T cells to tumors	CX3CL1, CXCL9, CXCL10, CCL5		
5. Infiltration of T cells into tumors	LFA1:ICAM1, selectins	VEGF, endothelin B receptor	
6. Recognition of cancer cells by T cells	T cell receptor	Reduced peptide-MHC expression on cancer cells	
7. Killing of cancer cells	IFN-γ, T cell granule content	PD-L1:PD-1, PD-L1:B7.1, TIM-3:phospholipids, BTLA, VISTA, LAG-3, IDO, Arginase, MICA:MICB, B7-H4, TGFβ	T regulatory cells, myeloid-derived suppressor cells, M2 macrophages, hypoxia

The theory that the immune system may interplay with cancerous cells was formulated in 1957 by Burnet and Thomas, nowadays known as the cancer immunosurveillance theory.[85,86] Cancer immunosurveillance comprises the first phase of the extended theory of immunoediting, the process of immunogenic changes of the tumor. Immunoediting can be divided into three phases: elimination (known as immunosurveillance), equilibrium and escape.[87] Cancer cells attempt to avoid elimination by the immune system generating poorly immunogenic tumor-cell variants, a mechanism called immunoselection.[88] This state of equilibrium between the immune system and cancer cells may extend over many years in which the immune system has to perpetually adjust their defense mechanisms to the new selected tumor cell variants [**Figure 7**]. At the time cancer cells breach the immune defense (immunosubversion), immunoediting enters the third phase: escape of the tumor.

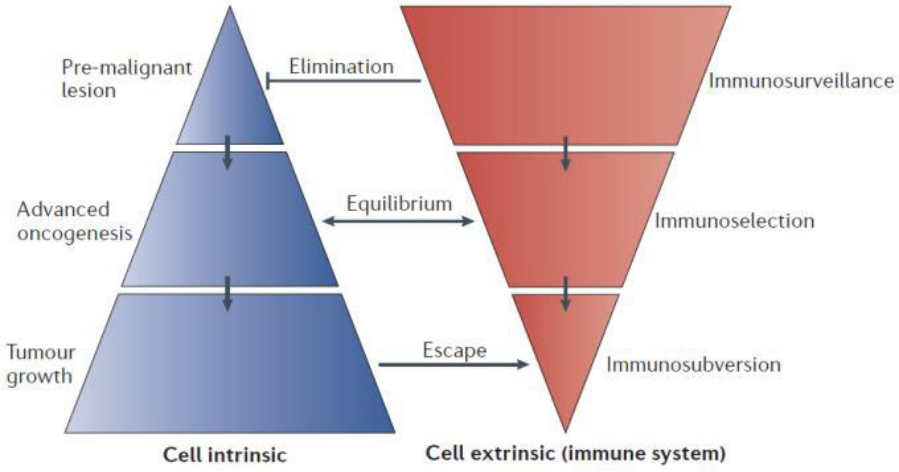

Figure 7: Relationship between the tumor and the immune system. The steps of carcinogenesis are depicted in blue. The steps of overcoming the immune system are depicted in blue. The three phases of this immunoediting are represented in the middle.[88]

Tumor escape occurs through loss of immunogenicity or resistance to suppressive or cytotoxic mechanisms of the immune cells within the tumor microenvironment.[87,89,90] Loss of immunogenicity can be achieved by reduced immune recognition (such as HLA loss/downregulation or dysregulation of antigen processing[91]). A mechanism for increased resistance to cytotoxic immune cell reaction is the induction of anti-apoptotic mechanisms. Immunosuppression of the microenvironment includes the production of immunosuppressive molecules, such as transforming growth factor-β (TGF-β), indoleamine-2,3-dioxygenase (IDO), vascular endothelial growth factor (VEGF) or galectin and the recruiting of regulatory immune cells, such as T_{reg} cells and myeloid-derived suppressor cells (MDSCs).[92] T_{reg} cells produce the immunosuppressive cytokines IL-10 and TGF-β, express the negative costimulatory molecules CTLA-4, PD-1 and PD-L1 and consume IL-2 which is important for proliferation and differentiation of tumor-infiltrating lymphocytes (TILs). Immunosuppressive mechanisms of MDSCs include the induction of T_{reg} cells, the production of immunosuppressive molecules such as TGF-β, the consumption of amino acids such as arginine and tryptophan or disabling TCR or chemokine receptors by nitration.[87]

1.8. Immunotherapy in cancer

Immunotherapy is the treatment of a disease which takes advantage of the immune system. The immunotherapy may either focus on the activation or enhancement of an immune response (such as reinforcing the immune activity in anti-cancer treatment) or focus on the suppression of the immune system (such as dampening the immune activity against autoimmune diseases or to prevent organ rejection in transplanted patients). The following section gives a short history and overview on treatment of cancer by immunotherapies.

The history of cancer immunotherapy started in the 1890s with the observation of William Coley that tumors may spontaneously regress after acute bacterial infections.[93] In the following time he started to inject bacterial preparations, nowadays known as "Coley's toxin", into cancer patients with several types of tumors, including sarcomas and lymphomas, with remarkable responses and a cure rate of 10%.[94] However, the unknown mechanism of action and the upcoming success of radiotherapy passed his approach into oblivion. Even the hypothesis of Paul Ehrlich in 1909 that the immune system may control cancers had no implications.[95] It took half a century until immunotherapy attracts attention with the cancer immunosurveillance theory (see section **1.7**).[85] However, the cancer immunosurveillance theory remained under debate until the 1990s. Several discoveries, such as the escape of auto-reactive T cells from thymic deletion[96,97], the genetic instability of tumor cells[98], the identification of TAAs[99,100] and the higher incidence of tumors in immunodeficient mice[101,102], changed the point of view.

The variety of immunotherapies nowadays can be grouped in active and passive immunotherapies. Active immunotherapies rely on activation of the body's own immune response, whereas passive approaches rely on intrinsic anti-cancer activity of administered drugs. Furthermore, a classification into specific or non-specific immunotherapies can be drawn dependent on direct targeting of cancer cells (specific) or a general activation of the immune system (non-specific). An overview of immunotherapeutic approaches is illustrated in **Table 2**.

Table 2: Overview of immunotherapeutic approaches. Modified from[103]

	Active Immunotherapy	**Passive Immunotherapy**
Specific	Vaccines - Prophylactic (HPV, HBV) - Therapeutic (peptide vaccines, peptide-loaded DCs, RNA vaccines, tumor lysates, whole cancer cells)	Adoptive T cell transfer (Tumor-infiltrating lymphocytes, TCR gene-modified lymphocytes, chimeric antigen receptors [CARs]) Monoclonal antibodies
Non-specific	Immune checkpoint inhibitors (α-CTLA-4, α-PD-1, α-PD-L1)	Cytokines (IL-2, IFNs, etc.)

Specific immunotherapeutic approaches are antigen-dependent, whereas non-specific approaches are antigen-independent. An antibody-based specific immunotherapy targets TAAs presented at the cell surface of tumor cells such as differentiation antigens (like CD20, CD30 or CD52), glycoproteins (like Mucins, CA9 or PSMA), or growth receptors (like EGFR or ERBB2). Furthermore, monoclonal antibodies may target TAAs which are not expressed by the tumor cell itself, such as the tumor vasculature antigen VEGF. The antibody application in cancer treatment was reviewed among others in [104,105]. Vaccines and adoptive T cell transfer (ACT) are based on antigen recognition in form of pHLA complexes presented by APCs and cancer cells. The presentation of antigens in form of pHLA complexes enhances the variety of targetable antigens and renders a personalized therapy feasible. Since the first part of this thesis deals with the identification of T-cell epitopes, ACT and therapeutic vaccination will be further explained.

ACT employs autologous T cells which are cultured and selected for high-avidity antigen recognition *ex vivo* [**Figure 8**]. Moreover, the antigen specificity can be genetically engineered *in vitro* modifying the TCR or including a chimeric antigen receptor (CAR) which may also provide non-HLA-restricted antigen recognition. Large numbers of T cells (>10^{10}) are expanded *ex vivo* using high amounts of IL-2 (6000 U/ml) and reinfused into the patient about five to six weeks after tumor resection.[106] Administered cells are able to proliferate and to maintain their effector function.[107] Their persistence *in vivo* correlates with tumor regression.[108] A lymphodepletion before ACT is applied to eliminate lymphocytes which would compete with the transferred T cells for cytokines such as IL-7 and IL-15[109] or would inhibit their function such as regulatory T cells[110]. The *ex vivo* expansion of antigen-specific T cells has the advantage of the missing inhibitory tumor microenvironment and the subsequent injection of high amounts of antigen-specific T-cells. However, the incorrect selection of the target antigen can lead to severe auto-reactivity of the reinfused cells.

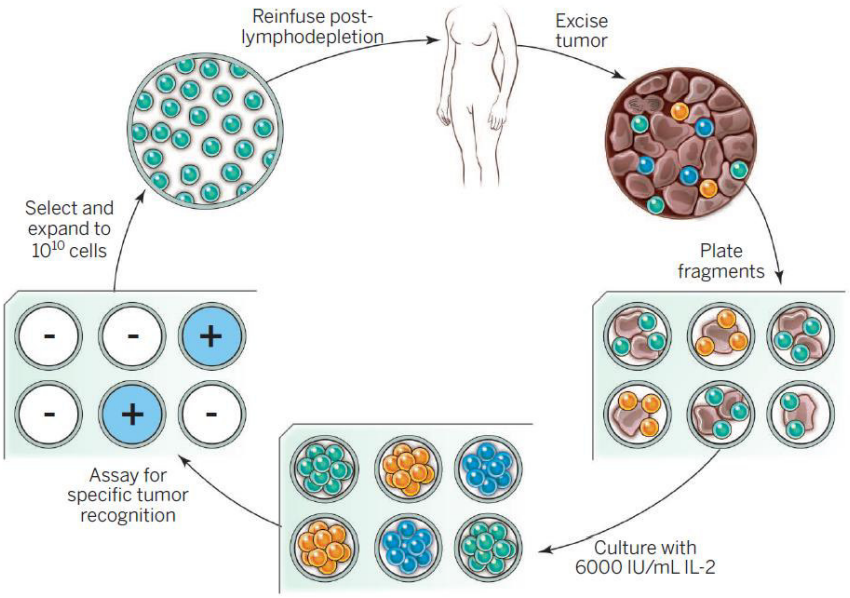

Figure 8: Adoptive T cell transfer using autologous antigen-specific tumor-infiltrating cells (TILs). The resected tumor is digested into a single-cell suspension following culture with high-dose IL-2. Cells are screened for antigen-specific T cell which are further expanded and reinfused into the patient after a lymphodepletion.[107]

Peptide vaccination approaches are based on *in vivo* stimulation of T cells by intradermal or subcutaneous injection of peptide formulations or autologous *in vitro* peptide-pulsed DCs. The basis of an effective vaccine is the appropriate activation of DCs. In general, the identification of TSAs or TAAs is based on mass spectrometry analysis of tumor samples and/or the prediction of HLA ligands from sequencing data (see section **1.6**). A subsequent *in vitro* immunogenicity screen reveals the recognition ability of T cells.[111]

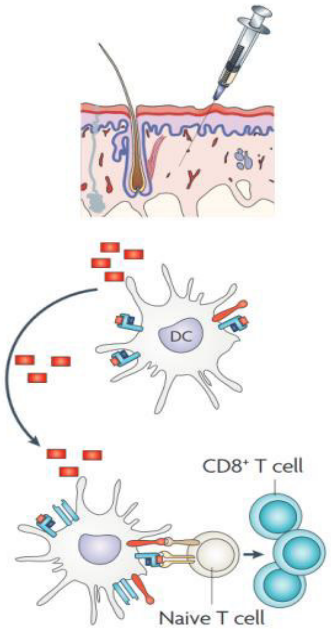

Figure 9: Peptide vaccination. Peptide formulation is injected intradermally or subcutaneously into the patients. Peptides are taken up by APCs and presented to T cells.[112]

Peptide formulations may include one to several peptides as well as short (minimal CTL epitope) to extended (CTL and T_H lymphocyte epitopes) peptides.[113] A proper selection of the peptides is mandatory to avoid immunological tolerance towards these peptides.[114,115] Short peptides are more prone to induce immunological tolerance because of the ability to directly replace peptides of cell surface-expressed HLA molecules of any cell.[116] On the other side, long peptides have to be endocytosed and processed by APCs overcoming the risk of tolerance induction by direct replacement at the cell surface. In addition, long peptides may be presented by HLA class II enabling the activation of T_H cells delivering additional activation signals to DCs through the CD40-CD40L signaling pathway.[117,118] However, short peptide are easier to produce and can be better screened for antigen-dependent immunogenicity. Cocktail formulations with several peptides (up to 12-15) may be superior compared to single peptide approaches in that the tumor can be attacked on various presented antigens hampering further immune escape. In addition, targeting of several antigens which are required for tumor cell survival may further restrict the adaption of the tumor. However, the typical poor immunogenicity of peptides alone requires an additional adjuvant with immunostimulatory effects.

Adjuvants act in several ways including depot formation for a slow and continuous release of peptides and/or activation of APCs by binding to pattern recognition receptors. Emulsions such as MF59 (oil-in-water)[119], incomplete Freund's adjuvant (water-in-oil)[120] or Montanide ISA 51 or ISA720 (both water-in-oil emulsions)[121] are some examples of adjuvants with depot formation ability. Recent research focuses on vaccine adjuvants which specifically activate APCs. Examples are the Toll-like receptor 4 (TLR4) agonist monophosphoryl lipid A (MPLA), the TLR7 agonist imiquimod, TLR9 agonists in form of CpG-containing oligonucleotides, the TLR3 agonist Poly(I:C) or the TLR1/2 agonist Pam_3Cys.[122] Up to date, 60 active clinical trials (plus many more in the pipeline) with peptide vaccines for several malignancies are listed on the clinicaltrials.gov website (Search term: "Peptide vaccine", Recruitment status: "Active", Date: 05.06.2017) displaying the upcoming era of immunotherapeutic strategies in disease combat.

1.9. Objectives

The objectives of this thesis were the identification of suitable T-cell epitopes for the immunotherapy of ccRCC and the unveiling of HLA-C, HLA-E and HLA-G peptide motifs. The results and discussion part I addresses the identification of T-cell epitopes for the immunotherapy of ccRCC. In the second part of the results and discussion the peptide presentation specificities of HLA-C, HLA-E and HLA-G will be addressed.

Renal cell carcinoma (RCC) is considered to be one of the most immunogenic tumors which is substantiated by spontaneous tumor rejections and high T cell infiltration.[123,124] Besides resection of the malignant kidney, current therapies focus on targeting the tumor or the tumor environment with small inhibitory molecules. However, frequent resistance against those drugs limits their applicability.[125] On the other side, non-specific immunotherapeutic approaches with either cytokines IL-2 or IFN-α or the lately approved checkpoint ab nivolumab demonstrates the potential of immunotherapies.[126,127] Specific or personalized approaches, such as peptide vaccination or ACT, as well as combinatorial strategies hold the potential in enhancing the frequency and specificity of anti-cancer T-cell responses. To that end a comprehensive analysis of the HLA ligandome of the most frequent subtype ccRCC should be conducted and compared to the HLA ligandome of the corresponding adjacent benign counterparts as well as to a benign in-house database. Immunopeptidomics should be performed by liquid chromatography (LC)-coupled mass spectrometry (MS). Finally, the immunogenicity of selected HLA ligands had to be addressed by priming of naïve $CD8^+$ T cells from healthy blood donors.

Classical HLA-C as well as the non-classical HLA-E and HLA-G molecules possess critical functions in both the innate and adaptive immunity. Compared to the well-defined immune activating functions of HLA-A and HLA-B molecules, the functions of HLA-C, HLA-E and HLA-G are diverse, ranging from immune activation, regulation and suppression depending on the receptor they interact with. This is mainly attributable to the interaction with NK cells. However, the characterization of peptide motifs has been lacking behind the more abundant HLA-A and HLA-B. For this purpose, peptide motifs of frequent HLA-C alleles as well as HLA-E and HLA-G should be analyzed. HLA ligands from monoallelic transfected lymphoblastoid C1R cells had to be analyzed by LC-MS/MS and employed for the definition of peptide motifs. The data should be utilized to establish SYFPEITHI matrices applicable for *in silico* binding prediction and for peptide assignment to the correct HLA.

2. Results and discussion, Part I: The immunopeptidomic landscape of clear cell renal cell carcinoma: identification and characterization of T-cell epitopes for immunotherapeutic approaches

2.1. Renal cell carcinoma

Renal cell carcinoma (RCC) arises from the glandular epithelium (adenocarcinoma) of the renal cortex and represents about 85% of all renal malignancies.[128] The other renal malignancies are the urothelial carcinoma, Non-Hodgkin lymphoma, sarcomas and Wilms tumor. It constitutes about 3% of all newly diagnosed cancers and is therefore among the ten most common cancers and the third common tumor of the urogenital tract after prostate and bladder carcinoma (US statistics illustrated in [**Figure 10**]). The average age at the time of diagnosis is between 65 and 70 years. The incidence of RCC is higher in men compared to women (2:1) and higher in more developed countries.[129] Worldwide about 295,000 people are annually diagnosed with RCC and about 134,000 deaths are related to the disease.[130]

Depending on the morphology of the tumor and their molecular characteristics over 10 subtypes can be distinguished.[131] The three main types with the highest incidence are clear cell RCC (ccRCC, with 75-85% the most frequent type), papillary RCC (pRCC, 10-15%) and chromophobe RCC (chRCC, 3-5%).[132,133] The other subtypes represent less than 1% of RCCs.

Hereditary predispositions, accounting for 2-3% of all RCC, are for instance the Von-Hippel Lindau disease (VHL) which is caused by mutations in the VHL tumor suppressor gene on chromosome 3 (predisposition for ccRCC)[134] and the Birt-Hogg-Dubé syndrome[135] caused by a mutation in the FLCN gene on chromosome 17 encoding for folliculin which is suggested to act as a tumor suppressor (predisposition for chRCC)[136]. An overview of further genetic predispositions was reviewed by Schmidt *et al.*[137] Further risk factors include smoking[138], obesity[139], hypertension and antihypertensive medication[140,141] and the acquired renal cystic disease[142] (reviewed in [143]).

RCC develops usually symptom-free over a longer time period and is often discovered accidently during screenings owing to another indication. Symptoms manifesting in an advanced stage are abdominal pain, palpable mass and haematuria. Therefore, it is not striking that at the time of diagnosis 30% of patients exhibit metastasis, whereas 25% display locally advanced disease and 45% localized RCC.[144] A suspected RCC is investigated through anamnesis, physical examination, laboratory tests of the blood and the urine, the medical imaging by ultrasonography or computed tomography and a possible biopsie.[145]

Estimated New Cases*

	Males			Females	
Prostate	233,000	27%		Breast	232,670	29%
Lung & bronchus	116,000	14%		Lung & bronchus	108,210	13%
Colorectum	71,830	8%		Colorectum	65,000	8%
Urinary bladder	56,390	7%		Uterine corpus	52,630	6%
Melanoma of the skin	43,890	5%		Thyroid	47,790	6%
Kidney & renal pelvis	39,140	5%		Non-Hodgkin lymphoma	32,530	4%
Non-Hodgkin lymphoma	38,270	4%		Melanoma of the skin	32,210	4%
Oral cavity & pharynx	30,220	4%		Kidney & renal pelvis	24,780	3%
Leukemia	30,100	4%		Pancreas	22,890	3%
Liver & intrahepatic bile duct	24,600	3%		Leukemia	22,280	3%
All Sites	**855,220**	**100%**		**All Sites**	**810,320**	**100%**

Estimated Deaths

	Males			Females	
Lung & bronchus	86,930	28%		Lung & bronchus	72,330	26%
Prostate	29,480	10%		Breast	40,000	15%
Colorectum	26,270	8%		Colorectum	24,040	9%
Pancreas	20,170	7%		Pancreas	19,420	7%
Liver & intrahepatic bile duct	15,870	5%		Ovary	14,270	5%
Leukemia	14,040	5%		Leukemia	10,050	4%
Esophagus	12,450	4%		Uterine corpus	8,590	3%
Urinary bladder	11,170	4%		Non-Hodgkin lymphoma	8,520	3%
Non-Hodgkin lymphoma	10,470	3%		Liver & intrahepatic bile duct	7,130	3%
Kidney & renal pelvis	8,900	3%		Brain & other nervous system	6,230	2%
All Sites	**310,010**	**100%**		**All Sites**	**275,710**	**100%**

Figure 10: Ten most frequent cancer types with estimated new cases and deaths in the US, 2014.[146] *Rounded values to the nearest 10. Basal cell and squamous cell skin cancers and in situ carcinoma except urinary bladder are excluded.

The standard classification of the disease progression into different tumor stages follows the TNM classification introduced by the Union for International Cancer Control [**Table 3**]. The TNM classification describes the disease progression based on three categories. The T refers to the size of the tumor and the spread into the kidney, the N indicates the infestation of regional lymph nodes, and the M indicates the presence of distal metastasis. The 5-year survival rate is dependent on the tumor stage. Observed survival rates published by the American Cancer Society are 81% for stage I, 74% for stage II, 53% for stage III and 8% for stage IV patients. Note, that these percentages include also people deceasing due to other diseases.

Table 3: TNM classification of RCC.[147] Schematic illustration of tumor staging, adapted from[148]. Illustration) A schematic stage I tumor localization is depicted in pink, a stage II tumor localization in blue, a stage III tumor localization in yellow and a stage IV tumor localization in red.

Primary tumor (T)		
TX		Primary tumor cannot be assessed
T0		No evidence of primary tumor in the kidneys
T1		Tumor ≤ 7 cm in greatest dimension, limited to the kidneys
	T1a	Tumor ≤ 4 cm in greatest dimension, limited to the kidneys
	T1b	Tumor > 4 cm but not > 7 cm in greatest dimension, limited to the kidneys
T2		Tumor > 7 cm in greatest dimension, limited to the kidneys
	T2a	Tumor > 7 cm but not > 10 cm in greatest dimension, limited to the kidneys
	T2b	Tumor > 10 cm in greatest dimension, limited to the kidneys
T3		Tumor extends into major veins or perinephric issues, but does not invade the adrenal gland or spread beyond Gerota's fascia
	T3a	Tumor spreads into renal vein or its muscles or perirenal and/or renal sinus fat, but not beyond Gerota's fascia
	T3b	Tumor grossly extends into vena cava below the diaphragm
	T3c	Tumor grossly extends into vena cava above the diaphragm or invades the wall of the vena cava
T4		Tumor invades beyond Gerota's fascia and extends into the contiguous adrenal gland
Regional lymph nodes (N)		
NX		Regional lymph nodes cannot be assessed
N0		No regional lymph node metastasis
N1		Metastasis to regional lymph nodes
Distant metastasis (M)		
M0		No distant metastasis
M1		Distant metastasis
Stage grouping		
Stage I		T1, N0, M0 (pink)
Stage II		T2, N0, M0 (blue)
Stage III		T1-T2, N1, M0 or T3a-T3c, N0-N1, M0 (yellow)
Stage IV		T4, NX-N1, M0 or TX-T4, NX-N1, M1 (red)

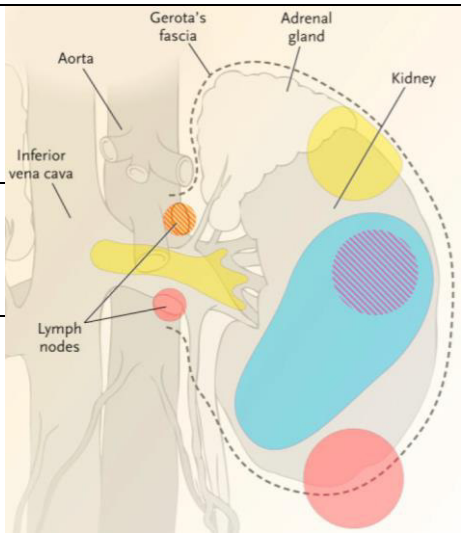

2.2. Therapy of renal cell carcinoma

The first intervention in the treatment of localized tumors is a partial or radical nephrectomy (surgical excision) of the affected kidney. The partial nephrectomy is used to preserve healthy kidney tissue in patients with stage I disease, one functional kidney, bilateral manifestation of RCC, VHL syndrome or other diseases impairing kidney function.[149] For metastatic RCC (mRCC) the additional treatment with targeted therapies or the checkpoint inhibitor nivolumab is exerted. These therapies

can be also applied for inoperable tumors. Alternative strategies are the active surveillance or ablative therapies such as radiofrequency ablation or cryotherapy.[150,151]

In former times, therapy of mRCC included single-agent or combinatorial chemotherapies and radiotherapy. However, due to high resistance against chemotherapy and radiotherapy the applicability was limited. In 1992, the first immunotherapeutic approach with high-dose IL-2 was approved. Until 2005, high-dose IL-2 and IFN-α were the state-of-the-art treatment for mRCC. Despite response rates of about 15%, these therapies implicate frequent adverse side effects on the cardiovascular, gastrointestinal, neurological, pulmonary, hepatic, renal and hematological systems.[152] Since 2005 nine therapeutic agents were approved belonging to the group of tyrosine kinase inhibitors targeting VEGFR and some other growth factor receptors, namely sorafenib, sunitinib, pazopanib, axitinib, lenvatinib and cabozantinib, the α-VEGF ab bevacizumab and the mammalian target of rapamycin (mTOR) inhibitors temsirolimus and everolimus [**Figure 11**]. The higher specificity of those drugs entails lower cytotoxicity and fewer side effects.[153]

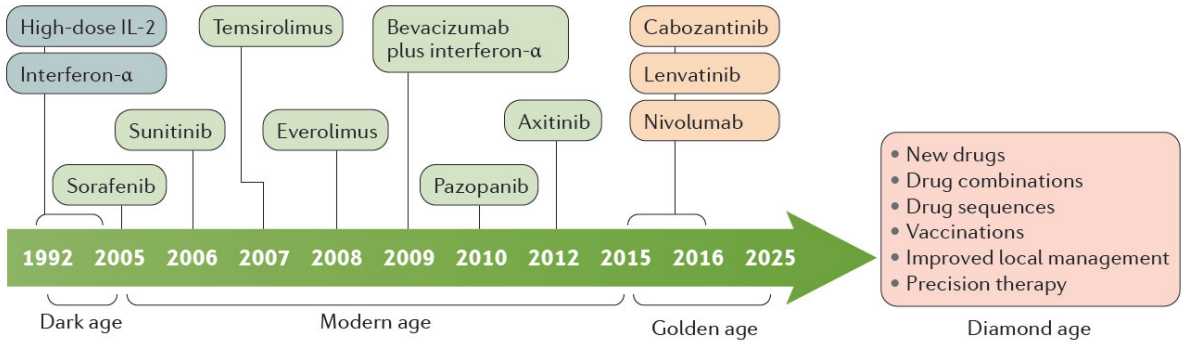

Figure 11: The evolution of the therapeutic treatment of mRCC. High-dose IL-2 and IFN-α were used until 2005 ("dark age") when the tyrosine kinase inhibitor sorafenib was introduced. In the following years several other tyrosine kinase inhibitors, a monoclonal ab and drugs inhibiting mTOR were developed ("modern age"). The new "golden era" was initiated by the checkpoint inhibitor nivolumab. The development of specific immunotherapeutic agents, such as vaccines or the adoptive T cell transfer, as well as drug combinations will lead to the "diamond age".[149]

The latest recommendations for the systematic treatment of patients with metastatic disease are illustrated in **Table 4** with sunitinib as standard of care for first-line therapy of most mRCC.[154] The clinical benefits of administered drugs in RCC in terms of overall response rate, progression-free survival and overall survival were highlighted among others by Tsao *et al.*[155] However, all targeted therapies have low response rates and a considerable risk of resistance development[125], rendering new approaches necessary.

The lately approved checkpoint ab nivolumab for treatment of mRCC is the first drug in the upcoming era of immunotherapy [**Figure 11**]. Nivolumab targets the checkpoint receptor programmed cell death protein 1 (PD-1) expressed on activated T cells, B cells and myeloid cells.[156,157] PD-1 interacts

with PD-L1 and PD-L2, which are preferentially expressed on DCs and cancer cells upon IFN-γ stimulation and exhibit immunoinhibitory signals.[157,158] For patients with prior failed sunitinib or pazopanib treatment the response rate of nivolumab was 25% compared to 5% for everolismus.[127] The progression-free survival was not improved. However, the overall survival was enhanced with 25.0 vs 19.6 months compared to everolimus.[127]

Table 4: Latest recommendations of the European Association of Urology for the treatment of mRCC patients.[159]

RCC type	MSKCC risk group [319]	First-line	LE^	Second-Line after VEGF therapy*	LE^	Third-line*	LE^	Later lines	LE
Clear cell*	Favourable, intermediate and poor	sunitinib pazopanib bevacizumab + IFN-α (favourable-intermediate only)	1b 1b 1b	based on OS: nivolumab based on PFS: cabozantinib axitinib sorafenib# everolimus&	 2a 2a 2a 2a 2a	after VEGF therapy: nivolumab cabozantinib everolimus& after VEGF and mTOR therapy: sorafenib after VEGF and nivolumab: cabozantinib axitinib everolimus	 2a 2a 2a 1b 4 4 4	any targeted agent	4
Clear cell*	poor¶	temsirolimus	1b	any targeted agent	4				
Non-clear cell §	any	sunitinib everolimus temsirolimus	2a 2b 2b	Any targeted agent	4				

MSKCC = Memorial Sloan-Kettering Cancer Center; LE = level of evidence

** Doses: IFN-α - 9 MU three times per week subcutaneously, bevacizumab 10 mg/kg biweekly intravenously; sunitinib 50 mg daily orally for 4 weeks, followed by 2 weeks of rest (37.5 mg continuous dosing did not show significant differences); temsirolimus 25 mg weekly intravenously; pazopanib 800 mg daily orally. Axitinib 5 mg twice daily, to be increased to 7 mg twice daily, unless greater than grade 2 toxicity, blood pressure higher than 150/90 mmHg, or the patient is receiving antihypertensive medication. Everolimus, 10 mg daily orally.*

§ No standard treatment available. Patients should be treated in the framework of clinical trials or a decision can be made in consultation with the patient to perform treatment in line with ccRCC.

¶ Poor risk criteria in the NCT00065468 trial consisted of MSKCC [319] risk plus metastases in multiple organs. Evidence for subsequent therapies unclear, making this option less appealing.

 # Sorafenib was inferior to axitinib in a RCT in terms of PFS but not OS [351].

^ Level of evidence was downgraded in instances when data were obtained from subgroup analysis within an RCT.

& everolimus was inferior in terms of OS to nivolumab and in terms of PFS to cabozantinib and should not routinely be given where other superior agents are available.

Several studies are currently investigating the application of further immune checkpoint inhibitors such as the anti-cytotoxic T lymphocyte-associated protein 4 (α-CTLA-4) antibodies ipilimumab and tremelimumab, the α-PD-1 antibodies nivolumab and pembrolizumab, and the anti-programmed cell death 1 ligand 1 (α-PD-L1) antibodies avelumab, atezolizumab and durvalumab.[160] Several immunotherapeutic approaches, such as the DC-based vaccine AGS-003 loaded with RNA[161], are currently in clinical trials (www.clinicaltrials.gov).

Moreover, the first therapeutic vaccine IMA901[162] demonstrated the potential of specific immunotherapies in a clinical phase 2 study, but ultimately failed to improve overall survival in phase 3 in combination with sunitinib compared to sunitinib monotherapy.[163] Because of significantly reduced $CD8^+$ T cell responses in the phase 3 study compared to prior studies, one may speculate an immunosuppressive effect of sunitinib. However, sunitinib treatment is so far suggested to possess an immune activating function by increasing the percentage of IFN-γ producing T cells and decreasing the percentage of IL-4 producing T cells as well as downregulating T_{reg} cells.[164] MDSC levels are reduced and myeloid DC levels are restored upon sunitinib treatment in RCC.[165-167] In mice, numbers of $CD8^+$ and $CD4^+$ T cells were elevated with reduced expression of immunosuppressive costimulatory molecules such as PD-1 and CTLA-4 as well as reduced levels of T_{reg} cells, MDSC and the immunosuppressive cytokine IL-10.[168] In addition, changes in the vaccination timeline with reduced vaccination cycles as well as focusing on patients with low and intermediate risk, which might be accounting for the overall exceptional good outcome in both treatment arms, are further explanations of the study fail.[163] Nonetheless, the phase 2 results emphasize the potential of specific immunotherapies.

2.3. Cellular aberrations of ccRCC

ccRCC is characterized by some recurring genetic alterations and a tremendous metabolic dysregulation.[169-171] The mutation rate of ccRCC is rather low with about four to five mutations per megabase.[172] However, there are some distinctive mutations recurring among patients. Frequent genetic aberrations involve the short arm of chromosome 3 which is lost in most of the ccRCC samples contained in The Cancer Genome Atlas (TCGA) database.[173]

Besides the common loss, the short arm of chromosome 3 encompasses the most frequent mutated genes, namely VHL, PBRM1, SETD2 and BAP1.[173] The most frequent mutations are found in VHL[174] which is part of the E3 ubiquitin ligase complex transferring ubiquitin molecules to targets for subsequent proteasomal degradation.[175] The main targets of VHL are the hypoxia-inducible factors HIF-1α and HIF-2α recognized subsequent to oxygen-dependent hydroxylation at specific proline residues by prolyl hydroxylases (PHD).[176,177] HIFs act as transcription factors in a heterodimeric complex with HIF-β, also called the aryl hydrocarbon receptor nuclear translocator (ARNT). Under normoxic conditions HIF proteins are hydroxylated and degraded. However, non-functional or missing VHL as well as a usually hypoxic (oxygen-deprived) environment result in unregulated activity of HIF transcription factors. The heterodimeric complex binds to hypoxia-response elements (HRE) activating several genes with functions in cell proliferation and differentiation (e.g. CCDN1,

IGFBP1/2), apoptosis (e.g. BNIP, Bax), angiogenesis (e.g. VEGF), cell invasion (e.g. GAS6/AXL, CDCP1, FYN), energy metabolism (e.g. GLUT1/3, ALDOA/C, PLIN2), matrix metabolism (P4H) or pH regulation (CA9).[178-181] Target genes of HIF-1α and HIF-2α are not completely overlapping and are cell-type dependent.[182] In ccRCC, both isoforms may possess opposing effects with a shift towards the tumor promoting HIF-2α.[181,183] Moreover, the gene for HIF-1α is often deleted due to a frequent (45% of ccRCC TCGA dataset[173]) loss of the long arm of chromosome 14 where the HIF1A gene is located. Beside chromosome loss and VHL mutations, gene silencing by methylation of the VHL gene is a further mechanism for the impaired or missing VHL activity.[184]

The other common mutated genes PBRM1, SETD2 and BAP1 are involved in histone remodeling or modification. The PBRM1 gene encodes for protein polybromo-1, a subunit of the SWI/SNF chromatin remodeling complex.[185] SETD2 encodes for a histone methyltransferase activating gene expression through the generation of H3K36me3.[186] BAP1 encodes for a histone deubiquitinase which acts as a tumor suppressor.[187]

Additionally to the VHL/HIF pathway and the chromatin remodeling, the PI(3)K/AKT/MTOR pathway plays a particular role in tumor progression. Genes encoding for proteins of the PI(3)K/AKT/MTOR pathway, in particular PTEN and MTOR, are often mutated. Moreover, PI(3)K signaling is often activated by a gain of copy numbers of the long arm of chromosome 5 comprising GNB2L1 and SQSTM1 which are associated with the activation of the PI(3)K signaling pathway.[173,188,189] The correlation of DNA methylation, RNA expression or protein expression of pathway involved genes, transcripts or proteins, respectively, with patient's survival demonstrates the importance of the PI(3)K/AKT/MTOR pathway.[173]

Overall, the genetic and epigenetic aberrations of ccRCC lead to a denoting metabolic shift including enhanced consumption of glucose along with downregulation of the tricarboxylic cycle and upregulation of the pentose phosphate pathway (NADPH production for lipid anabolism) and glutamine/glucose transporters.[169,173] AMPK, which senses cellular ATP levels protecting the cell against energy deprivation, is downregulated as well as the tumor suppressor PTEN which inhibits PI(3)K/AKT/MTOR pathway signaling.[173] Another apparent characteristic is the enhanced lipid storage of ccRCC which is the reason for the clear morphologic appearance of these cells.[190] Based on these metabolic shifts, ccRCC as well as other subtypes of RCC are considered as metabolic diseases.[191] The current therapeutic approaches focus on the metabolic shift of RCC. These approaches include the targets VEGF, produced by tumor cells in consequence of the disabled VHL pathway, VEGFR, presented by endothelial cells surrounding the tumor and leading to angiogenesis, and mTOR, activated by the PI(3)K/AKT/MTOR pathway subsequently leading to HIF transcription.

2.4. Tumor microenvironment of ccRCC

Besides the metabolic aberrations, ccRCC is characterized by enhanced infiltration of immune cells in the tumor microenvironment[123,192] considering ccRCC as immunogenic tumor. This is further emphasized by spontaneous regressions of the tumor even at metastatic stages[124] and sporadic responses to non-specific immunotherapies with IL-2 and IFN-α[126].

Immune cell populations infiltrating the tumor site of ccRCC include T cells representing half of the immune cell infiltrate, myeloid cells, NK cells and B cells, whereas granulocytes are only present at low levels.[193] Senbabaoglu *et al.*[192] found out that the $CD8^+$ T cell/T_{reg} ratio as well as the amount of Th_{17} cells is positively correlated to patient's survival in ccRCC, whereas Th_2 and T_{reg} amounts are negatively correlated.[192,194] The study by Geissler *et al.*[195] displays an increase in T cell numbers with a higher tumor grade which indicates the dedifferentiation level of tumors. T cells on RCC lesions of higher grade had enhanced CD69 and CTLA-4 expression, both immune regulatory receptors of activated T cells.[195] Moreover, patient's survival was positively correlated to NK cell and Th_1 infiltration, whereas a poor outcome was detected for patients with high T cell numbers, especially CD69 expressing cells.[195] The immune inhibitory molecule of activated immune cells PD-1 is also associated to high-risk RCC tumors.[196] The expression of effector T cell markers as well as the positive correlation to patient's survival supports the immunogenicity of RCC. However, there are many immune suppressive mechanisms of RCC preventing ultimately its defeat.

A general overview of immune escape mechanisms was highlighted in section **1.7**. Evidenced immune escape mechanisms for RCC were reviewed by Seliger[197] and Frankenberger *et al.*[198] RCC is able to evade or to suppress the immune system by several mechanisms. A reduction of immune recognition by downregulation of HLA molecules, however, is no mechanism to evade the immune system. Data show rather enhanced HLA expression in RCC.[199,200] The expression of inhibitory molecules, such as PD-L1 and B7-H4, is a mechanism to suppress T cell function and to induce apoptosis in T cells.[201-203] The non-classical HLA-G, usually restricted to immune-privileged organs (see section **3.1**), is expressed by RCC inhibiting NK cells as well as T cells.[204,205] In addition, RCC induces apoptosis in TILs by the expression of Fas ligand or CD70.[206,207] Overexpression of gangliosides, glycosphingolipids at the outer part of the cell membrane, may function in T cell inhibition or promotion of T cell dysfunctionality by the induction of the cytokines IFN-γ and IL-4.[208] Moreover, gangliosides may inhibit antigen processing and presentation.[208] The ganglioside-dependent induction of apoptosis by the activation of the transcription factor NF-κB was also demonstrated *in vitro*.[209] Several by RCC secreted soluble factors, such as VEGF, TGF-β and IDO, are also contributing to the immunosuppressive environment. VEGF inhibits DC maturation[210], while

TGF-β acts in several ways including the suppression of CTL and NK cell functionality.[211] IDO which degrades tryptophan leads to the inhibition of TIL proliferation and may recruit T_{reg} cells.[212,213]

Besides these direct mechanisms of immune suppression, RCC indirectly promotes an immunosuppressive microenvironment by the attraction of immunosuppressive MDSCs, T_{regs} and tumor-associated macrophages (TAMs).[214,215] Mechanisms of MDSCs and T_{regs} in immunosuppression were highlighted in section **1.7**. TAMs are attracted by chemokines produced among others by tumor cells such as monocyte chemotactic protein-1 (MCP-1), macrophage colony stimulating factor (M-CSF) or VEGF.[216] Attracted TAMs support tumor growth by the production of growth factors, such as EGF, FGF or TGF-β, and tumor spreading by the secretion of angiogenic factors, such as cytokines and matrix metalloproteinases (MMPs) -1, -3 and -10.[217,218] On the other side, secreted IL-10 suppresses the immune reaction.[219] Furthermore, low levels of Th_1 cells which provide IL-2 for CTLs and consumption of IL-2 by T_{regs} expressing the IL-2 receptor, lead to impeded CTL and NK functionality.[198,220] Defect TCR signaling caused by the downregulation of the CD3 ζ-chain is frequently found in RCC and may be induced by arginase I or nitric oxygen species produced by MDSCs.[221,222]

The immunosuppressive microenvironment of tumors is far more complex than presented here. Overcoming general mechanisms with appropriate drugs will improve immunotherapies. The first step was performed by the development of checkpoint inhibitors. Further strategies to overcome the immunosuppressive microenvironment were reviewed by Joyce and Fearon.[90] The reactivation of TILs impeding inhibitory signals through checkpoint inhibitors demonstrates the potential in intervening immune suppression.

Peptide vaccinations, by contrast, try to boost specific reactions against TAAs by the activation of APCs (through an adequate adjuvant) and the specific activation of TAA-specific T cells. On the other side, immunosuppressive effects can be simply overcome in a first step by the *in vitro* expansion of tumor-specific T cells for ACT. Priming and boosting a specific anti-cancer response with the prevention of immune suppressive mechanisms will revolutionize therapies against cancer. This part of the thesis addresses the identification of suitable T-cell epitopes for ccRCC which can be applied for specific immunotherapeutic approaches, such as vaccines or ACT.

2.5. Materials and methods

2.5.1. Samples

A cohort of 58 snap-frozen patient samples (tumors as well as adjacent benign tissues) was collected for HLA ligandome analysis. The histological clear-cell subtype was attested by the Institute of Pathology, Tübingen, Germany. Informed consent following the Helsinki protocol was obtained for all patients. The study was performed according to the guidelines of the local ethics committee (446/2008BO2). HLA typing was carried out by the Department of Hematology and Oncology, University of Tübingen, Germany. A list of the patient cohort for HLA ligandome analysis is illustrated in **Supplementary Table 1**. Whole blood for the isolation of peripheral blood mononuclear cells (PBMCs) and $CD8^+$ T cells for T cell assays was obtained from healthy volunteers by the blood transfusion unit of the University Hospital of Tübingen, Tübingen, Germany. A list of whole blood samples is illustrated in **Supplementary Table 4.**

2.5.2. Isolation of HLA ligands from tissue

HLA class I and II molecules were isolated by immunoaffinity purification[223,224] employing pan-HLA class I-specific mAb W6/32 as well as pan-HLA class II-specific mAb Tü39 and HLA-DR-specific mAb L243. Sample preparation and immunoaffinity purification were performed at 4°C or on ice. In a first step, tissue was covered with 10 mM CHAPS/PBS (AppliChem, Darmstadt, Germany/Lonza, Basel, Switzerland) containing protease inhibitor (Complete; Roche, Basel, Switzerland) and sliced into small pieces. Subsequent homogenization (Homogenizer: Rotwerk, München, Germany, Potter glass: Novodirect, Kehl, Germany) and sonification (Branson, Danbury, CT, USA) fostered cell lysis. Cell lysate was centrifuged at 4000 rpm for 45 min, supernatant was filtered and coupled to serially connected columns with HLA class I or HLA class II mAb, respectively, covalently linked to CNBr-activated sepharose (GE Healthcare, Little Chalfont, UK; pumps: Rotarus smart 30, Hirschmann, Eberstadt, Germany). Immunoaffinity purification was carried out overnight. On the following day, columns were washed for 30 min with ddH_2O and 1 h with PBS. HLA molecules and HLA ligands were eluted into a low-binding sample tube (Eppendorf, Hamburg, Germany) following a 15 min incubation step with 100 µl 0.2% trifluoroacetic acid (Merck, Darmstadt, Germany) on a shaker. Elution procedure was repeated eight times. In the first elution round, 10 µl of 10% trifluoroacetic acid was additionally added. HLA ligands were separated from HLA molecules (and further large contaminants) by ultrafiltration using 3 kDa or 10 kDa centrifugal filter units (Amicon; Merck Millipore) for HLA class I or HLA class II, respectively. Filters were subsequently washed by 500 µl 32.5% acetonitrile (Merck)/0.1% trifluoroacetic acid (AB_E) to recover hydrophobic peptides. The following steps were performed at room temperature (RT). Filtrates were concentrated by vacuum centrifugation (Bachofer, Reutligen, Germany) to a volume of about 50 µl. HLA ligands were

extracted and desalted using ZipTip C_{18} pipette tips (Merck Millipore) and eluted in 35 µl AB_E. Samples were vacuum-centrifuged to a volume of less than 5 µl and 1% acetonitrile/0.05% trifluoroacetic acid was added to a volume of 25 or 40 µl. Samples were stored at -80°C until LC-MS/MS analysis.

2.5.3. Analysis of HLA ligands by LC-MS/MS

Peptides were analyzed by reversed phase liquid chromatography (UltiMate 3000 RSLCnano, Dionex, Sunnyvale, CA, USA) coupled mass spectrometry (LTQ Orbitrap XL or Orbitrap Fusion Lumos, Thermo Fisher Scientific, Waltham, MA, USA). Overall, five technical replicates per sample with 5 µl each were measured. In a first step, sample was loaded onto a 75 µm x 2 cm C_{18} trap column (Acclaim PepMap RSLC, Thermo Fisher Scientific) for further purification and desalting at 4 µl/min for 5.75 min. Subsequent peptide separation took place at 50°C on a 50 µm x 25 cm separation column (Acclaim PepMap RSLC, Thermo Fisher Scientific) applying a gradient from 2.4 to 32.0% acetonitrile over a time course of 90 min. Eluting peptides were ionized by nanospray ionization and accelerated into the mass spectrometer. For samples measured in the LTQ Orbitrap XL, survey scans were recorded in the orbitrap with a resolution of 60,000. The top 5 peaks with the highest intensity were selected for fragmentation if they fulfill the following criteria: within a mass range of 400-650 m/z and a charge state of 2+ or 3+ for HLA class I or within a mass range of 300-1500 m/z and a charge state higher 2+ for HLA class II. Precursor ions were isolated in the ion trap and fragmented by collision induced dissociation. Fragment ions were recorded in the ion trap.

For samples measured in the Orbitrap Fusion Lumos [**Supplementary Table 2, Supplementary Table** 3] instrumentation-adapted changes were applied. The *TopSpeed* method was implemented and survey scans were generated in the Orbitrap at a resolution of 120,000. Precursor ions were isolated in the quadrupole, fragmented by collision induced dissociation (HLA class I) or higher-energy collisional dissociation (HLA class II) and fragment ions were recorded in the Orbitrap. For HLA class II the charge state of precursor selection was limited to 5+.

2.5.4. Spectral Annotation and data analysis

Data was processed against the human proteome as comprised in the Swiss-Prot database (www.uniprot.org, release: September 27th 2013; 20,279 reviewed protein sequences contained). The Mascot algorithm (Mascot 2.2.04, Matrix Science, London, UK)[225] was utilized for LTQ Orbitrap XL measured samples and the SequestHT algorithm[226] for Orbitrap Fusion Lumos measured samples within the Proteome Discoverer (v1.3, Thermo Fisher Scientific) software. Mass tolerance filters were set to 5 ppm for precursor ions and 0.5 Da (LTQ Orbitrap XL) or 0.02 Da (Orbitrap Fusion Lumos) for fragment ions. Search was not restricted to an enzymatic specificity. Oxidized methionine was

enabled as a dynamic modification. Percolator[227] assisted false discovery rate (FDR) calculation was set at a target value of q ≤ 0.05 (5% FDR). Results were restricted to rank 1 (best matches for each spectra) and a length of 8-12 aa for HLA class I or 9-25 aa for HLA class II, respectively. Replicates were processed independently to obtain consistent results for qualitative and quantitative analysis.

2.5.5. Peptide synthesis

Peptides used for immunogenicity tests were synthesized using the peptide synthesizers 433A (Applied Biosystems, Foster City, CA, USA) or LibertyBlue (CEM corporation, Matthews, NC, USA) applying the 9-fluorenylmethyloxycarbonyl/tert-butyl (Fmoc/tBu) strategy described in [228]. Purity and identity of synthesized peptides were determined by HPLC or MS, respectively.

2.5.6. Refolding and biotinylation of HLA-peptide complexes

HLA-peptide complexes were generated by incubation of HLA heavy chain, β_2m and the respective peptide under continuous and gentle stirring in 250 ml refolding buffer (pH 7.76) containing 6.97% L-arginine (Sigma-Aldrich, St. Louis, MO, USA)/2.4% HEPES (Roth, Karlsruhe, Germany)/0.4% 0.5 M EDTA, pH 8 (Sigma-Aldrich) in ddH_2O. Refolding was carried out for HLA-B*40 (HLA-B*40:02 heavy chain used). For the other HLA allotypes refolding was performed with an UV-sensitive peptide which was subsequently replaced by UV (see section **2.5.7**). All steps were performed at 4°C or on ice if not mentioned otherwise.

On day 1, following components were injected subsequently into the refolding buffer under continuous and fast stirring: 385 mg reduced gluthatione (Sigma-Aldrich), 77.5 mg oxidized gluthatione (Sigma-Aldrich), 250 µl 200 mM phenylmethylsulfonyl fluoride (PMSF; Sigma-Aldrich) in methanol (Merck), 7 mg peptide resolved in DMSO (Merck) to a concentration of 10 mg/ml, 8 mg HLA heavy chain resuspended in 700 µl 3 M guanidine HCl (Sigma-Aldrich)/10 mM sodium acetate (Sigma-Aldrich)/10 mM EDTA in ddH_2O, pH 4.2 (injection buffer) and 7 mg β_2m in 780 µl injection buffer. Reaction was performed overnight under gently stirring of the solution. On the next day, 8 mg HLA heavy chain resolved in 700 µl injection buffer was added under fast stirring once in the morning and once in the evening. On day 3, reaction was filtered through a 0.22 µm Stericup Express vacuum filter (Merck-Millipore) and concentrated to a volume of 20-25 ml in an Amicon stirring cell with a PBTK membrane, NMWL 30,000 (Merck-Millipore) at 60 psi. Retentate was collected in a 50 ml collection tube, while permeate was applied to a second round of refolding. Steps of day 1 to 3 were repeated with the following exception: only 250 µl 200 mM PMSF, 8 mg HLA heavy chain resuspended in 700 µl injection buffer and 7 mg β_2m in 780 µl injection buffer were injected into the permeate. Retentates were centrifuged for 5 min at 4000 rpm and concentrated to a volume of 5 ml using 10 kDa centrifugal filter units (Amicon Ultra-15; Merck-Millipore). On the following day (d6), a

size exclusion chromatography on a Superdex 75 column was conducted after centrifugation and filtration of the retentate. Tris-buffered saline (TBS; 20 mM Tris (Sigma-Aldrich) pH 8 at 4°C and 150 mM NaCl (Merck) in ddH_2O) was used as running buffer. Monomer fractions were collected and mixed with 200 µM PMSF, 1 µg/ml Leupeptin (Roche) and 0.7 µg/ml Pepstatin (Roche). Fractions were concentrated to a volume of 5 ml using 10 kDa centrifugal filter units. Biotinylation was carried out overnight at 27°C by subsequent addition of following components to the retentate: 80 mM Tris, pH 8 at 25°C, 5 mM $MgCl_2$ (Merck), 5 mM ATP (Sigma-Aldrich), 10-20 µg BirA ligase (in-house production) and 5.7 mM biotin (Sigma-Aldrich). Following biotinylation, a size exclusion chromatography was performed. Monomer fractions were collected, concentrated to 250-350 µl and protein concentration was determined by a Bradford assay. Aliquots of 50 µg monomer with a concentration of 2 mg/ml were frozen at -80°C until use. Successful refolding was additionally confirmed by MS.

2.5.7. UV-mediated peptide exchange in monomers

Monomers with UV-sensitive peptide and replacing peptide were exposed to UV for exchange. Therefore, 65 µl of monomer, diluted to 200 µg/ml in 2 mM EDTA in PBS, and 65 µl peptide, diluted to 400 µM in PBS-EDTA, were mixed in a 96-well polypropylene plate with V-bottom (Ref. 651201; Greiner Bio-One, Kremsmünster, Austria) and exposed to 366 nm UV light for 1 h. Plate was centrifuged at 4000 rpm for 5 min at RT and 100 µl of supernatant was collected in a 1.5 ml collection tube. For each monomer six wells were exchanged which was enough to perform the following experiments twice. A final concentration of 50 µg/ml was assumed (50% exchange rate). Aliquots of 115 µl for priming, 135 µl for tetramer staining and a leftover aliquot were frozen at -80°C.

2.5.8. Quality control of UV-exchanged monomers

Proper UV-exchange was proven employing pan-HLA class I mAb W6/32 and antibodies recognizing non-linear epitopes (HCA2, HC10) exposed by denaturated HLA molecules as described in[229]. The mAb GAP-A3 was used as control. All steps were conducted at 4°C or on ice. Streptavidin-coated microspheres (bead concentration 100,000/µl; Bangs Laboratories, Indiana, IN, USA) were washed twice in PBS (2500 rpm, 5 min) and resuspended in 100 µl FACS buffer (2 mM EDTA/2% FBS (Thermo Fisher Scientific, Gibco) in PBS) per 100,000 beads. 100 µl bead and 100 µl monomer solution, prior diluted in PBS to 0.1 µg/ml, were mixed in a 96 U-bottom well plate (Corning, New York, NY, USA) and incubated for 30 min. For each monomer four wells were used. Plate was washed twice with FACS buffer and wells were incubated with 50 µl of either 1 µg/ml W6/32, 0.5 µg/ml HCA2, 0.6 µg/ml HC10 or 1 µg/ml GAP-A3 for 30 min (all antibodies are in-house produced). After two washing steps, wells were incubated with 50 µl of 1:100 polyclonal goat anti-mouse FITC-labelled secondary Ab

(Agilent Technologies, Santa Clara, CA, USA, Dako) for 30 min. Following two washing steps, monomers were analyzed by flow cytometry (FACS Canto II analyzer; BD Biosciences, San Jose, CA, USA). Data analysis was conducted by FlowJo 10.0.7. (FlowJo, LLC, Ashland, OR, USA).

2.5.9. Tetramerization of monomers

Tetramerization of refolded monomers was performed by the addition of 6.28 µl strepavidin-phycoerythrin (Strep-PE, Thermo Fisher Scientific) in 20 µl 2 mg/ml monomer solution and subsequent rotation for 30 min in the dark. Step was repeated ten times. Tetramers were mixed with 3x glycerol solution (20 mM Tris, pH 8 at 4°C/48% glycerol (Roth)/1.5% human serum albumin (Biotest, Dreieich, Germany) and 3x protease inhibitor (Roche)) in a ratio of 1:3. For UV-exchanged monomers tetramerization was carried out by ten time addition of 1.06 µl Strep-PE in 135 µl 50 µg/ml monomer solution. Tetramers were mixed with 6x glycerol solution in a ratio of 1:6.

2.5.10. Isolation of PBMCs

PBMCs were isolated from whole blood of healthy donors using Ficoll (Merck-Millipore) separation solution. Blood was transferred into 50 ml collection tubes and centrifuged at 2000 rpm for 20 min at RT without break. The upper plasma layer was transferred into new 50 ml collection tubes. PBMC layer was generously collected and transferred into a 175 cm^2 cell culture flask (Greiner Bio-One), diluted 1:1 with PBS-EDTA (2mM) and carefully layered onto 15 ml Ficoll solution. After centrifugation at 2000 rpm for 20 min at RT without break, upper plasma layer was discarded and the middle PBMC layer was generously collected into new 50 ml collection tubes. PBMCs were diluted 1:1 with PBS-EDTA and centrifuged at 1500 rpm for 20 min at RT. Cells were washed twice with PBS-EDTA (10 min centrifugation steps at 1300 and 1100 rpm, respectively), resuspended in TCM (IMDM (Lonza) + 1x penicillin/streptomycin (Sigma-Aldrich) + 50 µM β-mercaptoethanol (Roth) + 25 µg/ml gentamycin (Thermo Fisher Scientific) + 10% autologous plasma), transferred into two 175 cm^2 cell culture flasks and incubated overnight at 37°C, 7.5% CO_2. $2x10^7$ PBMCs were frozen for recall ELISpot (see section **2.5.15**). Plasma was heat-inactivated at 56°C for 30 min and centrifuged at 2500 rpm for 20 min at RT. Supernatant was transferred into a new 50 ml collection tube. After another centrifugation step, supernatant was used for TCM preparation or frozen at -20°C.

2.5.11. Isolation of $CD8^+$ T cells

$CD8^+$ T cells were isolated from overnight culture of PBMCs by magnetic cell separation (MACS) using α-CD8 beads (Miltenyi Biotech, Bergisch Gladbach, Germany). PBMCs were transferred into 50 ml collection tubes and centrifuged at 1300 rpm for 10 min at RT. Cell pellet was resuspended in MACS buffer (0.5% BSA (Sigma-Aldrich)/2 mM EDTA in PBS), centrifuged at 1300 rpm for 10 min at 4°C, resuspended in 15 µl α-CD8 beads/$1*10^7$ cells and 50 µl MACS buffer/$1*10^7$ cells and incubated for 15 min at 4°C. Following incubation, cells were centrifuged, filtered and $CD8^+$ T cells were separated according to the manufacturer's instructions using LS columns (Miltenyi Biotech). Cells were washed once with MACS buffer and cultured in $75cm^2$ flasks with 15 ml TCM + 10 U/ml IL-2 (R&D systems, Minneapolis, MN, USA) and 2.5 ng/ml IL-7 (Promokine, Heidelberg, Germany) overnight at 37°C and 7.5% CO_2.

2.5.12. Priming of $CD8^+$ T cells

$CD8^+$ T cells were harvest, washed twice with PBS (1300 rpm, 10 min, RT) and resuspended in TCM at a concentration of $1*10^6$/100 µl. $1*10^6$ cells were distributed into wells of 96-well plates, U-bottom (Costar; Corning) and incubated at 37°C and 7.5% CO_2 (hereafter referred to as T-cell plates). Meanwhile, beads were prepared. 800,000 beads/well (bead stock: 100,000 beads/well) were washed twice with 20 ml MACS buffer (2500 rpm, 10 min 4°C) and resuspended to $8*10^6$ beads/ml. 96-well plates were prepared with 100 µl bead solution as well as 50 µl monomer solution, prior diluted to 4 µg/ml with MACS buffer, and incubated for 30 min at RT while shaking. In total, 20 wells were prepared for one monomer. 50 µl of biotinylated CD28 (in-house production) was added into the wells at a concentration of 12 µg/ml and plates were incubated for additional 30 min. Plates were washed five times with MACS buffer (2500 rpm, 2 min, 4°C) and beads were diluted in 200 µl MACS buffer/well (hereafter referred to as bead plates). Plates were stored at 4°C until use.

$CD8^+$ T cells were primed weekly for four times with streptavidin-coated microspheres coupled to biotinylated monomers and CD28. Therefore, 50 µl of bead stock was transferred from the bead plates into new 96-well plates and washed twice with TCM without plasma. Wells were resuspended in 100 µl TCM + 5 ng/ml IL-12 (Promokine) and beads were transferred to the T-cell plates. For stimulation rounds 2-4 100 µl medium was prior removed from the T-cell plate before adding the bead solution. Medium was changed when necessary. Two or three days after primings, 100 µl medium was removed and $CD8^+$ T cells were fed with 100 µl TCM + 40 U/ml IL-2 and 5 ng/ml IL-7 (final concentration in culture).

2.5.13. Tetramer staining

Recognition of pHLA complexes by *in vitro* primed $CD8^+$ T cells was ascertained by tetramer staining. All steps were performed at 4°C or on ice if not otherwise mentioned. Staining steps were performed for 20 min in the dark if not otherwise mentioned. Between staining steps, cells were washed with 150 µl PBS-EDTA or FACS buffer (after tetramer staining), respectively, by centrifugation at 1800 rpm for 2 min and removing the supernatant by flicking.

One third of cultured $CD8^+$ T cells were transferred into new 96-well plates and washed four times. Cells were stained with 50 µl Aqua live/dead solution (Thermo Fisher Scientific/Invitrogen) prior diluted 1:400 (if stored solution reconstituted within last 2 weeks) or 1:200 (if reconstituted 2-4 weeks before use) in PBS-EDTA. Subsequently, primed cells were stained with 50 µl of the corresponding tetramer solution (PE-labelled) which were prior diluted to 5 µg/ml in 50:50 PBS:FBS and 2 mM EDTA for 30 min at RT. After tetramer staining, cells were stained with 50 µl 1:100 diluted α-CD8-PerCP Ab (BioLegend, San Diego, CA, USA). Finally, fixation of the cells was performed with 100 µl FACS buffer/ 1% formaldehyde (Sigma-Aldrich). Cells were washed twice and resuspended in 200 µl FACS buffer. Samples were analyzed on a FACS Canto II analyzer. Data analysis was performed by FlowJo 10.0.7. Conditions for positive priming were a three-fold larger and distinct tetramer-positive population compared to the negative control.

For cells which were primed with UV-exchanged pHLA complexes, positive wells were additionally stained with the corresponding tetramer containing the UV-sensible peptide.

2.5.14. Intracellular IFN-γ and TNF-α staining of primed $CD8^+$ T cells

Functionality of *in vitro* primed $CD8^+$ T cells was determined by intracellular cytokine staining (ICS) of IFN-γ and TNF-α. One third of cultured cells of different tetramer positive wells were combined, centrifuged at 1800 rpm for 2 min at 4°C and split into three to five wells of a new 96-well plate (1x positive control, 1-2x peptide of interest, 1-2x negative control) with a volume of 50 µl each. 50 µl 150 ng/ml phorbol 12-myristate 13-acetate (PMA) + 3 µM ionomycin (Positive control; Company) or 10 µg/ml peptide diluted in TCM were added to the cells as well as 50 µl 10 µg/ml Brefeldin A (Sigma-Aldrich) + 10 µg/ml Golgi-Stop solution (BD Bioscience). Cells were cultured for 12-16 h at 37°C, 7.5% CO_2. On the following day, cells were washed and stained with Aqua Live/dead and α-CD8 Ab as described in **2.5.13**. Thereafter, cell membranes were permeabilized by incubation with 100 µl Cytoperm/Cytofix (BD Bioscience) for 20 min at 4°C in the dark and washed with Permwash buffer (0.1% saponine (AppliChem, St Louis, MO, USA)/0.5% BSA (Roth) in PBS). After permeabilization, intracellular IFN-γ and TNF-α were stained with 1:200 IFN-γ-PE (BD Bioscience) and 1:120 TNF-α-PacificBlue (BD Bioscience) diluted in Permwash buffer. Following two washing steps with Permwash

buffer, cells were diluted in 200 µl FACS buffer. Samples were analyzed on a FACS Canto II analyzer. Data analysis was performed by FlowJo 10.0.7. Conditions for positive ICS were a three-fold increase in IFN-γ and TNF-α staining compared to the negative control.

2.5.15. Recall IFN-γ ELISpot

To exclude memory responses of the positive tested peptides in priming experiments, ELISpot assay was conducted after 12-day stimulation of PBMCs from respective healthy donors. $2*10^7$ cells were thawed and washed twice with 10 ml IMDM + 1x penicillin/streptomycin + 50 µM β-mercaptoethanol + 25 µg/ml gentamycin + 3 µg/ml DNase (1400 rpm, 7 min). Subsequently, pellet was resuspended in 2 ml of TCM (5% pooled serum, instead of 10% used in TCM for priming experiments), distributed into four wells of a 24-well plate and incubated over night at 37°C, 7.5% CO_2. The following day, cells were stimulated with a 500 µl peptide mix containing 1 µg/ml of each peptide tested in the respective donor. On day 3, 6 and 8 cells were stimulated with a final concentration of 20 U/ml IL-2 prior diluted in 500 µl TCM. On day 10, medium was exchanged and ELISpot plate was coated with 100 µl of 2 µg/ml human 1-D1K IFN-γ Ab (MabTech, Stockholm, Sweden; 1:250 dilution with PBS) and incubated bubble-free at 4°C. On day 13, plate was washed twice with cold IMDM and incubated with 50 µl TCM for 2 h at 37°C to block unspecific binding sites. In the meantime cells were collected, washed twice with TCM and resuspended to $1*10^7$ cells/ml. 500,000 cells were distributed into the wells of the pre-coated plate and 50 µl of peptide diluted in TCM with a final concentration of 1 µg/ml was added. As positive control phytohaemagglutinin (PHA; Sigma-Aldrich) in a final concentration of 10 µg/ml was added to one additional well. Plate was incubated for 24 h at 37°C, 7.5% CO_2. On the following day, plate was washed twice with 200 µl PBS/0.05% Tween 20 (Merck), twice with 200 µl ddH_2O and again three times with 200 µl PBS/0.05% Tween 20 and subsequently incubated with 100 µl biotinylated secondary anti-IFN-γ Ab 7-B6-1 (1:3000 dilution in PBS/0.5% BSA; MabTech) bubble-free for 2 h at RT. Following six washing steps with 200 µl PBS/0.05% Tween 20, plate was incubated with 100 µl of avidin-conjugated alkaline phosphatase (1:1000 dilution in PBS/0.5% BSA; Sigma-Aldrich) for 1 h at RT. Finally, plate was washed three times with PBS/0.05% Tween 20 and three times with PBS and incubated with 50 µl of BCIP/NBT solution (one tablet dissolved in 10 ml ddH_2O; Sigma-Aldrich) for 7 min in the dark. Reaction was stopped washing the plate with water and plate was completely dried for one day and evaluated using the C.T.L ImmunoSPOT reader (Cellular Technology Inc., Kennesaw, GA, USA). Conditions for a positive response were a spot count of at least 10 and a three-fold higher spot count compared to the negative control.

2.6. Results

2.6.1. MS-based disclosure of the HLA ligandome

HLA class I ligandome analysis was performed for 58 ccRCC samples and corresponding adjacent benign tissue using mass spectrometry-based analysis of peptides after immunoprecipitation of HLA molecules. In total, 41,448 HLA ligands could be identified deriving from 11,521 antigens. HLA ligands were defined employing NetMHCpan-3.4 (Rank < 2 or 500 nM) and SYFPEITHI (≥ 60% of maximal score) [**Supplementary Table 1**]**.** The mean number of HLA ligands was 1573, ranging from 121 to 4934, for the tumor samples and 947, ranging from 42 to 2843, for the adjacent benign samples [**Figure 12, Supplementary Table 2**]. Sample purity, defined by the frequency of HLA ligands compared to the total number of identified peptides, was on average 90.1% for tumors and 86.7% for benign samples with a range of 77.9% to 96.7% and 60.3% to 95.0%, respectively. Overall, a broad range of HLA alleles could be covered gaining a comprehensive analysis of the immunopeptidome.

Investigation of the HLA class II ligandome was performed for 52 ccRCC samples and corresponding adjacent benign tissue with a total number of 32,158 peptides identified deriving from 6099 antigens. The mean number of peptides was 965 (range 240 to 5103) for the tumor samples and 860 (range 131 to 5414) for the adjacent benign samples [**Figure 13, Supplementary Table 3**]. Samples analyzed on the Orbitrap Fusion Lumos exhibited 5.22 times more peptides compared to LTQ Orbitrap XL analyzed samples (means: 3388 vs 649).

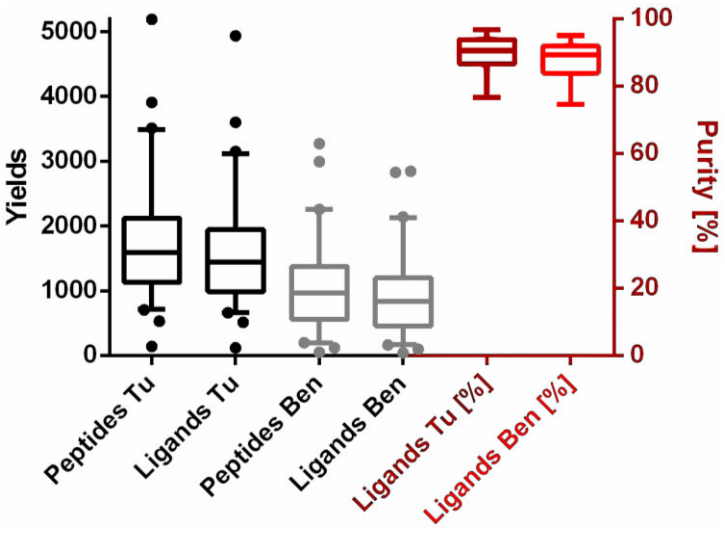

Figure 12: HLA class I peptide yields, ligand yields and sample purity. Yields are assigned to the left y-axis (black). Sample purity, which is defined by the frequency of ligands compared to the total number of identified peptides, is assigned to the right y-axis (red). Box & whiskers plot with 5-95% whiskers are displayed.

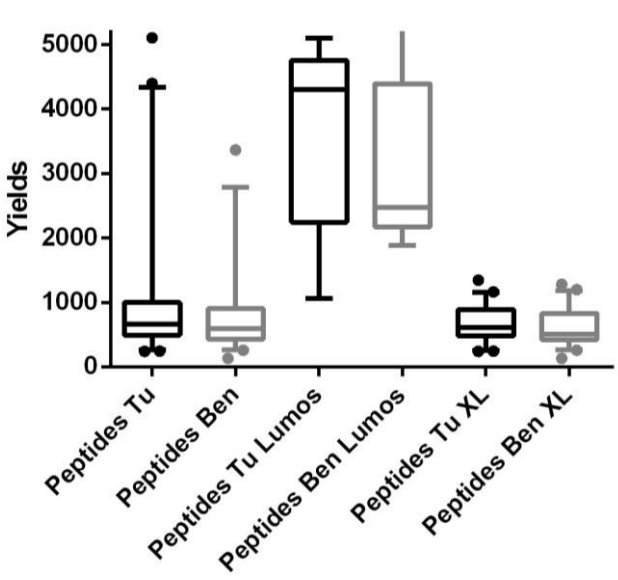

Figure 13: HLA class II peptide yields. Yields are plotted for all 52 samples (left), for the five samples analyzed on the Orbitrap Fusion Lumos (middle) and for the 47 samples analyzed on the LTQ Orbitrap XL (right). Box & whiskers plot with 5-95% whiskers are displayed.

2.6.2. Identification of HLA class I tumor-associated peptides using comparative profiling

Comparative profiling of HLA ligands of ccRCC and adjacent benign tissue was employed to identify tumor-exclusive peptides. Peptides unique to the tumor were defined as tumor-associated peptides (TUMAPs). A large in-house database containing 95,177 HLA ligands of 158 benign tissues from different organs (including blood, kidney, liver, lung, small intestine, heart, brain, and many more) was additionally included for HLA class I ligand comparison to ensure tumor-exclusivity of TUMAPs not only compared to the adjacent benign kidney, but also in relation to many other organs.

In total, 1591 TUMAPs could be identified which were presented in at least two ccRCC samples [**Figure 14**]. Restricting the dataset to TUMAPs with a representation frequency of at least three and a unique source protein origin the number of TUMAPs decreased to 433 deriving from 351 antigens. This set of TUMAPs was further analyzed for their HLA restriction and the gene expression (data from the TCGA database with 453 ccRCC samples and 68 benign kidney samples; kindly provided by the Institute for Clinical Pharmacology in Stuttgart) of the corresponding antigen.

Considering a fold change gene expression of the antigen of > 2 in ccRCC compared to the benign kidney cohort, the set of 433 TUMAPs originating from 351 antigens was further reduced to 170 TUMAPs from 112 antigens. Overexpressed antigens with one (or more) TUMAP represented in at least three samples are illustrated in **Supplementary Table 5** (in the appendix) and **Figure 15**.

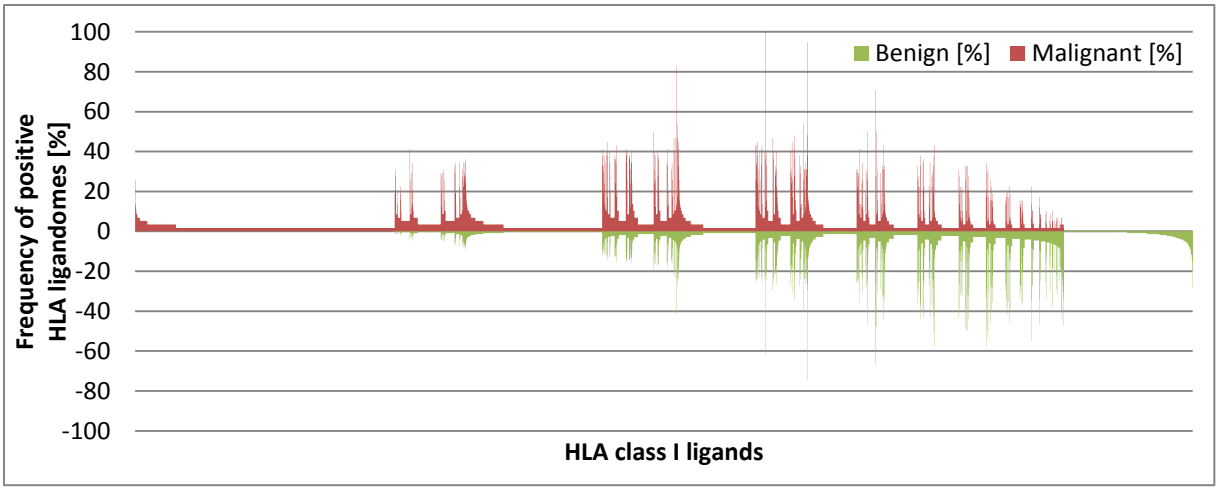

Figure 14: Comparative profiling of 58 ccRCC vs. corresponding adjacent benign tissues and 158 benign tissues. The frequency of HLA ligands in the tumor is illustrated in red (positive y-axis) and for the benign tissue in green (negative x-axis). Each bar represents one HLA class I ligand.

The antigen representing the highest diversity is PLIN2 (Perilipin-2) with 29 different HLA class I TUMAPs. PLIN2 is involved in the transport of long fatty acids and in the storage of lipids and is mainly expressed in fat tissue. It is upregulated upon VHL inactivation and is a main factor for the clear cell morphology (lipid droplets) of ccRCC.[230] The most frequently presented TUMAPs are GAVTGSVEK (5x, A*11), SINTVLGSR (5x, A*03), SVFRNAASF (4x, B*15) and TSSKGQLQK (4x, A*03).

However, several other antigens give rise to more frequently presented TUMAPs which would be more advantageous for so called off-the-shelf approaches.[163,231] The most frequent TUMAP is ILWREVVTL (15x, A*02) from the transcription factor HSF4 (heat shock factor protein 4). Interestingly, even the antigen is tumor-exclusive among the HLA ligandomes of ccRCC since no peptide was found in other benign tissues. Further examples of tumor-exclusive antigens are the NADH dehydrogenase subunit NDUFA4L2 (most frequent TUMAP: GSAALYLLR, 9x, A*11/A*68:01), the ion channel KCNN1 (RVFLISLEL, 8x, A*02), the metastasis suppressor KISS1R (RPAPADSAL, 6x, B*07/B*35), the growth factor PGF (YPSEVEHMF, 5x, B*35), and the angiogenesis modulator ANGPTL4 (two length variants: AQNSRIQQL[F], 7x, both B*15).

Other frequent TUMAPs are FLLSLIDRL (9x, A*02, EGLN3), HPIETLVDIF (9x, B*35, VEGFA), SEINTTHNL (9x, B*40/B*44, PRUNE2), ALIVSLPYL (8x, A*02, SLC17A3), GLVDIMVHL (8x, A*02, DNAH11) and SEAEALARTW (8x, B*44, DIRAS2). TUMAPs presented on more than two HLA allotypes are MPLGHIMRL (8x, B*07/B*35/B*51/B*53, EGLN3), AEKELVQSL (5x, B*40/B*41/B*44, P4HA2) or FPTEQINEI (5x, B*35/B*51/B*53, ADSSL1). These peptides are applicable for a larger population compared to peptides presented only on one of these HLA alloypes. An extended list of TUMAPs for the 112 target candidates is depicted in **Supplementary Table 5**.

Figure 15: Antigens with at least one frequent TUMAP (n ≥ 3) and > 2-fold higher expression in tumor compared to benign kidney within the TCGA cohort. The size of the letters is proportional to the frequency of the top TUMAP of the respective antigen. Range: The letters of the most frequent antigen HSF4 have a size of 15, whereas the letters from several antigens with a frequency of their top TUMAP of n = 3 have a size of 3.

2.6.3. Hypoxia-induced genes within the selected candidates

One characteristic of ccRCC is its hypoxic-like state which is the consequence of VHL mutations. The subsequent activation of hypoxia-induced antigens by HIFs renders these targets a promising approach for ccRCC treatment. Ortiz-Barahona *et al.*[182] used a computational strategy to specify the binding site of HIFs. Besides the core sequence („RCGTG", R = G or A [purine]) of HRE, several other nucleotides within position -1 to +17 displayed some particular variances. Overall, 216 genes could be identified to be probable targets of HIFs of which 61 were already known.

12 of the 112 overexpressed antigens with at least one frequent TUMAP are targets of HIFs. All of them were already known as HIF targets: CA9[232], EGLN3[233], IGFBP3[234], VEGFA[235], LOX[236], ADM[237], DDIT4[238], PFKP[239], P4HA2[240], BNIP3[241], PLOD1[240] and PLOD2[240]. The well characterized ccRCC tumor antigen CA9 is normally expressed in the stomach and is involved in the cellular pH regulation.[242] It is upregulated in many tumors. EGLN3 is a cellular oxygen sensor which hydroxylates substrates, such as the HIF proteins in a negative feedback, for proteasomal degradation.[243] IGFBP3 is an insulin growth factor (IGF) binding protein altering the interaction of IGF to their receptors. In pancreatic cancers IGFBP3 overexpression is correlated with the metastatic ability of the tumor.[244] The growth factor VEGFA promotes angiogenesis and cell migration.[245] LOX catalyzes the post-translational deamination of lysine residues and is correlated to the invasive potential of tumor cells.[246] ADM is involved in vasodilatation, whereas DDIT4 regulates cell survival and proliferation via the inhibition of mTORC1. PFKP is a key regulator of glycolysis. P4HA2 catalyzes the post-translational hydroxylation of proline residues, while BNIP3 is a cell death protein which may rather lead to necrosis instead of apoptosis.[247] PLOD1 and PLOD2 regulate the hydroxylation of lysine residues in procollagens.

2.6.4. Identification of HLA class I tumor-associated peptides from cancer-testis antigens

For the identification of TUMAPs from cancer-testis antigens (CTA) the CT database (www.cta.lncc.br/) was utilized. Moreover, the GTEx database (www.gtexportal.org/home/), containing RNA-Seq data of a plethora of tissues, was used to verify the cancer-testis specification.

Six TUMAPs derived from CTAs were presented on at least two ccRCC samples [**Table 5**]. The CTA PRAME (Melanoma antigen preferentially expressed in tumors) gives rise to the TUMAPs SLLQHLIGL[248] and GQHLHLETF. Additional peptides found in one ccRCC sample were MPMQDIKMIL, QLLALLPSL and SPSVSQLSVL. Other antigens with a TUMAP in at least two ccRCC samples were IGF2BP3, SYCP1, KDM5B and ODF2.

Table 5: TUMAPs derived from cancer-testis antigens. HLA restriction, number and frequency of positive samples are illustrated for each TUMAP.

TUMAP	Gene	HLA	Found on n allotype positive ccRCC samples	Allotype positive samples	% of respective allotype positive samples
SLLQHLIGL	PRAME	A*02	5	25	20
KIQEILTQV	IGF2BP3	A*02	3	25	12
AITTSEQYY	SYCP1	A*01	3	18	17
GQHLHLETF	PRAME	B*15	3	7	43
MPVMEQSVL	KDM5B	B*35	2	14	14
RDSLVERL	ODF2	B*37	2	2	100

2.6.5. Search for frequent tumor mutations

For the identification of mutated peptides arising from frequently mutated antigens the 600 most frequent mutations throughout all tumors contained in the COSMIC (Catalogue of somatic mutations in cancer) database were downloaded. The processing of the data including the 600 most frequent mutations exhibits no HLA ligand from frequently mutated antigens which is consistent with the low mutational burden of ccRCC.[172]

2.6.6. Biological involvement of target candidates

The biological involvements of the 112 antigens were analyzed for general tumor characteristics such as enhanced cell proliferation or angiogenesis, as well as for some ccRCC-specific characteristics such as hypoxic conditions and distorted lipid and glucose metabolism. For this purpose, the Uniprot database was screened with following keywords: “Response to hypoxia”, “Cell proliferation”, “Angiogenesis”, “Lipid” and “Glucose”, to identify those antigens within the 112 targets involved in the respective biological process.

Genes induced under hypoxic conditions (see section **2.6.3**) are highlighted in magenta [**Figure 16**]. Antigens involved in cell proliferation are transcription factors, such as HSF4, PRAME or CEBPA, histone-modifying proteins (SAP30), cell cycle regulators (CCND1) or growth factors (VEGFA, PGF) and their regulators (IGFBP3). Antigens involved in blood vessel formation are growth factors (VEGFA, PGF) and their receptors (MET) and other regulators, such as ANGPTL4 or extracellular matrix components (COL4A2, CSPG4) and modulators (LOXL2). The lipid metabolism involved antigens include transporters (SLC17A3, ABCA1), intracellular lipid transporting proteins (FABP7, PLIN2), lipid-modifying enzymes (CYP3A5, CYP2J2, LPCAT1), lipid storage proteins (PLIN2, HILPDA), homeostasis regulators (ANGPTL4, C3) or transcription factors (CEBPA). The glucose metabolism involved antigens include transporters (SLC17A3, C3), transport regulators (TRIB3), enzymes of the glucose metabolism (ALDOA, PFKP, ACLY, ACS) or transcription factors (CEBPA).

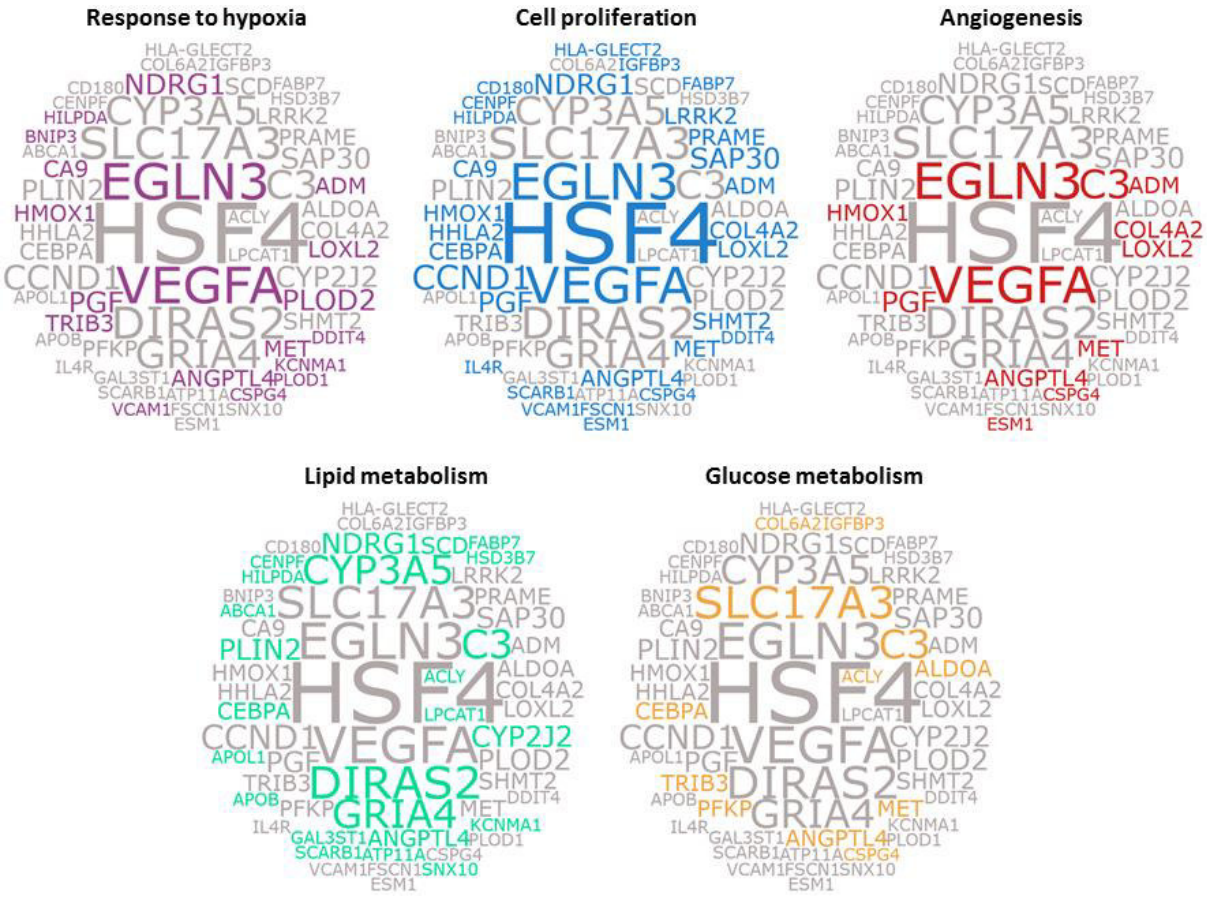

Figure 16: Biological involvement of target antigens. Antigens induced in response to hypoxia are highlighted in magenta; antigens important for cell proliferation are highlighted in blue; antigens relevant for angiogenesis are indicated in red; antigens involved in the lipid metabolism are marked in green and antigens involved in the glucose metabolism are indicated in orange.

2.6.7. Identification of HLA class I tumor-associated peptides using quantitative analysis

Quantitative analysis was exerted to identify HLA ligands which are overrepresented in ccRCC. For that purpose, 46 ccRCC samples were compared to each other [**Supplementary Table 2**]. Areas of peptides were picked from unfiltered peptide lists (without FDR and rank filter to include peptides which might miss the 5% FDR cut-off in a replicate but have been identified with statistical significance in another replicate of the same sample). Criterion for the inclusion of a peptide is its representation in at least two replicates. In replicates were the peptide is not detected the detection limit (area of the lowest detectable peptide) was applied. Only peptides which were predicted to be HLA ligands were included.

In total, 27,768 of 41,488 HLA class I ligands (66.9%) could be integrated into the analysis. The log_2 fold change presentation was calculated for each peptide. 6,145 HLA class I ligands (22.1%) were overrepresented in ccRCC with a log_2 fold change expression ≥ 2 (4-fold overrepresentation) [**Figure 17**]. Constraining the dataset to peptides emerging from unique antigens and a presentation frequency of n ≥ 3, 952 HLA class I ligands from 677 antigens remained [**Supplementary Table 6**].

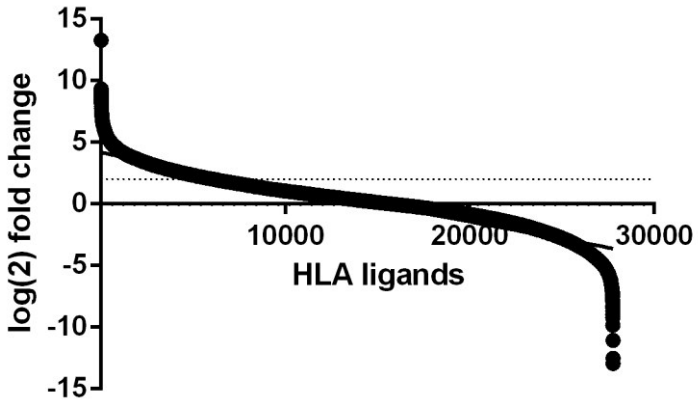

Figure 17: Quantitative analysis of 46 adjusted ccRCC and adjacent benign tissues. Log_2 fold change presentation of 27,768 HLA class I ligands is plotted.

Overlap analysis of the 677 antigens with overrepresented HLA class I ligands with the 112 antigens from comparative and expression-based analysis reveals 59 overlapping antigens [**Figure 18**, left] and 58 overlapping HLA class I ligands [**Figure 18**, right]. An overview of overlapping antigens is illustrated in **Table 6**.

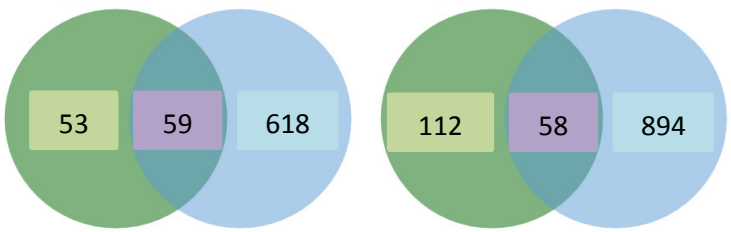

Figure 18: Overlap of the HLA class I ligand source antigens (left) and HLA class I ligands (right) from comparative and quantitative analysis. Green: comparative profiling, blue: quantitative analysis.

Table 6: Overlap of HLA class I ligands from comparative and quantitative analysis.

Sequence	UniprotID	Gene	HLA	Sequence	UniprotID	Gene	HLA
ILWREVVTL	Q9ULV5	HSF4	A*02	AESQILKHLL	P40261	NNMT	B*40/B*44
GSAALYLLR	Q9NRX3	NDUFA4L2	A*11/A*68	SPRAAEPVQL	Q16790	CA9	B*07
HPIETLVDIF	P15692	VEGFA	B*35	DEGKLSITL	Q8WUY3	PRUNE2	B*18
SEINTTHNL	Q8WUY3	PRUNE2	B*40/B*44	DEINLHQL	Q8WUY3	PRUNE2	B*18
ALIVSLPYL	O00476	SLC17A3	A*02	DPIDEISVIEY	Q86TB3	ALPK2	B*35
MPLGHIMRL	Q9H6Z9	EGLN3	B*07/B*35/B*51/B*53	FPWEKPTTL	Q86TB3	ALPK2	B*35
SEAEALARTW	Q96HU8	DIRAS2	B*44	GVIIAKKYFFK	Q96D42	HAVCR1	A*11
EIKIKLGI	O15539	RGS5	B*08	KIAQKALDL	P09601	HMOX1	G*01
IAYPRAVTL	P48029	SLC6A8	C*03/C*12	KIIAPLVTR	O00469	PLOD2	A*11
SVSPVKATQK	Q86XJ1	GAS2L3	A*03/A*11	KLLDATHVY	O15427	SLC16A3	A*03/A*02/B*15
VEKVVLVSL	P01024	C3	B*40/B*41	MPVDERDLQA	P55042	RRAD	B*35
AELPIFPQL	P78415	IRX3	B*40/B*41	RTVPPAVTGITF	P04075	ALDOA	B*57/B*58
FPIDKPPSF	P51805	PLXNA3	B*35/B*53	SEEEASINL	P04075	ALDOA	B*40
IAFSATRTI	P02746	C1QB	B*51	SLLHLGALY	O00767	SCD	A*29
RPAPADSAL	Q969F8	KISS1R	B*07/B*35	SPSPGKDPTL	Q9ULV5	HSF4	B*35
TPHDFIEHF	P24385	CCND1	B*35/B*53	TESETRILL	P01024	C3	B*40/B*44
AEKELVQSL	O15460	P4HA2	B*40/B*41/B*44	TSSKGQLQK	Q99541	PLIN2	A*03
LLAASVALA	P47972	NPTX2	A*02	DQYKFLAV	Q9NRX3	NDUFA4L2	B*08
REVTVDTTL	P51589	CYP2J2	B*40	AEVGDTIRVTF	P00450	CP	B*44
ALFEGVVRQI	P55042	RRAD	A*02	DEISIAQSL	A6NI28	ARHGAP42	B*18
FPTEQINEI	Q8N142	ADSSL1	B*35/B*51/B*53	GASLGARFY	Q9NRX3	NDUFA4L2	C*16
GAVTGSVEK	Q99541	PLIN2	A*11	GIASSSIAAK	P40305	IFI27	A*03/A*11
HALMEKDSL	O15539	RGS5	C*03/C*12	IQDAQDKLYL	Q99541	PLIN2	B*38
ILLQKPDSV	O15539	RGS5	A*02	SELLVEQY	Q99541	PLIN2	B*18
IPVNEKDTL	O75446	SAP30	B*35	SHVAPTETF	P00450	CP	B*38
KLLQNNYGL	O15539	RGS5	A*02	THEEVINLI	Q9Y6N9	USH1C	B*38
SINTVLGSR	Q99541	PLIN2	A*03	VPPVFVSVY	Q12791	KCNMA1	B*35
TTLRWALLY	P51589	CYP2J2	A*29/A*26	VPPVFVVSY	O15427	SLC16A3	B*35
YPSEVEHMF	P49763	PGF	B*35	WPDWALPRL	Q9UJY1	HSPB8	B*07/B*35
WPDWALPRL	Q9UJY1	HSPB8	B*07/B*35				

2.6.8. Identification of HLA class II tumor-associated peptides using comparative profiling

Comparative profiling of HLA class II presented peptides from 52 ccRCC and corresponding adjacent benign tissue was employed to identify tumor-exclusive peptides (see section **2.6.1**). Due to lack of an appropriate tool, HLA binding prediction was not exerted. A large in-house database of 123 benign tissues containing 94,896 HLA class II presented peptides was included to ascertain tumor-exclusivity of TUMAPs [**Figure 19**].

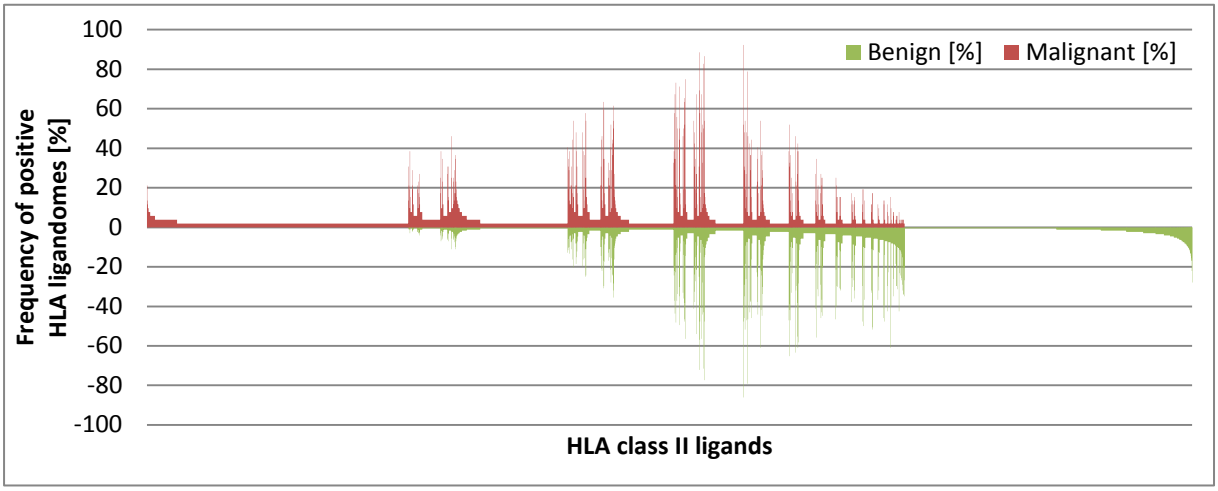

Figure 19: Comparative profiling of 52 ccRCC vs. corresponding adjacent benign tissues and 123 benign tissues. The frequency of HLA ligands in the tumor is illustrated in red (positive y-axis) and for the benign tissue in green (negative x-axis). Each bar represents one HLA class II ligand.

Overall, 917 TUMAPs could be identified which were presented in at least two ccRCC samples. Constraining the dataset to peptides originating from unique antigens and a representation frequency of n ≥ 3, 213 peptides from 135 antigens remained [**Supplementary Table 7**]. However, due to the limited HLA restriction of peptides as well as the limitations in predicting the HLA restriction of a peptide a high representation frequency is essential to increase the population coverage. With a representation frequency of n ≥ 5 (about 10% of all ccRCC) 30 peptides from 25 antigens remained [**Figure 20**].

Figure 20: Antigens with at least one frequent TUMAP (n ≥ 5). The size of the letters is proportional to the frequency of the top TUMAP of the respective antigen. Range: The letters of the most frequent antigen PXDN have a size of 11, whereas the letters from several antigens with a frequency of their top TUMAP of n = 5 have a size of 5.

Overlap analysis of the top 25 HLA class II antigens with HLA class I antigens revealed four antigens, NDUFA4L2, ENPP3, IGFBP3 and VCAM1, which present peptides on both HLA class I and HLA class II molecules [**Figure 21**]. Extending the HLA class II antigen list to the top 135 (antigens with TUMAPs with a representation frequency of n ≥ 3), 7 additional antigens were overlapping: NPTX2, C3, DNAH11, PLIN2, FGG, COL6A2 and COL4A2.

Figure 21: Overlap of HLA class I and HLA class II pathways. Green: HLA class I antigens, blue: HLA class II antigens. Four antigens provide ligands to both the class I and class II pathways.

2.6.9. Immunogenicity screening of selected HLA class I ligands

The immunological recognition of peptides was addressed by priming of $CD8^+$ T cells of healthy donors with pHLA complexes and costimulatory CD28 prior coated onto microspheres.[249,250] Outcome of $CD8^+$ T cell priming was read out by tetramer staining. HLA class I ligands in immunogenicity screens covered the HLA allotypes HLA-A*02, HLA-B*07, HLA-B*08, HLA-B*15, HLA-B*40 and HLA-B*44. Except for HLA-B*40 (refolding), all monomers were generated by UV exchange.

The success of UV-mediated peptide exchange was assessed by staining of monomers coated onto microspheres with the mAbs W6/32, HC10, HCA2 and GAP-A3 (control). Misfolded pHLA complexes can be detected by the mAbs HC10 and HCA2 which bind to linear structures usually not accessible in properly folded monomers. No staining with HCA2 and HC10 could be detected for all UV-exchanged monomers, but for monomers with UV-labile peptide exposed to UV without exchanging peptide [**Supplementary Figure 1**]. Some staining with HCA2 and HC10 was detected for the HLA-B*08/DQYKFLAV monomer. HLA-B*44 staining with HCA2 was detectable for some monomers. However, no staining with HC10 was detectable. Except for HLA-A*02, the mAb HC10 achieved higher fluorescence staining compared to HCA2 in the UV-sensitive monomer exposed to UV light. Still, HC10 staining of HLA-A*02 was substantial. Therefore, HC10 seems to be more appropriate for the quality control of UV-exchanged monomers.

An overview of tested HLA class I ligands, their HLA restriction and the identification strategy is illustrated in **Table 7**.

Overall, 26 HLA class I ligands were screened for their recognition by $CD8^+$ T cells. 19 of 26 HLA ligands (73%) were tested positive [**Figure 22**]. 3 of 26 HLA ligands displayed tetramer-positive populations, but as well exhibited positive populations in tetramer staining with the UV-sensitive tetramer. The populations of tetramer-positive cells ranged from 0.1% for YVKERSKAM (EGLN3, B*08) to 6.8% for KIQEILTQV (IGF2BP3, A*02). Furthermore, the amount of positive wells ranged from one to 18 (SQILKHLL, NNMT, B*08) out of 20 wells tested for one donor.

To access the functionality of the cells ICS was performed for 9 of the 19 HLA ligands tested positive. After KIQEILTQV and VLITGLPLI (CYP2J2, A*02) stimulation $CD8^+$ T cells displayed functionality producing IFN-γ and TNF-α [**Figure 23**]. ILWREVVTL (HSF4, A*02), KLLDEVTYL (CYP2J2, A*02) and MPLGHIMRL (EGLN3, B*07) stimulated $CD8^+$ T cells displayed IFN-γ and TNF-α production but the production was not significantly higher than the negative control.

To exclude memory T cell responses towards the peptides a recall IFN-γ ELISpot was performed after a 12 day stimulation of donor PBMCs. No IFN-γ secretion was detectable for all peptides [**Figure 24**]. However, memory T cells might recognize the peptide without IFN-γ secretion. Therefore, stimulated cells were additionally read out by tetramer staining. $CD8^+$ T cells displayed no binding to tetramers (not shown). In conclusion, the positive priming results of each of the 19 peptides could be confirmed by negative ELISpot and tetramer staining experiments after 12 day stimulation of respective PBMCs.

Table 7: Immunogenicity analysis of selected HLA class I ligands. Strategy for HLA ligand selection: Qual = Comparative profiling, Quan = Quantitative analysis, CTA = cancer-testis antigen, Qual_Antigen = HLA ligands from selected antigens from comparative profiling which do not fulfill all criteria. Positive tested HLA ligands are marked in green, ambiguous results are marked in orange, negative tested HLA ligands are marked in red. ICS =intracellular cytokine staining. *Ambiguous results in tetramer staining with peptide of interest and UV-sensitive peptide. N.s. = not significant, n.t = not tested, + = positive, - = negative.

Sequence	Source Protein	HLA	Identification strategy	Priming [Positive/Total]	Donor	Wells [Positve/Total]	Largest Tetramer^{+} population [%]	ICS
ILWREVVTL	HSF4	A*02	Qual/Quan	1/1	J263	10/16	4.51	n.s.
FLLSLIDRL	EGLN3	A*02	Qual	1/2	J263/J267	2/36	0.11	n.t.
KLLDEVTYL	CYP2J2	A*02	Qual	0/1	J263	1/20*	0.72	n.s.
ALIVSLPYL	SLC17A3	A*02	Qual/Quan	1/1	J263	3/14	1.99	-
LLAASVALA	NPTX2	A*02	Qual/Quan	0/1	J265	0/20	0	n.t.
KIQEILTQV	IGF2BP3	A*02	Qual/CTA	1/1	J263	1/11	6.76	+
VLITGLPLI	CYP2J2	A*02	Qual_Antigen	1/1	J263	3/20	1.4	+
RPPNNEKLSL	CYP2J2	B*07	Qual_Antigen	1/1	J262	2/20	0.1	-
VPREVTVDTTL	CYP2J2	B*07	Qual_Antigen	1/1	J262	3/20	0.37	-
MPLGHIMRL	EGLN3	B*07/B*08/B*35/B*51/B*53	Qual/Quan	1/1	J262	9/20	0.61	n.s.
EAKKKFRNL	EGLN3	B*08	Qual_Antigen	1/2	J265/J269	3/40	0.13	n.t.
YVKERSKAM	EGLN3	B*08	Qual_Antigen	1/2	J265/J269	2/40	0.1	n.t.
DQYKFLAV	NDUFA4L2	B*08	Qual/Quan	0/2	J265/J269	0/20	0	n.t.
SQILKHLL	NNMT	B*08	Qual	1/1	J265	18/20	0.49	-
AQNSRIQQLF	ANGPTL4	B*15	Qual	1/1	J268	5/20	0.75	n.t.
RSFAGNLNTY	PFKP	B*15	Qual	0/1	J268	0/20	0	n.t.
AQNSRIQQL	ANGPTL4	B*15	Qual	1/1	J268	3/20	1.19	n.t.
SLIDRLVLY	EGLN3	B*15	Qual	1/1	J268	1/20	0.48	n.t.
VQPSYATRY	EGLN3	B*15	Qual	0/1	J268	0/20	0	n.t.
GQHLHLETF	PRAME	B*15	Qual/CTA	1/1	J268	5/20	0.19	n.t.
REVTVDTTL	CYP2J2	B*40	Qual/Quan	1/1	J267	3/20	1.8	n.t.
AEKELVQSL	P4HA2	B*40/B*41/B*44	Qual/Quan	0/1	J267	1/20*	0.08	n.t.
AESQILKHLL	NNMT	B*40/B*44	Qual/Quan	1/1	J267	2/20	0.41	n.t.
TETTSTTLRW	CYP2J2	B*44	Qual_Antigen	1/1	J267	1/20	1.34	n.t.
AEVLPQHKF	ACAD11	B*44	Qual	1/1	J267	3/20	0.46	n.t.
AEAALSHSY	CDK18	B*44/B*18	Qual	0/1	J267	1/20*	0.04	n.t.

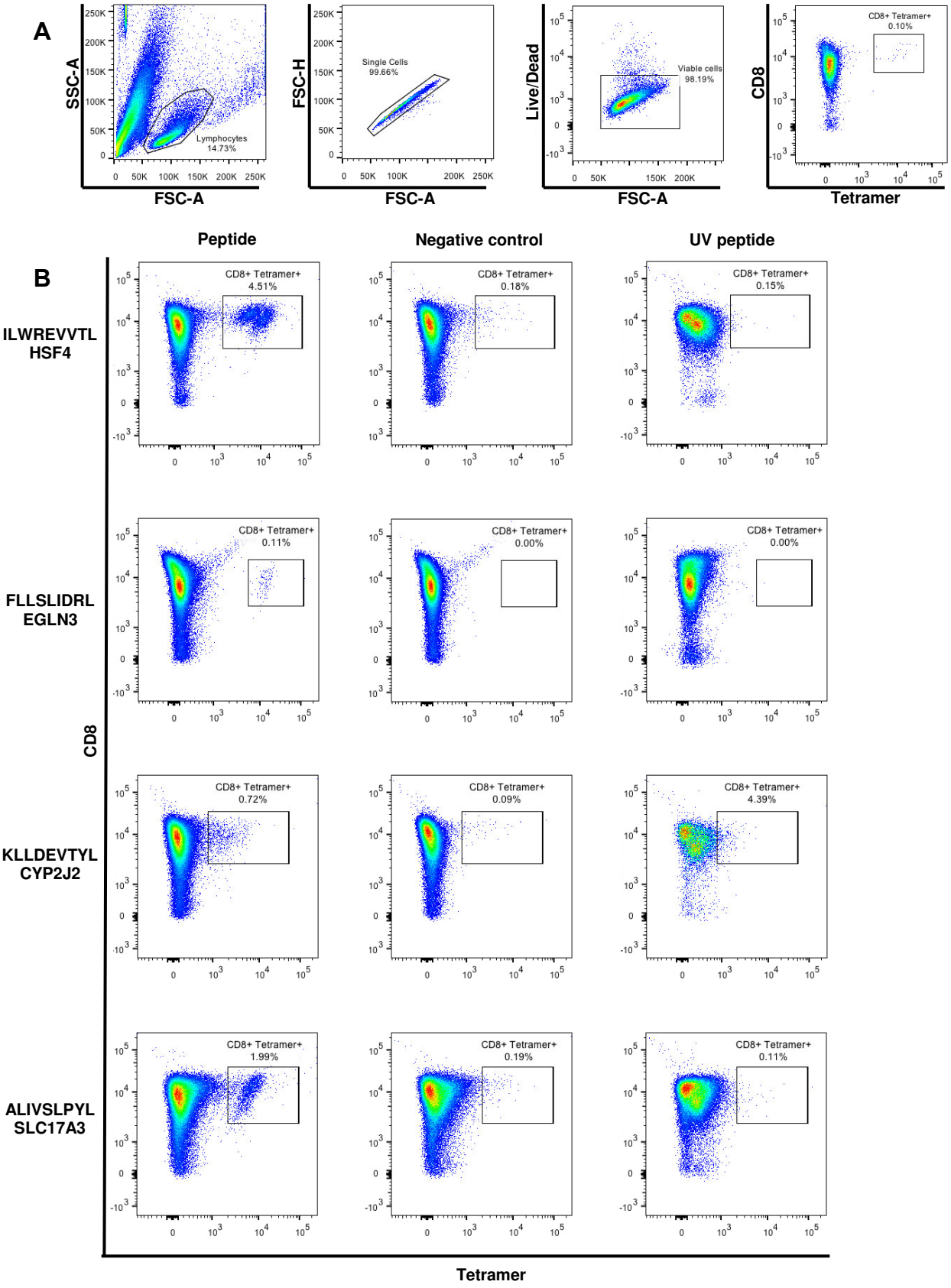

Figure 22: Tetramer staining (beginning, page 1/5)

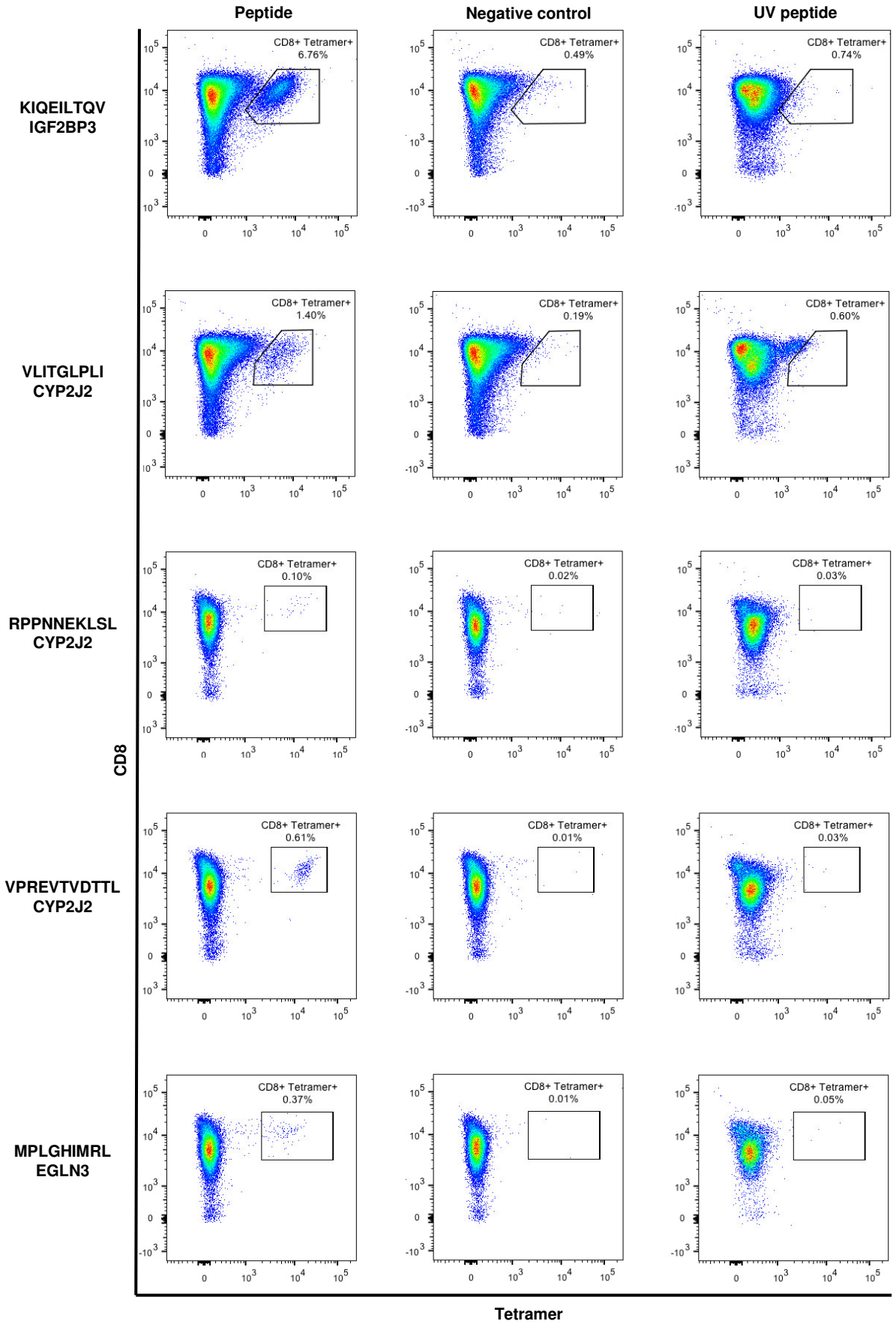

Figure 22: Tetramer staining (continued, page 2/5)

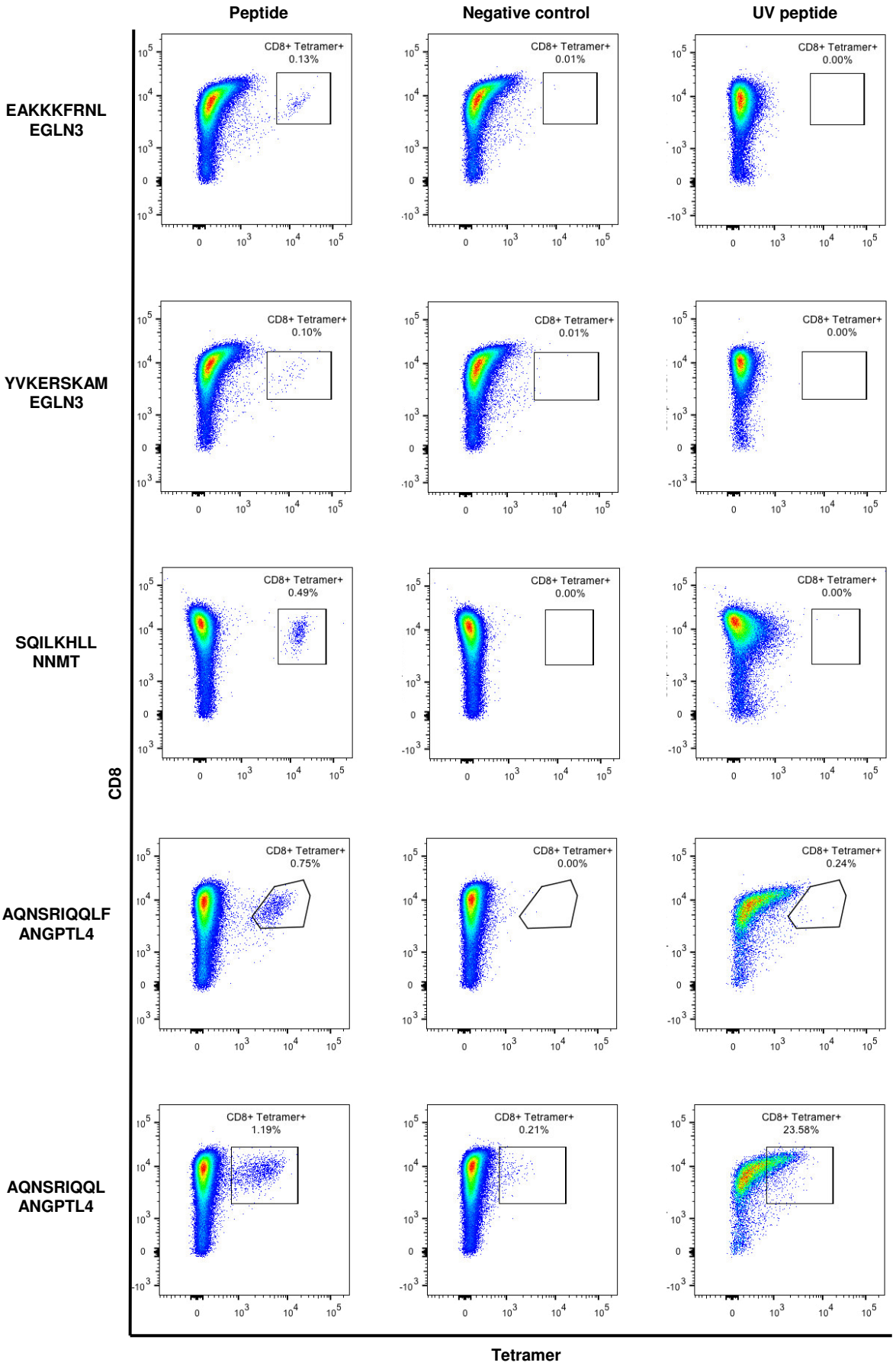

Figure 22: Tetramer staining (continued, page 3/5)

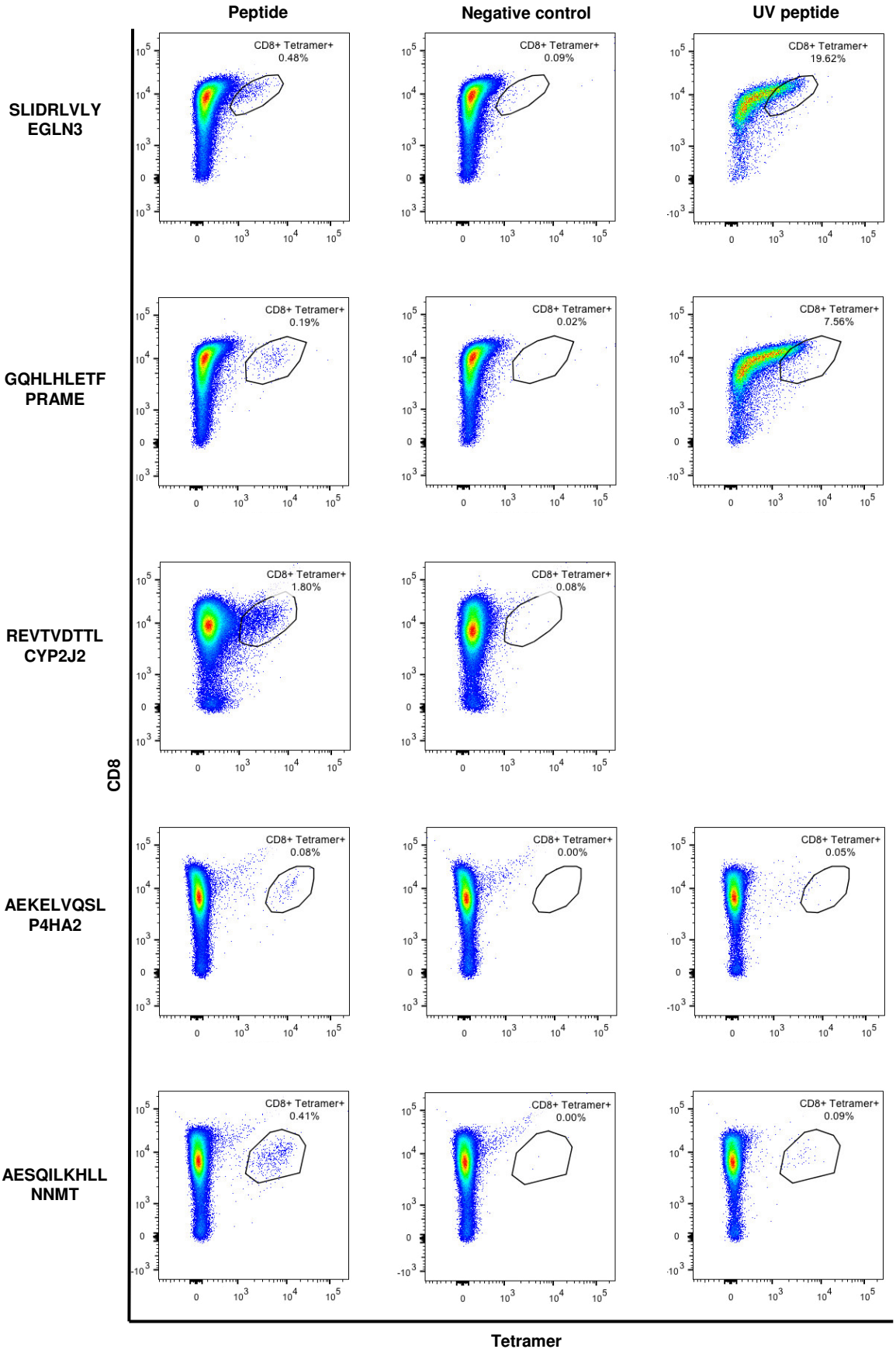

Figure 22: Tetramer staining (continued, page 4/5)

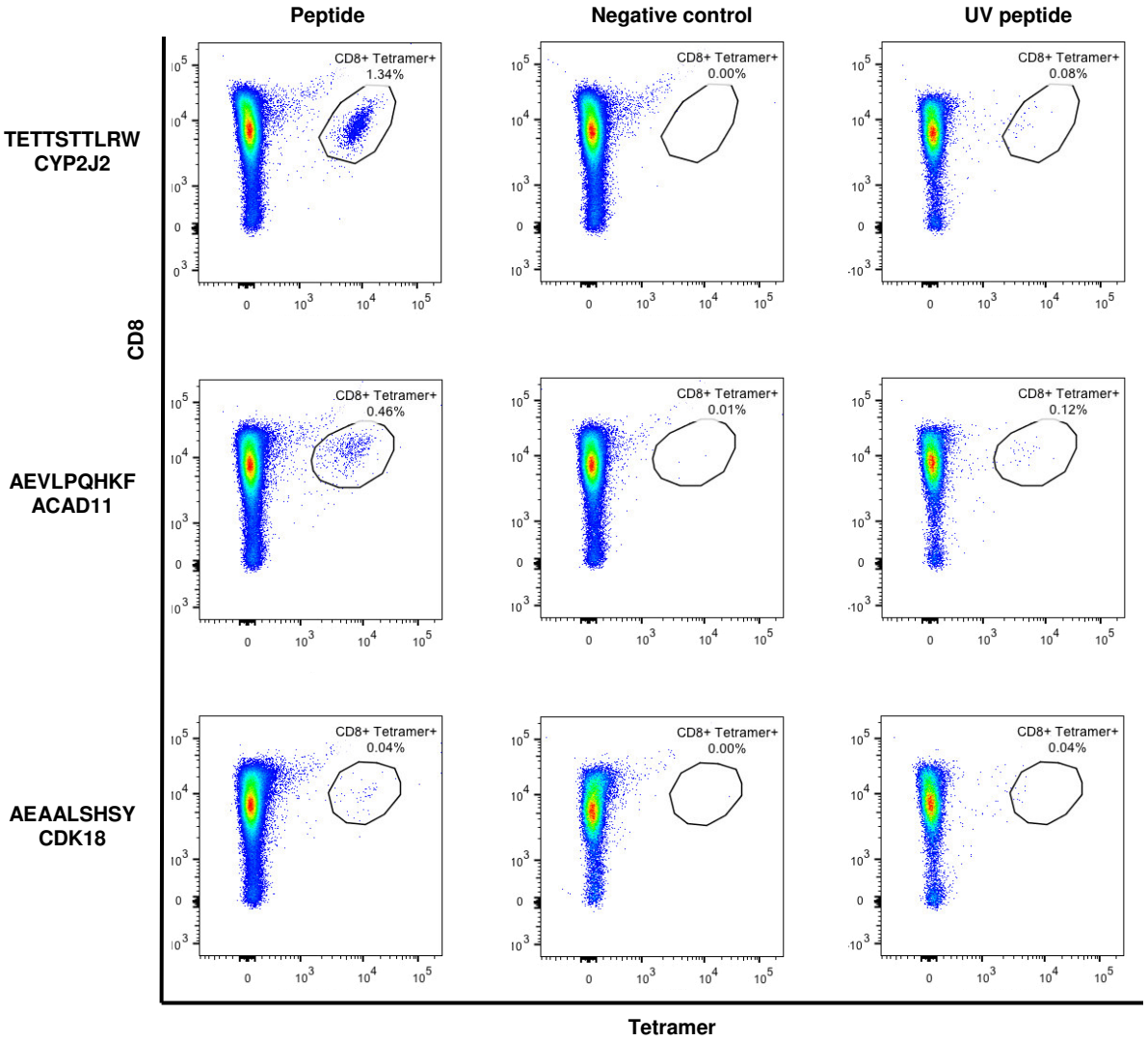

Figure 22: Tetramer staining. A) Gating strategy. Cells were gated for single and viable cells (Aqua Live/Dead staining), B) Tetramer staining of primed $CD8^+$ T cells. 700,000 events were measured. Negative control: Tetramer staining of $CD8^+$ T cells primed with a different tetramer. UV peptide: Positive wells were additionally stained with the tetramer comprising the respective UV-sensitive peptide used for UV-exchange.

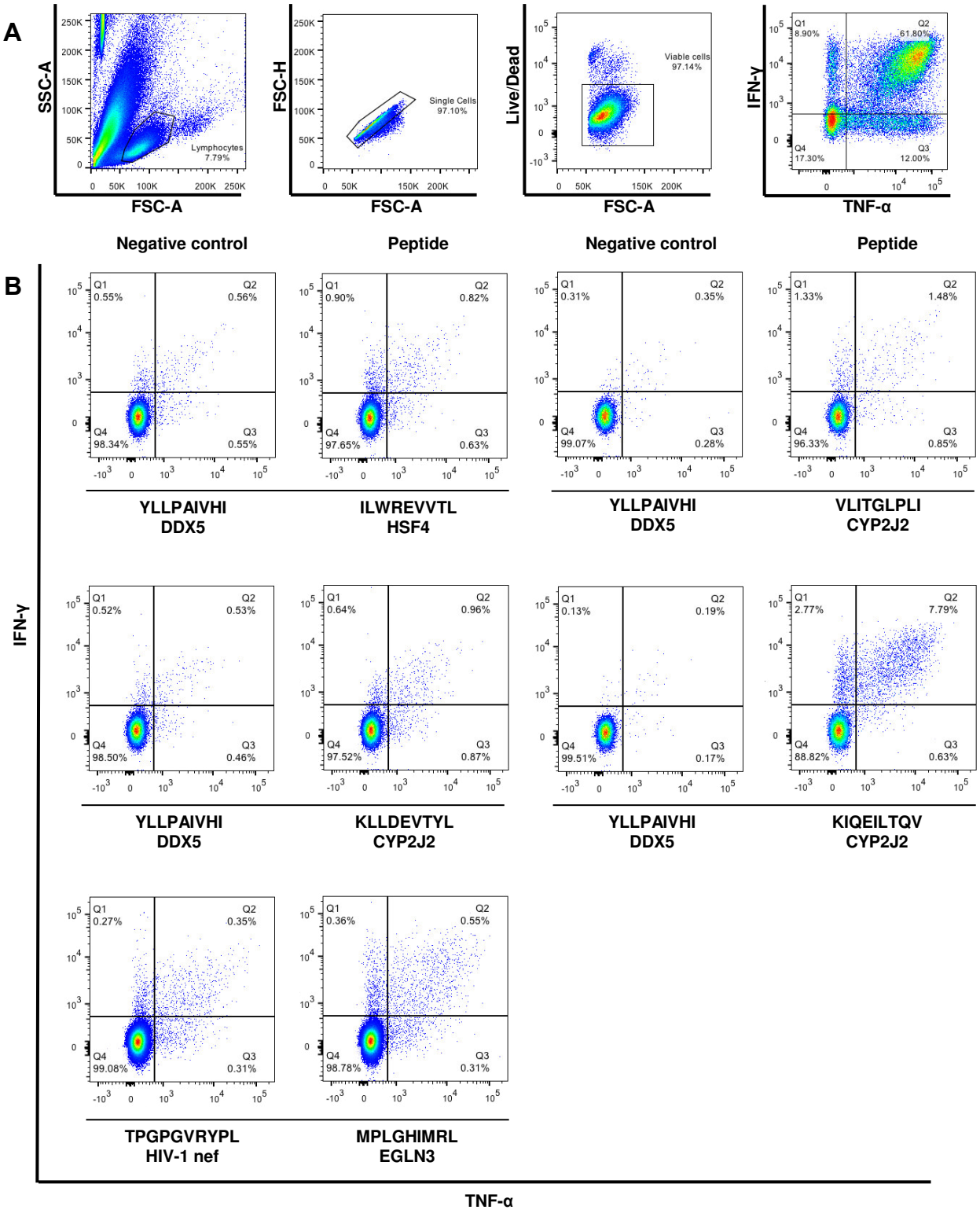

Figure 23: Intracellular cytokine staining. A) Gating strategy and example for positive control. Cells were gated for single and viable cells (Aqua Live/Dead staining), B) IFN-γ and TNF-α production of primed $CD8^+$ T cells. 700,000 events were measured.

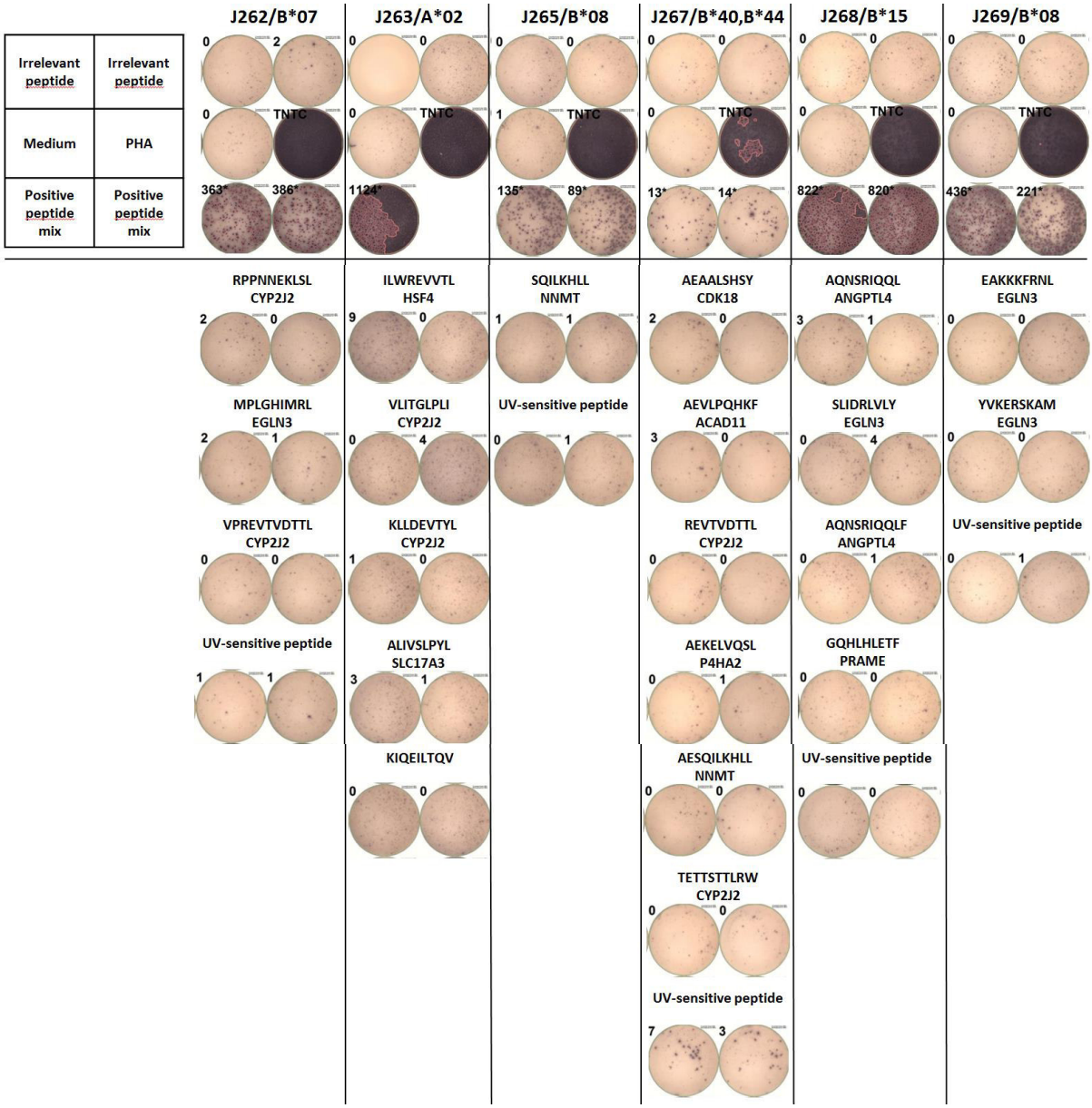

Figure 24: Recall ELISpot. PBMCs of healthy donors (same donors as for priming experiments) were stimulated for 12 days with peptides tested positive in respective priming experiments to exclude memory responses. 500,000 cells/well were stained. Irrelevant peptide for J262-J268 was YLLPAIVHI (A*02, DDX5), for J269 GSEELRSLY (A*01, POL_HV1H2). A mix of immunogenic viral HLA-A*02 peptides from Epstein-Barr virus (EBV) and cytomegalovirus (CMV) were used as positive control for J262-J268, for J269 a HLA-A*01 mix was employed. Additionally, PHA was employed as positive control. Numbers corresponds to spot count. Positive wells are marked with an asterisk. TNTC = too numerous to count.

2.7. Discussion

The immunogenic property of ccRCC is substantiated by sporadic responses in IL-2- or IFN-α-treated patients as well as beneficial effects demonstrated for nivolumab. These non-specific approaches reveal the potential of immunotherapy of ccRCC. On the other side, application of targeted therapies with tyrosine kinase inhibitors, mTOR inhibitors and bevacizumab are limited due to frequently occurring resistance to these drugs.[125] Specific immunotherapeutic approaches, like peptide vaccination or ACT, hold the potential to enhance and specify responses in patients. To that end, the identification of suitable T-cell epitopes is of major importance.

To address the identification of T-cell epitopes several methods are feasible and were employed in this part of the thesis. The main analysis was the comparative profiling of the naturally presented HLA ligandome of tumors compared to the benign counterpart which is an appropriate procedure to identify candidate targets. Compared to other approaches which include the *in silico* prediction of HLA ligands from tumor-associated antigens described in the literature or identified by gene expression analysis, exome sequencing or other approaches, the HLA ligandome analysis directly focuses on the presented immunopeptidome.[111,251] This includes the consideration of antigen processing which processes in antigen and peptide selection are thus far not well dissolved and cannot be predicted. Hence, in the immunopeptidomics approach peptides can be selected which are known to be presented by the tumor.

The comprehensive analysis in this project focuses on the main subtype of RCC. The restriction to ccRCC is an important approach to define the immunopeptidome of this subtype, since different subtypes of RCC are characterized by different cellular aberrations leading to individual HLA ligandomes.

Comparative profiling of HLA ligandomes is the major step in the selection of TUMAPs considering their tumor-exclusive presentation. Here, a cohort of 58 and 52 ccRCC and corresponding adjacent benign sample pairs were analyzed for HLA class I and HLA class II, respectively. The integration of an in-house database comprising 158 and 123 benign samples for HLA class I and HLA class II, respectively, provides crucial information of the immunopeptidomes of several other benign organs. In total, 1591 and 917 TUMAPs for HLA class I and HLA class II, respectively, could be identified which were presented in at least two ccRCC samples. The benign database acts as an important determinant for this preselection. However, some organs and less frequent HLA alleles lack with the risk of some remaining false TUMAPs. On the other hand, the comprehensive ccRCC cohort is appropriate for the identification of TUMAPs since HLA allotypes, especially for more common allotypes, are covered by several samples. Nevertheless, it is important to mention that this is a

preselection approach to identify targets which have to be further validated in immunogenicity screens.

The peptide yields display high variances which are mainly caused by three factors. The first factor is the weight of the tissue. Correlation of tissue weight with peptide yields exhibits a linear correlation up to the weight of about 0.8 to 1 g (not shown). The second factor is the improvement of sample processing in the course of time. The main improvement was the additional application of acetonitrile for washing of the filter units. In that way, peptide yields and peptide concentration (which correlates to the area under the curve in the survey scan summation of the respective identified peptide) could be tremendously improved.[252] In turn, sample sizes could be diminished. Third, five samples were measured on the Orbitrap Fusion Lumos which exhibits a 5-fold increase in peptide yields for HLA class II [**Figure 13**]. Peptide yields from JY cells exhibit a 4-fold increase for HLA class I ligands in the Orbitrap Fusion Lumos compared to the LTQ Orbitrap XL (not shown).

The differences in sample purity might be caused by the composition of the sample, for example necrotic areas, blood vessel or fat tissue amounts. This leads to increased amounts of soluble peptides (e.g. from necrotic cells) and proteins (e.g. structure proteins, histones and ribosomes from necrotic cells or hemoglobin and albumin from the blood stream) which might unspecifically bind to the column.

After the identification of TUMAPs by comparative profiling, the choice of the most promising candidates can be further addressed by several approaches. Here, approaches focusing on the HLA ligandome as well as the HLA ligand source antigens were applied. For HLA ligand selection the frequency of ligand presentation, the HLA restriction and the quantitative presentation were implemented. The selection of frequent HLA ligands is advantageous for the construction of a warehouse for an off-the-shelf approach.[163,231] Furthermore, the focus on frequent HLA alleles is important to cover the majority of the population. The quantitative analysis provides additional information of the overrepresentation of an antigen. This is relevant since sample sizes were not adjusted prior to immunoaffinity purification subsequently leading to varying peptide amounts and varying concentrations when diluting to the same volume. For quantitative analysis only adjusted sample pairs (sample volumes were adjusted on the basis of the total area of identifications in the "dose finding" runs) were used, whereas the comparative analysis comprises all samples including "dose finding" runs for subsequent sample adjustment and samples which were not adjusted. Further analysis of the HLA ligand source antigens using gene expression and cancer-testis association databases as well as literature search were used to select the most promising candidates.

Overlap analysis of comparative and quantitative analysis reveals 59 overlapping antigens with 58 overlapping HLA class I ligands [**Figure 18**]. The lower number of overlapping HLA class I ligands can be explained by the different focus of both methods. While comparative profiling focuses on all TUMAPs, the quantitative analysis does not consider TUMAPs which are only detected in one replicate.

Gene expression data from the TCGA database were included to search for antigens which are overexpressed in ccRCC compared to benign kidneys. Overexpressed antigens may have a considerable role in pathogenesis or are induced by cellular or microenvironmental aberrations. Targeting antigens with relevant functions in the tumor hold the promise for more effective therapies. Gene expression in other organs was not considered. However, gene expression and HLA ligand presentation were shown to be not correlated.[253] The integration of HLA ligandomes of several organs gives the essential information of HLA ligand presentation on these organs.

The adaption to hypoxia is one of the characteristic features of ccRCC following VHL mutation and is involved in tumor development. Disrupting the adaption to hypoxia is already considered as target therapy for ccRCC.[254] On the other side, genes induced via this commonly altered pathway may serve as suitable targets. Here, 12 hypoxia-induced antigens could be identified with enhanced gene expression and frequently presented TUMAPs.

Further targets are CTAs and mutated antigens which are not expressed in normal tissue. Six TUMAPs from five CTAs were identified which were at least presented on two ccRCC samples [**Table 5**]. On the other hand, no mutated peptide could be found by searching for the 600 most frequent mutations throughout all tumors, which is consistent with the low mutational burden of ccRCC.[172] However, the search was limited to the top 600 mutations, certainly missing some less frequent and ccRCC specific mutations. For the construction of a warehouse the search for infrequent and patient specific mutations is anyway inappropriate and the search for them should be only considered for personalized therapies.

Overall, a set of 26 HLA class I ligands from six HLA allotypes were chosen for the immunogenicity screening with 19 HLA ligands tested positive [**Table 7**].

Priming of $CD8^+$ T cells from healthy donors was applied to investigate the recognition ability of naïve T cells. This approach has several advantages compared to the *ex vivo* or short-term cytokine-stimulated screening for memory T cells in PBMCs or TILs of the corresponding patient. First of all, the limited availability of autologous blood samples or fresh tissue for TIL isolation is restricting the feasibility of this approach. The second limitation is the difficulty to detect memory T cells against tumor antigens due to the immunosuppressive microenvironment which leads to anergic T cells.

For the quality control of pHLA complexes required for priming experiments, UV-exchanged monomers were validated by staining with antibodies recognizing epitopes in misfolded HLA molecules. This method was suited for all tested HLA allotypes although the applicability of this method was so far only shown for HLA-A*02, HLA-B*07 and HLA-B*08.[229] Only for HLA-B*44 the applicability of the HCA2 ab might be inappropriate. Indications are the low binding capability to the UV-treated monomer without exchanging peptide and the inconsistent results of the UV-exchanged monomers compared to the corresponding staining with HC10 [**Supplementary Figure** 1]. The staining of the monomer exchanged with the DQYKFLAV peptide displayed binding of both HC10 and HCA2 abs implying an unsuccessful exchange. This could be the reason for the unsuccessful priming for this pHLA complex [**Table 7**]. Furthermore, only NetMHCpan-3.0 rank defines DQYKFLAV as HLA-B*08 ligand (NetMHC rank: 2, NetMHC affinity: 1623 nm, SYFPEITHI: 0%).

The high frequency of peptides tested positive displays the suitability of the applied strategies in the selection of peptides. Interestingly, the source antigens of most of the immunogenic peptides are not tumor-exclusive, neither on the RNA level nor on the immunopeptidome. One example is the highly on liver tissue expressed antigen NNMT. Several peptides from NNMT are presented on HLA molecules in benign livers. However, the HLA ligands AESQILKHLL and SQILKHLL are presented tumor-exclusive and display high immunogenicity with 2 of 20 and 18 of 20 positive tested wells, respectively [**Table 7**].

6 of 7 negative HLA ligands were tested once. Further testing is needed to ascertain their immunogenicity. Three HLA ligands tested negative displayed a positive population, but tetramer staining with the corresponding UV-labile pHLA complex used for exchange displayed positive populations, too. Therefore, these peptides have to be retested. For HLA-B*15, tetramers with UV-sensitive peptide exposed a banana-like shift in the tetramer staining [**Figure 22**] indicating misfolded and unspecifically binding tetramers. The repetition of the tetramerization procedure and a subsequent tetramer staining displayed the same results indicating the instability of the monomer itself. For that reason and the fact that no distinct population was detected, these controls were not considered.

ICS was performed for wells with primed $CD8^+$ T cells. Except for KIQEILTQV (IGF2BP3, A*02) and VLITGLPLI (CYP2J2, A*02) stimulation, cells displayed no functionality. A reason could be the exhaustion of the cells after four rounds of priming and IL-2 stimulation over a time course of five weeks. For that matter, ICS results may not reflect the functionality of the cells. A prolonged cultivation of the cells without IL-2 may have settled a probable over reactivity. However, the successful priming of $CD8^+$ T cells displays the immunogenicity of these targets.

The ability of the peptides to prime $CD8^+$ T cells was confirmed by ELISpot and tetramer staining experiments after a 12 day stimulation of memory T cells. Neither recognition of the pHLA complex in terms of positive tetramer staining, nor functionality in terms of IFN-γ secretion was detectable. Some spots were detected for the HLA-B*44 UV-sensitive peptide. However, this can be explained by carry over from the wells of the positive peptide mix to the wells of the UV-sensitive peptide which were directly located below.

HLA class II TUMAPs are potential targets for a $CD4^+$ T cell activation which may support $CD8^+$ T cells. Another option is the use of elongated, immunogenic HLA class I ligands which have to be processed by APCs and might additionally be presented on HLA class II molecules. Due to the unfeasibility to test peptides in the context of HLA class II in priming experiments (refolding of pHLA class II complexes are challenging) as well as the lack of patient blood or TILs for *ex vivo* stimulation of memory T cells, HLA class II TUMAPs were not tested.

2.8. Acknowledgements

This study was granted by the ICEPHA graduate school Tübingen-Stuttgart, the European Union (ERC AdG339842 Mutaediting) and the Deutsche Forschungsgemeinschaft (DFG, SFB 685 and GRK 794). The author thanks Nicole Bauer, Katharina Fiedler and Ulrich Wulle for peptide synthesis and the Cancer Genome Atlas initiative, all tissue donors, and investigators who contributed to the acquisition and analyses of the samples used in this study. Information about TCGA and the investigators and institutions who constitute the TCGA research network can be found at http://cancergenome.nih.gov/.

2.9. Supplementary data

Supplementary Table 1: RCC patient cohort and HLA typing

Samples	HLA class I	HLA class II
RCC137	A*32:01; B*35:02; C*04:01	DRB1*11:04; DQA1*05:05; DQB1*03:01
RCC160	A*01:01; A*03:01; B*27:05; B*35:01; C*02:02; C*04:01	DRB1*01:01; DRB1*04:01; DQB1*03:02; DQB1*05:01
RCC168	A*01:01; A*26:01; B*15:17; B*38:01; C*07:01; C*12:03	DRB1*14:33; DRB1*16:02; DQB1*05:02; DQB1*06:03
RCC171	A*01:01; B*08:01; C*07:01	DRB1*03:01; DQA1*05:01; DQB1*02:01
RCC203	A*01:01; B*08:01; C*07:01	DRB1*03:01; DQA1*05:01; DQB1*02:01
RCC224	A*03:01; B*38:01; C*12:03	DRB1*13:01; DQB1*06:03
RCC225	A*01:01; A*02:01; B*35:02; B*40:01; C*03:04; C*04:01	DRB1*03:01; DRB1*09:01; DQB1*02:01; DQB1*03:03
RCC243	A*02:01; A*11:01; B*44:02; C*05:01	DRB1*07:01; DRB1*12:01; DQA1*02:01; DQA1*05:05; DQB1*02:02; DQB1*03:01
RCC245	A*24:01; B*37:01; B*44:03; C*06:02; C*16:01	DRB1*08:01; DQA1*04:02; DQB1*04:02
RCC246	A*26:01:01; A*29:02:01:01; B*07:02:01; B*44:03:01; C*07:02:01:03; C*16:01:01	DRB1*07:01:01:01; DRB1*08:01:01; DQB1*02:02:01; DQB1*04:02:01
RCC247	A*11; A*30; B*13; B*15	DRB1*01; DRB1*07; DRB4
RCC296	A*03:01; A*24:02; B*35:03; B*55:01; C*07:02; C*12:03	DRB1*04:07; DRB1*04:08; DQA1*03:02; DQB1*03:01; DQB1*03:04
RCC301	A*23:01:01; A*33:01:01; B*14:02:01; B*44:03:01; C*04:01:01:01; C*08:02:01	-
RCC302	A*03; A*32; B*07; B*15	DRB1*04; DRB1*11; DRB3; DRB4
RCC318	A*02:01:01:01; A*24:02:01:01; B*08:01:01; B*51:01:01; C*02:02:02; C*07:01:01:01	-
RCC345	A*03:01; A*30:02; B*35:01; B*58:01; C*04:01; C*07:01	DRB1*01:01; DRB1*13:02; DQA1*01:01; DQA1*01:02; DQB1*05:01; DQB1*06:04
RCC432	A*11:01; A*31:01; B*35:01; B*44:02; C*04:01; C*05:01	DRB1*01:01; DRB1*11:04; DQB1*03:01; DQB1*05:01
RCC433	A*02:01:01:01; B*07:02:01; B*44:02:01:01; C*07:02:01:03; C*05:01:01:02	DRB1*04:01:01; DRB1*15:01:01:01
RCC440	A*02:01; B*27:05; B*44:02; C*01:02; C*05:01	DRB1*01:03; DRB1*15:01; DQA1*01:01; DQA1*01:02; DQB1*05:01; DQB1*06:02
RCC449	A*03:01; A*30:02; B*35:01; B*50:01; C*04:01	DRB1*03:01; DRB1*13:03; DQB1*02:01; DQB1*03:01
RCC451	A*24:02:01:01; A*31:01:02; B*07:02:01; B*40:01:02; C*07:02:01:03; C*03:04:01:01	DRB1*03:01:01:01; DRB1*15:01:01:01; DQB1*02:01:01; DQB1*06:02:01
RCC455	A*11:01; A*29:02; B*27:02; B*44:03; C*02:02; C*16:01	DRB1*07:01; DRB1*16:01; DQB1*02:02; DQB1*05:02

Supplementary Table 1 (continued)

Samples	HLA class I	HLA class II
RCC456	A*01:01; A*02:01; B*08:01; B*52:01; C*02:02; C*07:01	DRB1*15:02; DRB1*16:01; DQB1*05:02; DQB1*06:01
RCC467	A*01:01:01:01; A*02:01:01:01; B*18:01:01:02; B*37:01:01; C*06:02:01:01; C*07:01:01:01	DRB1*11:04:01; DRB1*13:02:01; DQB1*03:01:01:02; DQB1*06:04:01
RCC476	A*02:01:01:01; A*31:01:02; B*35:03:01; B*40:01:01; C*02:02:02; C*03:04:01:01	DRB1*11:02:01; DRB1*13:02:01; DRB3*02:02:01; DRB3*03:01:01; DQA1*01:02:01; DQA1*05:01:01; DQB1*03:19; DQB1*06:04:01; DPB1*04:01:01; DPB1*14:01
RCC792	A*02; A*03; B*15; B*27	-
RCC986	A*01:01; A*26:01; B*49:01; B*58:01; C*07:01	DRB1*01:01; DRB1*08:04; DQA1*01:01; DQA1*04:01; DQB1*04:02; DQB1*05:01
RCC990	A*02:01; B*27:05; B*55:01; C*02:02; C*03:03	DRB1*04:01; DRB1*14:01; DQA1*01:01; DQA1*03:01; DQB1*03:02; DQB1*05:03
RCC1005	A*02:01; B*51:01; B*57:01; C*06:02; C*15:02	DRB1*07:01; DRB1*13:01; DQA1*01:03; DQA1*02:01; DQB1*03:03; DQB1*06:03
RCC1056	A*02:01; A*31:01; B*44:02; B*44:03; C*05:01; C*07:02	DRB1*07:01; DRB1*11:03; DQA1*02:01; DQA1*05:05; DQB1*02:02; DQB1*03:01
RCC1060	A*03:01; B*13:02; B*51:01; C*01:02; C*06:02	DRB1*01:01; DRB1*07:01; DQA1*01:01; DQA1*02:01; DQB1*02:02; DQB1*05:01
RCC1083	A*01:01; A*68:02; B*08:01; B*53:01; C*07:01; C*04:01	DRB1*03:01; DRB1*13:02; DQB1*02:01; DQB1*06:04; DQA1*01:02; DQA1*05:01
RCC1086	A*01:01; A*03:01; B*07:02; B*08:01; C*07:02; C*07:01	DRB1*03:01; DRB1*15:01; DQB1*02:01; DQB1*06:02; DQA1*01:02; DQA1*05:01
RCC1117	A*02:01; B*07:02; B*15:01; C*03:04; C*07:02	DRB1*13:01; DRB1*15:01; DQA1*01:01; DQA1*01:03; DQB1*06:02; DQB1*06:03
RCC1148	A*01:01:01:01; A*11:01:01; B*07:02:01; B*44:03:01; C*07:02:01:01; C*16:01:01	DRB1*07:01:01:01; DRB1*13:02:01; DRB3*03:01:01; DRB4*01:01:01:01; DQB1*02:10; DQB1*06:04:01; DQA1*01:02:01; DQA1*02:01; DPB1*03:01:01; DPB1*11:01:01
RCC1152	A*29:01:01:01; A*25:01; B*44:02:01:01; B*07:05:01; C*05:01:01:01; C*15:05:01	DRB1*04:01:01; DRB1*11:01:01; DRB3*02:02:01; DRB4*01:01:01:01; DQB1*03:02:01; DQB1*03:01:01; DQA1*05:01:01; DQA1*03:01:01; DPB1*04:01:01; DPB1*04:02
RCC1154	A*01:01:01:01; A*02:01:01:01 B*08:01:01; B*27:05:02; C*07:01:01; C*02:02:02	DRB1*03:01:01:01; DRB1*01:01; DRB3*01:01:02:01; DQB1*02:01:01; DQB1*05:01:01; DQA1*05:01:01; DQA1*01:01:01; DPB1*03:01:01; DPB1*04:02
RCC1157	A*02:01; A*24:02; B*07:02; B*51:01; C*02:02; C*07:02	DRB1*11:01; DRB1*15:01; DQA1*01:01; DQA1*05:05; DQB1*03:01; DQB1*06:02
RCC1170	A*24:02:01:01; A*68:02:01:01; B*35:02:01; B*53:01:01; C*04:01:01:01	DRB1*13:02:01; DRB1*11:04:01; DRB3*03:01:01; DRB3*02:02:01; DQB1*03:01:01; DQB1*06:04:01; DQA1*01:02:01; DQA1*05:01:01; DPB1*04:01:01
RCC1187	A*24:02:01:01; A*68:01:02; B*51:01:01; B*18:01:01; C*07:01:01; C*14:02:01	DRB1*13:01:01; DRB1*07:01:01:01; DRB3*01:01:02:01; DRB4*01:01:01:01; DQB1*02:02; DQB1*06:03:01; DQA1*01:03; DQA1*02:01; DPB1*02:01:02; DPB1*04:02

Supplementary Table 1 (continued)

Samples	HLA class I	HLA class II
RCC1188	A*24:02:01:01; A*11:01:01; B*14:07N; B*18:01:01; C*07:01:01; C*08:02:01	DRB1*11:01:01; DRB1*07:01:01:01; DRB3*02:02:01; DRB4*01:01:01:01; DQB1*02:02; DQB1*03:01:01; DQA1*05:01:01; DQA1*02:01; DPB1*03:01:01; DPB1*04:01:01
RCC1192	A*03:01:01:01; A*11:01:01; B*08:01:01; B*51:01:01; C*07:01:01; C*15:02:01	DRB1*11:01:01; DRB1*03:01:01:01; DRB3*01:01:02:01; DRB3*02:02:01; DQB1*02:01:01; DQB1*03:01:01; DQA1*05:01:01; DPB1*02:01:02; DPB1*09:01
RCC1203	A*02:01; A*68:02; B*40:01; B*53:01; C*04:01; C*03:04	DRB1*13:02:01; DRB1*13:01:01; DRB3*01:01:02:01; DRB3*03:01:01; DQB1*06:04:01; DQB1*06:03:01; DQA1*01:02:01; DQA1*01:03; DPB1*13:01; DPB1*04:01:01
RCC1223	A*02:01:01:01; B*15:01:01:01; B*39:01:01:01; C*12:03:01:01; C*03:03:01	DRB1*13:01:01; DRB1*01:01:01; DRB3*02:02:01; DQB1*06:03:01; DQB1*05:01:01; DQA1*01:01:01; DQA1*01:03; DPB1:04:02; DPB1*03:01:01
RCC1238	A*68:01:02; B*44:02:01:01; B*51:01:01; C*07:04:01; C*15:02:01	DRB1*13:01:01; DRB1*01:01:01; DRB3*02:02:01; DQB1*06:03:01; DQB1*05:01:01; DQA1*01:02:01; DQA1*01:03; DPB1*06:01; DPB1*02:01:02
RCC1355	A*03:01; A*11:01; B*08:01; B*18:01; C*07:01	DRB1*03:01; DRB1*13:01; DQA1*01:03; DQA1*05:01; DQB1*02:01; DQB1*06:03
RCC1369	A*25:01; A*32:01; B*18:01; B*44:02; C*08:02; C*12:04	DRB1*04:01; DRB1*15:01; DQA1*01:02; DQA1*03:02; DQB1*03:02; DQB1*06:02
RCC1397	A*01:01; A*02:01; B*44:05; B*52:01; C*02:02; C*12:02	DRB1*07:01; DRB1*16:01; DQA1*01:02; DQA1*02:01; DQB1*03:03; DQB1*05:02
RCC1405	A*24:02; A*29:01; B*07:05; B*35:01; C*02:02; C*15:02	DRB1*11:01; DRB1*14:01; DQA1*01:01; DQA1*05:05; DQB1*03:01; DQB1*05:03
RCC1409	A*02:01; A*68:01; B*15:01; B*40:01; C*03:03; C*03:04	DRB1*04:01; DRB1*11:03; DQB1*03:02; DQB1*03:01; DQA1*03:01; DQA1*05:05
RCC1428	A*02:01; A*03:01; B*07:02; B*44:02; C*07:02; C*05:01	DRB1*07:01; DRB1*15:01; DQB1*02:02; DQB1*06:02; DQA1*01:02; DQA1*02:01
RCC1438	A*02:01; A*24:02; B*39:01; B*51:01; C*02:02	DRB1*01:01; DRB1*07:01; DQB1*05:01; DQB1*03:03; DQA1*01:01; DQA1*02:01
RCC1444	A*01:01; A*02:01; B*07:02; B*13:02; C*07:02; C*06:02	DRB1*07:01; DRB1*15:01; DQB1*02:02; DQB1*06:02; DQA1*01:02; DQA1*02:01
RCC1479	A*03:01; A*11:01; B*35:01; B*51:01; C*04:01; C*01:02	DRB1*01:01; DRB1*14:01; DQB1*05:01; DQB1*05:03; DQA1*01:01
RCC1483	A*01:01; A*24:02; B*40:01; B*57:01; C*03:04; C*06:02	DRB1*04:01; DRB1*07:01; DQA1*02:01; DQA1*03:01; DQB1*03:02; DQB1*03:03
RCC1491	A*01:01; A*66:01; B*08:01; B*41:02; C*07:01; C*17:03	DRB1*03:01; DRB1*13:03; DQB1*02:01; DQB1*03:01; DQA1*05:01
RCC1493	A*02:01; B*18:01; B*50:01; C*06:02; C*07:01	DRB1*07:01; DRB1*11:04; DQA1*02:01; DQA1*05:05; DQB1*02:02; DQB1*03:01
RCC1502	A*01:01; A*26:01; B*08:01; B*38:01; C*07:01; C*12:03	DRB1*03:01; DRB1*14:01; DQA1*01:01; DQA1*05:01; DQB1*02:01; DQB1*05:03

Supplementary Table 2: HLA class I sample overview. Peptide and ligands yields as well as the sample purity and measuring details are illustrated.

	Malignant			Benign					
Samples	**Peptides**	**Ligands**	**Ligands [%]**	**Peptides**	**Ligands**	**Ligands [%]**	**Mass Spectrometer**	**Search Algorithm**	**Adjusted**
RCC137	2010	1822	90,65	1745	1561	89,46	LTQ Orbitrap XL	Mascot	Yes
RCC160	1865	1791	96,03	1409	1329	94,32	LTQ Orbitrap XL	Mascot	Yes
RCC168	1919	1798	93,69	1504	1331	88,50	LTQ Orbitrap XL	Mascot	Yes
RCC171	2886	2506	86,83	1182	963	81,47	Orbitrap Fusion Lumos	SequestHT	Yes
RCC203	1105	987	89,32	501	446	89,02	LTQ Orbitrap XL	Mascot	Yes
RCC224	1771	1583	89,38	1257	1048	83,37	LTQ Orbitrap XL	Mascot	Yes
RCC225	2474	2347	94,87	49	42	85,71	LTQ Orbitrap XL	Mascot	No
RCC243	2134	2030	95,13	1683	1555	92,39	LTQ Orbitrap XL	Mascot	Yes
RCC245	849	764	89,99	703	588	83,64	LTQ Orbitrap XL	Mascot	Yes
RCC246	1192	961	80,62	1857	1724	92,84	LTQ Orbitrap XL	Mascot	Yes
RCC247	1406	1143	81,29	373	298	79,89	LTQ Orbitrap XL	Mascot	No
RCC296	1626	1457	89,61	1074	939	87,43	LTQ Orbitrap XL	Mascot	Yes
RCC301	2150	1859	86,47	1159	1010	87,14	LTQ Orbitrap XL	Mascot	No
RCC302	2027	1730	85,35	559	418	74,78	LTQ Orbitrap XL	Mascot	No
RCC318	2145	1721	80,23	195	164	84,10	LTQ Orbitrap XL	Mascot	No
RCC345	2498	2246	89,91	2227	1970	88,46	LTQ Orbitrap XL	Mascot	Yes
RCC432	1189	1112	93,52	1179	1074	91,09	LTQ Orbitrap XL	Mascot	Yes
RCC433	2450	2309	94,24	2255	2137	94,77	LTQ Orbitrap XL	Mascot	Yes
RCC440	5191	4934	95,05	3269	2826	86,45	Orbitrap Fusion Lumos	SequestHT	Yes
RCC449	2364	2155	91,16	1227	1114	90,79	LTQ Orbitrap XL	Mascot	Yes
RCC451	1188	1130	95,12	738	550	74,53	LTQ Orbitrap XL	Mascot	Yes
RCC455	1979	1856	93,78	839	750	89,39	LTQ Orbitrap XL	Mascot	Yes
RCC456	1681	1536	91,37	233	210	90,13	LTQ Orbitrap XL	Mascot	No
RCC467	2074	1991	96,00	881	828	93,98	LTQ Orbitrap XL	Mascot	Yes
RCC476	2146	1980	92,26	1408	1076	76,42	LTQ Orbitrap XL	Mascot	Yes
RCC792	910	761	83,63	117	99	84,62	LTQ Orbitrap XL	Mascot	No
RCC986	1589	1437	90,43	1162	1020	87,78	LTQ Orbitrap XL	Mascot	Yes
RCC990	1119	987	88,20	556	442	79,50	LTQ Orbitrap XL	Mascot	No
RCC1005	862	813	94,32	533	497	93,25	LTQ Orbitrap XL	Mascot	No

Supplementary Table 2 (continued)

	Malignant			Benign					
Samples	**Peptides**	**Ligands**	**Ligands [%]**	**Peptides**	**Ligands**	**Ligands [%]**	**Mass Spectrometer**	**Search Algorithm**	**Adjusted**
RCC1056	1880	1763	93,78	1256	1148	91,40	LTQ Orbitrap XL	Mascot	Yes
RCC1060	900	778	86,44	998	816	81,76	LTQ Orbitrap XL	Mascot	Yes
RCC1083	1264	1129	89,32	307	185	60,26	LTQ Orbitrap XL	Mascot	No
RCC1086	1004	879	87,55	829	588	70,93	LTQ Orbitrap XL	Mascot	Yes
RCC1117	1346	1237	91,90	1267	1150	90,77	LTQ Orbitrap XL	Mascot	Yes
RCC1148	2458	2261	91,99	1761	1638	93,02	LTQ Orbitrap XL	Mascot	Yes
RCC1152	3113	2547	81,82	1596	1357	85,03	LTQ Orbitrap XL	Mascot	Yes
RCC1154	946	772	81,61	553	474	85,71	LTQ Orbitrap XL	Mascot	Yes
RCC1157	1165	1127	96,74	455	431	94,73	LTQ Orbitrap XL	Mascot	Yes
RCC1170	2084	1796	86,18	1027	921	89,68	LTQ Orbitrap XL	Mascot	Yes
RCC1187	1279	1179	92,18	940	840	89,36	LTQ Orbitrap XL	Mascot	Yes
RCC1188	2113	1961	92,81	1302	1203	92,40	LTQ Orbitrap XL	Mascot	Yes
RCC1192	1414	1102	77,93	1286	1180	91,76	LTQ Orbitrap XL	Mascot	Yes
RCC1203	1382	1237	89,51	777	701	90,22	LTQ Orbitrap XL	Mascot	Yes
RCC1223	3507	3147	89,73	608	453	74,51	LTQ Orbitrap XL	Mascot	Yes
RCC1238	2073	1897	91,51	1900	1776	93,47	LTQ Orbitrap XL	Mascot	Yes
RCC1355	965	906	93,89	717	669	93,31	LTQ Orbitrap XL	Mascot	Yes
RCC1369	940	843	89,68	248	228	91,94	LTQ Orbitrap XL	Mascot	Yes
RCC1397	705	660	93,62	459	311	67,76	LTQ Orbitrap XL	Mascot	Yes
RCC1405	530	512	96,60	322	298	92,55	LTQ Orbitrap XL	Mascot	Yes
RCC1409	3906	3600	92,17	2117	1914	90,41	Orbitrap Fusion Lumos	SequestHT	Yes
RCC1428	2125	2041	96,05	510	451	88,43	Orbitrap Fusion Lumos	SequestHT	No
RCC1438	141	121	85,82	2992	2843	95,02	Orbitrap Fusion Lumos	SequestHT	No
RCC1444	1354	1139	84,12	1121	850	75,83	LTQ Orbitrap XL	Mascot	Yes
RCC1479	1949	1788	91,74	820	763	93,05	LTQ Orbitrap XL	Mascot	Yes
RCC1483	1583	1502	94,88	1402	1254	89,44	LTQ Orbitrap XL	Mascot	Yes
RCC1491	1383	1255	90,74	932	810	86,91	LTQ Orbitrap XL	Mascot	Yes
RCC1493	1154	1021	88,47	830	747	90,00	LTQ Orbitrap XL	Mascot	Yes
RCC1502	1417	1282	90,47	1063	907	85,32	LTQ Orbitrap XL	Mascot	Yes

Supplementary Table 3: HLA class II sample overview. Peptide yields as well as measuring details are illustrated.

Samples	Peptides Malignant	Peptides Benign	Mass Spectrometer	Search Algorithm
RCC137	1059	1019	LTQ Orbitrap XL	Mascot
RCC160	1165	1138	LTQ Orbitrap XL	Mascot
RCC168	993	785	LTQ Orbitrap XL	Mascot
RCC171	3420	1884	Orbitrap Fusion Lumos	SequestHT
RCC203	1128	382	LTQ Orbitrap XL	Mascot
RCC224	640	444	LTQ Orbitrap XL	Mascot
RCC225	979	485	LTQ Orbitrap XL	Mascot
RCC243	774	1165	LTQ Orbitrap XL	Mascot
RCC245	434	395	LTQ Orbitrap XL	Mascot
RCC246	240	280	LTQ Orbitrap XL	Mascot
RCC247	539	131	LTQ Orbitrap XL	Mascot
RCC296	773	742	LTQ Orbitrap XL	Mascot
RCC302	443	421	LTQ Orbitrap XL	Mascot
RCC345	1344	831	LTQ Orbitrap XL	Mascot
RCC432	474	696	LTQ Orbitrap XL	Mascot
RCC433	905	1030	LTQ Orbitrap XL	Mascot
RCC440	5103	5414	Orbitrap Fusion Lumos	SequestHT
RCC449	1029	594	LTQ Orbitrap XL	Mascot
RCC451	505	361	LTQ Orbitrap XL	Mascot
RCC456	856	458	LTQ Orbitrap XL	Mascot
RCC467	270	468	LTQ Orbitrap XL	Mascot
RCC476	609	463	LTQ Orbitrap XL	Mascot
RCC792	246	291	LTQ Orbitrap XL	Mascot
RCC986	1063	864	LTQ Orbitrap XL	Mascot
RCC990	890	789	LTQ Orbitrap XL	Mascot
RCC1005	503	275	LTQ Orbitrap XL	Mascot
RCC1056	1002	1025	LTQ Orbitrap XL	Mascot
RCC1060	485	879	LTQ Orbitrap XL	Mascot
RCC1083	791	591	LTQ Orbitrap XL	Mascot
RCC1086	516	1281	LTQ Orbitrap XL	Mascot
RCC1117	543	836	LTQ Orbitrap XL	Mascot
RCC1152	1151	641	LTQ Orbitrap XL	Mascot
RCC1157	503	515	LTQ Orbitrap XL	Mascot
RCC1170	490	433	LTQ Orbitrap XL	Mascot
RCC1188	490	274	LTQ Orbitrap XL	Mascot
RCC1192	431	511	LTQ Orbitrap XL	Mascot
RCC1203	727	256	LTQ Orbitrap XL	Mascot
RCC1223	391	432	LTQ Orbitrap XL	Mascot
RCC1238	415	448	LTQ Orbitrap XL	Mascot
RCC1355	605	456	LTQ Orbitrap XL	Mascot
RCC1369	676	478	LTQ Orbitrap XL	Mascot
RCC1397	697	909	LTQ Orbitrap XL	Mascot
RCC1405	425	380	LTQ Orbitrap XL	Mascot
RCC1409	4397	3366	Orbitrap Fusion Lumos	SequestHT
RCC1428	4305	2470	Orbitrap Fusion Lumos	SequestHT
RCC1438	1062	2454	Orbitrap Fusion Lumos	SequestHT
RCC1444	645	742	LTQ Orbitrap XL	Mascot
RCC1479	869	491	LTQ Orbitrap XL	Mascot
RCC1483	372	272	LTQ Orbitrap XL	Mascot
RCC1491	723	788	LTQ Orbitrap XL	Mascot
RCC1493	497	775	LTQ Orbitrap XL	Mascot
RCC1502	603	1199	LTQ Orbitrap XL	Mascot

Supplementary Table 4: Whole blood donors and HLA typing. Tested HLA alleles are underlined

Donor	HLA
J262	A*01, A*02, B*07, B*44
J263	A*02, A*03, B*15, B*51
J265	A*01, A*02, B*08, B*41
J267	A*02, A*29, B*40, B*44
J268	A*02, A*03, B*15, B*51
J269	A*01, B*08, B*35

Supplementary Table 5: HLA Class I TUMAPs of selected target candidates can be found in the Appendix.

Supplementary Table 6: HLA Class I candidates from quantitative analysis can be found in the Appendix.

Supplementary Table 7: HLA Class II TUMAPs of selected target candidates can be found in the Appendix.

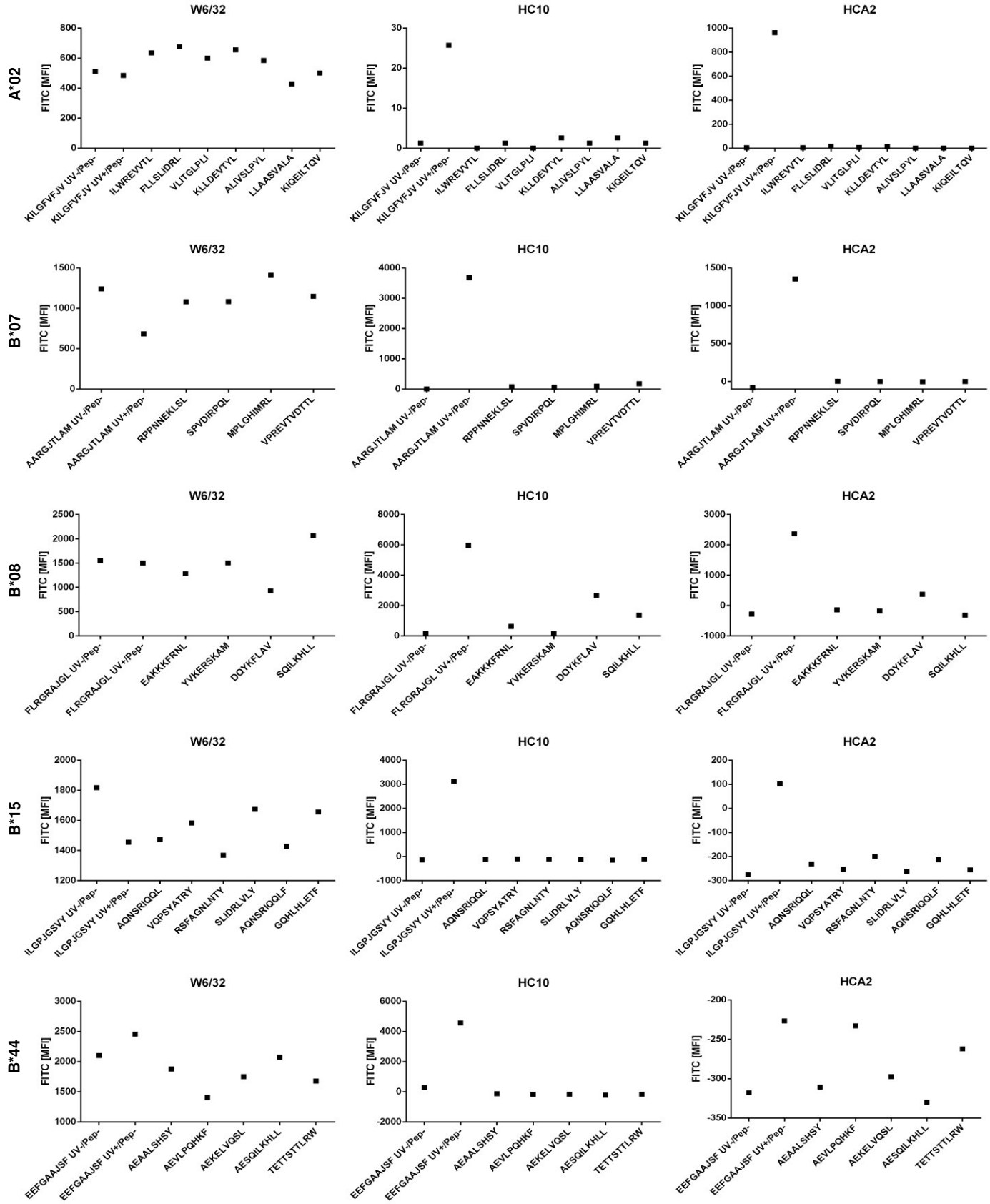

Supplementary Figure 1: Quality control of UV exchanged tetramers. UV-/Pep-: Control, Tetramer with UV-sensitive peptide, UV+/Pep-: misfolded control, Tetramer with UV-sensitive peptide exposed to UV light. mAb HC10 and HCA2 bind to exposed linear structures of unfolded HLA class I molecules. Values were substracted from background staining with mAb GAP-A3.

3. Results and discussion, Part II: Unveiling the peptide motifs of HLA-C and HLA-G from naturally presented peptides and generation of binding prediction matrices

The following part has been accepted for publication in the Journal of Immunology headed "Unveiling the peptide motifs of HLA-C and HLA-G from naturally presented peptides and generation of binding prediction matrices". Authors contributing to this work are listed below. All experiments (exceptions are stated in the following lines), data analysis and manuscript writing was performed by the author of this thesis. Heiko Schuster did the cell sorting, aided to the draft of the project layout and proofread the manuscript. Linus Backert gave bioinformatics support in data analysis and proofread the manuscript. Michael Ghosh supported the cell culture and proofread the manuscript.

Moreno Di Marco*, Heiko Schuster*†, Linus Backert*‡, Michael Ghosh*, Hans-Georg Rammensee*, Stefan Stevanović*

* Department of Immunology, Institute for Cell Biology, University of Tübingen, Tübingen, Germany
† Immatics Biotechnologies GmbH, Tübingen, Germany
‡ Applied Bioinformatics, Department of Computer Science, Center for Bioinformatics, University of Tübingen, Tübingen, Germany

3.1. Introduction

The HLA is a polygenic and polymorphic segment on human chromosome 6 which encodes histocompatibility antigens including the classical (or class Ia) and non-classical (or class Ib) HLA molecules (see section **1.2**). HLA-A, HLA-B and HLA-C belong to the classical HLA molecules which display a high degree of polymorphism. In contrary, HLA-E and HLA-G are considered non-classical HLA molecules showing limited polymorphism [**Table 8**]. Similar to classical HLA molecules, HLA-E and HLA-G are heterodimers consisting of a heavy α-chain and β_2m and take part in the peptide presentation pathway. HLA-C, -E and -G share the ability to interact with NK cell receptors as well as TCRs thereby bridging between innate and adaptive immunity.

Table 8: Characteristics of classical and non-classical HLA class I molecules. *Physiological expression on fetal derived placental cells and immune-privileged organs. Expression is induced in various diseases, such as autoimmune/inflammatory diseases, viral infections, transplantation, cancer, as an immune escape mechanism.

	HLA-A/B	HLA-C	HLA-E	HLA-G(*01)
MHC class	Ia = classical	Ia = classical	Ib = non-classical	Ib = non-classical
Polymorphism	High	High	Limited (non-polymorphic)	Limited (non-polymorphic)
Ligand	Peptide	Peptide	Peptide	Peptide
Binds β2m?	Yes	Yes	Yes	Yes
Binds TCR?	Yes	Yes	Yes	Yes
Binds NK-cell receptors?	Few	Yes	Yes	Yes
Immune activity	Activating	Activating	Inhibiting > activating	Inhibiting > activating
Expression	In most tissues	In most tissues	In most tissues	Tissue-specific expression*
Ligand repertoire	High	High	Low	High

Within the classical HLA molecules, HLA-C plays a special role in the interaction with NK cells. This feature manifests itself in the unusually conserved α1 domain[255] which in combination with a generally less polymorphic region in the α2 domain shape the binding site of killer cell immunoglobulin-like receptors (KIRs). Compared to HLA-A and HLA-B, HLA-C show a lower expression level at the cell surface representing only about 10% of classical HLA molecules. HLA-C allotypes have been implicated in many diseases, including viral infections, cancer or autoimmune disorders with HLA-C restricted epitopes recognized by either CTLs or NK cells. One of the most frequent cancer mutations, KRAS G12D, has been recently shown to be presented by HLA-C*08:02. Moreover, the corresponding epitope is able to induce T cell responses in cancer patients which can be harnessed for adoptive transfer immunotherapy.[256]

Many genetic associations of HLA-C alleles with several diseases have been reported which range from increased protection to higher susceptibility for a certain disease.[257] Last but not least, HLA-C expression on extravillous trophoblasts plays a central role in the development and tolerance of the fetus during pregnancy by interacting with maternal NK cells.[258]

Peptide motifs of HLA-C were first based on pool sequencing and few individual sequences.[259] The first high-throughput approach to determine the binding specificities of a larger set of HLA-C alleles was conducted by Rasmussen *et al.*[260] applying an *in vitro* peptide-HLA class I dissociation assay with synthetic peptides. By using this approach binding motifs for 16 HLA-C allotypes were uncovered, however with often less pronounced anchor residues.

The non-classical HLA-E has been implicated in the presentation of HLA class I leader peptides.[261,262] Its expression level is dependent on the HLA class Ia expression level and previous reports suggest it to be around 5% of the HLA-C expression.[263] The HLA-E-peptide complex acts as ligand for the family of CD94/NKG2 receptors expressed predominantly on NK cells but also on a subset of $CD8^+$ T cells.[264,265] Both, the KIR and CD94/NKG2 receptor family sense changes in HLA expression by interacting with HLA-C or HLA-E, respectively. While the conserved HLA-E-CD94/NKG2 system seems to be specialized in sensing HLA expression levels, polymorphic KIRs are able to detect early changes in the peptide repertoire presented on classical HLA, especially HLA-C.[266-268] HLA-E-CD94/NKG2 interaction has also been associated with fetal-maternal tolerance through inhibition of uterine NK cells by HLA-E expressing extravillous trophoblasts.[269] In addition to the presentation of HLA class I leader peptides, HLA-E is able to present pathogenic epitopes to CTLs.[270,271] However, the peptide binding pocket of HLA-E is highly hydrophobic and thus especially adapted for binding of HLA class I leader peptides. This unusual hydrophobicity within the binding pockets may further restrict the peptide repertoire. In fact, only few peptides could be shown to be presented *in vivo* by HLA-E.

The non-classical HLA-G is mainly expressed on fetal tissue exerting a major tolerogenic function and promoting fetal development.[272] In adults expression of HLA-G is found on immune-privileged organs, including cornea, thymus, pancreatic islets, endothelial, and erythroblasts. In addition, dendritic cells and macrophages may also express HLA-G.[273] Moreover, expression can be induced during various diseases, including cancer, viral infections, inflammatory diseases or autoimmune disorders mainly as an escape strategy to avoid immune recognition. Due to the checkpoint function, HLA-G is considered as an attractive target for anti-cancer treatment using blocking antibodies.[274] On the other hand, HLA-G expression in transplants is associated with better tolerance of the graft.[275] HLA-G interacts with different inhibitory receptors such as Immunoglobulin-like transcript 2 (ILT2) expressed by B cells, subsets of NK and T cells, monocytes and dendritic cells[276], ILT4 which is solely expressed by monocytes and dendritic cells[277] and KIR2DL4 which is expressed mainly on NK cells.[278]

Compared to HLA-E the peptide repertoire of HLA-G is larger but less complex than the peptide repertoire of HLA class Ia molecules.[279] The peptide motif of HLA-G was first defined by Diehl *et al.* from a small set of naturally eluted and pool sequenced peptides exhibiting anchors at position 2 (isoleucine or leucine), position 3 (proline) and position 9 (leucine).[280]

Considering the high importance of HLA-C, -E and -G in many immunological processes the clarification of ligand characteristics of these HLA molecules is of great relevance. In this study, peptide motifs were unveiled *via* comprehensive analyses of naturally presented HLA ligands. HLA presented peptides were analyzed by LC-MS/MS after immunoprecipitation of HLA molecules from transfected C1R cells. The EBV-transformed lymphoblastoid C1R cell line is well suited for this approach due to a functional antigen presentation pathway and low endogenous HLA expression[281,282] and we had applied this approach earlier for monoallelic motif determinations [56-59,283-287], and more recently also by Abelin *et al*.[60] We utilized this approach for the 15 most frequent HLA-C alleles (numbers according to www.allelefrequencies.net[288]) [**Table 9**]. Moreover, for the first time we comprehensively analyzed the peptide pool presented by the non-classical HLA molecules, HLA-E and HLA-G. For all analyzed HLA-C allotypes as well as HLA-G binding motifs were generated by Gibbs clustering.[289] SYFPEITHI[290] matrices were subsequently created for octa-, nona- and decamers and their predictive power has been analyzed in comparison to NetMHCpan-3.0.[291]

Table 9: Most frequent HLA-C alleles within the "Germany pop 8" cohort on allelefrequencies.net comprising data from 39,689 individuals. These alleles were also the most frequent within several other examined populations from different ethnic groups.

Rank	HLA-C	Allele Frequency in German population (n=39,689)
1	C*07:01	14.7%
2	C*07:02	13.4%
3	C*04:01	12.5%
4	C*06:02	10.0%
5	C*03:04	7.4%
6	C*05:01	6.4%
7	C*12:03	6.3%
8	C*02:02	5.4%
9	C*03:03	5.1%
10	C*01:02	3.6%
11	C*15:02	2.6%
12	C*08:02	2.4%
13	C*16:01	2.3%
14	C*14:02	1.5%
15	C*17:01	1.0%

3.2. Materials and methods

3.2.1. DNA vectors

DNA of HLA-C alleles, HLA-E and HLA-G were synthesized and integrated into the pcDNA3.1(+) plasmid utilizing the GeneArt™ gene synthesis service from Thermo Fisher Scientific. Nucleotide sequences were obtained from the IMGT/HLA database[292] for C*01:02:01, C*02:02:01, C*03:03:01, C*03:04:01:01, C*04:01:01:01, C*05:01:01:01, C*06:02:01:01, C*07:01:01:01, C*07:02:01:01, C*08:02:01:01, C*12:03:01:01, C*14:02:01, C*15:02:01, C*16:01:01, C*17:01:01:01, E*01:01:01:01, G*01:01:01:01. Codon usage was adapted to the codon bias of Homo sapiens genes without changing the protein sequence.

Vectors were linearized mixing 50 µg plasmid DNA with 50 µl CutSmart Buffer (NEB, MA, USA), 10 µl PvuI-HF (20,000 U/ml, NEB) and 390 µl ddH_2O and incubating for 2 h at 37°C. Complete linearization was confirmed by agarose gel electrophoresis. DNA was extracted by phenol/chloroform/isoamyl alcohol (Sigma-Aldrich /Merck/Sigma-Aldrich) and precipitated by adding 1/10 volume of 3 M sodium acetate (Roth) and 2.5 volume 100% ethanol (VWR Chemicals, Radnor, PA, USA). The linearized vector was frozen for 2 h at -80°C and afterwards centrifuged at 13000 rpm for 30 min at 4°C. The supernatant was removed and the pellet was dried under sterile conditions. The DNA pellet was solved in 40 µl sterile Ampuwa water and the concentration was determined by Nanodrop at 260 nm (NanoDrop 1000 Spectralphotometer; Peqlab, Erlangen, Germany).

3.2.2. Transfection and Selection

Prior to transfection, C1R cells were washed 3x with cold RPMI1640 (Thermo Fisher Scientific) and resuspended to a final concentration of $40*10^6$ cells/ml. For transfection, 500 µl mycoplasma-free cell suspension was mixed with 10 µg linearized plasmid DNA in a Gene Pulser® electroporation cuvette (0.4 cm gap, BioRad, Hercules, CA, USA). Electroporation was conducted using GenePulser II (BioRad) at 250 V and 975 µF. Afterwards, cells were incubated in 75 cm^2 flasks with 12 ml pre-warmed RPMI1640 + 10% FBS + 1x Penicillin/Streptomycin. Transfected cells were exposed to selection medium 24 h after electroporation by adding 1 mg/ml G418 (Merck) into the culture medium. Selection medium was exchanged twice a week.

3.2.3. HLA expression and cell sorting

HLA cell surface expression was verified by flow cytometry. For this purpose $1*10^6$ cells were washed with FACS buffer and transferred into a 96-well plate (Greiner Bio-One). After an additional wash, cells were incubated with 100 µl of 20 µg/ml of pan-HLA class I-specific monoclonal W6/32 Ab (in house production)[293] or the HLA-E specific monoclonal 3D-12 Ab (BioLegend, San Diego, CA, USA) on

ice for 20 min. Cells were washed twice and subsequently incubated with 100 µl 1:100 polyclonal α-mouse IG-FITC secondary Ab (Agilent Technologies) on ice for 20 min protected from light. After additional three washing steps cells were resuspended in 75 µl FACS buffer. Finally, 7.5 µl 7-aminoactinomycin D (BioLegend) was added to each sample and the cells were analyzed on a FACS Canto II analyzer. Data analysis was performed by FlowJo 10.0.7.

For intracellular staining of the C1R-E*01:01 transfectant, cells were fixed with 100 µl Cytoperm/Cytofix solution for 20 min prior to incubation with respective antibodies. For cell wash, 2% FBS/2 mM EDTA/0.1% saponine/0.5% BSA in PBS was used.

3.2.4. Cell sorting

Cell populations showing high expression of HLA were sorted using a BD FACS Jazz cell sorter (BD Biosciences) following the HLA cell surface staining procedure.

3.2.5. Cell harvest

Cells were cultured up to an amount of $2.5*10^9$ cells and harvested by centrifugation at 1500 rpm for 15 min at 4°C. After two washing steps with cold PBS, cells were collected in a 50 ml centrifugation tube and frozen at -80°C.

3.2.6. Isolation of HLA ligands by immunoaffinity purification

HLA class I molecules were isolated utilizing standard immunoaffinity purification as described in section **2.5.2** employing pan-HLA class I-specific monoclonal W6/32 Ab.

3.2.7. Analysis of HLA ligands by LC-MS/MS

Samples were analyzed by LC-MS/MS on the Orbitrap Fusion Lumos as described in section **2.5.3**.

3.2.8. Database Search and Spectral Annotation

Data was processed against the human proteome as comprised in the Swiss-Prot database (www.uniprot.org, release: September 27th 2013; 20,279 reviewed protein sequences contained) applying the SequestHT algorithm[226] in the Proteome Discoverer (v1.3, ThermoFisher) software as described in section **2.5.4**.

3.2.9. HLA ligands annotation, length distribution, ligand and source proteome overlap

Due to endogenous expression of HLA-B*35:03 and HLA-C*04:01 in C1R cells, isolated HLA ligands of these allotypes had to be excluded from further analysis in order to allow for identification of HLA ligands of the transfected allele. GibbsCluster 1.1[289] is an unsupervised way to cluster peptides in

dependency of their sequence similarity. For each transfectant clustering of nonameric peptides, which represent the most abundant length variant in all analyzed alleles, were carried out. The number of clusters was set to 1-3. A “trash cluster” with a threshold of 0 was incorporated to remove outliers. Sequence weighting type was set to “Clustering”. For all other options default settings were used. Peptide motifs of HLA-B*35:03 and HLA-C*04:01 were previously described[294,295] and could be confirmed performing exemplarily Gibbs clustering of some HLA-B*35:03 or HLA-C*04:01 positive samples of our in-house database containing different samples and corresponding HLA typings. Thus, clusters of these two allotypes could be well distinguished from the previously undefined analysis cluster which was assigned to the transfected HLA. The transfected HLA cluster was visualized employing Seq2Logo 2.0[296] and Kullback-Leibler logo type using default settings. Anchor and auxiliary anchor positions were defined based on respective nonamer clusters which were assigned to the transfected HLA and were subsequently adopted for octa- and decamers. This workaround was necessary since a clear distinction of all three expressed allotypes was not possible in all cases due to low peptide count and higher proportion of non-HLA peptides (Unsupervised clusters show combinations of transfected HLA, HLA-B*35:03 and HLA-C*04:01 motifs). With the exception of HLA-C*01:02 peptide anchor residues did not differ over the different length variants and clusters for octa- and decamers showed no obvious difference to the nonamer cluster. Peptides possessing anchor residues of the assigned transfected HLA cluster were selected from the initial peptide list for 8-11mers and were defined as ligands. SYFPEITHI matrices were determined for 8-10mers using frequencies of amino acids at each position from defined ligands according to established procedures.[290] The length distribution was calculated including 8-11mer ligands. Ligand overlap was determined using the 500 highest expressed ligands of each allele defined by the sum of all precursor areas in all five technical replicates. Source proteome overlap was determined using the source proteins of the respective top 500 presented ligands.

3.2.10. Validation of SYFPEITHI matrices

For SYFPEITHI matrix validation a *k*-fold (*k* = 5) cross-validation was used.[297] For this purpose, peptide lists of each transfected allotype were randomly split into five equal folds, whereby four folds were used as training dataset to determine a SYFPEITHI matrix applying the GibbsCluster approach described above. The fifth fold was used for evaluation of the matrix. Clustering was performed on the fifth fold and peptides in the transfected HLA cluster were defined as true binders, whereas peptides in the other clusters and outliers were defined as false binders for the transfected HLA. Evaluation was performed exemplarily for one nonamer evaluation dataset. Receiver operating characteristic (ROC) curve analysis was conducted to visualize the performance. Area under the curve (AUC) was calculated for each ROC curve. For comparison to NetMHCpan-3.0 commonly used

thresholds were set to decide whether a peptide is defined as binder or not. For SYFPEITHI a threshold of ≥ 60% of the maximal score (defined by the sum of the highest possible scores in each position of the peptide) was set, for NetMHCpan-3.0 a threshold of rank < 2 was employed.

3.3. Results

3.3.1. HLA expression of transfected C1R cells

HLA expression of transfected C1R cells was analyzed by flow cytometry using the pan-HLA class I-specific antibody W6/32. Untransfected C1R cells were included as a negative control to distinguish expression of the transfected HLA from endogenous HLA-B*35:03 and HLA-C*04:01 expression. All transfectants, except C1R-HLA-E*01:01, demonstrated expression of the transfected HLA at the cell surface [**Supplementary Figure 2**]. C1R-HLA-E*01:01, stained by either W6/32 or HLA-E specific antibody 3D-12, exhibited no cell surface expression of transfected HLA-E*01:01. However, intracellular staining of C1R-HLA-E*01:01 with 3D-12 antibody revealed the presence of intracellular pools of HLA-E*01:01. Furthermore, PCR of isolated plasmid DNA and subsequent sequencing of the HLA-E*01:01 locus confirmed the persistence of the transfected gene as well as the correct sequence (data not shown). Since the C1R cell line is HLA-E*01:03^{+298}, which has a higher affinity to HLA class Ia leader peptides[299], this might explain missing expression of transfected HLA-E*01:01 due to a lack of sufficient leader peptides. However, neither HLA-E*01:01 nor HLA-E*01:03 could be detected on the cell surface by flow cytometry which in turn might be reasoned by the overall low expression of endogenous HLA [**Supplementary Figure 2C**]. For all remaining transfected HLA, cell surface expression was sufficient for subsequent characterization of naturally processed and presented HLA ligands.

3.3.2. Peptide motifs of HLA-C

Peptides were obtained after immunoaffinity chromatography of HLA molecules from cell lysates. After separation by reversed-phase liquid chromatography peptides were analyzed by mass spectrometry. GibbsCluster 1.1[289] was used to separate ligands of the transfected HLA from those of endogenously expressed alleles in an unbiased manner [**Supplementary Figure 3**]. For HLA-C*05:01 and HLA-C*08:02 clustering revealed a similar motif to the endogenously expressed HLA-C*04:01. To avoid cross-contamination within the groups, clustering was repeated after exclusion of all peptides extracted from the C1R-HLA-C*04:01 transfectant.

In total, 392 to 3,463 ligands could be identified for respective HLA transfectants possessing the anchor amino acids defined by clustering of nonamers [**Table 10**]. **Figure 25** displays the peptide motifs of the 15 analyzed HLA-C molecules. All HLA-C allotypes share a hydrophobic C-terminal anchor position with differences in the preferred amino acid residues. This varies from aliphatic residues such as valine or leucine in HLA-C*15:02 to aromatic residues phenylalanine and tyrosine in HLA-C*02:02. Most allotypes accept multiple hydrophobic or aromatic anchor residues at the C-terminus, while a few have a clear preference for a single amino acid (e.g. leucine in HLA-C*01:02,

Table 10: HLA ligand yields for each corresponding C1R transfectant and numbers of source proteins. Overlapping ligands and source proteins are removed from the sum of ligands and the sum of source proteins.

	8mers	9mers	10mers	11mers	# ligands	# source proteins	# source proteins (cumulative)
C*01:02	102	987	235	36	1360	1165	1165
C*02:02	116	1533	214	100	1963	1589	2483
C*03:03	91	852	99	38	1080	945	2963
C*03:04	251	1601	176	91	2119	1716	3530
C*04:01	467	1161	153	35	1816	1484	4243
C*05:01	626	1563	249	64	2502	1898	4985
C*06:02	47	870	32	4	953	846	5271
C*07:01	55	310	19	8	392	366	5357
C*07:02	116	589	53	19	777	700	5472
C*08:02	792	2231	330	110	3463	2444	5981
C*12:03	146	1160	53	29	1388	1158	6143
C*14:02	484	1604	313	38	2439	1879	6590
C*15:02	191	1639	56	22	1908	1522	6834
C*16:01	685	1899	106	50	2740	2086	7133
C*17:01	120	418	49	45	632	542	7184
E*01:01	0	5	0	0	5	5	7184
G*01:01	248	1725	204	81	2258	1816	7536
				Sum	**22,197**	**7,536**	

-C*03:03/04 or -C*17:01). The frequency of aromatic residues correlates with the polymorphism at position 116 within the HLA molecules [**Table 11**].[29] Allotypes with a serine at position 116 favor more often aromatic residues at the C-terminal position of the peptide, while phenylalanine, tyrosine or leucine at position 116 may interfere with the binding of aromatic residues. 11 of 15 HLA-C allotypes accept a second anchor shaped by peptide residues at position 2 (HLA-C*02:02, -C*03:03, -C*03:04, -C*06:02, -C*07:01, -C*07:02, -C*12:03, -C*14:02, -C*15:02, -C*16:01 and -C*17:01), while residues at position 3 constitute the second anchor for 4 of 15 HLA-C alleles (HLA-C*01:02, -C*04:01, -C*05:01 and -C*08:02). In contrast to small variations with regard to the C-terminal anchor residues, preferred residues at position 2 or 3 display a high degree of variability. A unique preference of proline in position 3 is favored by HLA-C*01:02. Small aliphatic or hydrophilic residues at position 2 constitute the anchor of HLA-C*02:02, -C*03:03, -C*03:04, -C*12:03, -C*15:02, -C*16:01 and -C*17:01. All of these allotypes possess a tyrosine at position 9 which may inhibit binding of larger anchor residues.[29] Of note, 6 of them favor large aromatic residues at position 1 which may support the interaction provided by the small anchor residue at position 2. Only HLA-C*15:02 displays preferences for basic residues at position 1 which are also able to support the binding of the peptide.

HLA-C*01:02

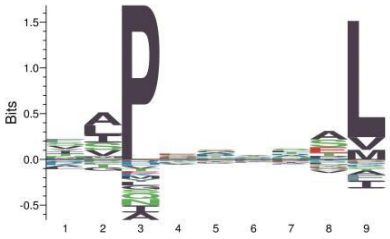

HLA-C*01:02 10mers

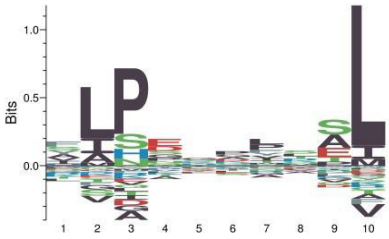

HLA-C*02:02

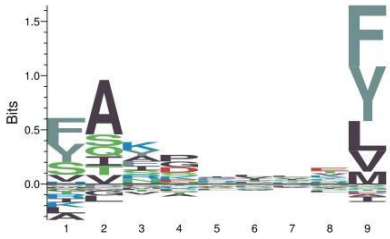

HLA-C*03:03

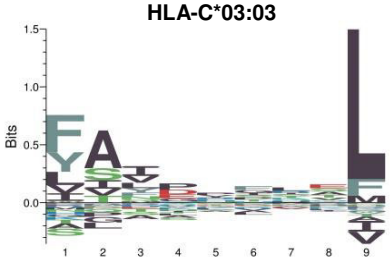

HLA-C*03:04

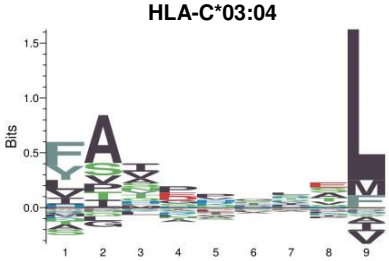

HLA-C*04:01

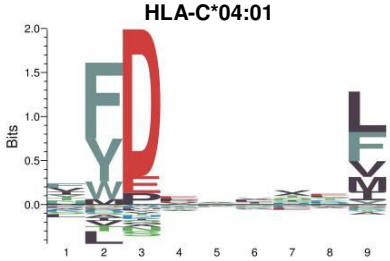

HLA-C*05:01

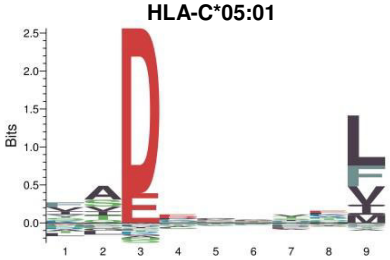

HLA-C*06:02

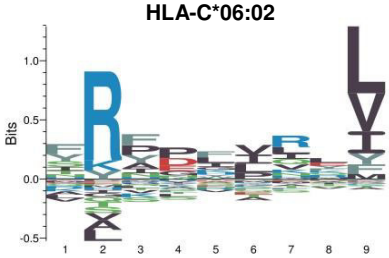

HLA-C*07:01

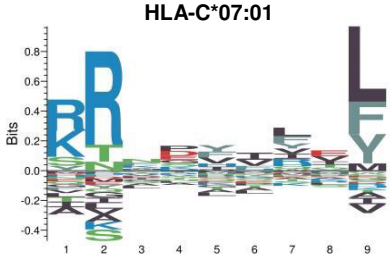

HLA-C*07:02

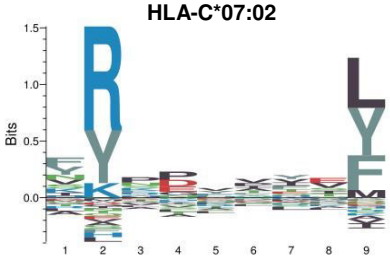

HLA-C*08:02

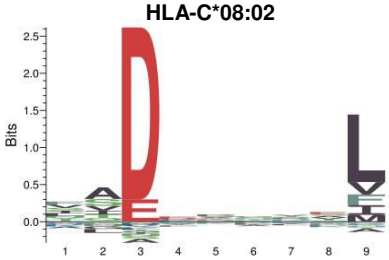

HLA-C*12:03

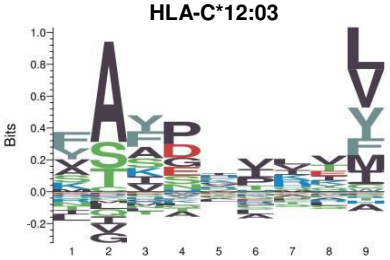

HLA-C*14:02

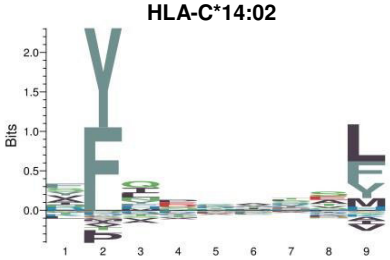

HLA-C*15:02

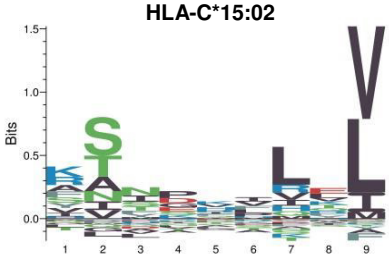

HLA-C*16:01

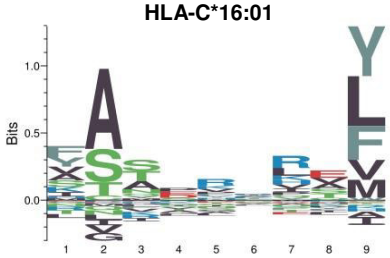

HLA-C*17:01

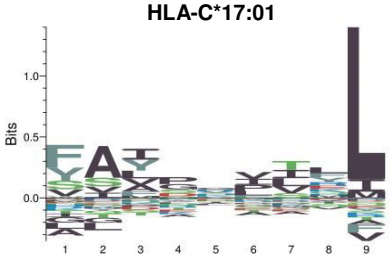

HLA-G*01:01

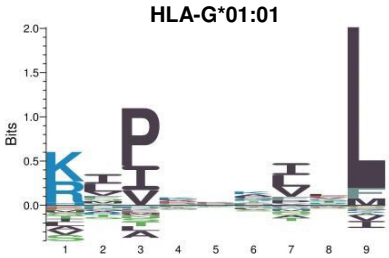

Figure 25: Sequence logos of the clusters corresponding to the transfected HLA allotype visualized using Seq2Logo 2.0.[296] The size of the letter indicates the impact of the corresponding amino acid presented by a given position in either positive or negative fashion. Black = aliphatic residues, gray = aromatic residues, green = hydrophilic residues, blue = basic residues, red = acidic residues.

This may be feasible due to an asparagine at position 66 instead of a lysine which constitutes this position in most allotypes. Within the HLA-C*03 subtypes differences in peptide specificities are marginal. Acidic residues at position 3 form the anchor for HLA-C*04:01, -C*05:01 and -C*08:02. All three molecules combine an asparagine at position 114 and an arginine at position 156. The arginine may serve for electrostatic interaction, whereas the asparagine at position 114 instead of aspartic acid may enable the binding of an acidic residue. While HLA-C*04:01 has a clear preference for aromatic residues at position 2, HLA-C*05:01 and -C*08:02 accept only small residues at this position. An explanation may be the phenylalanine at position 9 of HLA-C*05:01 and -C*08:02 reducing the space to accomodate larger resides.[29] HLA-C*04:01 possesses a serine at this position which may enable the binding of large aromatic residues. Basic anchor residues at position 2 are preferred by HLA-C*06:02, -C*07:01 and -C*07:02. This may be explained by the aspartic acid at position 9 of HLA-C*06:02, -C*07:01 and -C*07:02. Major differences in the peptide specificities of the HLA-C*07 subtypes HLA-C*07:01 and -C*07:02 are revealed at position 1 and the anchor position 2. Both subtypes prefer arginine as anchor residue whereas alternatively accepted anchor residues are threonine or asparagine for HLA-C*07:01 and tyrosine or lysine for HLA-C*07:02. The tyrosine in position 2 of HLA-C*07:02 ligands may be accepted due to a serine at position 99 where usually an aromatic residue is located. Further, HLA-C*07:01 favors basic residues at position 1 whereas HLA-C*07:02 does not have such a preference. As for HLA-C*15:02, the preference for basic residues at position 1 of HLA-C*07:01 ligands can be explained by an asparagine at position 66. Unique to HLA-C*14:02 is its preference for aromatic residues at anchor position 2. Again, a serine at position 9 instead of an aromatic amino acid which is generally placed at this position may enable binding of large aromatic residues. Further allotypes favoring aromatic residues at anchor position 2 are HLA-A*23 and -A*24 which as well possess a serine at position 9. Auxiliary anchors (defined by a percentage share of > 50% of amino acids with similar features) are located at position 1 of HLA-C*03:03, -C*03:04 and -C*17:01 ligands and at position 2 of HLA-C*04:01 ligands with a preference for aromatic residues. Remarkable is the higher frequency of aromatic residues at position 5 and 7 of HLA-C*07:01 and -C*07:02 ligands and at position 8 of HLA-C*17:01 ligands which may be explained by a leucine at position 147 instead of a tryptophan situated in this position in the other allotypes. The preference for aromatic residues at position 5 and 7 of HLA-C*07:01 and -C*07:02 ligands may also be explained by an alanine at position 152 which may provide a larger

Table 11: Polymorphic residues within HLA-C molecules and the position within the peptide interacting with respective residue.[27,29] Boldface: Polymorphic residues which may explain differences in the peptide motifs.

	Polymorphic residues within HLA-C molecules															
Allotype	9	24	66	73	77	80	95	97	99	114	116	143	147	152	156	163
C*01:02	**F**	S	K	T	S	N	L	W	C	D	Y	T	W	E	R	T
C*02:02	**Y**	A	K	T	N	K	L	R	Y	D	**S**	T	W	E	W	E
C*03:03	**Y**	A	K	T	S	N	I	R	Y	D	Y	T	W	E	L	L
C*03:04	**Y**	A	K	T	S	N	I	R	Y	D	Y	T	W	E	L	L
C*04:01	**S**	A	K	A	N	K	L	R	F	**N**	F	T	W	E	**R**	T
C*05:01	**Y**	A	K	T	N	K	L	R	Y	**N**	F	T	W	E	**R**	T
C*06:02	**D**	S	K	A	N	K	L	W	Y	D	**S**	T	W	E	W	T
C*07:01	**D**	S	**N**	A	S	N	L	R	Y	D	**S**	T	**L**	**A**	L	T
C*07:02	**D**	S	K	A	S	N	L	R	**S**	D	**S**	T	**L**	**A**	L	T
C*08:02	**Y**	A	K	T	S	N	L	R	Y	**N**	F	T	W	E	**R**	T
C*12:03	**Y**	A	K	A	S	N	L	W	Y	D	**S**	T	W	E	W	T
C*14:02	**S**	A	K	T	S	N	L	W	F	D	**S**	T	W	E	R	T
C*15:02	**Y**	A	**N**	T	N	K	I	R	Y	D	L	T	W	E	L	T
C*16:01	**Y**	A	K	T	S	N	L	W	Y	D	**S**	T	W	A	Q	T
C*17:01	**Y**	A	K	A	N	K	I	R	Y	N	F	S	**L**	E	L	E
	2	2	1-4/6	5-8	7/8	8/9	9	3/5/6/9	2/3	3/5-7	5/7/9	9	5/7-9	3/5-7	3-7	1/2/4
	Position in Peptide interacting with respective residue															

pocket for residues at position 5 and 7 of the ligands, a feature not shared by HLA-C*17:01. Exceptional to HLA-C*01:02 is its change at the anchor position 3 with proline for octameric and nonameric HLA ligands to a shared anchor with aliphatic residues at position 2 and proline, serine or histidine at position 3 for longer ligands. In sum, peptide motifs of all analyzed HLA-C molecules could be identified and are in agreement with our knowledge of allotype specific pocket characteristics. All HLA allotypes that have been analyzed in this study prefer nonameric ligands with frequencies varying from 62.5% to 91.3% [**Figure 26**]. Octamer frequency ranges from 4.9% to 25.0%. Decamers and undecamers were less frequent with 2.9% to 17.3% or 0.4% to 7.1%, respectively.

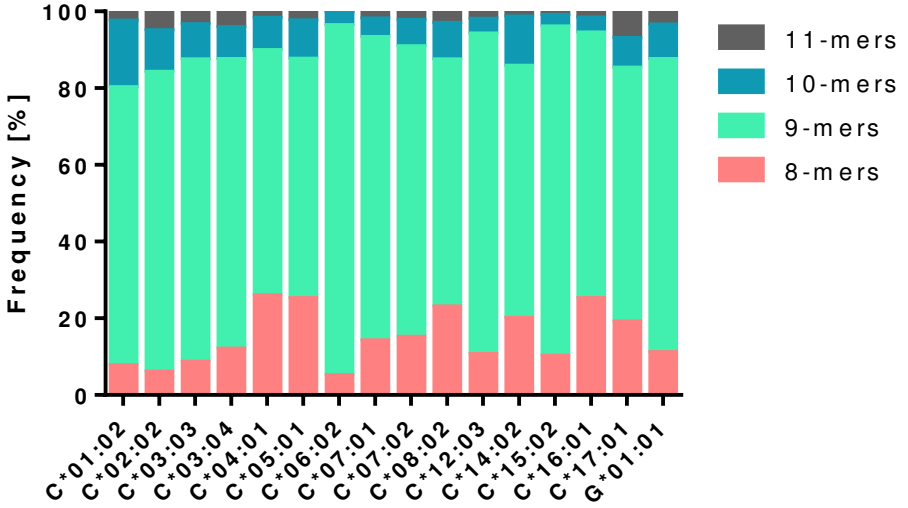

Figure 26: Length distribution of HLA-C and HLA-G alleles.

3.3.3. HLA-C in the context of the supertype concept

The concept of grouping HLA allotypes into supertypes depending on their main anchor specificities was introduced in 1995.[287,300] In sum, nine supertypes could be defined covering most of the HLA-A and HLA-B alleles: HLA-A*01, -A*02, -A*03, -A*24, -B*07, -B*27, -B*44, -B*58, -B*62.[301,302] In 2004, Doytchinova *et al.* applied a bioinformatics approach based on structural similarities between allotypes integrating also the HLA-C alleles.[303] Using this strategy, two HLA-C supertypes could be defined, named C1 and C4. Supertype C1 was defined by a serine or glycine at position 77, whereas C4 supertypic allotypes possess an asparagine at this position. Allotypes from our study belonging to the C1 supertype are HLA-C*01:02, -C*03:03, -C*03:04, -C*07:02, -C*08:02, -C*12:03, -C*14:02 and -C*16:01. Whereas HLA-C*02:02, -C*04:01, -C*05:01, -C*06:02, -C*07:01, -C*15:02 and -C*17:01 belong to the C4 supertype. However, this definition is not in line with the peptide motifs of HLA-C allotypes unveiled here [**Figure 25**]. Considering the peptide motifs of HLA-C we propose now a new categorization into five groups. Three of these groups may be integrated into HLA-A and HLA-B supertypes (HLA-C*02:02, -C*03:03, -C*03:04, -C*12:03, -C*15:02, -C*16:01 and -C*17:01 into the

A*01, B*58 or B*62 supertype, and HLA-C*14:02 into the A*24 supertype, HLA-C*06:02, -C*07:01 and -C*07:02 into the B*27 supertype). Allotypes with an anchor at position 3 may deserve additional supertype definitions. A C*01 supertype with proline at position 3 and aliphatic residues at the C-terminus may account for the uniqueness of HLA-C*01. A C*04 supertype would integrate HLA-C*04:01, -C*05:01 and -C*08:02 into the supertype concept.

3.3.4. Characteristics of HLA-E and HLA-G ligands

HLA-E*01:01 transfected C1R cells present two HLA class I leader peptides, namely VMAPRTL**I**L derived from HLA-C*04:01 and VMAPRTL**V**L derived from HLA-A*02:01. The latter one is to some extent surprising because there is no evidence for surface expression of HLA-A*02:01 in C1R.[281,304] VMAPRTL**V**L was detected in every C1R transfectant (Note: C1R is HLA-E*01:03^{+}) ensuring that it is not a false positive but most probably derived from a DRiP. Overall three additional HLA class I leader peptides VMAPRTL**L**L (HLA-C*02:02 and -C*15:02), VMAPR**A**LLL (HLA-C*07:01 and -C*07:02) and VMAPRTL**F**L (HLA-G*01:01) were detected which are presented by HLA-E*01:03. MHC class I leader peptides of HLA-B*35:03 (V**T**APRTVLL) and HLA-C*17:01 (VMAP**QA**LLL) are not presented by HLA-E*01:01 (Note: only HLA-B*35:03 signal sequence could have been expressed on C1R-E*01:01) or the endogenously expressed HLA-E*01:03. This discrimination of peptides with one or two amino acid changes, mostly in positions contributing less to the interaction to HLA, illustrates the adaption of HLA-E in HLA leader peptide presentation and its restricted peptide repertoire.

HLA-G*01:01 reveals a marked peptide motif with anchors at position 3, composed of proline, isoleucine and valine, and at the C-terminal position (Ω) formed by leucine. An auxiliary anchor with lysine and arginine is shaped at position 1. Hydrophobic residue preferences show up at position 2 and position Ω-2 [**Figure 25**]. Contrary to HLA-E, HLA-G*01:01 exhibits a large peptide binding repertoire with 2258 identified ligands eluted solely from HLA-G*01:01 transfected C1R cells.

3.3.5. Ligand overlap

In order to look for ligand overlap across the analyzed allotypes the top 500 most abundant ligands (defined by the sum of the area under the curve values of five technical replicates) of each HLA molecule were integrated. For HLA-C*07:01 only 392 ligands could be considered [**Table 12**]. The overlap in HLA presented peptides among allotypes with clearly distinguishable peptide motifs (one or both anchor residues are different) was marginal with a maximal overlap of 2.46% between HLA-C*03:04 and HLA-C*08:02. Allotypes with consistent anchor residue preferences display higher overlap within the presented peptides ranging from 3.20% between HLA-C*07:02 and HLA-C*14:02 and up to 11.98% between HLA-C*02:02 and HLA-C*12:03. Notably HLA-C*05:01 and HLA-C*08:02

Table 12: Ligand overlap [%] of the top 500 HLA ligands of each allele. Ligand overlap was determined using the top 500 ligands of each allele defined by the sum of area in all five technical replicates. Crossed out numbers are not representative.

C*01:02	0.10	0.10	0.10	0.00	0.00	0.10	0.11	0.10	0.00	0.20	0.60	0.10	0.00	0.20	0.70
	C*02:02	7.53	6.38	1.63	0.00	0.00	0.90	0.00	0.00	11.98	0.00	2.25	5.82	4.82	0.00
		C*03:03	42.86	1.01	1.52	0.00	1.02	0.00	1.73	5.26	0.00	3.41	6.38	8.70	0.30
			C*03:04	1.32	2.15	0.00	0.79	0.00	2.46	3.73	0.00	3.41	7.41	6.16	0.10
				C*04:01	~~0.00~~	0.00	1.13	0.00	~~0.00~~	0.60	0.00	0.50	1.01	1.63	0.00
					C*05:01*	0.00	0.00	0.00	27.39	0.00	0.00	0.30	0.00	0.50	0.00
						C*06:02	3.96	5.26	0.00	0.00	0.60	0.00	0.00	0.00	0.40
							C*07:01**	10.12	0.00	1.13	0.00	1.02	0.56	0.00	0.22
								C*07:02	0.00	0.00	3.20	0.00	0.00	0.00	0.30
									C*08:02*	0.00	0.00	0.40	0.00	0.20	0.00
										C*12:03	0.00	3.41	7.64	3.31	0.00
											C*14:02	0.00	0.00	0.00	1.42
												C*15:02	2.67	2.88	0.40
													C*16:01	2.56	0.00
														C*17:01	0.20
															G*01:01

* C1R-C*04:01 peptides removed
** only 392 ligands

show a high overlap, sharing 27.39% ligands. Comparison to HLA-C*04:01 is limited due to endogenous expression of the allotype on C1R and its similarity to HLA-C*05:01 and -C*08:02. Since peptides from C1R-C*04:01 had to be excluded for ligand definition of HLA-C*05:01 and -C*08:02 the overlap is consequently 0. Nevertheless, overlap of HLA-C*05:01 and HLA-C*08:02 to HLA-C*04:01 should be markedly lower since HLA-C*04:01 favors large aromatic residues in position 2 whereas HLA-C*05:01 and HLA-C*08:02 prefer small residues. In fact, including intrinsic HLA-C*04:01 ligands (no exclusion of peptides of C1R-C*04:01 from C1R-C*05:01 and -C*08:02 peptide lists) the overlap is higher between HLA-C*05:01 and -C*08:02 with 40.45% compared to 26.26% between HLA-C*04:01 and -C*05:01 or 25.31% between HLA-C*04:01 and -C*08:02, respectively. High overlap is seen between the HLA-C*03 subtypes HLA-C*03:03 and HLA-C*03:04 with 42.86% of shared ligands. The HLA-C*07 subtypes HLA-C*07:01 and HLA-C*07:02 display with 10.12% a rather small overlap within their ligands compared to the HLA-C*03 subtypes which can be explained by differences in the preferred residues in anchor position 2. In general, ligand overlap is marginal within HLA allotypes unless the same anchor residues are shared.[305]

3.3.6. Source proteome overlap

Theoretically all proteins within a cell may be used as source for peptide presentation. However, different factors such as source protein expression level, antigen processing and transport efficiency and affinity of the peptide to the HLA and their stability may select for a smaller set of source proteins which are presented by one allotype. The source proteins of the 500 most abundant ligands were selected for the overlap analysis of the source proteome [**Table 13**]. The source protein overlap was the highest for allotypes with a high ligand overlap which is obvious since the overlapping ligands derive from the same source protein. More interesting is the overlap of the source proteome added by non-overlapping ligands. In fact, the additional overlap contributed by non-overlapping ligands is comparable within all allotypes, independent of their peptide motifs, with a median increase of 5.42%. This allotype- and also subtype-independent low increase in the source proteome overlap displays the high diversification which is added by an additional HLA molecule.

3.3.7. Performance of established SYFPEITHI matrices

Identified peptides were used to establish SYFPEITHI matrices. Therefore peptides were clustered using GibbsCluster 1.1.[289] Anchor positions and residues were defined from clusters of the transfected HLA. Peptides harboring predefined anchor residues were defined as ligands and were used to establish SYFPEITHI matrices [**Supplementary Figure 3, Appendix 8.2**]. In order to examine the performance of the established SYFPEITHI matrices *5*-fold cross-validation was performed.[297]

Table 13: Source proteome overlap [%]. Source proteins of the top 500 expressed HLA ligands, defined by the sum of area in all five technical replicates, were included.

C*01:02	4.73	4.79	5.95	4.59	5.63	5.26	3.95	5.36	7.33	5.47	5.80	5.37	7.09	4.98	5.59
	C*02:02	13.07	14.00	7.56	7.82	5.65	5.81	5.88	8.18	17.30	5.96	8.45	11.90	9.70	5.38
		C*03:03	41.70	7.33	6.83	4.86	4.93	4.03	7.95	10.67	7.75	10.18	11.20	13.76	6.39
			C*03:04	9.21	8.72	4.72	5.71	4.95	9.60	9.83	6.72	11.36	12.79	11.86	7.10
				C*04:01	7.65	5.37	5.91	5.12	8.52	6.83	5.56	7.76	7.25	7.65	5.23
					C*05:01	5.83	5.89	6.19	32.49	6.44	7.30	7.51	6.49	4.68	4.83
						C*06:02	9.21	10.45	6.56	5.43	6.99	5.82	5.13	4.81	6.51
							C*07:01	13.51	5.18	5.57	4.99	5.74	4.96	4.74	5.44
								C*07:02	5.31	3.86	7.10	5.44	4.88	5.05	5.66
									C*08:02	7.31	7.27	9.46	7.61	4.67	6.03
										C*12:03	7.12	9.29	13.36	7.86	5.16
											C*14:02	7.02	5.67	4.74	6.84
												C*15:02	9.44	8.71	6.91
													C*16:01	7.90	4.98
														C*17:01	5.04
															G*01:01

For that purpose, the initial peptide list of each analyzed transfectant was split into five parts. Four parts were used for clustering and subsequent definition of the SYFPEITHI matrix, while one part remained to validate the matrix. Peptides in the cluster corresponding to the transfected HLA were defined as true binders whereas peptides of the other clusters and peptides fitting to no cluster were defined as false binders. ROC points were calculated in 5% steps of the SYFPEITHI maximal score. AUC values extend from 0.88 for HLA-C*14:02 and HLA-C*17:01 to 0.97 for HLA-C*01:02 nonamer matrix. Only the HLA-C*16:01 matrix performed less good with an AUC = 0.78 [**Supplementary Figure** 4]. In conclusion, the performance of the matrices is excellent for discrimination of true and false binders within the dataset.

3.3.8. Comparing SYFPEITHI and NetMHCpan-3.0 binding predictions

SYFPEITHI[290] and NetMHC[291,306] are commonly used tools for HLA binding predictions. However, both prediction tools are based on different strategies. SYFPEITHI uses a position based matrix scoring system depending on amino acid frequencies at each position and the definition of anchor and auxiliary anchor positions utilizing naturally eluted HLA ligands. In contrast, NetMHCpan-3.0 uses artificial neural networks which were trained on quantitative *in vitro* binding data of peptides-HLA class I complexes from IEDB.[307] Thus, all ligands are also binders, but peptides identified to be binders *in vitro* are not necessarily natural ligands. To compare both prediction tools peptides of each transfectant were split into true or false binders for the transfected HLA by clustering (peptides of the transfected HLA cluster = “true binders”, other peptides = ”false binders”). Commonly used thresholds for binder definition were used with ≥ 60% of the maximal score for SYFPEITHI and Rank < 2 for NetMHCpan-3.0. The rate of false positive (FP) and true positive (TP) predicted binders is illustrated in **Figure 27** for all analyzed allotypes except for HLA-E*01:01. SYFPEITHI illustrates a powerful prediction with a high TP rate ranging from 0.66 to 0.91 and a low FP rate ranging from 0.00 to 0.22. Only the nonameric matrix for HLA-C*14:02 with a FP rate of 0.54 performed poorly which can be explained by their motif similarities to HLA-C*04:01 (endogenously expressed by C1R) at position 2 (anchor and auxiliary anchor, respectively, preferring aromatic residues) and anchor position 9. NetMHCpan-3.0 exhibits higher TP rates between 0.71 and 0.97 but at the same time higher FP rates between 0.07 and 0.65. Similar to SYFPEITHI, NetMHCpan-3.0 prediction for HLA-C*14:02 performs with a FP rate of 0.72. The highest disparity is seen for HLA-G*01:01 with a TP rate of 0.91 and a FP rate of 0.05 for SYFPEITHI and a TP rate of 0.67 and a FP rate of 0.65 for NetMHCpan-3.0. Hence, NetMHCpan-3.0 displays a rather random prediction. In conclusion, the performance of the established SYFPEITHI matrices could be confirmed by comparison to NetMHCpan-3.0. SYFPEITHI outperformed with higher precision for all allotypes [**Figure 28**].

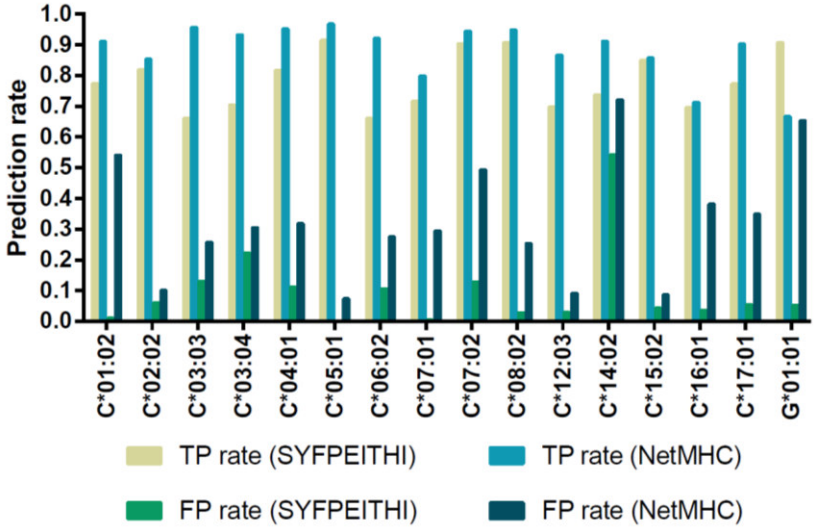

Figure 27: Performance of SYFPEITHI matrices and NetMHCpan-3.0 prediction. Dataset of each transfectant was divided into true and false binders to the respective HLA using unbiased clustering. Peptides in cluster of the corresponding transfected HLA were defined as true binders; peptides in clusters representing the endogenously expressed HLA molecules were defined as false binders of the transfected HLA. Peptides were defined as ligands with a SYFPEITHI score of ≥ 60% or NetMHCpan-3.0 Rank < 2. TP = true positive, FP = false positive.

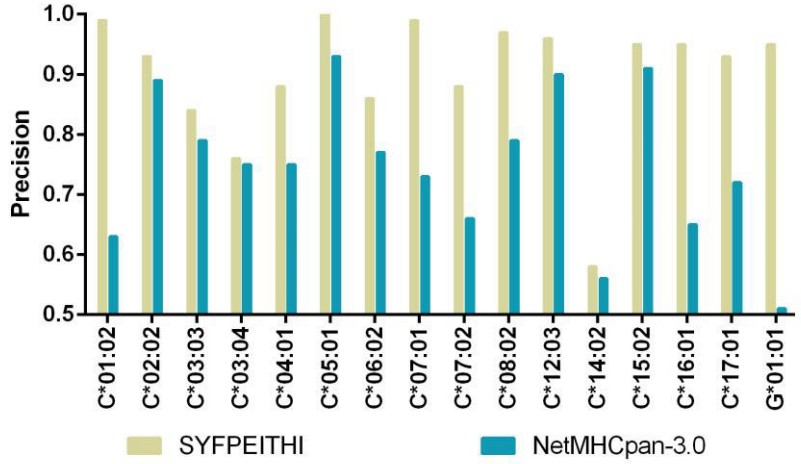

Figure 28: Precision of SYFPEITHI and NetMHCpan-3.0. The precision is defined by the true positive rate divided by the sum of true and false positives (= TP/TP+FP)

3.4. Discussion

It is not only the definition of the binding specificities of classical but often underestimated HLA-C alleles and the non-classical HLA-E and HLA-G, which is of great importance. With regard to their roles in many diseases, like cancer, viral infections, inflammatory diseases, autoimmune disorders and transplantation, naturally processed and presented HLA ligands may contribute to our understanding of disease and foster approaches for intervention.

3.4.1. HLA-C

In this study, the peptide motifs of the 15 most frequently represented HLA-C alleles were comprehensively analyzed using mass spectrometry based characterization of naturally presented HLA ligands [**Figure 25**]. Due to the low expression of HLA-C[308-312], it is hardly feasible to determine the peptide motifs in a system with simultaneous normal expression of HLA-A and -B in an unsupervised clustering approach. Hence, the lymphoblastoid C1R cell line with a low endogenous expression of HLA-B*35:03, which is strongly repressed due to a point mutation in the translation initiation codon[281], and HLA-C*04:01 was utilized to uncover the peptide motifs of HLA-C alleles.

The ligand yields encompass a wide range, which is owed to differences in the expression levels, but may also be caused by performance variances of mass spectrometric measurements. Nevertheless, yields of extracted HLA ligands were sufficient for all alleles to determine the binding motif of predominating nonamers in an unsupervised manner utilizing GibbsCluster 1.1.[289] Peptide yields for less frequent length variants were in some cases insufficient leading to contaminated clusters of the transfected HLA with peptides from the endogenously expressed HLA molecules. However, except for HLA-C*01:02 no changes in the preferred anchor residues emerged between the less frequent lengths and nonamers. Therefore, anchor residues were defined from the cluster of nonamers and assigned to the other length variants. This was helpful for the definition of ligands of all length variants. For HLA-C*01:02 additional anchor residues for longer length variants were included.

A common feature of all allotypes is their preference for hydrophobic and/or aromatic residues at the C-terminal position similar to HLA-B, whereas some HLA-A allotypes accept basic amino acids as C-terminal anchors. The restricted repertoire of anchor residues at the C-terminal position could be a result of the proximity to the interaction side of KIRs with HLA-C. KIRs interact with residues α73 to α90 of the HLA molecule[313,314] which are less polymorphic in HLA-C compared to HLA-A and -B. This region is also mainly involved in the C-terminal anchor contacts.[29] The low polymorphism of the α2 domain of HLA-C molecules restricts the binding repertoire of HLA-C alleles reducing the number of potential ligands. This appears at a glance to be rather unfavorable for the body's defense, since in theory fewer pathogen-derived or tumor-associated antigens could be presented on HLA-C

molecules. This low polymorphism could be associated with the particular role of HLA-C in delivering inhibitory signals to NK cells to ensure self-tolerance. HLA-C alleles guarantee NK cell inhibition in every individual regardless of their HLA allele combination, since compared to HLA-A and -B (only few alleles show epitopes for KIR recognition) all HLA-C molecules have either the C1 or C2 epitope for KIR recognition.[315,316] Thereby, HLA-C allows combinatorial diversity of HLA-A and -B molecules and a still sufficient broad binding repertoire within the population without the disadvantage of a loss of self-tolerance due to missing-self signals.

The anchors in position 2 or 3, respectively, display high variability and thus contribute most to the peptide repertoire of HLA-C alleles. Based on the motif variability five groups can be determined: 1) small residues in position 2 of HLA-C*02:02, -C*03:03, -C*03:04, -C*12:03, -C*15:02, -C*16:01 and -C*17:01, 2) acidic residues in position 3 of HLA-C*04:01, -C*05:01 and -C*08:02, 3) basic residues in position 2 of HLA-C*06:02, -C*07:01 and -C*07:02, 4) proline in position 3 of HLA-C*01:02 and 5) aromatic residues in position 2 of HLA-C*14:02. Interestingly, small residues in position 2 are often attended by aromatic residues in position 1 or 3 which may stabilize the binding of the position 2 anchor. A striking change in the peptide motif is seen for longer length variants of HLA-C*01:02 where the auxiliary anchor in position 2 almost reaches the importance of the anchor at position 3.

The predominating length variant in HLA-C is 9 aa. However, a higher rate of shorter HLA ligands were obtained for HLA-C*04:01, -C*05:01, -C*07:01, -C*07:02, -C*08:02, -C*14:02, -C*15:02 and -C*17:01. Interestingly, 6 of 8 listed allotypes prefer charged or aromatic anchor residues leading to the assumption that stronger interaction with the HLA molecule by charged or aromatic anchor residues may stabilize shorter peptides in the binding pocket.

Peptide overlap was generally low among the HLA alleles ranging from 0% in allotypes with non-overlapping motifs (Note: C-terminal anchor has low variance throughout the HLA-C alleles) to 10.86% in allotypes with similar motifs (HLA-C*02:02 and HLA-C*12:03). This underlines the distinct peptide repertoire of allotypes with similar binding specificities, a feature that has also been reported for members of the HLA-B*44 supertype.[305] However, high overlap is observed between HLA-C*05:01 and HLA-C*08:02 displaying peptide motifs which are virtually indistinguishable from each other. On the other hand, HLA subtypes usually demonstrate a high degree of binding similarity (41.24% peptide overlap between HLA-C*03:03 and HLA-C*03:04). Exceptional is the lower promiscuity (8.12%) in the HLA-C*07 subtypes HLA-C*07:01 and -C*07:02 caused primarily by distinct differences in the favored anchor residues in position 2 and differences in position 1 (basic auxiliary anchor in HLA-C*07:01 or uncharged residues in HLA-C*07:02, respectively).

The source proteome overlap of the top 500 ligands of each allotype was particularly increased by overlapping ligands. A limitation is the consideration of only the source proteome of the top 500 ligands which will underestimate the source proteome overlap since the probability for further included ligands (up to 3463 ligands were detected for one HLA molecule [**Table 10**]) to derive from already included source proteins is higher. However, this was necessary due to high variations in the ligand yields. Including the source proteins of all ligands the source proteome overlap of non-overlapping ligands would increase from 5.42% to approximately 10%. This percentage still illustrates the high diversification added by a second allotype, including subtypes.

The SYFPEITHI matrices resulting of this work reveal high TP prediction rates for HLA-C ligands in combination with a low FP prediction rate, whereas NetMHCpan-3.0 generally gains slightly higher TP rates which are often accompanied by a high FP rate. This high FP rate is problematic in that HLA-C*04:01 and HLA-B*35:03 peptides used for this comparison (endogenously expressed by C1R) exhibit distinguishable anchor residues. In general, SYFPEITHI prediction is more conservative (lower TP rates but outperforming low FP rates) than binding prediction with NetMHCpan-3.0 coming along with a higher precision.

The importance of HLA-C becomes apparent in that several peptides of tumor associated antigens are known to be presented by HLA-C and are recognized by $CD8^+$ T cells. HLA-C ligands which are known to be recognized by $CD8^+$ T cells arise from the shared tumor specific antigens MAGE[317-320], BAGE[321], GAGE[322] and NY-ESO1[323], the differentiation antigens DCT, PMEL[324] and SLC45A3[325], the overexpressed antigen TPBG[326], and the antigen PARP12[327]. Indeed, SAFPTTINF (MAGEA1) and VYPEYVIQY (PARP12) were also found within our dataset. Furthermore, neoepitopes are known arising from KRAS[328] or MUM2[329]. Within our dataset further peptides of tumor associated antigens (according to [330]) were found to be presented by HLA-C alleles which may be targets of $CD8^+$ T cells and NK cells [**Table 14**].

3.4.2. HLA-E

C1R cells transfected with HLA-E*01:01 exhibit no increase in cell surface expression, although successful transfection was demonstrated by sequencing. This is in line with results of Braud *et al.*[298] revealing a correlation of HLA-E surface expression with the presence of HLA molecules. In fact, the presentation of the HLA-C*04:01 signal peptide VMAPRTLIL was higher in C1R transfected with an HLA allele harboring the same signal peptide (HLA-C*01:01, -C*03:03, -C*03:04, -C*05:01, -C*06:02, -C*08:02, -C*12:03, -C*14:02 and -C*16:01) compared to HLA-E*01:01 transfected cells (not shown).

In accordance to Braud *et al.*[298] only HLA signal peptides, in total five, could be found to be presented by HLA-E looking for recurring sequence similarities throughout the transfectants after the exclusion

of HLA-B*35:03 and HLA-C*04:01 ligands (Clustering did also not work). However, some conventional peptides from pathogens[331-334] and a prostate cancer-associated antigen[335] were reported to elicit HLA-E-dependent T cell responses. Furthermore, a broader binding repertoire of HLA-E was reported with similarities to the HLA-A*02 binding motif in TAP-deficient K562 cells.[336]

3.4.3. HLA-G

In contrast to HLA-E*01:01, HLA-G*01:01 displayed a much larger peptide repertoire with over 2200 detected HLA ligands including peptides of tumor associated antigens such as PSA, Cyclin B1, Sperm protein 17 and LCK [**Table 14**] which may elicit inhibitory effects on T and NK cells. The peptide motif displays unusual and highly specialized binding preferences. In contrast to the conclusion made by

Table 14: HLA-C and HLA-G ligands of tumor associated antigens according to Cheever *et al.*[330] and the allotype by which the ligand is presented. Proteins in brackets may be also the source of the HLA ligand.

Protein	Uniprot ID	Ligand	HLA
MAGEA3	P43357	FQAALSRKV	C*02:02
MAGEA3	P43357	FVQENYLEY	C*02:02
MAGEA3	P43357	TFPDLESEF	C*14:02
MAGEA3	P43357	NYPLWSQSY	C*14:02
TP53	P04637	TAKSVTCTY	C*02:02
PSMA	Q04609	FTEIASKF	C*12:03
gp100/PMEL	P40967	HFLRNQPL	C*14:02
PSA	P55786	ISTVEVLKV	C*15:02
PSA (PSAL)	P55786	VVPKDRVAL	G*01:01
PSA	P55786	RSPVYLTVL	G*01:01
Cyclin B1	P14635	VQDLAKAV	C*05:01/C*08:02
Cyclin B1	P14635	FRLLQETMY	C*07:02
Cyclin B1	P14635	VQVQMKFRL	G*01:01
RhoC (RhoA)	P08134	FSIDSPDSL	C*03:03
RhoC	P08134	MATRAGLQV	C*15:02
RhoC (RhoB)	P08134	KTKEGVREV	C*15:02/C*16:01
SART3	Q15020	YIDFEMKI	C*05:01
SART3	Q15020	IGDPARIQL	C*05:01
SART3	Q15020	NADFAKLFL	C*08:02
SART3	Q15020	IFSNRGDF	C*14:02
SART3	Q15020	VAAATYKTM	C*16:01
SART3	Q15020	AAFTRALEY	C*16:01
Sperm protein 17	Q15506	RIPQGFGNLL	G*01:01
LCK	P06239	ITFPGLHEL	C*07:01/C*12:03/C*15:02
LCK	P06239	FYISPRITF	C*14:02
LCK	P06239	KTPSGIKL	G*01:01
B7H3	Q5ZPR3	FSPEPGFSL	C*01:02
B7H3	Q5ZPR3	LFDVHSVL	C*04:01
B7H3	Q5ZPR3	VAAPYSKPSM	C*16:01

Diehl *et al.*[280] assuming three anchor residues (I/L in position 2, P in position 3 and L in position 9), our results indicate that position 2 seems to be less important for peptide binding. The preferred length of HLA-G*01:01 ligands is 9 aa with a sparse peptide overlap to the analyzed HLA-C alleles. The SYFPEITHI matrix for nonameric HLA-G*01:01 reveals a strong performance with a TP rate of 0.91 and a FP rate of 0.05 using the C1R-HLA-G*01:01 peptide dataset, whereas NetMHCpan-3.0 exhibits a random prediction with a TP rate of 0.67 and a FP rate of 0.65. In summary, the peptide motif of HLA-G*01:01 was uncovered making use of over 2200 HLA-G*01:01 ligands. The SYFPEITHI matrix for nonamers outperforms prediction by NetMHCpan-3.0.

3.5. Acknowledgements

This study was granted by the ICEPHA graduate school Tübingen-Stuttgart, the European Union (ERC AdG339842 Mutaediting) and the Deutsche Forschungsgemeinschaft (DFG, SFB 685 and GRK 794). The authors thank Claudia Falkenburger, Zsofia Bittner and Martin Laure for supporting some of the cell culture experiments and Beate Pömmerl for PCR of isolated plasmid DNA.

3.6. Supplementary data

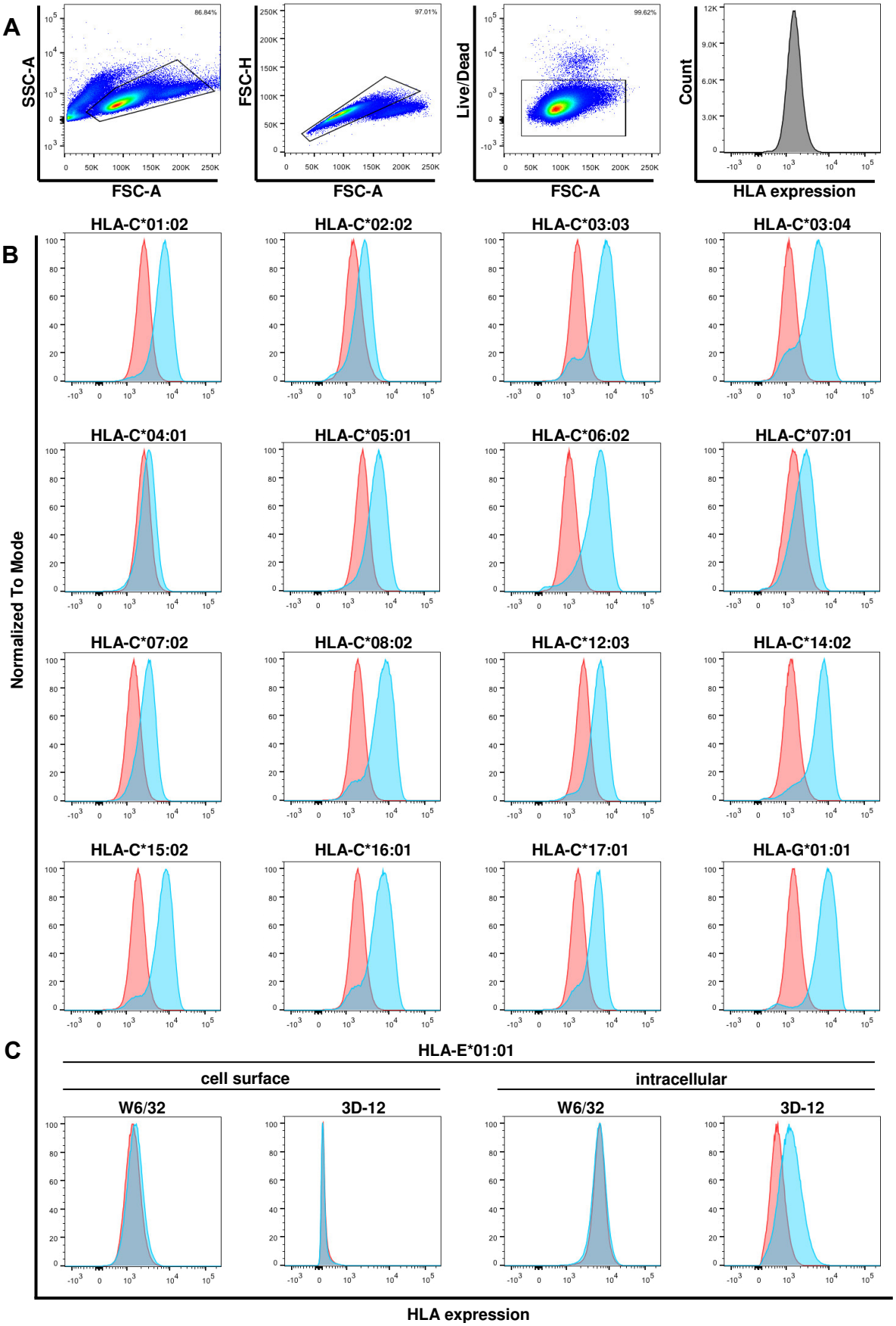

Supplementary Figure 2: HLA expression of transfected C1R cells. A) Gating strategy. C1R cells were gated for single and viable cells (7-AAD-negative). B) HLA expression of transfected C1R cells (blue) and C1R control (red). Cells were stained with pan-HLA class I-specific mAb W6/32. 500,000 cells were counted. C) Cell surface and intracellular staining of C1R-HLA-E*01:01 with W6/32 and HLA-E specific Ab 3D-12.

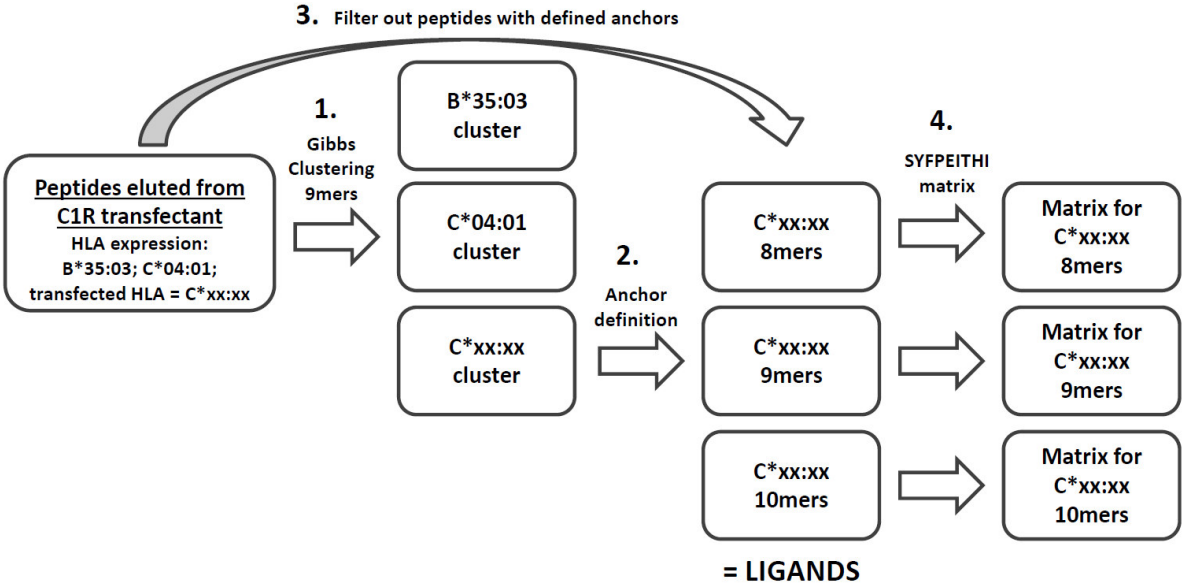

Supplementary Figure 3: Method overview. Clustering of nonameric peptides was performed using GibbsCluster1.1 (30). Cluster of transfected HLA could be distinguished from the previously described motifs of endogenously expressed HLA-B*35:03 and HLA-C*04:01 (39, 40). Anchor positions and residues were defined using frequencies of amino acids at each position of peptides in the transfected HLA cluster. Peptides harboring both anchor residues were defined as ligands in length variants 8-11. SYFPEITHI matrices were established using the defined ligands.

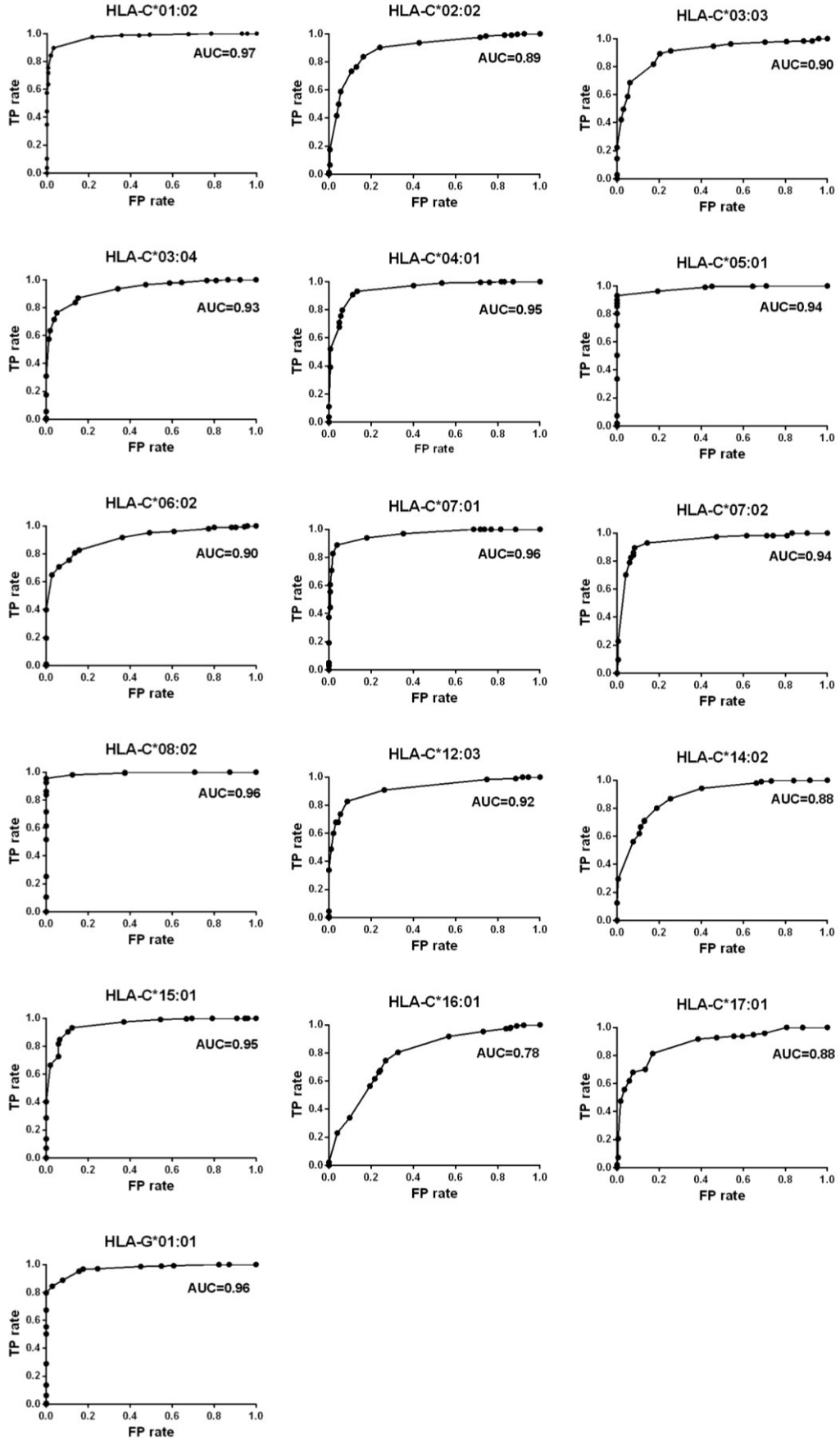

Supplementary Figure 4: ROC analysis of SYFPEITHI matrices of nonamers. Each point represents the true and false positive predicted ligands applying SYFPEITHI thresholds in 5% steps from 0-100% of the maximal score.

4. Summary

Current therapy of ccRCC is commonly constrained by low response rates and frequent resistance against administered drugs. In recent years, drug discovery is focusing on the positive modulation of the immune system. The lately approved checkpoint ab nivolumab for treatment of ccRCC is the first drug in the upcoming era of immunotherapy. Being an immunogenic tumor entity, specific immunotherapies have the potential to increase the anti-cancer response with lower side effects.

To identify suitable targets for a specific immunotherapy a comprehensive analysis on the HLA ligandome of 58 ccRCC samples and corresponding adjacent benign tissues was conducted by LC-MS/MS and compared to an additional in-house database of benign immunopeptidomes. TUMAPs were selected according to several evaluations focusing on tumor-exclusivity, quantitative expression and HLA restriction as well as the biological role of the source antigens. Overall, 26 peptides from six HLA alleles were selected and screened for their immunogenicity in $CD8^+$ T cell priming experiments, with 19 peptides exhibiting immune recognition. This set of peptides can be considered for future specific immunotherapeutic approaches.

HLA-C as well as HLA-E and HLA-G molecules possess important roles in both the innate and adaptive immunity with different immunomodulatory functions. However, the uncovering of the peptide motifs received insufficient attention until recent data from *in vitro* binding experiments for HLA-C allotypes.

For this purpose, the characterization of the binding specificities of the most frequent HLA-C allotypes as well as HLA-E and HLA-G were accomplished by LC-MS/MS-based identification of naturally processed and presented HLA ligands from monoallelic C1R transfectants. HLA-C allotypes display anchors in the B or C pocket (position 2 or 3 within the peptide) and a less variable anchor in pocket F (C-terminal position within the peptide). Overall, 20,156 HLA-C ligands were identified. For HLA-E the previously reported small ligand repertoire could be confirmed with five identified ligands, whereas a large ligand repertoire for HLA-G (2258 ligands) could be unveiled with anchor positions 3 and 9 and an auxiliary anchor at position 1. The data was utilized to establish SYFPEITHI matrices for epitope prediction and for peptide assignment to the correct HLA. Especially for HLA-G the number of HLA ligands could be tremendously increased from three prior known HLA ligands within the IEDB database to more than 2000 HLA ligands.

5. Zusammenfassung

Die gegenwärtige Therapie vom klarzelligem Nierenzellkarzinom ist, sowohl durch eine niedrige Ansprechrate als auch durch die häufig auftretenden Resistenzen gegenüber der angewandten Medikation begrenzt. Dies ist ein Grund weshalb der Fokus immer weiter in Richtung Modulation des Immunsystems gesetzt wird. Der kürzlich für ccRCC zugelassene Checkpoint-Inhibitor-Antikörper Nivolumab ist das erste Medikament der bevorstehenden Ära der Immuntherapie. Spezifische Immuntherapien haben aufgrund der Immunogenität von ccRCC das Potential höherer Anspruchsraten als auch geringerer Nebenwirkungen.

Um geeignete Angriffsziele für eine spezifische Immuntherapie zu identifizieren wurde eine umfangreiche Analyse des HLA Ligandoms von 58 ccRCC Proben und entsprechendem benachbarten Normalgewebe mittels LC-MS/MS durchgeführt und zusätzlich mit einer internen Immunpeptidom-Datenbank von diversen gesunden Organen verglichen. TUMAPs wurden durch Anwendung unterschiedlicher Auswertungen ausgewählt, die sowohl deren Tumorexklusivität, quantitative Expression und HLA-Restriktion als auch die Funktion des Quellantigens berücksichtigten. Insgesamt wurden 26 Peptide von sechs HLA-Allotypen ausgewählt und auf deren Immunogenität in $CD8^+$ T-Zell-Priming-Experimenten überprüft. 19 von 26 Peptiden konnten im Komplex mit HLA durch $CD8^+$ T-Zellen gesunder Spender erkannt werden. Dieses Set an Peptiden kann für zukünftige spezifische immuntherapeutische Ansätze in Betracht gezogen werden.

HLA-C- als auch HLA-E- und HLA-G-Moleküle nehmen sowohl in der angeborenen als auch in der adaptiven Immunität diverse immunmodulatorische Funktionen ein. Nichtsdestotrotz wurden viele HLA-C-Bindemotive erst kürzlich über *in vitro* Bindungsexperimenten angegangen.

Aus diesem Grund wurden die Bindungsspezifitäten der häufigsten HLA-C-Allotypen als auch die Bindungsspezifitäten von HLA-E und HLA-G charakterisiert. Hierfür wurden natürlich prozessierte und präsentierte HLA-Liganden aus monoallelischen C1R-Transfektanten mittels LC-MS/MS identifiziert. HLA-C-Allotypen zeigen Ankerpositionen in der B- oder C-Tasche (Interaktion mit Position 2 bzw. 3 im Peptid) und einen wenig variablen Anker in der F-Tasche (Interaktion mit C-terminaler Position im Peptid). Insgesamt wurden 20.156 HLA-C-Liganden identifiziert. Für HLA-E wurde das bekannte kleine Ligandenrepertoire (5 identifizierte Liganden) bestätigt, wohingegen das breite Repertoire von HLA-G (2258 Liganden) aufgedeckt werden konnte. Position 3 und der C-Terminus des Liganden bilden hierbei die Ankerpositionen und Position 1 einen Hilfsanker. Die Daten wurden verwendet um SYFPEITHI-Matrizen für die Epitopvorhersage als auch für die Peptidzuordnung zum entsprechenden HLA Molekül zu etablieren. Insbesondere für HLA-G konnte die Anzahl der HLA-Liganden massiv von bisher drei bekannten Liganden IEDB Datenbank) auf über 2000 Liganden gesteigert werden.

6. Abbreviations

aa	amino acid
ab	antibody
ACT	adoptive T cell transfer
APC	antigen presenting cell
AUC	area under the curve
ccRCC	clear cell renal cell carcinoma
chRCC	chromophobe renal cell carcinoma
CTA	cancer-testis antigen
CTL	cytotoxic T lymphocyte
CTLA-4	cytotoxic T lymphocyte-associated protein 4
DC	dendritic cell
DRiP	defective ribosomal product
ER	endoplasmic reticulum
FDR	false discovery rate
FP	false positive
HIF	hypoxia-inducible factor
HLA	human leukocyte antigen
HRE	hypoxia-response element
ICS	intracellular cytokine staining
IDO	indoleamine-2,3-dioxygenase
IGF	insulin growth factor
IL	interleukin
IFN	interferon
KIR	killer cell immunoglobulin-like receptor
LC	liquid chromatography
LC-MS/MS	liquid chromatographic tandem mass spectrometry
MDSC	myeloid-derived suppressor cell
MHC	major histocompatibility complex
mRCC	metastatic renal cell carcinoma
MS	mass spectrometry
mTOR	mammalian target of rapamycin
NK cell	natural killer cell
PBMC	peripheral blood mononuclear cell

PD-1	programmed cell death protein 1
PD-L1	programmed cell death 1 ligand 1
pHLA	HLA-peptide complex
pMHC	MHC-peptide complex
pRCC	papillary renal cell carcinoma
RCC	Renal cell carcinoma
ROC	receiver operating characteristic
RT	room temperature
TAA	tumor-associated antigen
TAM	tumor-associated macrophage
TAP	transporter associated with antigen processing
TCGA	The Cancer Genome Atlas
TCR	T-cell receptor
TGF-β	transforming growth factor-β
T_H cell	T helper cell
TIL	tumor-infiltrating lymphocyte
TLR	Toll-like receptor
TP	true positive
T_{reg} cell	regulatory T cell
TSA	tumor-specific antigen
TUMAP	tumor-associated peptide
VEGF	vascular endothelial growth factor
VHL	Von-Hippel Lindau

7. References

1 Dranoff, G. Cytokines in cancer pathogenesis and cancer therapy. *Nat Rev Cancer* **4**, 11-22, (2004).

2 Medzhitov, R. & Janeway, C., Jr. Innate immune recognition: mechanisms and pathways. *Immunol Rev* **173**, 89-97, (2000).

3 Tang, D., Kang, R., Coyne, C. B., Zeh, H. J. & Lotze, M. T. PAMPs and DAMPs: signal 0s that spur autophagy and immunity. *Immunol Rev* **249**, 158-175, (2012).

4 Kambayashi, T. & Laufer, T. M. Atypical MHC class II-expressing antigen-presenting cells: can anything replace a dendritic cell? *Nat Rev Immunol* **14**, 719-730, (2014).

5 Lodoen, M. B. & Lanier, L. L. Viral modulation of NK cell immunity. *Nat Rev Microbiol* **3**, 59-69, (2005).

6 Wang, W., Erbe, A. K., Hank, J. A., Morris, Z. S. & Sondel, P. M. NK Cell-Mediated Antibody-Dependent Cellular Cytotoxicity in Cancer Immunotherapy. *Front Immunol* **6**, 368, (2015).

7 Trambas, C. M. & Griffiths, G. M. Delivering the kiss of death. *Nat Immunol* **4**, 399-403, (2003).

8 Kolev, M., Le Friec, G. & Kemper, C. Complement--tapping into new sites and effector systems. *Nat Rev Immunol* **14**, 811-820, (2014).

9 Matzinger, P. Tolerance, danger, and the extended family. *Annu Rev Immunol* **12**, 991-1045, (1994).

10 Yatim, K. M. & Lakkis, F. G. A brief journey through the immune system. *Clin J Am Soc Nephrol* **10**, 1274-1281, (2015).

11 Klein, L., Kyewski, B., Allen, P. M. & Hogquist, K. A. Positive and negative selection of the T cell repertoire: what thymocytes see (and don't see). *Nat Rev Immunol* **14**, 377-391, (2014).

12 den Haan, J. M., Arens, R. & van Zelm, M. C. The activation of the adaptive immune system: cross-talk between antigen-presenting cells, T cells and B cells. *Immunol Lett* **162**, 103-112, (2014).

13 Malissen, B. & Bongrand, P. Early T cell activation: integrating biochemical, structural, and biophysical cues. *Annu Rev Immunol* **33**, 539-561, (2015).

14 Pennock, N. D., White, J. T., Cross, E. W., Cheney, E. E., Tamburini, B. A. & Kedl, R. M. T cell responses: naive to memory and everything in between. *Adv Physiol Educ* **37**, 273-283, (2013).

15 LeBien, T. W. & Tedder, T. F. B lymphocytes: how they develop and function. *Blood* **112**, 1570-1580, (2008).

16 Turner, S. J., Doherty, P. C., McCluskey, J. & Rossjohn, J. Structural determinants of T-cell receptor bias in immunity. *Nat Rev Immunol* **6**, 883-894, (2006).

17 Notarangelo, L. D., Kim, M. S., Walter, J. E. & Lee, Y. N. Human RAG mutations: biochemistry and clinical implications. *Nat Rev Immunol* **16**, 234-246, (2016).

18 Kaech, S. M., Wherry, E. J. & Ahmed, R. Effector and memory T-cell differentiation: implications for vaccine development. *Nat Rev Immunol* **2**, 251-262, (2002).

19 Kurosaki, T., Kometani, K. & Ise, W. Memory B cells. *Nat Rev Immunol* **15**, 149-159, (2015).

20 Janeway, C. A., Jr., Travers, P., Walport, M. *Immunobiology*. (Garland Science, New York, 2012).

21 Neefjes, J., Jongsma, M. L., Paul, P. & Bakke, O. Towards a systems understanding of MHC class I and MHC class II antigen presentation. *Nat Rev Immunol* **11**, 823-836, (2011).

22 Bjorkman, P. J., Saper, M. A., Samraoui, B., Bennett, W. S., Strominger, J. L. & Wiley, D. C. Structure of the human class I histocompatibility antigen, HLA-A2. *Nature* **329**, 506-512, (1987).

23 Yaneva, R., Schneeweiss, C., Zacharias, M. & Springer, S. Peptide binding to MHC class I and II proteins: new avenues from new methods. *Mol Immunol* **47**, 649-657, (2010).

24 Bouvier, M. & Wiley, D. C. Importance of peptide amino and carboxyl termini to the stability of MHC class I molecules. *Science* **265**, 398-402, (1994).

25 Matsumura, M., Fremont, D. H., Peterson, P. A. & Wilson, I. A. Emerging principles for the recognition of peptide antigens by MHC class I molecules. *Science* **257**, 927-934, (1992).
26 Rotzschke, O., Falk, K., Stevanovic, S., Jung, G. & Rammensee, H. G. Peptide motifs of closely related HLA class I molecules encompass substantial differences. *Eur J Immunol* **22**, 2453-2456, (1992).
27 Rammensee, H.-G., Bachmann, J. & Stevanovic, S. *MHC Ligands and Peptide Motifs*. 1 edn, (Springer-Verlag Berlin Heidelberg, 1997).
28 Chelvanayagam, G. A roadmap for HLA-A, HLA-B, and HLA-C peptide binding specificities. *Immunogenetics* **45**, 15-26, (1996).
29 Huyton, T., Ladas, N., Schumacher, H., Blasczyk, R. & Bade-Doeding, C. Pocketcheck: updating the HLA class I peptide specificity roadmap. *Tissue Antigens* **80**, 239-248, (2012).
30 Rich R.R., F. T. A., Shearer W.T., Schroeder H.W., Jr., Frew A.J., Weyand C.M. *Clinical Immunology: Principles and Practice*. 3 edn, (Mosby Elsevier, 2008).
31 Kjer-Nielsen, L., Patel, O., Corbett, A. J., Le Nours, J., Meehan, B., Liu, L., Bhati, M., Chen, Z., Kostenko, L., Reantragoon, R., Williamson, N. A., Purcell, A. W. *et al.* MR1 presents microbial vitamin B metabolites to MAIT cells. *Nature* **491**, 717-723, (2012).
32 Trowsdale, J. & Knight, J. C. Major histocompatibility complex genomics and human disease. *Annu Rev Genomics Hum Genet* **14**, 301-323, (2013).
33 Hauptmann, G. & Bahram, S. Genetics of the central MHC. *Curr Opin Immunol* **16**, 668-672, (2004).
34 Ackerman, A. L. & Cresswell, P. Cellular mechanisms governing cross-presentation of exogenous antigens. *Nat Immunol* **5**, 678-684, (2004).
35 Guermonprez, P. & Amigorena, S. Pathways for antigen cross presentation. *Springer Semin Immunopathol* **26**, 257-271, (2005).
36 Schubert, U., Anton, L. C., Gibbs, J., Norbury, C. C., Yewdell, J. W. & Bennink, J. R. Rapid degradation of a large fraction of newly synthesized proteins by proteasomes. *Nature* **404**, 770-774, (2000).
37 Yewdell, J. W., Reits, E. & Neefjes, J. Making sense of mass destruction: quantitating MHC class I antigen presentation. *Nat Rev Immunol* **3**, 952-961, (2003).
38 Hershko, A. & Ciechanover, A. The ubiquitin system. *Annu Rev Biochem* **67**, 425-479, (1998).
39 Voges, D., Zwickl, P. & Baumeister, W. The 26S proteasome: a molecular machine designed for controlled proteolysis. *Annu Rev Biochem* **68**, 1015-1068, (1999).
40 Tanaka, K. The proteasome: from basic mechanisms to emerging roles. *Keio J Med* **62**, 1-12, (2013).
41 Schoenborn, J. R. & Wilson, C. B. Regulation of interferon-gamma during innate and adaptive immune responses. *Adv Immunol* **96**, 41-101, (2007).
42 Vigneron, N. & Van den Eynde, B. J. Proteasome subtypes and the processing of tumor antigens: increasing antigenic diversity. *Curr Opin Immunol* **24**, 84-91, (2012).
43 Gaczynska, M., Rock, K. L. & Goldberg, A. L. Gamma-interferon and expression of MHC genes regulate peptide hydrolysis by proteasomes. *Nature* **365**, 264-267, (1993).
44 Gray, C. W., Slaughter, C. A. & DeMartino, G. N. PA28 activator protein forms regulatory caps on proteasome stacked rings. *J Mol Biol* **236**, 7-15, (1994).
45 Groettrup, M., Soza, A., Eggers, M., Kuehn, L., Dick, T. P., Schild, H., Rammensee, H. G., Koszinowski, U. H. & Kloetzel, P. M. A role for the proteasome regulator PA28alpha in antigen presentation. *Nature* **381**, 166-168, (1996).
46 Kunisawa, J. & Shastri, N. The group II chaperonin TRiC protects proteolytic intermediates from degradation in the MHC class I antigen processing pathway. *Mol Cell* **12**, 565-576, (2003).
47 Stevanovic, S. & Schild, H. Quantitative aspects of T cell activation--peptide generation and editing by MHC class I molecules. *Semin Immunol* **11**, 375-384, (1999).
48 Yewdell, J. W. Not such a dismal science: the economics of protein synthesis, folding, degradation and antigen processing. *Trends Cell Biol* **11**, 294-297, (2001).

49 Reits, E., Griekspoor, A., Neijssen, J., Groothuis, T., Jalink, K., van Veelen, P., Janssen, H., Calafat, J., Drijfhout, J. W. & Neefjes, J. Peptide diffusion, protection, and degradation in nuclear and cytoplasmic compartments before antigen presentation by MHC class I. *Immunity* **18**, 97-108, (2003).
50 Kobayashi, K. S. & van den Elsen, P. J. NLRC5: a key regulator of MHC class I-dependent immune responses. *Nat Rev Immunol* **12**, 813-820, (2012).
51 Munz, C. Antigen Processing for MHC Class II Presentation via Autophagy. *Front Immunol* **3**, 9, (2012).
52 Dengjel, J., Schoor, O., Fischer, R., Reich, M., Kraus, M., Muller, M., Kreymborg, K., Altenberend, F., Brandenburg, J., Kalbacher, H., Brock, R., Driessen, C. *et al.* Autophagy promotes MHC class II presentation of peptides from intracellular source proteins. *Proc Natl Acad Sci U S A* **102**, 7922-7927, (2005).
53 Poluektov, Y. O., Kim, A., Hartman, I. Z. & Sadegh-Nasseri, S. HLA-DO as the optimizer of epitope selection for MHC class II antigen presentation. *PLoS One* **8**, e71228, (2013).
54 Lazarski, C. A., Chaves, F. A. & Sant, A. J. The impact of DM on MHC class II-restricted antigen presentation can be altered by manipulation of MHC-peptide kinetic stability. *J Exp Med* **203**, 1319-1328, (2006).
55 Hillen, N. & Stevanovic, S. Contribution of mass spectrometry-based proteomics to immunology. *Expert Rev Proteomics* **3**, 653-664, (2006).
56 Falk, K., Rotzschke, O., Takiguchi, M., Gnau, V., Stevanovic, S., Jung, G. & Rammensee, H. G. Peptide motifs of HLA-B38 and B39 molecules. *Immunogenetics* **41**, 162-164, (1995).
57 Falk, K., Rotzschke, O., Takiguchi, M., Gnau, V., Stevanovic, S., Jung, G. & Rammensee, H. G. Peptide motifs of HLA-B51, -B52 and -B78 molecules, and implications for Behcet's disease. *Int Immunol* **7**, 223-228, (1995).
58 Falk, K., Rotzschke, O., Takiguchi, M., Gnau, V., Stevanovic, S., Jung, G. & Rammensee, H. G. Peptide motifs of HLA-B58, B60, B61, and B62 molecules. *Immunogenetics* **41**, 165-168, (1995).
59 Falk, K., Rotzschke, O., Takiguchi, M., Grahovac, B., Gnau, V., Stevanovic, S., Jung, G. & Rammensee, H. G. Peptide motifs of HLA-A1, -A11, -A31, and -A33 molecules. *Immunogenetics* **40**, 238-241, (1994).
60 Abelin, J. G., Keskin, D. B., Sarkizova, S., Hartigan, C. R., Zhang, W., Sidney, J., Stevens, J., Lane, W., Zhang, G. L., Eisenhaure, T. M., Clauser, K. R., Hacohen, N. *et al.* Mass Spectrometry Profiling of HLA-Associated Peptidomes in Mono-allelic Cells Enables More Accurate Epitope Prediction. *Immunity* **46**, 315-326, (2017).
61 Valastyan, S. & Weinberg, R. A. Tumor metastasis: molecular insights and evolving paradigms. *Cell* **147**, 275-292, (2011).
62 Alizadeh, A. M., Shiri, S. & Farsinejad, S. Metastasis review: from bench to bedside. *Tumour Biol* **35**, 8483-8523, (2014).
63 Hanahan, D. & Weinberg, R. A. Hallmarks of cancer: the next generation. *Cell* **144**, 646-674, (2011).
64 Blasco, M. A. Telomeres and human disease: ageing, cancer and beyond. *Nat Rev Genet* **6**, 611-622, (2005).
65 Elmore, S. Apoptosis: a review of programmed cell death. *Toxicol Pathol* **35**, 495-516, (2007).
66 Adams, J. M. & Cory, S. The Bcl-2 apoptotic switch in cancer development and therapy. *Oncogene* **26**, 1324-1337, (2007).
67 Lowe, S. W., Cepero, E. & Evan, G. Intrinsic tumour suppression. *Nature* **432**, 307-315, (2004).
68 Carmeliet, P. Angiogenesis in life, disease and medicine. *Nature* **438**, 932-936, (2005).
69 Weis, S. M. & Cheresh, D. A. Tumor angiogenesis: molecular pathways and therapeutic targets. *Nat Med* **17**, 1359-1370, (2011).
70 Potente, M., Gerhardt, H. & Carmeliet, P. Basic and therapeutic aspects of angiogenesis. *Cell* **146**, 873-887, (2011).
71 Warburg, O. On the origin of cancer cells. *Science* **123**, 309-314, (1956).

72 DeBerardinis, R. J. & Chandel, N. S. Fundamentals of cancer metabolism. *Sci Adv* **2**, e1600200, (2016).
73 Cobbold, M., De La Pena, H., Norris, A., Polefrone, J. M., Qian, J., English, A. M., Cummings, K. L., Penny, S., Turner, J. E., Cottine, J., Abelin, J. G., Malaker, S. A. *et al.* MHC class I-associated phosphopeptides are the targets of memory-like immunity in leukemia. *Sci Transl Med* **5**, 203ra125, (2013).
74 Marino, F., Bern, M., Mommen, G. P., Leney, A. C., van Gaans-van den Brink, J. A., Bonvin, A. M., Becker, C., van Els, C. A. & Heck, A. J. Extended O-GlcNAc on HLA Class-I-Bound Peptides. *J Am Chem Soc* **137**, 10922-10925, (2015).
75 Brentville, V. A., Metheringham, R. L., Gunn, B., Symonds, P., Daniels, I., Gijon, M., Cook, K., Xue, W. & Durrant, L. G. Citrullinated Vimentin Presented on MHC-II in Tumor Cells Is a Target for CD4+ T-Cell-Mediated Antitumor Immunity. *Cancer Res* **76**, 548-560, (2016).
76 Peper, J. K., Bosmuller, H. C., Schuster, H., Guckel, B., Horzer, H., Roehle, K., Schafer, R., Wagner, P., Rammensee, H. G., Stevanovic, S., Fend, F. & Staebler, A. HLA ligandomics identifies histone deacetylase 1 as target for ovarian cancer immunotherapy. *Oncoimmunology* **5**, e1065369, (2016).
77 Chen, D. S. & Mellman, I. Oncology meets immunology: the cancer-immunity cycle. *Immunity* **39**, 1-10, (2013).
78 Ferguson, T. A., Choi, J. & Green, D. R. Armed response: how dying cells influence T-cell functions. *Immunol Rev* **241**, 77-88, (2011).
79 Masopust, D. & Schenkel, J. M. The integration of T cell migration, differentiation and function. *Nat Rev Immunol* **13**, 309-320, (2013).
80 Franciszkiewicz, K., Boissonnas, A., Boutet, M., Combadiere, C. & Mami-Chouaib, F. Role of chemokines and chemokine receptors in shaping the effector phase of the antitumor immune response. *Cancer Res* **72**, 6325-6332, (2012).
81 Qin, S., Rottman, J. B., Myers, P., Kassam, N., Weinblatt, M., Loetscher, M., Koch, A. E., Moser, B. & Mackay, C. R. The chemokine receptors CXCR3 and CCR5 mark subsets of T cells associated with certain inflammatory reactions. *J Clin Invest* **101**, 746-754, (1998).
82 Rothlein, R., Dustin, M. L., Marlin, S. D. & Springer, T. A. A human intercellular adhesion molecule (ICAM-1) distinct from LFA-1. *J Immunol* **137**, 1270-1274, (1986).
83 Franciszkiewicz, K., Le Floc'h, A., Boutet, M., Vergnon, I., Schmitt, A. & Mami-Chouaib, F. CD103 or LFA-1 engagement at the immune synapse between cytotoxic T cells and tumor cells promotes maturation and regulates T-cell effector functions. *Cancer Res* **73**, 617-628, (2013).
84 Ley, K. The role of selectins in inflammation and disease. *Trends Mol Med* **9**, 263-268, (2003).
85 Burnet, M. Cancer; a biological approach. I. The processes of control. *Br Med J* **1**, 779-786, (1957).
86 Dunn, G. P., Old, L. J. & Schreiber, R. D. The immunobiology of cancer immunosurveillance and immunoediting. *Immunity* **21**, 137-148, (2004).
87 Schreiber, R. D., Old, L. J. & Smyth, M. J. Cancer immunoediting: integrating immunity's roles in cancer suppression and promotion. *Science* **331**, 1565-1570, (2011).
88 Zitvogel, L., Tesniere, A. & Kroemer, G. Cancer despite immunosurveillance: immunoselection and immunosubversion. *Nat Rev Immunol* **6**, 715-727, (2006).
89 Beatty, G. L. & Gladney, W. L. Immune escape mechanisms as a guide for cancer immunotherapy. *Clin Cancer Res* **21**, 687-692, (2015).
90 Joyce, J. A. & Fearon, D. T. T cell exclusion, immune privilege, and the tumor microenvironment. *Science* **348**, 74-80, (2015).
91 Khong, H. T. & Restifo, N. P. Natural selection of tumor variants in the generation of "tumor escape" phenotypes. *Nat Immunol* **3**, 999-1005, (2002).
92 Vesely, M. D., Kershaw, M. H., Schreiber, R. D. & Smyth, M. J. Natural innate and adaptive immunity to cancer. *Annu Rev Immunol* **29**, 235-271, (2011).

93 Coley, W. B. The treatment of malignant tumors by repeated inoculations of erysipelas: with a report of ten original cases. *Am J Med Sci* **105**, 487-511, (1893).
94 Wiemann, B. & Starnes, C. O. Coley's toxins, tumor necrosis factor and cancer research: a historical perspective. *Pharmacol Ther* **64**, 529-564, (1994).
95 Ehrlich, P. Über den jetzigen Stand der Karzinomforschung. *Ned Tijdschr Geneeskd* **5**, 273-290, (1909).
96 Arnold, B., Schonrich, G. & Hammerling, G. J. Multiple levels of peripheral tolerance. *Immunol Today* **14**, 12-14, (1993).
97 Fowlkes, B. J. & Ramsdell, F. T-cell tolerance. *Curr Opin Immunol* **5**, 873-879, (1993).
98 Fenton, R. G. & Longo, D. L. Genetic instability and tumor cell variation: implications for immunotherapy. *J Natl Cancer Inst* **87**, 241-243, (1995).
99 Urban, J. L. & Schreiber, H. Tumor antigens. *Annu Rev Immunol* **10**, 617-644, (1992).
100 Boon, T., Cerottini, J. C., Van den Eynde, B., van der Bruggen, P. & Van Pel, A. Tumor antigens recognized by T lymphocytes. *Annu Rev Immunol* **12**, 337-365, (1994).
101 Dighe, A. S., Richards, E., Old, L. J. & Schreiber, R. D. Enhanced in vivo growth and resistance to rejection of tumor cells expressing dominant negative IFN gamma receptors. *Immunity* **1**, 447-456, (1994).
102 Shankaran, V., Ikeda, H., Bruce, A. T., White, J. M., Swanson, P. E., Old, L. J. & Schreiber, R. D. IFNgamma and lymphocytes prevent primary tumour development and shape tumour immunogenicity. *Nature* **410**, 1107-1111, (2001).
103 Ito, F. & Chang, A. E. Cancer immunotherapy: current status and future directions. *Surg Oncol Clin N Am* **22**, 765-783, (2013).
104 Scott, A. M., Wolchok, J. D. & Old, L. J. Antibody therapy of cancer. *Nat Rev Cancer* **12**, 278-287, (2012).
105 Weiner, L. M., Surana, R. & Wang, S. Monoclonal antibodies: versatile platforms for cancer immunotherapy. *Nat Rev Immunol* **10**, 317-327, (2010).
106 Rosenberg, S. A., Restifo, N. P., Yang, J. C., Morgan, R. A. & Dudley, M. E. Adoptive cell transfer: a clinical path to effective cancer immunotherapy. *Nat Rev Cancer* **8**, 299-308, (2008).
107 Rosenberg, S. A. & Restifo, N. P. Adoptive cell transfer as personalized immunotherapy for human cancer. *Science* **348**, 62-68, (2015).
108 Robbins, P. F., Dudley, M. E., Wunderlich, J., El-Gamil, M., Li, Y. F., Zhou, J., Huang, J., Powell, D. J., Jr. & Rosenberg, S. A. Cutting edge: persistence of transferred lymphocyte clonotypes correlates with cancer regression in patients receiving cell transfer therapy. *J Immunol* **173**, 7125-7130, (2004).
109 Gattinoni, L., Finkelstein, S. E., Klebanoff, C. A., Antony, P. A., Palmer, D. C., Spiess, P. J., Hwang, L. N., Yu, Z., Wrzesinski, C., Heimann, D. M., Surh, C. D., Rosenberg, S. A. *et al.* Removal of homeostatic cytokine sinks by lymphodepletion enhances the efficacy of adoptively transferred tumor-specific CD8+ T cells. *J Exp Med* **202**, 907-912, (2005).
110 Antony, P. A., Piccirillo, C. A., Akpinarli, A., Finkelstein, S. E., Speiss, P. J., Surman, D. R., Palmer, D. C., Chan, C. C., Klebanoff, C. A., Overwijk, W. W., Rosenberg, S. A. & Restifo, N. P. CD8+ T cell immunity against a tumor/self-antigen is augmented by CD4+ T helper cells and hindered by naturally occurring T regulatory cells. *J Immunol* **174**, 2591-2601, (2005).
111 Di Marco, M., Peper, J. K. & Rammensee, H. G. Identification of Immunogenic Epitopes by MS/MS. *Cancer J* **23**, 102-107, (2017).
112 Melief, C. J. & van der Burg, S. H. Immunotherapy of established (pre)malignant disease by synthetic long peptide vaccines. *Nat Rev Cancer* **8**, 351-360, (2008).
113 Yamada, A., Sasada, T., Noguchi, M. & Itoh, K. Next-generation peptide vaccines for advanced cancer. *Cancer Sci* **104**, 15-21, (2013).
114 Toes, R. E., Blom, R. J., Offringa, R., Kast, W. M. & Melief, C. J. Enhanced tumor outgrowth after peptide vaccination. Functional deletion of tumor-specific CTL induced by peptide vaccination can lead to the inability to reject tumors. *J Immunol* **156**, 3911-3918, (1996).

115 Toes, R. E., Offringa, R., Blom, R. J., Melief, C. J. & Kast, W. M. Peptide vaccination can lead to enhanced tumor growth through specific T-cell tolerance induction. *Proc Natl Acad Sci U S A* **93**, 7855-7860, (1996).
116 Bijker, M. S., van den Eeden, S. J., Franken, K. L., Melief, C. J., van der Burg, S. H. & Offringa, R. Superior induction of anti-tumor CTL immunity by extended peptide vaccines involves prolonged, DC-focused antigen presentation. *Eur J Immunol* **38**, 1033-1042, (2008).
117 Schoenberger, S. P., Toes, R. E., van der Voort, E. I., Offringa, R. & Melief, C. J. T-cell help for cytotoxic T lymphocytes is mediated by CD40-CD40L interactions. *Nature* **393**, 480-483, (1998).
118 Bennett, S. R., Carbone, F. R., Karamalis, F., Flavell, R. A., Miller, J. F. & Heath, W. R. Help for cytotoxic-T-cell responses is mediated by CD40 signalling. *Nature* **393**, 478-480, (1998).
119 Singh, M. & O'Hagan, D. Advances in vaccine adjuvants. *Nat Biotechnol* **17**, 1075-1081, (1999).
120 Kenter, G. G., Welters, M. J., Valentijn, A. R., Lowik, M. J., Berends-van der Meer, D. M., Vloon, A. P., Essahsah, F., Fathers, L. M., Offringa, R., Drijfhout, J. W., Wafelman, A. R., Oostendorp, J. *et al.* Vaccination against HPV-16 oncoproteins for vulvar intraepithelial neoplasia. *N Engl J Med* **361**, 1838-1847, (2009).
121 Aucouturier, J., Dupuis, L., Deville, S., Ascarateil, S. & Ganne, V. Montanide ISA 720 and 51: a new generation of water in oil emulsions as adjuvants for human vaccines. *Expert Rev Vaccines* **1**, 111-118, (2002).
122 Black, M., Trent, A., Tirrell, M. & Olive, C. Advances in the design and delivery of peptide subunit vaccines with a focus on toll-like receptor agonists. *Expert Rev Vaccines* **9**, 157-173, (2010).
123 Van den Hove, L. E., Van Gool, S. W., Van Poppel, H., Baert, L., Coorevits, L., Van Damme, B. & Ceuppens, J. L. Phenotype, cytokine production and cytolytic capacity of fresh (uncultured) tumour-infiltrating T lymphocytes in human renal cell carcinoma. *Clin Exp Immunol* **109**, 501-509, (1997).
124 Lokich, J. Spontaneous regression of metastatic renal cancer. Case report and literature review. *Am J Clin Oncol* **20**, 416-418, (1997).
125 Rini, B. I. & Atkins, M. B. Resistance to targeted therapy in renal-cell carcinoma. *Lancet Oncol* **10**, 992-1000, (2009).
126 Negrier, S., Escudier, B., Lasset, C., Douillard, J. Y., Savary, J., Chevreau, C., Ravaud, A., Mercatello, A., Peny, J., Mousseau, M., Philip, T. & Tursz, T. Recombinant human interleukin-2, recombinant human interferon alfa-2a, or both in metastatic renal-cell carcinoma. Groupe Francais d'Immunotherapie. *N Engl J Med* **338**, 1272-1278, (1998).
127 Motzer, R. J., Escudier, B., McDermott, D. F., George, S., Hammers, H. J., Srinivas, S., Tykodi, S. S., Sosman, J. A., Procopio, G., Plimack, E. R., Castellano, D., Choueiri, T. K. *et al.* Nivolumab versus Everolimus in Advanced Renal-Cell Carcinoma. *N Engl J Med* **373**, 1803-1813, (2015).
128 Motzer, R. J., Bander, N. H. & Nanus, D. M. Renal-cell carcinoma. *N Engl J Med* **335**, 865-875, (1996).
129 Torre, L. A., Bray, F., Siegel, R. L., Ferlay, J., Lortet-Tieulent, J. & Jemal, A. Global cancer statistics, 2012. *CA Cancer J Clin* **65**, 87-108, (2015).
130 Global Burden of Disease Cancer, C., Fitzmaurice, C., Dicker, D., Pain, A., Hamavid, H., Moradi-Lakeh, M., MacIntyre, M. F., Allen, C., Hansen, G., Woodbrook, R., Wolfe, C., Hamadeh, R. R. *et al.* The Global Burden of Cancer 2013. *JAMA Oncol* **1**, 505-527, (2015).
131 Moch, H., Cubilla, A. L., Humphrey, P. A., Reuter, V. E. & Ulbright, T. M. The 2016 WHO Classification of Tumours of the Urinary System and Male Genital Organs-Part A: Renal, Penile, and Testicular Tumours. *Eur Urol* **70**, 93-105, (2016).
132 Cheville, J. C., Lohse, C. M., Zincke, H., Weaver, A. L. & Blute, M. L. Comparisons of outcome and prognostic features among histologic subtypes of renal cell carcinoma. *Am J Surg Pathol* **27**, 612-624, (2003).
133 Rini, B. I., Campbell, S. C. & Escudier, B. Renal cell carcinoma. *Lancet* **373**, 1119-1132, (2009).

134 Ben-Skowronek, I. & Kozaczuk, S. Von Hippel-Lindau Syndrome. *Horm Res Paediatr* **84**, 145-152, (2015).
135 Nickerson, M. L., Warren, M. B., Toro, J. R., Matrosova, V., Glenn, G., Turner, M. L., Duray, P., Merino, M., Choyke, P., Pavlovich, C. P., Sharma, N., Walther, M. *et al.* Mutations in a novel gene lead to kidney tumors, lung wall defects, and benign tumors of the hair follicle in patients with the Birt-Hogg-Dube syndrome. *Cancer Cell* **2**, 157-164, (2002).
136 Baba, M., Hong, S. B., Sharma, N., Warren, M. B., Nickerson, M. L., Iwamatsu, A., Esposito, D., Gillette, W. K., Hopkins, R. F., 3rd, Hartley, J. L., Furihata, M., Oishi, S. *et al.* Folliculin encoded by the BHD gene interacts with a binding protein, FNIP1, and AMPK, and is involved in AMPK and mTOR signaling. *Proc Natl Acad Sci U S A* **103**, 15552-15557, (2006).
137 Schmidt, L. S. & Linehan, W. M. Genetic predisposition to kidney cancer. *Semin Oncol* **43**, 566-574, (2016).
138 Hunt, J. D., van der Hel, O. L., McMillan, G. P., Boffetta, P. & Brennan, P. Renal cell carcinoma in relation to cigarette smoking: meta-analysis of 24 studies. *Int J Cancer* **114**, 101-108, (2005).
139 Renehan, A. G., Tyson, M., Egger, M., Heller, R. F. & Zwahlen, M. Body-mass index and incidence of cancer: a systematic review and meta-analysis of prospective observational studies. *Lancet* **371**, 569-578, (2008).
140 Chow, W. H., Gridley, G., Fraumeni, J. F., Jr. & Jarvholm, B. Obesity, hypertension, and the risk of kidney cancer in men. *N Engl J Med* **343**, 1305-1311, (2000).
141 Weikert, S., Boeing, H., Pischon, T., Weikert, C., Olsen, A., Tjonneland, A., Overvad, K., Becker, N., Linseisen, J., Trichopoulou, A., Mountokalakis, T., Trichopoulos, D. *et al.* Blood pressure and risk of renal cell carcinoma in the European prospective investigation into cancer and nutrition. *Am J Epidemiol* **167**, 438-446, (2008).
142 Denton, M. D., Magee, C. C., Ovuworie, C., Mauiyyedi, S., Pascual, M., Colvin, R. B., Cosimi, A. B. & Tolkoff-Rubin, N. Prevalence of renal cell carcinoma in patients with ESRD pre-transplantation: a pathologic analysis. *Kidney Int* **61**, 2201-2209, (2002).
143 Ljungberg, B., Campbell, S. C., Choi, H. Y., Jacqmin, D., Lee, J. E., Weikert, S. & Kiemeney, L. A. The epidemiology of renal cell carcinoma. *Eur Urol* **60**, 615-621, (2011).
144 Corgna, E., Betti, M., Gatta, G., Roila, F. & De Mulder, P. H. Renal cancer. *Crit Rev Oncol Hematol* **64**, 247-262, (2007).
145 Sokoloff, M. H., deKernion, J. B., Figlin, R. A. & Belldegrun, A. Current management of renal cell carcinoma. *CA Cancer J Clin* **46**, 284-302, (1996).
146 Siegel, R., Ma, J., Zou, Z. & Jemal, A. Cancer statistics, 2014. *CA Cancer J Clin* **64**, 9-29, (2014).
147 Edge, S. B. & Compton, C. C. The American Joint Committee on Cancer: the 7th edition of the AJCC cancer staging manual and the future of TNM. *Ann Surg Oncol* **17**, 1471-1474, (2010).
148 Cohen, H. T. & McGovern, F. J. Renal-cell carcinoma. *N Engl J Med* **353**, 2477-2490, (2005).
149 Hsieh, J. J., Purdue, M. P., Signoretti, S., Swanton, C., Albiges, L., Schmidinger, M., Heng, D. Y., Larkin, J. & Ficarra, V. Renal cell carcinoma. *Nat Rev Dis Primers* **3**, 17009, (2017).
150 Ljungberg, B., Bensalah, K., Canfield, S., Dabestani, S., Hofmann, F., Hora, M., Kuczyk, M. A., Lam, T., Marconi, L., Merseburger, A. S., Mulders, P., Powles, T. *et al.* EAU guidelines on renal cell carcinoma: 2014 update. *Eur Urol* **67**, 913-924, (2015).
151 Motzer, R. J., Jonasch, E., Agarwal, N., Beard, C., Bhayani, S., Bolger, G. B., Chang, S. S., Choueiri, T. K., Costello, B. A., Derweesh, I. H., Gupta, S., Hancock, S. L. *et al.* Kidney cancer, version 3.2015. *J Natl Compr Canc Netw* **13**, 151-159, (2015).
152 Fyfe, G., Fisher, R. I., Rosenberg, S. A., Sznol, M., Parkinson, D. R. & Louie, A. C. Results of treatment of 255 patients with metastatic renal cell carcinoma who received high-dose recombinant interleukin-2 therapy. *J Clin Oncol* **13**, 688-696, (1995).
153 Hutson, T. E. Targeted therapies for the treatment of metastatic renal cell carcinoma: clinical evidence. *Oncologist* **16 Suppl 2**, 14-22, (2011).

154 Motzer, R. J., Hutson, T. E., Tomczak, P., Michaelson, M. D., Bukowski, R. M., Rixe, O., Oudard, S., Negrier, S., Szczylik, C., Kim, S. T., Chen, I., Bycott, P. W. *et al.* Sunitinib versus interferon alfa in metastatic renal-cell carcinoma. *N Engl J Med* **356**, 115-124, (2007).
155 Tsao, C. K., Liaw, B., He, C., Galsky, M. D., Sfakianos, J. & Oh, W. K. Moving beyond vascular endothelial growth factor-targeted therapy in renal cell cancer: latest evidence and therapeutic implications. *Ther Adv Med Oncol* **9**, 287-298, (2017).
156 Vibhakar, R., Juan, G., Traganos, F., Darzynkiewicz, Z. & Finger, L. R. Activation-induced expression of human programmed death-1 gene in T-lymphocytes. *Exp Cell Res* **232**, 25-28, (1997).
157 Freeman, G. J., Long, A. J., Iwai, Y., Bourque, K., Chernova, T., Nishimura, H., Fitz, L. J., Malenkovich, N., Okazaki, T., Byrne, M. C., Horton, H. F., Fouser, L. *et al.* Engagement of the PD-1 immunoinhibitory receptor by a novel B7 family member leads to negative regulation of lymphocyte activation. *J Exp Med* **192**, 1027-1034, (2000).
158 Flies, D. B. & Chen, L. The new B7s: playing a pivotal role in tumor immunity. *J Immunother* **30**, 251-260, (2007).
159 Ljungberg, B. e. a. EAU Guidelines on Renal Cell Carcinoma. *European Association of Urology*, (2016).
160 Ghatalia, P., Zibelman, M., Geynisman, D. M. & Plimack, E. R. Checkpoint Inhibitors for the Treatment of Renal Cell Carcinoma. *Curr Treat Options Oncol* **18**, 7, (2017).
161 Amin, A., Dudek, A. Z., Logan, T. F., Lance, R. S., Holzbeierlein, J. M., Knox, J. J., Master, V. A., Pal, S. K., Miller, W. H., Jr., Karsh, L. I., Tcherepanova, I. Y., DeBenedette, M. A. *et al.* Survival with AGS-003, an autologous dendritic cell-based immunotherapy, in combination with sunitinib in unfavorable risk patients with advanced renal cell carcinoma (RCC): Phase 2 study results. *J Immunother Cancer* **3**, 14, (2015).
162 Walter, S., Weinschenk, T., Stenzl, A., Zdrojowy, R., Pluzanska, A., Szczylik, C., Staehler, M., Brugger, W., Dietrich, P. Y., Mendrzyk, R., Hilf, N., Schoor, O. *et al.* Multipeptide immune response to cancer vaccine IMA901 after single-dose cyclophosphamide associates with longer patient survival. *Nat Med* **18**, 1254-1261, (2012).
163 Rini, B. I., Stenzl, A., Zdrojowy, R., Kogan, M., Shkolnik, M., Oudard, S., Weikert, S., Bracarda, S., Crabb, S. J., Bedke, J., Ludwig, J., Maurer, D. *et al.* IMA901, a multipeptide cancer vaccine, plus sunitinib versus sunitinib alone, as first-line therapy for advanced or metastatic renal cell carcinoma (IMPRINT): a multicentre, open-label, randomised, controlled, phase 3 trial. *Lancet Oncol* **17**, 1599-1611, (2016).
164 Finke, J. H., Rini, B., Ireland, J., Rayman, P., Richmond, A., Golshayan, A., Wood, L., Elson, P., Garcia, J., Dreicer, R. & Bukowski, R. Sunitinib reverses type-1 immune suppression and decreases T-regulatory cells in renal cell carcinoma patients. *Clin Cancer Res* **14**, 6674-6682, (2008).
165 Kusmartsev, S., Su, Z., Heiser, A., Dannull, J., Eruslanov, E., Kubler, H., Yancey, D., Dahm, P. & Vieweg, J. Reversal of myeloid cell-mediated immunosuppression in patients with metastatic renal cell carcinoma. *Clin Cancer Res* **14**, 8270-8278, (2008).
166 Ko, J. S., Zea, A. H., Rini, B. I., Ireland, J. L., Elson, P., Cohen, P., Golshayan, A., Rayman, P. A., Wood, L., Garcia, J., Dreicer, R., Bukowski, R. *et al.* Sunitinib mediates reversal of myeloid-derived suppressor cell accumulation in renal cell carcinoma patients. *Clin Cancer Res* **15**, 2148-2157, (2009).
167 van Cruijsen, H., van der Veldt, A. A., Vroling, L., Oosterhoff, D., Broxterman, H. J., Scheper, R. J., Giaccone, G., Haanen, J. B., van den Eertwegh, A. J., Boven, E., Hoekman, K. & de Gruijl, T. D. Sunitinib-induced myeloid lineage redistribution in renal cell cancer patients: CD1c+ dendritic cell frequency predicts progression-free survival. *Clin Cancer Res* **14**, 5884-5892, (2008).
168 Ozao-Choy, J., Ma, G., Kao, J., Wang, G. X., Meseck, M., Sung, M., Schwartz, M., Divino, C. M., Pan, P. Y. & Chen, S. H. The novel role of tyrosine kinase inhibitor in the reversal of immune

suppression and modulation of tumor microenvironment for immune-based cancer therapies. *Cancer Res* **69**, 2514-2522, (2009).

169 Hakimi, A. A., Reznik, E., Lee, C. H., Creighton, C. J., Brannon, A. R., Luna, A., Aksoy, B. A., Liu, E. M., Shen, R., Lee, W., Chen, Y., Stirdivant, S. M. *et al.* An Integrated Metabolic Atlas of Clear Cell Renal Cell Carcinoma. *Cancer Cell* **29**, 104-116, (2016).

170 Sato, Y., Yoshizato, T., Shiraishi, Y., Maekawa, S., Okuno, Y., Kamura, T., Shimamura, T., Sato-Otsubo, A., Nagae, G., Suzuki, H., Nagata, Y., Yoshida, K. *et al.* Integrated molecular analysis of clear-cell renal cell carcinoma. *Nat Genet* **45**, 860-867, (2013).

171 Yang, W., Yoshigoe, K., Qin, X., Liu, J. S., Yang, J. Y., Niemierko, A., Deng, Y., Liu, Y., Dunker, A., Chen, Z., Wang, L., Xu, D. *et al.* Identification of genes and pathways involved in kidney renal clear cell carcinoma. *BMC Bioinformatics* **15 Suppl 17**, S2, (2014).

172 Alexandrov, L. B., Nik-Zainal, S., Wedge, D. C., Aparicio, S. A., Behjati, S., Biankin, A. V., Bignell, G. R., Bolli, N., Borg, A., Borresen-Dale, A. L., Boyault, S., Burkhardt, B. *et al.* Signatures of mutational processes in human cancer. *Nature* **500**, 415-421, (2013).

173 Cancer Genome Atlas Research, N. Comprehensive molecular characterization of clear cell renal cell carcinoma. *Nature* **499**, 43-49, (2013).

174 Gnarra, J. R., Tory, K., Weng, Y., Schmidt, L., Wei, M. H., Li, H., Latif, F., Liu, S., Chen, F., Duh, F. M. & et al. Mutations of the VHL tumour suppressor gene in renal carcinoma. *Nat Genet* **7**, 85-90, (1994).

175 Kibel, A., Iliopoulos, O., DeCaprio, J. A. & Kaelin, W. G., Jr. Binding of the von Hippel-Lindau tumor suppressor protein to Elongin B and C. *Science* **269**, 1444-1446, (1995).

176 Ivan, M., Kondo, K., Yang, H., Kim, W., Valiando, J., Ohh, M., Salic, A., Asara, J. M., Lane, W. S. & Kaelin, W. G., Jr. HIFalpha targeted for VHL-mediated destruction by proline hydroxylation: implications for O2 sensing. *Science* **292**, 464-468, (2001).

177 Jaakkola, P., Mole, D. R., Tian, Y. M., Wilson, M. I., Gielbert, J., Gaskell, S. J., von Kriegsheim, A., Hebestreit, H. F., Mukherji, M., Schofield, C. J., Maxwell, P. H., Pugh, C. W. *et al.* Targeting of HIF-alpha to the von Hippel-Lindau ubiquitylation complex by O2-regulated prolyl hydroxylation. *Science* **292**, 468-472, (2001).

178 Wenger, R. H., Stiehl, D. P. & Camenisch, G. Integration of oxygen signaling at the consensus HRE. *Sci STKE* **2005**, re12, (2005).

179 Schodel, J., Oikonomopoulos, S., Ragoussis, J., Pugh, C. W., Ratcliffe, P. J. & Mole, D. R. High-resolution genome-wide mapping of HIF-binding sites by ChIP-seq. *Blood* **117**, e207-217, (2011).

180 Smaldone, M. C. & Maranchie, J. K. Clinical implications of hypoxia inducible factor in renal cell carcinoma. *Urol Oncol* **27**, 238-245, (2009).

181 Schodel, J., Grampp, S., Maher, E. R., Moch, H., Ratcliffe, P. J., Russo, P. & Mole, D. R. Hypoxia, Hypoxia-inducible Transcription Factors, and Renal Cancer. *Eur Urol* **69**, 646-657, (2016).

182 Ortiz-Barahona, A., Villar, D., Pescador, N., Amigo, J. & del Peso, L. Genome-wide identification of hypoxia-inducible factor binding sites and target genes by a probabilistic model integrating transcription-profiling data and in silico binding site prediction. *Nucleic Acids Res* **38**, 2332-2345, (2010).

183 Kim, C. M., Vocke, C., Torres-Cabala, C., Yang, Y., Schmidt, L., Walther, M. & Linehan, W. M. Expression of hypoxia inducible factor-1alpha and 2alpha in genetically distinct early renal cortical tumors. *J Urol* **175**, 1908-1914, (2006).

184 Herman, J. G., Latif, F., Weng, Y., Lerman, M. I., Zbar, B., Liu, S., Samid, D., Duan, D. S., Gnarra, J. R., Linehan, W. M. & et al. Silencing of the VHL tumor-suppressor gene by DNA methylation in renal carcinoma. *Proc Natl Acad Sci U S A* **91**, 9700-9704, (1994).

185 Varela, I., Tarpey, P., Raine, K., Huang, D., Ong, C. K., Stephens, P., Davies, H., Jones, D., Lin, M. L., Teague, J., Bignell, G., Butler, A. *et al.* Exome sequencing identifies frequent mutation of the SWI/SNF complex gene PBRM1 in renal carcinoma. *Nature* **469**, 539-542, (2011).

186 Sun, X. J., Wei, J., Wu, X. Y., Hu, M., Wang, L., Wang, H. H., Zhang, Q. H., Chen, S. J., Huang, Q. H. & Chen, Z. Identification and characterization of a novel human histone H3 lysine 36-specific methyltransferase. *J Biol Chem* **280**, 35261-35271, (2005).
187 Jensen, D. E., Proctor, M., Marquis, S. T., Gardner, H. P., Ha, S. I., Chodosh, L. A., Ishov, A. M., Tommerup, N., Vissing, H., Sekido, Y., Minna, J., Borodovsky, A. *et al.* BAP1: a novel ubiquitin hydrolase which binds to the BRCA1 RING finger and enhances BRCA1-mediated cell growth suppression. *Oncogene* **16**, 1097-1112, (1998).
188 He, X., Wang, J., Messing, E. M. & Wu, G. Regulation of receptor for activated C kinase 1 protein by the von Hippel-Lindau tumor suppressor in IGF-I-induced renal carcinoma cell invasiveness. *Oncogene* **30**, 535-547, (2011).
189 Duran, A., Amanchy, R., Linares, J. F., Joshi, J., Abu-Baker, S., Porollo, A., Hansen, M., Moscat, J. & Diaz-Meco, M. T. p62 is a key regulator of nutrient sensing in the mTORC1 pathway. *Mol Cell* **44**, 134-146, (2011).
190 Gebhard, R. L., Clayman, R. V., Prigge, W. F., Figenshau, R., Staley, N. A., Reesey, C. & Bear, A. Abnormal cholesterol metabolism in renal clear cell carcinoma. *J Lipid Res* **28**, 1177-1184, (1987).
191 Linehan, W. M., Srinivasan, R. & Schmidt, L. S. The genetic basis of kidney cancer: a metabolic disease. *Nat Rev Urol* **7**, 277-285, (2010).
192 Senbabaoglu, Y., Gejman, R. S., Winer, A. G., Liu, M., Van Allen, E. M., de Velasco, G., Miao, D., Ostrovnaya, I., Drill, E., Luna, A., Weinhold, N., Lee, W. *et al.* Tumor immune microenvironment characterization in clear cell renal cell carcinoma identifies prognostic and immunotherapeutically relevant messenger RNA signatures. *Genome Biol* **17**, 231, (2016).
193 Chevrier, S., Levine, J. H., Zanotelli, V. R. T., Silina, K., Schulz, D., Bacac, M., Ries, C. H., Ailles, L., Jewett, M. A. S., Moch, H., van den Broek, M., Beisel, C. *et al.* An Immune Atlas of Clear Cell Renal Cell Carcinoma. *Cell* **169**, 736-749 e718, (2017).
194 Liotta, F., Gacci, M., Frosali, F., Querci, V., Vittori, G., Lapini, A., Santarlasci, V., Serni, S., Cosmi, L., Maggi, L., Angeli, R., Mazzinghi, B. *et al.* Frequency of regulatory T cells in peripheral blood and in tumour-infiltrating lymphocytes correlates with poor prognosis in renal cell carcinoma. *BJU Int* **107**, 1500-1506, (2011).
195 Geissler, K., Fornara, P., Lautenschlager, C., Holzhausen, H. J., Seliger, B. & Riemann, D. Immune signature of tumor infiltrating immune cells in renal cancer. *Oncoimmunology* **4**, e985082, (2015).
196 Thompson, R. H., Dong, H., Lohse, C. M., Leibovich, B. C., Blute, M. L., Cheville, J. C. & Kwon, E. D. PD-1 is expressed by tumor-infiltrating immune cells and is associated with poor outcome for patients with renal cell carcinoma. *Clin Cancer Res* **13**, 1757-1761, (2007).
197 Seliger, B. Immune Escape Mechanisms of Renal Cell Carcinoma. *European Urology Supplements* **6**, 616-622, (2007).
198 Frankenberger, B., Noessner, E. & Schendel, D. J. Immune suppression in renal cell carcinoma. *Semin Cancer Biol* **17**, 330-343, (2007).
199 Saenz-Lopez, P., Gouttefangeas, C., Hennenlotter, J., Concha, A., Maleno, I., Ruiz-Cabello, F., Cozar, J. M., Tallada, M., Stenzl, A., Rammensee, H. G., Garrido, F. & Cabrera, T. Higher HLA class I expression in renal cell carcinoma than in autologous normal tissue. *Tissue Antigens* **75**, 110-118, (2010).
200 Stickel, J. S., Stickel, N., Hennenlotter, J., Klingel, K., Stenzl, A., Rammensee, H. G. & Stevanovic, S. Quantification of HLA class I molecules on renal cell carcinoma using Edman degradation. *BMC Urol* **11**, 1, (2011).
201 Jung, D., Hilmes, C., Knuth, A., Jaeger, E., Huber, C. & Seliger, B. Gene transfer of the Co-stimulatory molecules B7-1 and B7-2 enhances the immunogenicity of human renal cell carcinoma to a different extent. *Scand J Immunol* **50**, 242-249, (1999).
202 Lang, S., Atarashi, Y., Nishioka, Y., Stanson, J., Meidenbauer, N. & Whiteside, T. L. B7.1 on human carcinomas: costimulation of T cells and enhanced tumor-induced T-cell death. *Cell Immunol* **201**, 132-143, (2000).

203 Dong, H., Strome, S. E., Salomao, D. R., Tamura, H., Hirano, F., Flies, D. B., Roche, P. C., Lu, J., Zhu, G., Tamada, K., Lennon, V. A., Celis, E. *et al.* Tumor-associated B7-H1 promotes T-cell apoptosis: a potential mechanism of immune evasion. *Nat Med* **8**, 793-800, (2002).
204 Bukur, J., Malenica, B., Huber, C. & Seliger, B. Altered expression of nonclassical HLA class Ib antigens in human renal cell carcinoma and its association with impaired immune response. *Hum Immunol* **64**, 1081-1092, (2003).
205 Ibrahim, E. C., Guerra, N., Lacombe, M. J., Angevin, E., Chouaib, S., Carosella, E. D., Caignard, A. & Paul, P. Tumor-specific up-regulation of the nonclassical class I HLA-G antigen expression in renal carcinoma. *Cancer Res* **61**, 6838-6845, (2001).
206 Uzzo, R. G., Rayman, P., Kolenko, V., Clark, P. E., Bloom, T., Ward, A. M., Molto, L., Tannenbaum, C., Worford, L. J., Bukowski, R., Tubbs, R., Hsi, E. D. *et al.* Mechanisms of apoptosis in T cells from patients with renal cell carcinoma. *Clin Cancer Res* **5**, 1219-1229, (1999).
207 Adam, P. J., Terrett, J. A., Steers, G., Stockwin, L., Loader, J. A., Fletcher, G. C., Lu, L. S., Leach, B. I., Mason, S., Stamps, A. C., Boyd, R. S., Pezzella, F. *et al.* CD70 (TNFSF7) is expressed at high prevalence in renal cell carcinomas and is rapidly internalised on antibody binding. *Br J Cancer* **95**, 298-306, (2006).
208 Biswas, K., Richmond, A., Rayman, P., Biswas, S., Thornton, M., Sa, G., Das, T., Zhang, R., Chahlavi, A., Tannenbaum, C. S., Novick, A., Bukowski, R. *et al.* GM2 expression in renal cell carcinoma: potential role in tumor-induced T-cell dysfunction. *Cancer Res* **66**, 6816-6825, (2006).
209 Thornton, M. V., Kudo, D., Rayman, P., Horton, C., Molto, L., Cathcart, M. K., Ng, C., Paszkiewicz-Kozik, E., Bukowski, R., Derweesh, I., Tannenbaum, C. S. & Finke, J. H. Degradation of NF-kappa B in T cells by gangliosides expressed on renal cell carcinomas. *J Immunol* **172**, 3480-3490, (2004).
210 Ohm, J. E. & Carbone, D. P. VEGF as a mediator of tumor-associated immunodeficiency. *Immunol Res* **23**, 263-272, (2001).
211 Romero, J. M., Aptsiauri, N., Vazquez, F., Cozar, J. M., Canton, J., Cabrera, T., Tallada, M., Garrido, F. & Ruiz-Cabello, F. Analysis of the expression of HLA class I, proinflammatory cytokines and chemokines in primary tumors from patients with localized and metastatic renal cell carcinoma. *Tissue Antigens* **68**, 303-310, (2006).
212 Uyttenhove, C., Pilotte, L., Theate, I., Stroobant, V., Colau, D., Parmentier, N., Boon, T. & Van den Eynde, B. J. Evidence for a tumoral immune resistance mechanism based on tryptophan degradation by indoleamine 2,3-dioxygenase. *Nat Med* **9**, 1269-1274, (2003).
213 Prendergast, G. C., Metz, R. & Muller, A. J. IDO recruits Tregs in melanoma. *Cell Cycle* **8**, 1818-1819, (2009).
214 Zea, A. H., Rodriguez, P. C., Atkins, M. B., Hernandez, C., Signoretti, S., Zabaleta, J., McDermott, D., Quiceno, D., Youmans, A., O'Neill, A., Mier, J. & Ochoa, A. C. Arginase-producing myeloid suppressor cells in renal cell carcinoma patients: a mechanism of tumor evasion. *Cancer Res* **65**, 3044-3048, (2005).
215 Cesana, G. C., DeRaffele, G., Cohen, S., Moroziewicz, D., Mitcham, J., Stoutenburg, J., Cheung, K., Hesdorffer, C., Kim-Schulze, S. & Kaufman, H. L. Characterization of CD4+CD25+ regulatory T cells in patients treated with high-dose interleukin-2 for metastatic melanoma or renal cell carcinoma. *J Clin Oncol* **24**, 1169-1177, (2006).
216 Bingle, L., Brown, N. J. & Lewis, C. E. The role of tumour-associated macrophages in tumour progression: implications for new anticancer therapies. *J Pathol* **196**, 254-265, (2002).
217 Mickley, A., Kovaleva, O., Kzhyshkowska, J. & Gratchev, A. Molecular and immunologic markers of kidney cancer-potential applications in predictive, preventive and personalized medicine. *EPMA J* **6**, 20, (2015).
218 Petrella, B. L. & Vincenti, M. P. Interleukin-1beta mediates metalloproteinase-dependent renal cell carcinoma tumor cell invasion through the activation of CCAAT enhancer binding protein beta. *Cancer Med* **1**, 17-27, (2012).

219 Daurkin, I., Eruslanov, E., Stoffs, T., Perrin, G. Q., Algood, C., Gilbert, S. M., Rosser, C. J., Su, L. M., Vieweg, J. & Kusmartsev, S. Tumor-associated macrophages mediate immunosuppression in the renal cancer microenvironment by activating the 15-lipoxygenase-2 pathway. *Cancer Res* **71**, 6400-6409, (2011).
220 Nakagomi, H., Pisa, P., Pisa, E. K., Yamamoto, Y., Halapi, E., Backlin, K., Juhlin, C. & Kiessling, R. Lack of interleukin-2 (IL-2) expression and selective expression of IL-10 mRNA in human renal cell carcinoma. *Int J Cancer* **63**, 366-371, (1995).
221 Bukowski, R. M., Rayman, P., Uzzo, R., Bloom, T., Sandstrom, K., Peereboom, D., Olencki, T., Budd, G. T., McLain, D., Elson, P., Novick, A. & Finke, J. H. Signal transduction abnormalities in T lymphocytes from patients with advanced renal carcinoma: clinical relevance and effects of cytokine therapy. *Clin Cancer Res* **4**, 2337-2347, (1998).
222 Baniyash, M. TCR zeta-chain downregulation: curtailing an excessive inflammatory immune response. *Nat Rev Immunol* **4**, 675-687, (2004).
223 Falk, K., Rotzschke, O., Stevanovic, S., Jung, G. & Rammensee, H. G. Allele-specific motifs revealed by sequencing of self-peptides eluted from MHC molecules. *Nature* **351**, 290-296, (1991).
224 Kowalewski, D. J. & Stevanovic, S. Biochemical large-scale identification of MHC class I ligands. *Methods Mol Biol* **960**, 145-157, (2013).
225 Perkins, D. N., Pappin, D. J., Creasy, D. M. & Cottrell, J. S. Probability-based protein identification by searching sequence databases using mass spectrometry data. *Electrophoresis* **20**, 3551-3567, (1999).
226 Eng, J. K., McCormack, A. L. & Yates, J. R. An approach to correlate tandem mass spectral data of peptides with amino acid sequences in a protein database. *J Am Soc Mass Spectrom* **5**, 976-989, (1994).
227 Kall, L., Canterbury, J. D., Weston, J., Noble, W. S. & MacCoss, M. J. Semi-supervised learning for peptide identification from shotgun proteomics datasets. *Nat Methods* **4**, 923-925, (2007).
228 Sturm, T., Leinders-Zufall, T., Macek, B., Walzer, M., Jung, S., Pommerl, B., Stevanovic, S., Zufall, F., Overath, P. & Rammensee, H. G. Mouse urinary peptides provide a molecular basis for genotype discrimination by nasal sensory neurons. *Nat Commun* **4**, 1616, (2013).
229 Chandran, P. A., Heidu, S., Zelba, H., Schmid-Horch, B., Rammensee, H. G., Pascolo, S. & Gouttefangeas, C. A Simple and Rapid Method for Quality Control of Major Histocompatibility Complex-Peptide Monomers by Flow Cytometry. *Front Immunol* **8**, 96, (2017).
230 Yao, M., Tabuchi, H., Nagashima, Y., Baba, M., Nakaigawa, N., Ishiguro, H., Hamada, K., Inayama, Y., Kishida, T., Hattori, K., Yamada-Okabe, H. & Kubota, Y. Gene expression analysis of renal carcinoma: adipose differentiation-related protein as a potential diagnostic and prognostic biomarker for clear-cell renal carcinoma. *J Pathol* **205**, 377-387, (2005).
231 Gulley, J. L. Toward an off-the-shelf vaccine for B-cell malignancies. *Blood* **120**, 1539-1540, (2012).
232 Potter, C. & Harris, A. L. Hypoxia inducible carbonic anhydrase IX, marker of tumour hypoxia, survival pathway and therapy target. *Cell Cycle* **3**, 164-167, (2004).
233 Pescador, N., Cuevas, Y., Naranjo, S., Alcaide, M., Villar, D., Landazuri, M. O. & Del Peso, L. Identification of a functional hypoxia-responsive element that regulates the expression of the egl nine homologue 3 (egln3/phd3) gene. *Biochem J* **390**, 189-197, (2005).
234 Ragel, B. T., Couldwell, W. T., Gillespie, D. L. & Jensen, R. L. Identification of hypoxia-induced genes in a malignant glioma cell line (U-251) by cDNA microarray analysis. *Neurosurg Rev* **30**, 181-187; discussion 187, (2007).
235 Forsythe, J. A., Jiang, B. H., Iyer, N. V., Agani, F., Leung, S. W., Koos, R. D. & Semenza, G. L. Activation of vascular endothelial growth factor gene transcription by hypoxia-inducible factor 1. *Mol Cell Biol* **16**, 4604-4613, (1996).

236 Erler, J. T., Bennewith, K. L., Nicolau, M., Dornhofer, N., Kong, C., Le, Q. T., Chi, J. T., Jeffrey, S. S. & Giaccia, A. J. Lysyl oxidase is essential for hypoxia-induced metastasis. *Nature* **440**, 1222-1226, (2006).
237 Ma, Y., Freitag, P., Zhou, J., Brune, B., Frede, S. & Fandrey, J. Thyroid hormone induces erythropoietin gene expression through augmented accumulation of hypoxia-inducible factor-1. *Am J Physiol Regul Integr Comp Physiol* **287**, R600-607, (2004).
238 Jin, H. O., An, S., Lee, H. C., Woo, S. H., Seo, S. K., Choe, T. B., Yoo, D. H., Lee, S. B., Um, H. D., Lee, S. J., Park, M. J., Kim, J. I. *et al.* Hypoxic condition- and high cell density-induced expression of Redd1 is regulated by activation of hypoxia-inducible factor-1alpha and Sp1 through the phosphatidylinositol 3-kinase/Akt signaling pathway. *Cell Signal* **19**, 1393-1403, (2007).
239 Olbryt, M., Jarzab, M., Jazowiecka-Rakus, J., Simek, K., Szala, S. & Sochanik, A. Gene expression profile of B 16(F10) murine melanoma cells exposed to hypoxic conditions in vitro. *Gene Expr* **13**, 191-203, (2006).
240 Hofbauer, K. H., Gess, B., Lohaus, C., Meyer, H. E., Katschinski, D. & Kurtz, A. Oxygen tension regulates the expression of a group of procollagen hydroxylases. *Eur J Biochem* **270**, 4515-4522, (2003).
241 Bruick, R. K. Expression of the gene encoding the proapoptotic Nip3 protein is induced by hypoxia. *Proc Natl Acad Sci U S A* **97**, 9082-9087, (2000).
242 Wykoff, C. C., Beasley, N. J., Watson, P. H., Turner, K. J., Pastorek, J., Sibtain, A., Wilson, G. D., Turley, H., Talks, K. L., Maxwell, P. H., Pugh, C. W., Ratcliffe, P. J. *et al.* Hypoxia-inducible expression of tumor-associated carbonic anhydrases. *Cancer Res* **60**, 7075-7083, (2000).
243 Marxsen, J. H., Stengel, P., Doege, K., Heikkinen, P., Jokilehto, T., Wagner, T., Jelkmann, W., Jaakkola, P. & Metzen, E. Hypoxia-inducible factor-1 (HIF-1) promotes its degradation by induction of HIF-alpha-prolyl-4-hydroxylases. *Biochem J* **381**, 761-767, (2004).
244 Hansel, D. E., Rahman, A., House, M., Ashfaq, R., Berg, K., Yeo, C. J. & Maitra, A. Met proto-oncogene and insulin-like growth factor binding protein 3 overexpression correlates with metastatic ability in well-differentiated pancreatic endocrine neoplasms. *Clin Cancer Res* **10**, 6152-6158, (2004).
245 Ferrara, N., Gerber, H. P. & LeCouter, J. The biology of VEGF and its receptors. *Nat Med* **9**, 669-676, (2003).
246 Kirschmann, D. A., Seftor, E. A., Fong, S. F., Nieva, D. R., Sullivan, C. M., Edwards, E. M., Sommer, P., Csiszar, K. & Hendrix, M. J. A molecular role for lysyl oxidase in breast cancer invasion. *Cancer Res* **62**, 4478-4483, (2002).
247 Sowter, H. M., Ratcliffe, P. J., Watson, P., Greenberg, A. H. & Harris, A. L. HIF-1-dependent regulation of hypoxic induction of the cell death factors BNIP3 and NIX in human tumors. *Cancer Res* **61**, 6669-6673, (2001).
248 Kessler, J. H., Beekman, N. J., Bres-Vloemans, S. A., Verdijk, P., van Veelen, P. A., Kloosterman-Joosten, A. M., Vissers, D. C., ten Bosch, G. J., Kester, M. G., Sijts, A., Wouter Drijfhout, J., Ossendorp, F. *et al.* Efficient identification of novel HLA-A(*)0201-presented cytotoxic T lymphocyte epitopes in the widely expressed tumor antigen PRAME by proteasome-mediated digestion analysis. *J Exp Med* **193**, 73-88, (2001).
249 Peper, J. K. & Stevanovic, S. A combined approach of human leukocyte antigen ligandomics and immunogenicity analysis to improve peptide-based cancer immunotherapy. *Cancer Immunol Immunother* **64**, 1295-1303, (2015).
250 Walter, S., Herrgen, L., Schoor, O., Jung, G., Wernet, D., Buhring, H. J., Rammensee, H. G. & Stevanovic, S. Cutting edge: predetermined avidity of human CD8 T cells expanded on calibrated MHC/anti-CD28-coated microspheres. *J Immunol* **171**, 4974-4978, (2003).
251 Bassani-Sternberg, M. & Coukos, G. Mass spectrometry-based antigen discovery for cancer immunotherapy. *Curr Opin Immunol* **41**, 9-17, (2016).
252 Di Marco, M. Peptidmotive von HLA-B*58:01, HLA-B*58:02 und HLA-A*32:01 und Unterschiede im HLA-Ligandom von HLA-B*58:01 und HLA-B*58:02. *Diploma thesis*, (2014).

253 Weinzierl, A. O., Lemmel, C., Schoor, O., Muller, M., Kruger, T., Wernet, D., Hennenlotter, J., Stenzl, A., Klingel, K., Rammensee, H. G. & Stevanovic, S. Distorted relation between mRNA copy number and corresponding major histocompatibility complex ligand density on the cell surface. *Mol Cell Proteomics* **6**, 102-113, (2007).
254 Martinez-Saez, O., Gajate Borau, P., Alonso-Gordoa, T., Molina-Cerrillo, J. & Grande, E. Targeting HIF-2 alpha in clear cell renal cell carcinoma: A promising therapeutic strategy. *Crit Rev Oncol Hematol* **111**, 117-123, (2017).
255 Zemmour, J. & Parham, P. Distinctive polymorphism at the HLA-C locus: implications for the expression of HLA-C. *J Exp Med* **176**, 937-950, (1992).
256 Rech, A. J. & Vonderheide, R. H. T-Cell Transfer Therapy Targeting Mutant KRAS. *N Engl J Med* **376**, e11, (2017).
257 Blais, M. E., Dong, T. & Rowland-Jones, S. HLA-C as a mediator of natural killer and T-cell activation: spectator or key player? *Immunology* **133**, 1-7, (2011).
258 Trowsdale, J. & Moffett, A. NK receptor interactions with MHC class I molecules in pregnancy. *Semin Immunol* **20**, 317-320, (2008).
259 Falk, K., Rotzschke, O., Grahovac, B., Schendel, D., Stevanovic, S., Gnau, V., Jung, G., Strominger, J. L. & Rammensee, H. G. Allele-specific peptide ligand motifs of HLA-C molecules. *Proc Natl Acad Sci U S A* **90**, 12005-12009, (1993).
260 Rasmussen, M., Harndahl, M., Stryhn, A., Boucherma, R., Nielsen, L. L., Lemonnier, F. A., Nielsen, M. & Buus, S. Uncovering the peptide-binding specificities of HLA-C: a general strategy to determine the specificity of any MHC class I molecule. *J Immunol* **193**, 4790-4802, (2014).
261 Braud, V., Jones, E. Y. & McMichael, A. The human major histocompatibility complex class Ib molecule HLA-E binds signal sequence-derived peptides with primary anchor residues at positions 2 and 9. *Eur J Immunol* **27**, 1164-1169, (1997).
262 Aldrich, C. J., DeCloux, A., Woods, A. S., Cotter, R. J., Soloski, M. J. & Forman, J. Identification of a Tap-dependent leader peptide recognized by alloreactive T cells specific for a class Ib antigen. *Cell* **79**, 649-658, (1994).
263 Apps, R., Meng, Z., Del Prete, G. Q., Lifson, J. D., Zhou, M. & Carrington, M. Relative expression levels of the HLA class-I proteins in normal and HIV-infected cells. *J Immunol* **194**, 3594-3600, (2015).
264 Braud, V. M., Allan, D. S., O'Callaghan, C. A., Soderstrom, K., D'Andrea, A., Ogg, G. S., Lazetic, S., Young, N. T., Bell, J. I., Phillips, J. H., Lanier, L. L. & McMichael, A. J. HLA-E binds to natural killer cell receptors CD94/NKG2A, B and C. *Nature* **391**, 795-799, (1998).
265 Borrego, F., Masilamani, M., Marusina, A. I., Tang, X. & Coligan, J. E. The CD94/NKG2 family of receptors: from molecules and cells to clinical relevance. *Immunol Res* **35**, 263-278, (2006).
266 Malnati, M. S., Peruzzi, M., Parker, K. C., Biddison, W. E., Ciccone, E., Moretta, A. & Long, E. O. Peptide specificity in the recognition of MHC class I by natural killer cell clones. *Science* **267**, 1016-1018, (1995).
267 Fadda, L., Borhis, G., Ahmed, P., Cheent, K., Pageon, S. V., Cazaly, A., Stathopoulos, S., Middleton, D., Mulder, A., Claas, F. H., Elliott, T., Davis, D. M. *et al.* Peptide antagonism as a mechanism for NK cell activation. *Proc Natl Acad Sci U S A* **107**, 10160-10165, (2010).
268 Borhis, G., Ahmed, P. S., Mbiribindi, B., Naiyer, M. M., Davis, D. M., Purbhoo, M. A. & Khakoo, S. I. A peptide antagonist disrupts NK cell inhibitory synapse formation. *J Immunol* **190**, 2924-2930, (2013).
269 King, A., Allan, D. S., Bowen, M., Powis, S. J., Joseph, S., Verma, S., Hiby, S. E., McMichael, A. J., Loke, Y. W. & Braud, V. M. HLA-E is expressed on trophoblast and interacts with CD94/NKG2 receptors on decidual NK cells. *Eur J Immunol* **30**, 1623-1631, (2000).
270 Adams, E. J. & Luoma, A. M. The adaptable major histocompatibility complex (MHC) fold: structure and function of nonclassical and MHC class I-like molecules. *Annu Rev Immunol* **31**, 529-561, (2013).

271 Sullivan, L. C., Hoare, H. L., McCluskey, J., Rossjohn, J. & Brooks, A. G. A structural perspective on MHC class Ib molecules in adaptive immunity. *Trends Immunol* **27**, 413-420, (2006).
272 Curigliano, G., Criscitiello, C., Gelao, L. & Goldhirsch, A. Molecular pathways: human leukocyte antigen G (HLA-G). *Clin Cancer Res* **19**, 5564-5571, (2013).
273 Carosella, E. D., Favier, B., Rouas-Freiss, N., Moreau, P. & Lemaoult, J. Beyond the increasing complexity of the immunomodulatory HLA-G molecule. *Blood* **111**, 4862-4870, (2008).
274 Lin, A., Zhang, X., Xu, H. H., Xu, D. P., Ruan, Y. Y. & Yan, W. H. HLA-G expression is associated with metastasis and poor survival in the Balb/c nu/nu murine tumor model with ovarian cancer. *Int J Cancer* **131**, 150-157, (2012).
275 Lila, N., Carpentier, A., Amrein, C., Khalil-Daher, I., Dausset, J. & Carosella, E. D. Implication of HLA-G molecule in heart-graft acceptance. *Lancet* **355**, 2138, (2000).
276 Colonna, M., Navarro, F., Bellon, T., Llano, M., Garcia, P., Samaridis, J., Angman, L., Cella, M. & Lopez-Botet, M. A common inhibitory receptor for major histocompatibility complex class I molecules on human lymphoid and myelomonocytic cells. *J Exp Med* **186**, 1809-1818, (1997).
277 Colonna, M., Samaridis, J., Cella, M., Angman, L., Allen, R. L., O'Callaghan, C. A., Dunbar, R., Ogg, G. S., Cerundolo, V. & Rolink, A. Human myelomonocytic cells express an inhibitory receptor for classical and nonclassical MHC class I molecules. *J Immunol* **160**, 3096-3100, (1998).
278 Rajagopalan, S. & Long, E. O. A human histocompatibility leukocyte antigen (HLA)-G-specific receptor expressed on all natural killer cells. *J Exp Med* **189**, 1093-1100, (1999).
279 Lee, N., Malacko, A. R., Ishitani, A., Chen, M. C., Bajorath, J., Marquardt, H. & Geraghty, D. E. The membrane-bound and soluble forms of HLA-G bind identical sets of endogenous peptides but differ with respect to TAP association. *Immunity* **3**, 591-600, (1995).
280 Diehl, M., Munz, C., Keilholz, W., Stevanovic, S., Holmes, N., Loke, Y. W. & Rammensee, H. G. Nonclassical HLA-G molecules are classical peptide presenters. *Curr Biol* **6**, 305-314, (1996).
281 Zemmour, J., Little, A. M., Schendel, D. J. & Parham, P. The HLA-A,B "negative" mutant cell line C1R expresses a novel HLA-B35 allele, which also has a point mutation in the translation initiation codon. *J Immunol* **148**, 1941-1948, (1992).
282 Storkus, W. J., Howell, D. N., Salter, R. D., Dawson, J. R. & Cresswell, P. NK susceptibility varies inversely with target cell class I HLA antigen expression. *J Immunol* **138**, 1657-1659, (1987).
283 Yamada, N., Ishikawa, Y., Dumrese, T., Tokunaga, K., Juji, T., Nagatani, T., Miwa, K., Rammensee, H. G. & Takiguchi, M. Role of anchor residues in peptide binding to three HLA-A26 molecules. *Tissue Antigens* **54**, 325-332, (1999).
284 Dumrese, T., Stevanovic, S., Seeger, F. H., Yamada, N., Ishikawa, Y., Tokunaga, K., Takiguchi, M. & Rammensee, H. HLA-A26 subtype A pockets accommodate acidic N-termini of ligands. *Immunogenetics* **48**, 350-353, (1998).
285 Shiga, H., Shioda, T., Tomiyama, H., Takamiya, Y., Oka, S., Kimura, S., Yamaguchi, Y., Gojoubori, T., Rammensee, H. G., Miwa, K. & Takiguchi, M. Identification of multiple HIV-1 cytotoxic T-cell epitopes presented by human leukocyte antigen B35 molecules. *AIDS* **10**, 1075-1083, (1996).
286 Kikuchi, A., Sakaguchi, T., Miwa, K., Takamiya, Y., Rammensee, H. G., Kaneko, Y. & Takiguchi, M. Binding of nonamer peptides to three HLA-B51 molecules which differ by a single amino acid substitution in the A-pocket. *Immunogenetics* **43**, 268-276, (1996).
287 Sidney, J., del Guercio, M. F., Southwood, S., Engelhard, V. H., Appella, E., Rammensee, H. G., Falk, K., Rotzschke, O., Takiguchi, M., Kubo, R. T., Grey, H. M. & Sette, A. Several HLA alleles share overlapping peptide specificities. *J Immunol* **154**, 247-259, (1995).
288 Gonzalez-Galarza, F. F., Takeshita, L. Y., Santos, E. J., Kempson, F., Maia, M. H., da Silva, A. L., Teles e Silva, A. L., Ghattaoraya, G. S., Alfirevic, A., Jones, A. R. & Middleton, D. Allele frequency net 2015 update: new features for HLA epitopes, KIR and disease and HLA adverse drug reaction associations. *Nucleic Acids Res* **43**, D784-788, (2015).

289 Andreatta, M., Lund, O. & Nielsen, M. Simultaneous alignment and clustering of peptide data using a Gibbs sampling approach. *Bioinformatics* **29**, 8-14, (2013).
290 Rammensee, H., Bachmann, J., Emmerich, N. P., Bachor, O. A. & Stevanovic, S. SYFPEITHI: database for MHC ligands and peptide motifs. *Immunogenetics* **50**, 213-219, (1999).
291 Nielsen, M. & Andreatta, M. NetMHCpan-3.0; improved prediction of binding to MHC class I molecules integrating information from multiple receptor and peptide length datasets. *Genome Med* **8**, 33, (2016).
292 Robinson, J., Halliwell, J. A., Hayhurst, J. D., Flicek, P., Parham, P. & Marsh, S. G. The IPD and IMGT/HLA database: allele variant databases. *Nucleic Acids Res* **43**, D423-431, (2015).
293 Barnstable, C. J., Bodmer, W. F., Brown, G., Galfre, G., Milstein, C., Williams, A. F. & Ziegler, A. Production of monoclonal antibodies to group A erythrocytes, HLA and other human cell surface antigens-new tools for genetic analysis. *Cell* **14**, 9-20, (1978).
294 Steinle, A., Falk, K., Rötzschke, O., Gnau, V., Stevanovic, S., Jung, G., Schendel, D.J., Rammensee, H.-G. Motif of HLA-B*35:03 peptide ligands. *Immunogenetics* **43**, 105-107, (1995).
295 Schittenhelm, R. B., Dudek, N. L., Croft, N. P., Ramarathinam, S. H. & Purcell, A. W. A comprehensive analysis of constitutive naturally processed and presented HLA-C*04:01 (Cw4)-specific peptides. *Tissue Antigens* **83**, 174-179, (2014).
296 Thomsen, M. C. & Nielsen, M. Seq2Logo: a method for construction and visualization of amino acid binding motifs and sequence profiles including sequence weighting, pseudo counts and two-sided representation of amino acid enrichment and depletion. *Nucleic Acids Res* **40**, W281-287, (2012).
297 Backert, L. & Kohlbacher, O. Immunoinformatics and epitope prediction in the age of genomic medicine. *Genome Med* **7**, 119, (2015).
298 Braud, V. M., Allan, D. S., Wilson, D. & McMichael, A. J. TAP- and tapasin-dependent HLA-E surface expression correlates with the binding of an MHC class I leader peptide. *Curr Biol* **8**, 1-10, (1998).
299 Strong, R. K., Holmes, M. A., Li, P., Braun, L., Lee, N. & Geraghty, D. E. HLA-E allelic variants. Correlating differential expression, peptide affinities, crystal structures, and thermal stabilities. *J Biol Chem* **278**, 5082-5090, (2003).
300 del Guercio, M. F., Sidney, J., Hermanson, G., Perez, C., Grey, H. M., Kubo, R. T. & Sette, A. Binding of a peptide antigen to multiple HLA alleles allows definition of an A2-like supertype. *J Immunol* **154**, 685-693, (1995).
301 Sette, A. & Sidney, J. Nine major HLA class I supertypes account for the vast preponderance of HLA-A and -B polymorphism. *Immunogenetics* **50**, 201-212, (1999).
302 Sidney, J., Peters, B., Frahm, N., Brander, C. & Sette, A. HLA class I supertypes: a revised and updated classification. *BMC Immunol* **9**, 1, (2008).
303 Doytchinova, I. A., Guan, P. & Flower, D. R. Identifiying human MHC supertypes using bioinformatic methods. *J Immunol* **172**, 4314-4323, (2004).
304 Barth, S. M., Schreitmuller, C. M., Proehl, F., Oehl, K., Lumpp, L. M., Kowalewski, D. J., Di Marco, M., Sturm, T., Backert, L., Schuster, H., Stevanovic, S., Rammensee, H. G. *et al.* Characterization of the Canine MHC Class I DLA-88*50101 Peptide Binding Motif as a Prerequisite for Canine T Cell Immunotherapy. *PLoS One* **11**, e0167017, (2016).
305 Hillen, N., Mester, G., Lemmel, C., Weinzierl, A. O., Muller, M., Wernet, D., Hennenlotter, J., Stenzl, A., Rammensee, H. G. & Stevanovic, S. Essential differences in ligand presentation and T cell epitope recognition among HLA molecules of the HLA-B44 supertype. *Eur J Immunol* **38**, 2993-3003, (2008).
306 Nielsen, M., Lundegaard, C., Worning, P., Lauemoller, S. L., Lamberth, K., Buus, S., Brunak, S. & Lund, O. Reliable prediction of T-cell epitopes using neural networks with novel sequence representations. *Protein Sci* **12**, 1007-1017, (2003).

307 Vita, R., Overton, J. A., Greenbaum, J. A., Ponomarenko, J., Clark, J. D., Cantrell, J. R., Wheeler, D. K., Gabbard, J. L., Hix, D., Sette, A. & Peters, B. The immune epitope database (IEDB) 3.0. *Nucleic Acids Res* **43**, D405-412, (2015).
308 McCutcheon, J. A., Gumperz, J., Smith, K. D., Lutz, C. T. & Parham, P. Low HLA-C expression at cell surfaces correlates with increased turnover of heavy chain mRNA. *J Exp Med* **181**, 2085-2095, (1995).
309 Neisig, A., Melief, C. J. & Neefjes, J. Reduced cell surface expression of HLA-C molecules correlates with restricted peptide binding and stable TAP interaction. *J Immunol* **160**, 171-179, (1998).
310 Neefjes, J. J. & Ploegh, H. L. Allele and locus-specific differences in cell surface expression and the association of HLA class I heavy chain with beta 2-microglobulin: differential effects of inhibition of glycosylation on class I subunit association. *Eur J Immunol* **18**, 801-810, (1988).
311 Setini, A., Beretta, A., De Santis, C., Meneveri, R., Martayan, A., Mazzilli, M. C., Appella, E., Siccardi, A. G., Natali, P. G. & Giacomini, P. Distinctive features of the alpha 1-domain alpha helix of HLA-C heavy chains free of beta 2-microglobulin. *Hum Immunol* **46**, 69-81, (1996).
312 Schaefer, M. R., Williams, M., Kulpa, D. A., Blakely, P. K., Yaffee, A. Q. & Collins, K. L. A novel trafficking signal within the HLA-C cytoplasmic tail allows regulated expression upon differentiation of macrophages. *J Immunol* **180**, 7804-7817, (2008).
313 Mandelboim, O., Reyburn, H. T., Sheu, E. G., Vales-Gomez, M., Davis, D. M., Pazmany, L. & Strominger, J. L. The binding site of NK receptors on HLA-C molecules. *Immunity* **6**, 341-350, (1997).
314 Boyington, J. C., Brooks, A. G. & Sun, P. D. Structure of killer cell immunoglobulin-like receptors and their recognition of the class I MHC molecules. *Immunol Rev* **181**, 66-78, (2001).
315 Colonna, M., Borsellino, G., Falco, M., Ferrara, G. B. & Strominger, J. L. HLA-C is the inhibitory ligand that determines dominant resistance to lysis by NK1- and NK2-specific natural killer cells. *Proc Natl Acad Sci U S A* **90**, 12000-12004, (1993).
316 Hilton, H. G. & Parham, P. Missing or altered self: human NK cell receptors that recognize HLA-C. *Immunogenetics* **69**, 567-579, (2017).
317 Chaux, P., Luiten, R., Demotte, N., Vantomme, V., Stroobant, V., Traversari, C., Russo, V., Schultz, E., Cornelis, G. R., Boon, T. & van der Bruggen, P. Identification of five MAGE-A1 epitopes recognized by cytolytic T lymphocytes obtained by in vitro stimulation with dendritic cells transduced with MAGE-A1. *J Immunol* **163**, 2928-2936, (1999).
318 Breckpot, K., Heirman, C., De Greef, C., van der Bruggen, P. & Thielemans, K. Identification of new antigenic peptide presented by HLA-Cw7 and encoded by several MAGE genes using dendritic cells transduced with lentiviruses. *J Immunol* **172**, 2232-2237, (2004).
319 Vantomme, V., Boel, P., De Plaen, E., Boon, T. & van der Bruggen, P. A new tumor-specific antigenic peptide encoded by MAGE-6 is presented to cytolytic T lymphocytes by HLA-Cw16. *Cancer Immun* **3**, 17, (2003).
320 Heidecker, L., Brasseur, F., Probst-Kepper, M., Gueguen, M., Boon, T. & Van den Eynde, B. J. Cytolytic T lymphocytes raised against a human bladder carcinoma recognize an antigen encoded by gene MAGE-A12. *J Immunol* **164**, 6041-6045, (2000).
321 Boel, P., Wildmann, C., Sensi, M. L., Brasseur, R., Renauld, J. C., Coulie, P., Boon, T. & van der Bruggen, P. BAGE: a new gene encoding an antigen recognized on human melanomas by cytolytic T lymphocytes. *Immunity* **2**, 167-175, (1995).
322 Van den Eynde, B., Peeters, O., De Backer, O., Gaugler, B., Lucas, S. & Boon, T. A new family of genes coding for an antigen recognized by autologous cytolytic T lymphocytes on a human melanoma. *J Exp Med* **182**, 689-698, (1995).
323 Gnjatic, S., Nagata, Y., Jager, E., Stockert, E., Shankara, S., Roberts, B. L., Mazzara, G. P., Lee, S. Y., Dunbar, P. R., Dupont, B., Cerundolo, V., Ritter, G. *et al.* Strategy for monitoring T cell responses to NY-ESO-1 in patients with any HLA class I allele. *Proc Natl Acad Sci U S A* **97**, 10917-10922, (2000).

324 Castelli, C., Tarsini, P., Mazzocchi, A., Rini, F., Rivoltini, L., Ravagnani, F., Gallino, F., Belli, F. & Parmiani, G. Novel HLA-Cw8-restricted T cell epitopes derived from tyrosinase-related protein-2 and gp100 melanoma antigens. *J Immunol* **162**, 1739-1748, (1999).
325 Friedman, R. S., Spies, A. G. & Kalos, M. Identification of naturally processed CD8 T cell epitopes from prostein, a prostate tissue-specific vaccine candidate. *Eur J Immunol* **34**, 1091-1101, (2004).
326 Redchenko, I., Harrop, R., Ryan, M. G., Hawkins, R. E. & Carroll, M. W. Identification of a major histocompatibility complex class I-restricted T-cell epitope in the tumour-associated antigen, 5T4. *Immunology* **118**, 50-57, (2006).
327 Nagata, Y., Hanagiri, T., Takenoyama, M., Fukuyama, T., Mizukami, M., So, T., Ichiki, Y., Sugaya, M., Sugio, K. & Yasumoto, K. Identification of the HLA-Cw*0702-restricted tumor-associated antigen recognized by a CTL clone from a lung cancer patient. *Clin Cancer Res* **11**, 5265-5272, (2005).
328 Tran, E., Ahmadzadeh, M., Lu, Y. C., Gros, A., Turcotte, S., Robbins, P. F., Gartner, J. J., Zheng, Z., Li, Y. F., Ray, S., Wunderlich, J. R., Somerville, R. P. *et al.* Immunogenicity of somatic mutations in human gastrointestinal cancers. *Science* **350**, 1387-1390, (2015).
329 Chiari, R., Foury, F., De Plaen, E., Baurain, J. F., Thonnard, J. & Coulie, P. G. Two antigens recognized by autologous cytolytic T lymphocytes on a melanoma result from a single point mutation in an essential housekeeping gene. *Cancer Res* **59**, 5785-5792, (1999).
330 Cheever, M. A., Allison, J. P., Ferris, A. S., Finn, O. J., Hastings, B. M., Hecht, T. T., Mellman, I., Prindiville, S. A., Viner, J. L., Weiner, L. M. & Matrisian, L. M. The prioritization of cancer antigens: a national cancer institute pilot project for the acceleration of translational research. *Clin Cancer Res* **15**, 5323-5337, (2009).
331 Heinzel, A. S., Grotzke, J. E., Lines, R. A., Lewinsohn, D. A., McNabb, A. L., Streblow, D. N., Braud, V. M., Grieser, H. J., Belisle, J. T. & Lewinsohn, D. M. HLA-E-dependent presentation of Mtb-derived antigen to human CD8+ T cells. *J Exp Med* **196**, 1473-1481, (2002).
332 Salerno-Goncalves, R., Fernandez-Vina, M., Lewinsohn, D. M. & Sztein, M. B. Identification of a human HLA-E-restricted CD8+ T cell subset in volunteers immunized with Salmonella enterica serovar Typhi strain Ty21a typhoid vaccine. *J Immunol* **173**, 5852-5862, (2004).
333 Romagnani, C., Pietra, G., Falco, M., Mazzarino, P., Moretta, L. & Mingari, M. C. HLA-E-restricted recognition of human cytomegalovirus by a subset of cytolytic T lymphocytes. *Hum Immunol* **65**, 437-445, (2004).
334 Garcia, P., Llano, M., de Heredia, A. B., Willberg, C. B., Caparros, E., Aparicio, P., Braud, V. M. & Lopez-Botet, M. Human T cell receptor-mediated recognition of HLA-E. *Eur J Immunol* **32**, 936-944, (2002).
335 Housseau, F., Bright, R. K., Simonis, T., Nishimura, M. I. & Topalian, S. L. Recognition of a shared human prostate cancer-associated antigen by nonclassical MHC-restricted CD8+ T cells. *J Immunol* **163**, 6330-6337, (1999).
336 Lampen, M. H., Hassan, C., Sluijter, M., Geluk, A., Dijkman, K., Tjon, J. M., de Ru, A. H., van der Burg, S. H., van Veelen, P. A. & van Hall, T. Alternative peptide repertoire of HLA-E reveals a binding motif that is strikingly similar to HLA-A2. *Mol Immunol* **53**, 126-131, (2013).

8. Appendix

8.1. Lists of TUMAPs of selected target candidates

Supplementary Table 5: Class I TUMAPs of selected target candidates. All TUMAPs of the 112 filtered antigens are listed with number of ccRCC positive samples, Ensembl ID of the corresponding gene, Uniprot ID of the corresponding protein, fold change gene expression within the TCGA dataset and its statistical significance. Gene expression data was downloaded on 12/9/16 from the Genomic Data Commons Portal (https://gdc-portal.nci.nih.gov/, HTSeq – FPKM-UQ normalized data).

Gene TUMAP	Found on n ccRCC patients	Ensembl_ID	Uniprot_ID	FC expression (Tum/Ben)	p-Value
ABCA1	6	ENSG00000165029	O95477	3.17	1.73E-34
QEMDLVRML	1				
RLSDLGISSY	3				
SAGLLVVILK	2				
ACAD11	16	ENSG00000240303	Q709F0	2.84	3.55E-14
AEVLPQHKF	7				
DLAHFSLFY	1				
FPVPKPILY	2				
IYVATVETL	1				
RTQNTSLSR	1				
RVPATNLIL	2				
SVIGTEFYV	2				
ACLY	25	ENSG00000131473	P53396	2.85	5.45E-37
ATADYICKV	1				
ATVGKATGFLK	1				
ETMNYAQIR	3				
EVEKITTSK	1				
EVPPPTVPMDY	1				
FHHEGGVDV	1				
FISGLFNFY	2				
GEIIQSVYEDL	1				
GVAIGGDRY	2				
HFPATPLLDY	2				
KEILIPVF	2				
LPKYSCQFI	1				
SRHTKAIVW	1				
TAVAKNQAL	1				
TMFSSEVQF	1				
VSSLTSGLLTI	1				
YPFTGDHKQKF	2				
YVLPEHMSM	1				
ADM	5	ENSG00000148926	P35318	8.87	6.75E-38
KLVSVALMY	1				
LPEAGPGRTL	4				
ADSSL1	16	ENSG00000185100	Q8N142	6.14	1.08E-25
AVKWVGVGK	1				
FPTEQINEI	5				
GEVKVGVSY	1				

Supplementary Table 5 (continued)

KEYDFHLLP	2				
QHQSMFPTL	1				
VENHVGVAVKW	1				
VLGEVKVGV	4				
WLDLMILRY	1				
AHNAK2	14	ENSG00000185567	Q8IVF2	24.43	7.59E-37
DALKILQY	1				
GRLEGDLSL	1				
IPEPHTQARVY	1				
KLMVPRFSF	1				
KLPEGHMPEV	1				
MPKFKIPSL	2				
MPKFKMPSF	1				
RPQVHIPSL	1				
RRKFLNLRF	1				
SLDVSAPKV	3				
SVDVSPPKV	1				
ALDOA	19	ENSG00000149925	P04075	2.32	9.69E-32
DGRPFPQVI	1				
GRALQASALK	1				
PLLKPWAL	1				
QEEYVKRAL	2				
RALQASALK	2				
RRFYRQLLL	1				
RTVPPAVTGITF	4				
SEEEASINL	4				
SIAKRLQSI	1				
TENTEENRRF	2				
ALPK2	18	ENSG00000198796	Q86TB3	4.64	4.63E-33
AEAQPLEGF	1				
DELIQRNY	2				
DPIDEISVIEY	4				
DTIDSLVGR	2				
FPWEKPTTL	4				
KELSVTDSL	1				
NPKKPNANL	2				
SENNPLVQF	1				
YVFPVSQKR	1				
ANGPTL4	13	ENSG00000167772	Q9BY76	79.23	3.21E-39
AQNSRIQQL	3				
AQNSRIQQLF	4				
DEMNVLAH	1				
LPRDCQELF	1				
RPWEAYKAGF	1				
RTRSQLSALER	2				
SRIQQLFHK	1				
APOB	30	ENSG00000084674	P04114	4.78	2.99E-13
AEARSEILAHW	1				

Supplementary Table 5 (continued)

AEAVLKTLQEL	1				
AFTDLHLRY	1				
FELPTGAGL	1				
FTDLHLRY	1				
GEATLQRIY	2				
GRFREHNAKF	1				
HSTKNHLQL	1				
IFMENAFEL	1				
IRWKNEVRI	1				
KLRLEPLKL	1				
KLVELAHQY	1				
KPQEFTIVAF	1				
LPDFRLPEI	1				
QRANLFNKL	1				
SEPINIIDAL	1				
SLDGKAALTEL	1				
SPAKLLLQM	1				
SSASLAHMK	2				
SSPITLQAL	1				
TAYGSTVSKR	1				
TLLDSPIKV	1				
VASHIANIL	1				
VLMDKLVEL	3				
VPDGVSKVL	1				
YQMDIQQEL	1				
APOL1	11	ENSG00000100342	O14791	2.62	8.41E-27
DVAPVSFFL	3				
IGKDIRALR	1				
KEKVSTQNL	1				
KLTDVAPVSF	1				
QELEEKLNIL	1				
RGIGKDIRALR	2				
SVPHASASR	2				
ARHGAP42	5	ENSG00000165895	A6NI28	2.51	1.27E-25
AEPLMTYKL	1				
DEISIAQSL	3				
VQKLMNTTF	1				
ARSE	9	ENSG00000157399	P51690	2.12	1.13E-12
DVFPTVVRL	2				
HSDHEFLMHY	4				
LTHLIPVSW	2				
SSIGYRVLQW	1				
ATP11A	5	ENSG00000068650	P98196	2.82	5.17E-27
ALINTVLKY	1				
EVALVEGVQR	1				
VLFELSKTV	3				
BCO1	3	ENSG00000135697	Q9HAY6	3.02	3.51E-25
IVSTDPQKL	3				

Supplementary Table 5 (continued)

BNIP3	6	ENSG00000176171	Q12983	3.18	1.53E-33
LAIGLGIYI	1				
LAIGLGIYIGR	3				
RRKEVESILKK	1				
TLSMRNTSV	1				
C1QB	7	ENSG00000173369	P02746	7.86	2.6E-36
IAFSATRTI	6				
LEQGENVFL	1				
C3	35	ENSG00000125730	P01024	40.66	8.94E-34
AEDLVGKSLY	3				
FTIPANREF	1				
HRIHWESASLL	1				
HRIHWESASLLR	1				
IPIEDGSGEVVL	2				
IPSFRLVAY	1				
KIWDVVEKA	3				
LSSEKTVL	1				
QEVEVKAAVY	1				
SEFPESWLW	3				
SPAYRVPVA	1				
TESETRILL	4				
VEIRAVLY	1				
VEKVVLVSL	7				
VTITARFLY	4				
YSIITPNILRL	1				
CA9	10	ENSG00000107159	Q16790	1072.87	2.9E-39
APLCPSPWLPL	1				
EHTVEGHRF	1				
GTKGGVSYR	1				
SPRAAEPVQL	4				
SPVDIRPQL	2				
SVAFLVQMR	1				
CCND1	19	ENSG00000110092	P24385	4.97	1.54E-37
ALLESSLRQA	5				
IEALLESSL	2				
KHAQTFVAL	1				
MELLLVNKL	1				
RAYPDANLL	1				
RSPNNFLSY	1				
SPNNFLSYY	2				
TPHDFIEHF	6				
CD180	3	ENSG00000134061	Q99467	6.32	5.23E-28
QELDLTATHL	3				
CDK18	13	ENSG00000117266	Q07002	6.30	6.24E-38
AEAALSHSY	6				
AEAALSHSYF	1				
EELHLIFRL	2				
SEFRTYSF	4				

Supplementary Table 5 (continued)

CEBPA	4	ENSG00000245848	P49715	2.36	3.08E-21
YLDGRLEPLY	4				
CENPF	4	ENSG00000117724	P49454	4.51	3.41E-32
KNKEIQEL	1				
LEKLKLAV	3				
COL1A1	4	ENSG00000108821	P02452	9.18	5.38E-24
FSFVDLRLL	3				
TGNLKKAL	1				
COL4A2	4	ENSG00000134871	P08572	3.40	5.56E-30
HPIIAPTGVTF	4				
COL6A2	15	ENSG00000142173	P12110	4.69	3.89E-30
ALCDRDVTV	2				
DSLHESAHSMR	1				
DTINRIIKV	1				
FLLDGSERL	3				
HEKHESENL	1				
NEFYLDQVAL	1				
RPVDIVFLL	2				
RRFVEQVAR	1				
TAIGIGDMF	1				
TPSALKFAY	1				
TWTPSALKF	1				
CP	35	ENSG00000047457	P00450	24.92	5.17E-29
AEDRVKWYL	1				
AEVGDTIRVTF	3				
DSTFRVPVER	1				
DVGDKVKIIFK	1				
ETFRTTIEK	1				
FLDKGEFY	1				
GTTRIGGSY	1				
HFHGHSFQY	1				
IEKPVWLGF	1				
NAFLDKGEFY	2				
NEIDLHTVHF	3				
NEVDVHAAF	3				
NEVDVHAAFF	3				
RLYKKALYL	1				
RQSEDSTFY	1				
RTTIEKPVW	1				
SHVAPTETF	3				
SIEPIGVRF	1				
STFRVPVERK	2				
TDSTFRVPVER	1				
TFYLGERTYY	1				
YLGERTYYI	1				
YTDASFTNR	1				
CSPG4	9	ENSG00000173546	Q6UVK1	8.44	2.87E-36
GRLGLEVGR	1				

Supplementary Table 5 (continued)

GRLQVRLVL	1				
LSTDPQHHAY	1				
QAEVYAGNILY	3				
STDPQHHAY	2				
TLAPPLLRV	1				
CYP2J2	25	ENSG00000134716	P51589	48.52	9.5E-36
ARTELFIFF	2				
DHFLENGQF	1				
ETRDFIDAY	1				
GTETTSTTLRW	1				
ITISPVSHR	1				
REVTVDTTL	5				
RPPNNEKLSL	2				
TALHRDPTEW	1				
TETTSTTLRW	1				
TTLRWALLY	5				
VLITGLPLI	2				
VPREVTVDTTL	2				
VVHPRTLLL	1				
CYP3A5	7	ENSG00000106258	P20815	5.96	5.82E-24
RLFPVAIRL	7				
DDIT4	6	ENSG00000168209	Q9NX09	5.87	1.28E-33
FSSANSPFL	1				
LALDPSLVPTF	1				
REEGFDRSTSL	3				
RLWPKIQGL	1				
DIRAS2	10	ENSG00000165023	Q96HU8	9.61	1.08E-33
AEALARTW	1				
EAEALARTW	1				
SEAEALARTW	8				
DNAH11	11	ENSG00000105877	Q96DT5	34.34	6.71E-31
GLVDIMVHL	8				
HYSTLVHMF	1				
NLDLLVQGY	1				
TPARVIVLL	1				
EGLN3	34	ENSG00000129521	Q9H6Z9	25.50	1.99E-39
AEERAEAKKKF	1				
EAKKKFRNL	1				
FLLSLIDRL	9				
GSRLGKYYVK	2				
LSLIDRLVL	1				
LSLIDRLVLY	1				
MPLGHIMRL	8				
SLIDRLVLY	3				
SRLGKYYVK	2				
VPCLHEVGF	2				
VQPSYATRY	3				
YVKERSKAM	1				

Supplementary Table 5 (continued)

EHD2	11	ENSG00000024422	Q9NZN4	6.51	2.11E-36
AERVDLIIL	1				
DEMLTHDI	2				
ERVDLIILL	1				
GTHMGPFVER	2				
SVLGRIWKL	4				
TEVGVQGGAF	1				
ENPP3	12	ENSG00000154269	O14638	47.97	1.9E-38
GETRLEASL	2				
HAGGPVSAR	4				
KEQNNPAWW	1				
KTCGIHSKY	1				
RAMYPTKTF	1				
TLMPNINKL	2				
YQGLKAATY	1				
ESM1	3	ENSG00000164283	Q9NQ30	14.25	6.67E-38
KSVLLLTTL	3				
FABP7	6	ENSG00000164434	O15540	2038.46	6.1E-38
EYMKALGVGF	1				
LTFGDVVAVR	3				
YMKALGVGF	2				
FGG	16	ENSG00000171557	P02679	5.56	7.33E-07
FLSTYQTKV	1				
GVYYQGGTYSK	1				
KMLEEIMKY	2				
KQSGLYFIK	2				
KRLDGSVDF	1				
KSRKMLEEI	1				
KVGPEADKY	1				
PYALRVEL	1				
SAIPYALRV	1				
SLEDILHQV	3				
THDSSIRYL	1				
TPNGYDNGIIW	1				
FSCN1	6	ENSG00000075618	Q16658	2.77	5.14E-30
ASASSLKKK	3				
HDDGRWSL	1				
SVQTADHRFLR	1				
TLDANRSSY	1				
GABRD	5	ENSG00000187730	O14764	83.47	4.56E-39
AAVPARVSL	1				
AFAHFNADY	1				
VTQELAISR	3				
GAL3ST1	4	ENSG00000128242	Q99999	7.98	4.94E-37
RLFESSFHY	1				
SLDPSSPQV	3				
GALNT14	9	ENSG00000158089	Q96FL9	2.16	6.77E-31
GEDAKSQVW	1				

Supplementary Table 5 (continued)

RPFGNVESRL	1				
SIPKESSIQK	5				
SRLDLRKNL	1				
TYIESASEL	1				
GAS2L3	7	ENSG00000139354	Q86XJ1	10.56	3.33E-38
SVSPVKATQK	7				
GJA4	3	ENSG00000187513	P35212	2.51	1.11E-25
NLLELVHLL	3				
GRIA4	11	ENSG00000152578	P48058	5.48	6.84E-08
APFNLVPHV	1				
DTDRGYSIL	1				
NILEQIVSV	7				
RIISRQIVL	2				
HAVCR1	9	ENSG00000113249	Q96D42	6.13	1.47E-20
GVIIAKKYFFK	4				
HPQVVILSL	1				
IIAKKYFFK	3				
VILSLILHL	1				
HHLA2	4	ENSG00000114455	Q9UM44	13.50	7.77E-29
VYPRPIITW	4				
HILPDA	4	ENSG00000135245	Q9Y5L2	45.21	5.29E-39
LPDHPSRSM	3				
TLLSIFVRV	1				
HLA-DMA	3	ENSG00000204257	P28067	2.80	5.4E-35
FPIAEVFTL	3				
HLA-DOA	7	ENSG00000204252	P06340	2.27	1.16E-18
HEFDEEQLF	1				
LPKSRVEL	1				
VTEGVAQTSFY	5				
HLA-DQB2	6	ENSG00000232629	P05538	8.55	4.22E-26
FPKDFLVQF	2				
VMLSTPVAEA	4				
HLA-G	5	ENSG00000204632	P17693	10.21	2.28E-32
SEASSHTLQW	1				
TGAAVAAVLW	1				
YPAEIILTW	3				
HMOX1	16	ENSG00000100292	P09601	5.25	1.81E-36
AALEQDLAFW	1				
ATKFKQLYR	1				
EVIPYTPAMQRY	1				
IEEAKTAFL	4				
KAALEQDLAFW	1				
KESPVFAPVYF	1				
KIAQKALDL	4				
QVLKKIAQK	1				
RTEPELLVAHAY	1				
TEPELLVAHAY	1				

Supplementary Table 5 (continued)

HSD3B7	11	ENSG00000099377	Q9H2F3	4.43	1.81E-36
AALNALLQW	3				
IPASVEHGRVY	1				
NTKGHPFYR	2				
QWLLRPLVL	1				
RHFGYEPLF	2				
TTFTVSTDKAQR	2				
HSF4	21	ENSG00000102878	Q9ULV5	50.40	1.12E-39
ILWREVVTL	15				
RLLGEVQAL	1				
SPSPGKDPTL	4				
VPERGEPEL	1				
HSPB8	4	ENSG00000152137	Q9UJY1	5.08	9.16E-37
KQQEGGIVSK	1				
WPDWALPRL	3				
IFI27	7	ENSG00000165949	P40305	2.48	3.37E-23
AGIASSSIAAK	2				
GIASSSIAAK	3				
IASSSIAAK	1				
SGLTKFIL	1				
IGF2BP3	4	ENSG00000136231	O00425	3.65	2.49E-17
IMKKIRESY	1				
KIQEILTQV	3				
IGFBP3	5	ENSG00000146674	P17936	15.47	7.98E-38
NASAVSRLR	1				
NHLKFLNVL	1				
RPTLWAAA	3				
IL4R	3	ENSG00000077238	P24394	3.14	3.41E-38
VLWPESISV	3				
IRX3	11	ENSG00000177508	P78415	3.25	1.11E-26
AELPIFPQL	6				
FPQLGAQYEL	1				
LPIFPQLGAQY	2				
RTDEEGNAY	2				
KCNAB1	3	ENSG00000169282	Q14722	3.39	2.14E-24
VEVQLPELY	3				
KCNMA1	3	ENSG00000156113	Q12791	6.96	5.37E-27
VPPVFVSVY	3				
KCNN1	8	ENSG00000105642	Q92952	10.13	7.79E-30
RVFLISLEL	8				
KISS1R	11	ENSG00000116014	Q969F8	201.06	5.94E-35
EAFPSRALER	1				
RLSPGPRAY	1				
RPAPADSAL	6				
SEAFPSRAL	3				
LECT2	3	ENSG00000145826	O14960	2.14	0.00025002
GTLLPLQK	3				

Supplementary Table 5 (continued)

LOX	7	ENSG00000113083	P28300	11.63	8.04E-34
DVKPGNYILK	1				
GAWRQQIQW	2				
IQWENNGQVF	1				
IRYTGHHAY	3				
LOXL2	7	ENSG00000134013	Q9Y4K0	9.19	3.34E-34
FGFPGERTY	4				
GMFGFPGERTY	1				
KSWTASSSY	2				
LPCAT1	8	ENSG00000153395	Q8NF37	5.51	2.5E-39
ALAEGQLRL	1				
EEEKRNPAL	1				
GRNPFVHEL	1				
LEVPVSDLL	3				
YPNKLDTITW	2				
LRRK2	18	ENSG00000188906	Q5S007	2.15	5.76E-19
DGKKRHTL	1				
DIIRFLQQR	1				
ESSPKLVEL	1				
GEEHQKILL	4				
HETSLPVQL	2				
HHSFDLVIF	2				
KIMAQILTV	1				
KLPDPVKEY	1				
KPWLFNIKA	1				
MHSSSKEVF	1				
QTILAILKL	1				
TLLKKWAL	1				
VELEKIIL	1				
MET	11	ENSG00000105976	P08581	2.17	4.12E-25
APLEGGTRL	1				
FPIKYVNDFF	1				
HYVHVNATY	1				
KPFEKPVMI	1				
RISAIFSTF	4				
SYREDPIVY	1				
YVDPVITSI	2				
MS4A6A	3	ENSG00000110077	Q9H2W1	7.12	8.39E-34
MLICTLLEF	3				
NDRG1	26	ENSG00000104419	Q92597	2.64	4.93E-32
ALPDMVVSH	2				
FALNNPEM	1				
FPAGYMYPSM	5				
LPDMVVSHLF	1				
MPGTHTVTL	1				
MPSASMTRLM	1				
NPEMVEGLVL	1				
NVEVVHTYR	1				

Supplementary Table 5 (continued)

PSASMTRL	1				
QPAKLAEAF	3				
RPMPGTHTVTL	1				
SAGPKSMEV	1				
SHTSEGAHL	1				
SNVEVVHTYR	2				
YFVQGMGY	3				
YILTRFAL	1				
NDUFA4L2	22	ENSG00000185633	Q9NRX3	153.58	1.7E-38
AGASLGARFYR	1				
ASLGARFYR	2				
AVSTDYKKLKK	1				
DQYKFLAV	3				
GASLGARFY	3				
GSAALYLLR	9				
KRHPGIIPM	1				
RLSPNDQYK	1				
SLGARFYR	1				
NNMT	20	ENSG00000166741	P40261	35.86	1.8E-37
AESQILKHL	2				
AESQILKHLL	4				
GLFSLVARK	1				
KEIVVTDY	3				
LPLGREAVEA	1				
LVARKLSRPL	1				
RVKGPEKEEK	1				
SQILKHLL	4				
VEAAVKEAGY	2				
YTIEWFEVI	1				
NPTX2	15	ENSG00000106236	P47972	194.64	4.61E-38
ALLAASVALA	2				
ALLQRVTEL	2				
LLAASVALA	5				
PGDFREVL	1				
SPDAFKVSL	3				
VSLPLRTNY	2				
P4HA2	8	ENSG00000072682	O15460	3.21	3.03E-27
AEKELVQSL	5				
FHERGQEFL	1				
GEEATTTKSQVL	1				
WPALEDLVL	1				
PFKP	15	ENSG00000067057	Q01813	5.18	1.47E-36
GQIDKEAVQK	2				
GQLEHVQPWSV	1				
ILGTKRVL	1				
KEWSGLLEEL	3				
KVYFIYEGY	1				
LGYDTRVTI	1				

Supplementary Table 5 (continued)

MEWITAKL	1				
RRFQDAVRL	1				
RSFAGNLNTY	4				
PGF	5	ENSG00000119630	P49763	16.65	1.07E-36
YPSEVEHMF	5				
PLIN2	61	ENSG00000147872	Q99541	11.95	1.66E-36
AVDPQPSVV	1				
AVTTTVTGAK	2				
ESRTLAIAR	1				
EVSDSLLTSSK	1				
GAVTGSVEK	5				
GVMAGDIYSV	2				
HIESRTLAI	1				
IEERLPIL	1				
IEFARKNVY	3				
IQDAQDKLYL	3				
KEAKKVEGF	1				
LVGPFYPQL	1				
MAGDIYSVF	1				
RTLAIARNL	1				
SALPIIQKL	1				
SELLVEQY	3				
SINTVLGSR	5				
SLSTKLHSR	3				
SRVKEAKQK	1				
STKDQYPYLK	1				
STVHLIEFAR	3				
STVHLIEFARK	1				
SVASTITGVMDK	3				
SVFRNAASF	4				
TSSKGQLQK	4				
TVHLIEFAR	3				
VTTTVTGAK	3				
YPYLKSVC	1				
YQQALSRV	1				
PLOD1	6	ENSG00000083444	Q02809	2.62	1.62E-34
DVFMFLTNR	2				
KRFLGSGGF	1				
QLFYTKIFL	3				
PLOD2	24	ENSG00000152952	O00469	2.89	1.3E-30
AEARNMGMDF	1				
ALLNFVVKY	1				
GRLLSTANY	2				
IPTDKLLVI	5				
KESDGFHRF	1				
KIIAPLVTR	4				
LMKEVMEHY	1				
NPVDWKEKY	2				

Supplementary Table 5 (continued)

REFIAPVTL	2				
RPHHDASTF	2				
RYLNSGGFIGY	2				
YSKIFTENI	1				
PLOD3	8	ENSG00000106397	O60568	2.75	1.07E-37
AETEGYLRF	1				
HHDSSTFTL	1				
NPVDWKEQY	2				
SPRKGWAL	3				
YTVRTLGL	1				
PLXNA3	6	ENSG00000130827	P51805	2.53	1.27E-30
FPIDKPPSF	6				
PRAME	12	ENSG00000185686	P78395	3.88	0.0000177
GQHLHLETF	3				
KMILKMVQL	1				
MPMQDIKMIL	1				
QLLALLPSL	1				
SLLQHLIGL	4				
SPSVSQLSVL	1				
TVWSGNRASL	1				
PRUNE2	38	ENSG00000106772	Q8WUY3	2.63	3.23E-20
DEGKLSITL	4				
DEINLHQL	4				
DNSERNLSL	1				
ETRFILEEL	1				
FHSNITSDL	1				
IESPFEREL	1				
ITDSEQREL	1				
KVYEKVDSW	1				
LEEDSLKQSL	2				
NPSSDLDHTW	2				
NRLPGSQL	1				
REDPESVYL	2				
REFVPSNAEL	1				
SEAAFDHSF	4				
SEINTTHNL	9				
TEQLAHRL	1				
THNLDENEL	1				
YVMENLFLY	1				
RASSF4	4	ENSG00000107551	Q9H2L5	3.52	1.95E-34
EVPHEVAQY	3				
YHEGKSFQL	1				
RGS5	36	ENSG00000143248	O15539	5.54	4.78E-32
ALMEKDSL	1				
EIKIKLGI	7				
HALMEKDSL	5				
ILLQKPDSV	5				
KAKQIYEEF	1				

Supplementary Table 5 (continued)

KEIKIKLGI	1				
KEIKIKLGILL	1				
KIKSPAKMAEK	6				
KLLQNNYGL	5				
PAKTQKTSL	2				
VRSEFYQEL	2				
RNF145	4	ENSG00000145860	Q96MT1	2.09	3.86E-32
EAVLNVALR	3				
LEIADPIVL	1				
RPLP0	4	ENSG00000089157	P05388	2.04	3.1E-30
IEILSDVQL	3				
RGNVGFVF	1				
RPS19	4	ENSG00000105372	P39019	2.66	3.04E-34
ASTARHLYL	1				
TARHLYLR	3				
RRAD	14	ENSG00000166592	P55042	3.45	1.53E-20
ALFEGVVRQI	5				
EAAGHTYDR	2				
MPVDERDL	1				
MPVDERDLQA	4				
TSAALHHNV	1				
WPEDSEDSL	1				
SAP30	6	ENSG00000164105	O75446	6.28	1.04E-39
IPVNEKDTL	5				
RPGLNKAQL	1				
SCARB1	9	ENSG00000073060	Q8WTV0	20.59	1.55E-38
DVMNPSEILK	1				
GVFEGIPTYR	2				
HPNQEAHSL	3				
IVMPNILVL	1				
KEIPIPFYL	1				
VLMPKVMHY	1				
SCD	18	ENSG00000099194	O00767	13.09	1.44E-36
AVGEGFHNY	1				
ETHADPHNSRR	1				
FPYDYSASEY	1				
ITAGAHRL	1				
ITAGAHRLW	3				
LPLRLFLI	1				
RRYYKPGLLM	1				
RYAVVLNATW	2				
SEYRWHINF	1				
SLLHLGALY	4				
VVLNATWLV	1				
YAVVLNATW	1				
SHMT2	4	ENSG00000182199	P34897	4.43	6.27E-39
ALLERGYSL	4				

Supplementary Table 5 (continued)

SLC16A3	12	ENSG00000141526	O15427	11.29	1.86E-38
DTAWISSILL	1				
FVAGLGKVR	1				
KLLDATHVY	4				
KLLDATHVYM	1				
VPPVFVVSY	3				
VVHTPETSV	2				
SLC17A3	29	ENSG00000124564	O00476	5.61	1.03E-13
ALIVSLPYL	8				
APRYSSFL	2				
ARYGIALVL	1				
FLMGASRGF	2				
GYITATALL	2				
IPRKVPSL	2				
ITATALLTL	1				
KEYIISSL	1				
LPSSALIVSL	3				
MVVYIPTYI	2				
SALPFIVAW	3				
SEKEYIISSL	1				
SEVLPVDSF	1				
SLC6A13	6	ENSG00000010379	Q9NSD5	3.05	2.66E-11
SLYRLGTLK	1				
VMLPFSPLW	1				
YLYPNLTRL	4				
SLC6A8	9	ENSG00000130821	P48029	2.95	3.91E-25
IAYPRAVTL	7				
LPASYYFRF	1				
VVYYEPLVY	1				
SNX10	5	ENSG00000086300	Q9Y5X0	2.08	1.38E-28
ALLVQLPEL	3				
KVLQNALLL	1				
RQRLQSNAL	1				
STBD1	5	ENSG00000118804	O95210	2.07	4.71E-26
AEKLPSSNLL	1				
GRWNTYIPLHY	1				
VENGGVTRW	3				
TLR3	14	ENSG00000164342	O15455	3.31	1.88E-32
INTSILLIF	4				
LPMLKVLNL	4				
LSYNKYLQL	1				
RLFGLFLNNV	1				
TRYSQLTSL	1				
VPSLQRLML	2				
YAAYIIHAY	1				
TLR7	5	ENSG00000196664	Q9NYK1	5.14	2.46E-27
DTKDPAVTEW	2				
VLAELVAKL	3				

Supplementary Table 5 (continued)

TMEM176A	7	ENSG00000002933	Q96HP8	2.77	1.06E-28
GSSRLLVASW	1				
HQESALAKLLL	1				
QESALAKLLL	3				
QHTHIDVHI	1				
SSRLLVASW	1				
TMEM91	5	ENSG00000142046	Q6ZNR0	12.81	1.4E-38
AESLRGLQF	1				
FLSPPLPSV	4				
TRIB3	5	ENSG00000101255	Q96RU7	7.56	1.5E-35
ASYSGKAADVW	1				
YPFQDSEPVL	4				
USH1C	17	ENSG00000006611	Q9Y6N9	2.37	1.81E-18
AEAALQKAW	2				
AEAALQKAWNQ	1				
AEAEAALQKAW	5				
DEIVRINGY	1				
EEQGEQDFRKY	2				
KSSPDEPLTW	1				
SPIGKVVVSA	1				
TAEVHPVPL	1				
THEEVINLI	3				
VCAM1	5	ENSG00000162692	P19320	3.97	7.19E-29
AQIGDSVSL	1				
SPKNTVISV	1				
YPFDRLEIDL	3				
VEGFA	10	ENSG00000112715	P15692	12.30	2.58E-39
GQHIGEMSF	1				
HPIETLVDIF	9				

Supplementary Table 6: Class I candidates from quantitative analysis. All HLA class I ligands with a mean log(2) fold change expression of ≥2 in ccRCC samples compared to adjacent benign samples.

Gene HLA ligand	Uniprot_ID	Quantified samples	Mean area (log2)	Found on n benign samples [n=158]	Found on n adjacent benign samples [n=58]	Found on n malignant samples [n=58]	Malignant/ Total [%]
AATF	Q9NY61						
PQPDVFPLF		3	2.00	20	3	5	17.86
ABCA1	O95477						
ALFEEQGIGV		4	2.72	4	1	7	58.33
DAFLNKNSI		5	2.94	4	1	7	58.33
DGYTIVVRI		5	2.47	5	7	8	40.00
MLRADVIL		3	2.05	1	0	1	50.00
NVINNAILR		3	2.06	5	1	3	33.33
ABCC1	P33527						
QILKLLIKF		3	4.42	0	0	2	100.00
ABCC3	O15438						
AYLHTTTTF		6	2.48	20	2	9	29.03
VILPLAVLY		3	3.68	1	0	3	75.00
ABCF3	Q9NUQ8						
VLLDAPIQL		7	2.97	7	1	11	57.89
ABI1	Q8IZP0						
NYIEKVVAI		3	2.40	23	2	4	13.79
ABLIM3	O94929						
FPIGDKVTF		4	4.71	15	0	6	28.57
ACLY	P53396						
FMDHVLRY		3	2.19	0	2	3	60.00
KLYRPGSVAY		3	2.09	13	1	5	26.32
NFTNVAATF		4	2.68	9	1	7	41.18
THMTAIVGM		3	2.19	2	3	4	44.44
ACO1	P21399						
TYIKSPPFF		5	2.99	17	3	8	28.57
ACTN1	P12814						
ETIDQLYLEY		3	2.64	2	2	3	42.86
VSKIVQTY		3	2.32	32	1	1	2.94
ACTR2	P61160						
LPDGRIIKV		3	2.68	9	2	4	26.67
STMYPGLPSRL		6	3.59	23	0	7	23.33
ADCK2	Q7Z695						
SLLSSVFKL		3	2.20	4	0	6	60.00
ADGRE2	Q9UHX3						
TIINSLQGV		3	2.13	0	1	5	83.33
ADPGK	Q9BRR6						
DEFHLILEY		5	3.03	4	2	6	50.00
RLLEVVTSI		3	2.63	3	0	6	66.67
SEFPGAQHY		3	2.14	7	2	7	43.75
ADSSL1	Q8N142						
FPTEQINEI		4	5.08	0	0	5	100.00

Supplementary Table 6 (continued)

AFF1	P51825						
EAFPEKIPLF		3	3.09	1	0	3	75.00
AFF4	Q9UHB7						
MPSPVSPKL		10	2.31	24	6	14	31.82
AGAP1	Q9UPQ3						
DEISFQTVY		4	2.17	1	2	4	57.14
AGR2	O95994						
KIPVSAFLL		3	3.36	18	0	2	10.00
AGRN	O00468						
APDVARALL		4	2.76	0	0	5	100.00
AHNAK	Q09666						
FEGPDAKL		3	2.32	0	1	4	80.00
AHR	P35869						
AIMDPLPLRTK		7	2.60	24	3	7	20.59
AIM1	Q9Y4K1						
SLSPVILIK		8	2.30	24	4	10	26.32
AKR1C3	P42330						
HPNYPYSDEY		5	3.03	14	3	5	22.73
ALDOA	P04075						
ALSDHHIYL		14	3.16	23	9	20	38.46
ASINLNAINK		5	3.37	1	0	6	85.71
ESTGSIAKRL		3	3.98	0	1	2	66.67
HHIYLEGTLL		4	3.59	0	1	4	80.00
LFVSNHAY		5	3.62	7	0	1	12.50
LSDHHIYL		9	3.94	1	2	12	80.00
RTVPPAVTGITF		3	4.34	0	0	4	100.00
SEEEASINL		3	3.91	0	0	4	100.00
SESLFVSNHAY		10	2.07	21	8	14	32.56
SLFVSNHAY		5	2.53	23	6	9	23.68
ALDOB	P05062						
TEKVLAAVY		7	2.50	3	5	7	46.67
ALDOC	P09972						
ESVGSMAKR		3	2.71	2	0	4	66.67
ALKBH6	Q3KRA9						
EEYLLRQVF		3	3.67	8	1	3	25.00
ALOX5	P09917						
KIVPIAIQL		11	3.46	1	0	11	91.67
QVVEEDPEL		3	3.33	0	0	2	100.00
ALPK2	Q86TB3						
DPIDEISVIEY		3	4.07	0	0	4	100.00
FPWEKPTTL		3	4.35	0	0	4	100.00
AMN	Q9BXJ7						
READTEIQVVL		3	3.44	0	1	4	80.00
ANKRD13A	Q8IZ07						
TSWVPLVSR		3	3.46	2	0	5	71.43
ANKRD18B	A2A2Z9						
MQAIEKLEEI		3	4.00	0	0	1	100.00
ANXA2	P07355						
LIDQDARDLY		3	3.71	0	0	5	100.00

Supplementary Table 6 (continued)

ANXA4	P09525						
DEVKFLTV		3	2.66	0	1	4	80.00
DEVKFLTVL		5	4.54	1	1	5	71.43
IRSDTSFMF		3	4.81	1	0	3	75.00
NAMEDAQTL		5	3.56	5	2	6	46.15
SAYFAEKLYK		6	3.97	4	0	7	63.64
ANXA5	P08758						
DAYELKHAL		4	2.10	22	6	7	20.00
AOC1	P19801						
KAVHSFLW		3	4.70	0	0	3	100.00
AP2S1	P53680						
VYTVVDEMFL		3	2.93	10	0	4	28.57
AP3D1	O14617						
MPNHSASIQL		3	3.83	1	0	3	75.00
APLP2	Q06481						
SLLYKVPYV		3	2.91	2	1	3	50.00
APOL1	O14791						
FLVLDVVYL		3	2.16	0	2	8	80.00
IFIEDAIKY		3	3.06	0	1	4	80.00
SLAGNTYQL		5	2.01	3	2	6	54.55
AQP2	P41181						
GQAVTVELFL		3	2.32	0	0	1	100.00
AQP3	Q92482						
LYYDAIWHF		5	2.74	12	4	6	27.27
ARCN1	P48444						
ETTFLVDKY		5	2.42	2	1	8	72.73
FVETESVRY		5	2.65	0	1	7	87.50
IQVTKVTQV		5	2.38	5	1	2	25.00
ARHGAP42	A6NI28						
DEISIAQSL		3	2.61	0	0	3	100.00
ARHGEF2	Q92974						
KYPLLISRI		4	2.41	10	1	5	31.25
ARL2BP	Q9Y2Y0						
IYTPIFNEY		3	2.13	6	1	3	30.00
ARL4C	P56559						
KLYEMILKR		4	4.46	17	2	5	20.83
ARL6IP1	Q15041						
NQHGIILKY		3	3.73	1	0	3	75.00
ARPC3	O15145						
FPIPGEPGF		10	2.24	22	3	12	32.43
ARRDC3	Q96B67						
KVKSLTISF		3	3.26	4	0	5	55.56
ARSB	P15848						
VPLDEKLLPQL		4	2.71	4	1	2	28.57
ASPA	P45381						
VYLIEHPSL		4	4.15	0	0	6	100.00
ATF4	P18848						
YLKDLIEEV		4	2.54	8	1	9	50.00

Supplementary Table 6 (continued)

ATL2	Q8NHH9						
HEDDHNFEL		3	2.28	0	0	4	100.00
ATM	Q13315						
SVYDALPLTR		6	2.33	22	2	6	20.00
SVYDALPLTRL		3	3.40	6	0	1	14.29
ATP1B1	P05026						
AYVLNIVRF		9	2.53	3	10	10	43.48
KAYGENIGY		3	2.79	3	3	6	50.00
YPYYGKLL		5	2.74	0	4	6	60.00
ATP5G1	P05496						
SPVNSSKQPSY		5	2.10	4	2	6	50.00
ATP6V1E1	P36543						
MPEVRGALF		3	2.18	4	2	6	50.00
BAK1	Q16611						
NAYEYFTKI		3	2.25	6	3	5	35.71
BARX2	Q9UMQ3						
RLSSPGQLK		4	3.09	1	0	5	83.33
BAZ2A	Q9UIF9						
GEVQDLLVRL		3	2.04	2	1	3	50.00
BBS4	Q96RK4						
IYQKAFEHL		5	2.55	13	2	8	34.78
QYASAFHFL		4	3.22	16	3	6	24.00
BCAS2	O75934						
VYNENLVHMI		7	2.49	21	3	9	27.27
BHLHE41	Q9C0J9						
GQKLEPLAY		3	4.17	24	0	5	17.24
BHMT2	Q9H2M3						
DEARIKKLF		3	4.93	0	0	4	100.00
YPFGLESRV		6	3.86	0	2	8	80.00
BICC1	Q9H694						
MPAETIKEL		10	2.98	1	5	11	64.71
BIRC2	Q13490						
KLGDSPIQK		3	2.73	5	0	4	44.44
BPIFB4	P59827						
LLGGIKVKL		5	2.31	0	1	7	87.50
BTBD9	Q96Q07						
GEIDHVHIL		3	2.57	6	1	5	41.67
BTNL9	Q6UXG8						
APHRVALTL		4	2.41	5	1	6	50.00
BZW2	Q9Y6E2						
FLDSTGSRLDY		3	2.81	8	1	5	35.71
C11orf52	Q96A22						
MSEDSNLHY		4	2.23	6	3	8	47.06
C12orf4	Q9NQ89						
EVVQQVVLY		3	3.00	0	0	3	100.00
C14orf166	Q9Y224						
TEFRNFIVW		5	2.70	9	1	5	33.33

Supplementary Table 6 (continued)

C16orf58	Q96GQ5						
NLAKCIVSV		3	4.25	1	0	4	80.00
C16orf87	Q6PH81						
KIINQRLIL		4	5.14	0	0	4	100.00
C1QB	P02746						
FLLFPDMEA		9	2.54	61	0	9	12.86
IAFSATRTI		3	4.51	0	0	6	100.00
RFDHVITNM		7	4.00	4	2	10	62.50
VTTGGMVLK		3	4.28	11	0	4	26.67
C1S	P09871						
TLFGSVIRY		3	2.81	9	0	3	25.00
C2	P06681						
DHIREILNI		3	3.17	0	2	3	60.00
C3	P01024						
ATFGTQVVEK		4	4.16	29	0	5	14.71
TEFEVKEY		4	3.63	0	1	4	80.00
TESETRILL		3	2.80	0	0	4	100.00
TPTVIAVHY		3	4.70	2	0	3	60.00
VEKVVLVSL		6	4.13	0	0	7	100.00
C3orf70	A6NLC5						
ISDLFIDNY		3	2.29	1	1	5	71.43
C6orf106	Q9H6K1						
SEFQRLLGF		4	2.27	4	2	4	40.00
CA9	Q16790						
SPRAAEPVQL		3	5.41	0	0	4	100.00
CABIN1	Q9Y6J0						
SVLPWIILH		4	2.71	22	1	6	20.69
CAD	P27708						
HPQPGAVEL		4	2.28	4	2	5	45.45
CALML4	Q96GE6						
DEFIHKITL		3	2.82	1	2	3	50.00
CARD11	Q9BXL7						
FLMNEVIKL		4	2.20	11	2	10	43.48
CASD1	Q96PB1						
TSIAPLLEK		7	5.44	9	0	8	47.06
CCND1	P24385						
ETIPLTAEK		4	4.57	5	0	4	44.44
ETIPLTAEKL		4	2.45	18	3	6	22.22
TPHDFIEHF		4	3.68	0	0	6	100.00
CCND2	P30279						
ALTELLAKI		9	2.44	7	4	18	62.07
ATDFKFAMY		12	2.71	18	4	18	45.00
CCT5	P48643						
HVIETLIGK		9	2.24	33	4	10	21.28
CCT6A	P40227						
HPRIITEGF		3	2.62	2	1	5	62.50
CCT8	P50990						
AEELLRIGL		6	2.33	6	5	7	38.89
FLAKLIAQA		3	3.84	8	1	6	40.00

Supplementary Table 6 (continued)

CD24	P25063						
ARLGLGLLL		3	5.22	2	1	5	62.50
RAMVARLGL		3	4.10	2	0	6	75.00
CDC42SE2	Q9NRR3						
AHVGSGDLF		3	3.00	0	1	3	75.00
CDH2	P19022						
EEIVFPRQF		3	3.64	1	0	4	80.00
CDH5	P33151						
GSDPREELLY		3	3.66	1	0	5	83.33
CDK18	Q07002						
DTASIFSLK		7	4.33	4	0	7	63.64
CDKL1	Q00532						
FTETSKLQY		3	3.05	2	1	3	50.00
CDKN2A	P42771						
LPVDLAEEL		3	3.08	1	0	6	85.71
CDKN2AIPNL	Q96HQ2						
IEVEDLPQF		3	3.45	0	0	5	100.00
CECR1	Q9NZK5						
APVFRDYVF		6	3.41	12	1	7	35.00
CFI	P05156						
AEGKFSVSL		4	2.72	0	0	5	100.00
CFL1	P23528						
ILEEGKEILV		4	2.54	6	2	5	38.46
CHD4	Q14839						
RIPPVAVRL		4	5.16	1	0	6	85.71
CIB1	Q99828						
AEYQDLTFL		6	2.57	3	3	7	53.85
FASSFKIVL		3	3.80	11	0	3	21.43
FLTKQEILL		15	2.10	17	16	24	42.11
CIITA	P33076						
GVSSIFIYH		8	2.06	3	5	9	52.94
CIT	O14578						
YLDIPNPRY		8	3.39	1	0	11	91.67
CLASP1	Q7Z460						
AEYDNFFQHL		3	2.72	17	1	3	14.29
CLNS1A	P54105						
YPTISLHAL		3	3.38	10	1	5	31.25
CLTC	Q00610						
KMYDAAKLLY		3	4.47	8	0	7	46.67
MFTELAILY		3	2.27	0	3	3	50.00
CMBL	Q96DG6						
SEFRAGVSVY		3	2.13	0	1	4	80.00
VEYQIKTF		5	3.71	0	1	5	83.33
CMTR1	Q8N1G2						
GEELLHSVL		4	2.39	5	0	5	50.00
CNDP2	Q96KP4						
QEIPVNVRF		8	2.10	8	6	9	39.13

Supplementary Table 6 (continued)

CNOT1	A5YKK6						
YHDINVYSL		3	2.16	2	2	4	50.00
COL6A2	P12110						
EVISPDTTER		3	3.36	12	1	3	18.75
FVIDSSESIGY		4	3.87	4	1	4	44.44
COPB1	P53618						
FEWENKVTV		4	2.37	15	2	8	32.00
COPB2	P35606						
GELKIAYQL		3	3.01	2	1	4	57.14
COPG1	Q9Y678						
ALVSSLHLL		9	2.06	3	3	13	68.42
DTVTMQVTAR		3	2.13	9	2	4	26.67
COX8A	P10176						
SVLTPLLLR		3	2.51	1	0	3	75.00
CP	P00450						
AEVGDTIRVTF		3	3.33	0	0	3	100.00
FLDKGEFYI		6	3.80	0	1	8	88.89
KVYPGEQYTY		3	5.64	4	0	4	50.00
NEADVHGIYF		8	2.73	2	3	8	61.54
SHVAPTETF		3	2.50	0	0	3	100.00
TVDQVKDLY		13	2.55	15	10	17	40.48
VVDENFSWY		3	2.95	0	1	7	87.50
CPE	P16870						
ASAPGYLAITK		3	5.20	13	0	4	23.53
CREB3L2	Q70SY1						
VLLELQQHL		3	3.10	3	2	7	58.33
CRIP1	P50238						
GGAESHTFK		5	2.27	7	0	5	41.67
CRYAB	P02511						
DEHGFISREF		3	2.72	0	1	4	80.00
CRYL1	Q9Y2S2						
KLFAGLVHV		6	2.64	18	3	10	32.26
CSPG4	Q6UVK1						
TMLARLASA		18	3.28	2	7	24	72.73
CTNNA1	P35221						
SEFKAMDSI		4	2.24	19	2	7	25.00
CTNNB1	P35222						
HAIMRSPQM		3	2.63	4	1	6	54.55
CTSL	P07711						
KVFQEPLFY		10	4.23	11	3	14	50.00
CUBN	O60494						
PYSQVWIHF		3	4.79	1	3	7	63.64
CXCL13	O43927						
KFISTSLLL		3	2.38	5	0	4	44.44
CYP2J2	P51589						
ITFGERFEY		5	4.84	2	0	6	75.00
KLLDEVTYL		12	6.01	2	0	16	88.89
REVTVDTTL		4	4.86	0	0	5	100.00
TTLRWALLY		4	4.47	0	0	5	100.00

Supplementary Table 6 (continued)

CYP7B1	O75881						
KLLEKAFSI		4	2.09	14	2	9	36.00
DARS	P14868						
AEPRLPLQL		3	3.61	1	0	6	85.71
TSTSQAVFR		3	2.44	2	0	3	60.00
DBR1	Q9UK59						
RIGGISGIFK		3	2.22	25	2	3	10.00
DCLK1	O15075						
IPATITERY		3	2.78	6	0	3	33.33
DCPS	Q96C86						
ATEKHLQKY		3	3.04	10	0	6	37.50
DDOST	P39656						
DSFFNSAVQK		3	2.17	5	1	3	33.33
FPDKPITQY		6	2.06	39	6	9	16.67
VQFKLPDVY		3	2.16	21	2	3	11.54
YSSTQVSVR		3	2.43	6	1	3	30.00
DDRGK1	Q96HY6						
REHEEYLKL		3	2.05	3	2	5	50.00
DDX27	Q96GQ7						
LPVLERLIY		5	3.05	5	0	6	54.55
DDX42	Q86XP3						
GSVLLFVTK		6	2.50	8	2	6	37.50
DDX60	Q8IY21						
YLWNTVSKL		3	2.75	0	1	4	80.00
DEGS1	O15121						
EVINTVAQV		5	2.09	14	3	6	26.09
FPNIPGKSL		18	2.07	48	16	22	25.58
LPIGIPYSISF		3	2.76	3	2	4	44.44
SMTLAIHEI		9	2.03	7	8	17	53.13
DEPP	Q9NTK1						
RPSSVLRTL		5	3.82	9	1	9	47.37
SHLPVIHEL		3	2.81	0	3	3	50.00
DERA	Q9Y315						
DEWLKPELF		3	3.15	2	1	3	50.00
DERL1	Q9BUN8						
TVAVPLVGKL		12	2.30	14	2	8	33.33
DHX15	O43143						
RIFEPPPPK		8	2.82	52	2	8	12.90
DHX32	Q7L7V1						
SEFPLDPQL		3	2.01	1	0	3	75.00
DHX40	Q8IX18						
VPISKSEAL		3	3.79	5	1	4	40.00
DIRAS2	Q96HU8						
SEAEALARTW		5	3.99	0	0	8	100.00
DNAJA2	O60884						
KEISFAYEVL		3	3.15	1	0	3	75.00
DNAJB12	Q9NXW2						
EAFKAIGTAY		3	2.48	9	0	5	35.71

Supplementary Table 6 (continued)

DNAJB14	Q8TBM8						
FPSGSVHSF		5	2.94	4	1	5	50.00
DNAJB9	Q9UBS3						
REIAEAYETL		3	2.72	2	0	4	66.67
DNPEP	Q9ULA0						
PSLSHNLLVD		7	2.57	32	0	2	5.88
DOCK2	Q92608						
AYTLLLHTW		7	2.12	21	3	10	29.41
KMWEEAISL		6	2.59	14	2	12	42.86
DOCK8	Q8NF50						
AEIPADPKLY		3	2.57	8	1	4	30.77
DOK3	Q7L591						
TPIKDGILY		4	2.48	16	1	5	22.73
DPP9	Q86TI2						
MPYGSRENSL		3	3.13	3	0	5	62.50
DPYSL3	Q14195						
MPYKGMTTV		3	2.63	2	2	7	63.64
DST	Q03001						
LPSDKALVL		4	2.35	8	2	4	28.57
DTX3L	Q8TDB6						
NVIEVDSAHY		4	2.99	2	3	4	44.44
DUSP1	P28562						
KLDEAFEFV		3	3.93	2	1	4	57.14
EDNRA	P25101						
NHVDDFTTF		3	2.78	0	3	3	50.00
EEF1G	P26641						
FPAGKVPAF		3	2.97	10	1	6	35.29
EEF2	P13639						
GLKEGIPAL		7	2.26	8	4	13	52.00
KSTAISLFY		4	3.50	13	0	4	23.53
LEPEELYQTF		3	2.31	4	1	3	37.50
LPSPVTAQKY		5	2.31	21	5	7	21.21
RVFSGLVSTGLK		13	2.92	28	7	16	31.37
TAISLFYEL		4	2.35	17	1	5	21.74
EEF2K	O00418						
VVDIQGVGDLY		6	2.01	9	3	10	45.45
EGLN1	Q9GZT9						
NPHEVQPAY		4	2.74	1	1	4	66.67
EGLN3	Q9H6Z9						
AEERAEAKKKF		3	2.91	0	0	1	100.00
EVQPSYATR		5	3.97	2	0	8	80.00
MPLGHIMRL		4	5.18	0	0	8	100.00
NPHEVQPSY		5	6.18	1	1	5	71.43
EHD2	Q9NZN4						
ALASHLIEA		13	2.36	11	6	20	54.05
FGAFHSPAL		4	3.15	8	2	10	50.00
KLPNSVLGR		3	3.85	1	0	3	75.00
LPVIFAKI		3	2.33	1	3	5	55.56
RVHAYIISY		13	3.50	25	4	17	36.96

Supplementary Table 6 (continued)

EHHADH	Q08426						
APRTFGLTL		3	3.60	10	1	7	38.89
EIF3K	Q9UBQ5						
LPHTDFTL		3	2.37	0	2	4	66.67
TVTAQILLK		8	2.12	9	4	8	38.10
EIF4A1	P60842						
MPLNVADLI		4	3.50	2	1	6	66.67
EIF4G1	Q04637						
FVAEQKVEY		7	2.11	22	3	7	21.88
EIF6	P56537						
TVADQVLVGSY		5	3.16	0	5	6	54.55
ELAC2	Q9BQ52						
RYQQWMERF		3	2.11	17	0	4	19.05
EMC1	Q8N766						
IPPEVQRI		4	3.19	3	3	5	45.45
YPSKQFDVL		5	2.98	4	3	6	46.15
EML2	O95834						
IHTDGNEQI		3	2.75	0	0	3	100.00
EML4	Q9HC35						
SHDNFIYLY		3	2.36	0	0	3	100.00
ENC1	O14682						
YLPELLQTV		4	2.26	5	1	5	45.45
ENGASE	Q8NFI3						
SPDPLPVRY		3	2.68	10	0	3	23.08
ENO1	P06733						
KTIAPALVSK		4	2.70	2	0	5	71.43
ENPP2	Q13822						
STEERHLLY		10	3.46	6	2	13	61.90
VRPPLIIF		4	3.50	1	1	6	75.00
YSEQPDFSGHKY		6	4.37	1	0	9	90.00
EPPK1	P58107						
YPDPYGGEKL		3	3.37	2	1	4	57.14
YPDPYSRASL		5	5.39	8	0	7	46.67
EPRS	P07814						
FTDVNSILRY		14	2.24	39	12	18	26.09
KEDFEKVIL		3	2.75	0	0	5	100.00
EPSTI1	Q96J88						
EAFREHQQY		3	2.13	6	0	3	33.33
QELANLEKW		3	4.28	3	0	3	50.00
ERBB3	P21860						
LPLPNLRVV		5	2.61	0	5	5	50.00
VYDGKFAIF		4	3.10	4	1	4	44.44
ERCC2	P18074						
YPLEVTKLIY		4	2.48	3	1	5	55.56
ERGIC1	Q969X5						
YILKIVPTV		3	4.77	3	0	5	62.50
EVL	Q9UI08						
VVINYSIVK		4	3.52	35	0	6	14.63

Supplementary Table 6 (continued)

EXD2	Q9NVH0						
FPLDKSLLL		3	3.49	9	2	7	38.89
EXOC3	O60645						
EAVATAVQR		3	2.52	12	0	4	25.00
EZR	P15311						
AEYTAKIAL		6	3.34	8	4	8	40.00
EYTAKIALL		3	2.79	2	2	5	55.56
YPEDVAEEL		4	3.45	2	2	6	60.00
FAM109A	Q8N4B1						
EEFAFAVRF		3	2.16	5	1	3	33.33
FAM120A	Q9NZB2						
MYPYIFHVL		5	2.47	22	2	8	25.00
FAM120B	Q96EK7						
FVYPGNPLRH		6	2.20	14	0	1	6.67
FAM129A	Q9BZQ8						
VLFEKEVNEV		4	2.21	2	2	5	55.56
FAM149A	A5PLN7						
AVLDLGSLLAK		13	3.80	6	2	14	63.64
FAM32A	Q9Y421						
TEHYDIPKVSW		3	3.37	4	0	3	42.86
FAM65B	Q9Y4F9						
IEVNGKQSW		3	2.60	13	3	4	20.00
FANCI	Q9NVI1						
KLQEFLQTL		3	3.26	10	0	5	33.33
FAR1	Q8WVX9						
VFMHVSTAY		3	2.33	10	1	5	31.25
FASN	P49327						
HPLGDIVAF		4	3.94	17	0	4	19.05
FAU	P35544						
APLEDEATL		3	3.66	1	0	4	80.00
FBXL17	Q9UF56						
VQQYPHITF		3	2.00	30	1	4	11.43
FBXO28	Q9NVF7						
ILAAVETRL		3	2.25	3	1	8	66.67
FBXO3	Q9UK99						
KIFNVAIPRF		4	2.12	10	3	7	35.00
FBXW5	Q969U6						
DEFLWREQF		5	2.21	2	4	5	45.45
FCGR3A	P08637						
RVLEKDSVTLK		5	4.17	14	1	7	31.82
FCHO2	Q0JRZ9						
FPSGIIKVF		6	2.21	10	4	10	41.67
KTFALPGIIK		5	3.46	7	1	6	42.86
KTFALPGIIKK		6	2.32	18	6	9	27.27
FEM1B	Q9UK73						
FPNALVTKL		5	2.66	15	2	6	26.09
FGA	P02671						
GDSTFESKSYK		4	3.11	20	0	7	25.93

Supplementary Table 6 (continued)

FGG	P02679						
IPYALRVEL		3	3.42	1	1	4	66.67
FIBP	O43427						
VTDAVALRV		8	2.06	3	5	10	55.56
FLII	Q13045						
FARLPEEEF		3	3.46	3	0	3	50.00
VLNGNPLLH		3	2.73	10	1	5	31.25
FLNB	O75369						
SPFKADIEM		6	2.84	7	3	7	41.18
FLOT1	O75955						
GEVLDILTRL		4	2.42	1	2	6	66.67
FMR1	Q06787						
VLLDYHLNYL		5	2.02	9	5	13	48.15
FNDC3B	Q53EP0						
ILWETVPSM		13	2.22	5	10	20	57.14
FXYD2	P54710						
YETVRNGGL		5	2.26	1	3	6	60.00
GALK2	Q01415						
TQDVLIFKL		3	2.27	0	3	3	50.00
GANAB	Q14697						
FLDDGHTFNY		6	2.27	16	2	13	41.94
GAS2L3	Q86XJ1						
SVSPVKATQK		4	2.15	0	0	7	100.00
GBA	P04062						
LTDPEAAKY		9	2.20	19	3	15	40.54
YFVKFLDAY		3	2.33	0	0	3	100.00
GBA3	Q9H227						
YHFDLPQTL		3	4.60	0	2	4	66.67
YPSSRLPEF		3	5.85	0	0	3	100.00
GBP1	P32455						
QEQLLKEGF		3	3.93	6	0	4	40.00
GBP2	P32456						
AQIENSAAVEK		7	2.36	17	2	8	29.63
GBP5	Q96PP8						
RLKNLVLTY		5	2.80	12	0	5	29.41
SLLSELQHA		8	2.88	12	3	14	48.28
GFPT1	Q06210						
ETADTLMGLRY		4	2.08	3	4	5	41.67
GMPPA	Q96IJ6						
ALYASRLYL		9	3.40	5	1	13	68.42
QEFNLPVRY		3	2.07	2	0	5	71.43
GNL3	Q9BVP2						
VPLDKQITI		5	2.32	9	6	8	34.78
GPAA1	O43292						
LHQSFFLYL		3	2.35	0	0	4	100.00
GPNMB	Q14956						
KGLSVFLNR		5	3.06	2	4	4	40.00

Supplementary Table 6 (continued)

GRB7	Q14451						
WPVGGDSRFVF		6	2.83	1	2	8	72.73
GSN	P06396						
WSVDPLDR		8	4.11	53	0	1	1.85
WSVDPLDRAM		7	3.73	42	1	10	18.87
GUCY1A3	Q02108						
KFSNVTMLF		5	3.55	7	0	7	50.00
GUCY1B3	Q02153						
DLYTRFDTL		4	2.43	5	2	6	46.15
MYGFVNHAL		3	2.39	6	0	3	33.33
RYDNVTILF		3	4.76	14	0	5	26.32
GZMK	P49863						
VLIDPQWVL		6	2.21	3	0	8	72.73
HADHA	P40939						
SPNSKVNTL		4	2.53	17	2	8	29.63
HAVCR1	Q96D42						
ALLGVIIAK		12	4.33	0	2	16	88.89
GVIIAKKYFFK		4	4.65	0	0	4	100.00
HBA1	P69905						
ALTNAVAHV		3	2.16	13	0	3	18.75
ASVSTVLTSKYR		8	2.07	57	2	0	0.00
HCFC1R1	Q9NWW0						
SLIPEALRL		4	4.23	2	0	3	60.00
HDLBP	Q00341						
IPAKLHNSL		6	2.10	17	5	9	29.03
HEATR1	Q9H583						
FLFDTQHFI		3	2.35	9	2	6	35.29
HEYL	Q9NQ87						
ATGIILPAR		6	2.19	12	1	5	27.78
HIF1A	Q16665						
ELNPKILAL		3	2.17	6	2	7	46.67
HLA-DPA1	P20036						
WEAQEPIQM		3	2.12	0	3	5	62.50
HLA-DQA1	P01909						
VVGTVFIIR		4	4.11	2	1	4	57.14
HLA-DQB1	P01920						
SPEDFVYQF		6	2.26	6	3	7	43.75
HLA-DRA	P01903						
IIGTIFIIK		8	4.00	25	3	8	22.22
LPFLPSTEDVY		5	2.99	18	1	7	26.92
HM13	Q8TCT9						
FPASFPNRQY		5	2.61	7	5	6	33.33
HMOX1	P09601						
AENAEFMRNF		3	4.67	4	1	4	44.44
APLLRWVL		13	3.48	19	9	21	42.86
DSAPVETPR		4	3.91	14	1	5	25.00
EVIPYTPAM		8	3.89	9	4	9	40.91
FPNIASATKF		4	4.67	3	0	6	66.67
KIAQKALDL		3	4.91	0	0	4	100.00

Supplementary Table 6 (continued)

RVIEEAKTAF		3	5.30	18	0	6	25.00
SLYHIYVAL		4	4.09	1	2	4	57.14
HNRNPA2B1	P22626						
FGPGPGSNF		4	3.26	13	2	3	16.67
HNRNPA3	P51991						
DTVDKIVVQKY		3	2.31	0	1	2	66.67
HNRNPU	Q00839						
AENPGKYNIL		3	2.82	2	0	3	60.00
HPS3	Q969F9						
IYPWVHVVI		3	4.69	11	0	5	31.25
HPS4	Q9NQG7						
SLNGLEVHL		4	2.65	13	0	5	27.78
HSD3B7	Q9H2F3						
RVYVGNVAW		4	4.62	1	1	5	71.43
HSF2	Q03933						
LVQNNQLVSL		6	5.33	5	0	6	54.55
HSF4	Q9ULV5						
ILWREVVTL		12	3.87	0	0	15	100.00
SPSPGKDPTL		3	3.84	0	0	4	100.00
HSP90AB1	P08238						
IPNPQERTLTL		4	2.96	0	1	4	80.00
RRLSELLRY		4	2.05	13	4	5	22.73
HSP90B1	P14625						
HPTDITSLDQY		3	3.76	1	0	4	80.00
HSPA5	P11021						
AEAYLGKKV		3	2.27	10	1	4	26.67
KVYEGERPLTK		4	2.77	11	0	4	26.67
QARIEIESF		5	3.80	8	1	3	25.00
QPTVTIKVY		4	4.32	1	0	5	83.33
HSPA7	P48741						
TVFDAKRLIGR		8	2.99	28	3	8	20.51
HSPA8	P11142						
ILNVSAVDK		5	2.12	9	2	6	35.29
NAVVTVPAY		3	2.59	2	0	3	60.00
HSPB8	Q9UJY1						
AEVDPVTVF		3	2.40	2	1	7	70.00
SWPDWALPRL		5	2.22	1	3	6	60.00
WPDWALPRL		3	2.92	0	0	3	100.00
HSPD1	P10809						
DGVAVLKV		3	2.26	10	4	7	33.33
RTVIIEQSW		4	2.28	11	3	6	30.00
HSPG2	P98160						
DASPPPVKI		5	2.06	0	3	5	62.50
EVAQPGPSNR		4	2.19	1	2	4	57.14
GLNLHTLLY		4	3.90	4	2	5	45.45
ID2	Q02363						
TPVDDPMSLLY		3	3.65	2	0	4	66.67

Supplementary Table 6 (continued)

IDE	P14735						
FPIPDLQKY		3	2.26	18	1	6	24.00
IDO1	P14902						
NPKAFFSVL		3	2.67	7	1	6	42.86
NPSVREFVL		4	3.22	0	2	5	71.43
RSYHLQIVTK		12	3.10	28	4	13	28.89
IFI16	Q16666						
EVPNKIINR		3	3.44	25	2	3	10.00
IFI27	P40305						
GIASSSIAAK		3	2.49	0	0	3	100.00
IFT57	Q9NWB7						
RPFEQPQEY		5	2.42	4	2	5	45.45
IFT81	Q8WYA0						
RQQASIISR		3	2.46	0	0	3	100.00
IGFBP3	P17936						
RPTLWAAAL		10	4.82	5	2	11	61.11
IGKV2-30	P06310						
LPAQLLGLLM		4	2.81	3	2	4	44.44
IKBIP	Q70UQ0						
EPLVNDLTL		3	2.43	0	1	4	80.00
IL1B	P01584						
SVDPKNYPK		5	3.03	41	0	10	19.61
IL32	P24001						
YLETVAAYY		6	2.35	3	1	7	63.64
IPO9	Q96P70						
RLIPTLVSI		3	2.85	4	0	5	55.56
IQCB1	Q15051						
ELQLSMLEI		4	2.46	0	4	4	50.00
IQGAP1	P46940						
DEIGLPKIFY		4	3.24	3	1	5	55.56
DPLQKEEL		4	2.11	2	3	6	54.55
IRAK1	P51617						
SVLWPWINR		4	3.20	8	1	4	30.77
IRF7	Q92985						
SEADARIFKAW		4	2.41	2	1	4	57.14
IRX3	P78415						
AELPIFPQL		5	3.11	0	0	6	100.00
IST1	P53990						
AELKIVADQL		3	2.18	2	1	6	66.67
ITGA3	P26006						
FPAHPSLLL		3	3.70	1	0	5	83.33
ITGA4	P13612						
SVINPGAIYR		10	2.42	35	3	10	20.83
ITGA5	P08648						
IEDKAQILL		6	2.83	1	1	6	75.00
ITGA7	Q13683						
EAVGIKSFGY		3	3.69	0	1	3	75.00

Supplementary Table 6 (continued)

ITGAV	P06756						
KSLLWTETF		5	2.11	17	6	9	28.13
NPMKAGTQL		4	2.45	12	6	6	25.00
ITGB2	P05107						
AENNIQPIF		3	2.97	6	1	5	41.67
IVNS1ABP	Q9Y6Y0						
DAYIQEHLL		5	3.64	4	0	6	60.00
SPRSNAGIATV		3	3.76	1	0	5	83.33
VEVLLNYAY		3	2.77	3	0	4	57.14
JAK1	P23458						
KYLATLETL		3	2.01	7	2	6	40.00
JKAMP	Q9P055						
ALFQHITAL		9	2.66	8	3	15	57.69
KANSL1L	A0AUZ9						
LPSDVPLHF		6	2.54	0	0	6	100.00
KARS	Q15046						
LTDFIQKY		4	2.54	2	2	8	66.67
KBTBD7	Q8WVZ9						
NHDQKLLLI		3	2.01	0	2	3	60.00
KCNMA1	Q12791						
VPPVFVSVY		3	4.65	0	0	3	100.00
KDSR	Q06136						
YPSRAVITTM		3	3.23	7	0	3	30.00
KHK	P50053						
DVISLVDKY		4	3.81	0	2	3	60.00
RSVQEALRF		3	5.74	0	0	3	100.00
KIF11	P52732						
RVITALVER		3	3.40	3	0	3	50.00
KIFAP3	Q92845						
NEVEQLLYY		6	2.11	3	3	8	57.14
KISS1R	Q969F8						
RPAPADSAL		3	4.68	0	0	6	100.00
KLHL12	Q53G59						
SPIDVVEKY		5	2.44	22	5	8	22.86
KLHL22	Q53GT1						
LPLEKVYSL		3	3.78	8	1	4	30.77
KMO	O15229						
MPFEEFEKL		3	4.95	1	0	6	85.71
KRR1	Q13601						
HPIYNIKSL		4	3.31	17	2	5	20.83
KRT18	P05783						
ALLNIKVKL		10	2.80	7	6	19	59.38
ILLHLESEL		9	3.39	0	3	16	84.21
IMADIRAQY		5	4.81	2	0	7	77.78
KVKLEAEIATY		4	2.42	2	0	2	50.00
LLNIKVKL		6	3.08	1	1	5	71.43
REVEARYAL		5	4.04	1	1	6	75.00
RLESKIREH		4	3.86	0	0	4	100.00
RVKYETELAMR		4	3.28	0	0	4	100.00

Supplementary Table 6 (continued)

RVRSLETENR		3	3.01	0	0	3	100.00
RYALQMEQL		8	2.28	4	4	8	50.00
SETNDTKVL		4	3.44	0	0	6	100.00
YEALLNIKV		5	2.62	10	3	6	31.58
KRT19	P08727						
ALISGIEAQL		3	5.12	0	1	7	87.50
KRT8	P05787						
AESMYQIKY		6	3.10	0	2	8	80.00
KLSELEAAL		10	3.28	1	6	17	70.83
NMDNMFESY		5	4.02	2	0	12	85.71
LAMB1	P07942						
AEYIEKVVY		5	2.66	0	3	6	66.67
LAMB3	Q13751						
HINGRVLYY		7	4.05	6	2	9	52.94
LAMP2	P13473						
FPVPGSGLVL		4	2.36	10	1	6	35.29
LCP2	Q13094						
KVYNIQIRY		7	3.38	27	5	8	20.00
TAKLPAPSI		5	2.15	12	3	6	28.57
LDHA	P00338						
SVADLAESIMK		4	3.23	3	0	5	62.50
LDOC1L	Q6ICC9						
FPGEAERVAF		7	2.65	10	2	8	40.00
LEMD3	Q9Y2U8						
IENPFGETF		6	2.10	4	2	6	50.00
LGALS2	P05162						
SEVKFTVTF		9	4.06	4	0	11	73.33
LGALS3	P17931						
KPNANRIAL		10	2.20	20	5	9	26.47
LIN7A	O14910						
TAIREVYQY		4	3.95	2	0	5	71.43
LITAF	Q99732						
VYVQHPITF		8	2.21	26	5	10	24.39
LMTK2	Q8IWU2						
EIYTGTSVAR		4	2.08	6	1	4	36.36
LONRF1	Q17RB8						
LKERLTKI		3	2.38	5	0	1	16.67
LOXL3	P58215						
LPYTGAETRI		3	3.56	13	4	4	19.05
LPCAT1	Q8NF37						
IQYIRPVFV		3	2.17	6	0	4	40.00
KEPEQPPALW		4	3.93	4	1	5	50.00
TLFPVRLLV		11	4.28	12	0	14	53.85
LPCAT3	Q6P1A2						
RLIQESPTL		9	2.25	18	5	16	41.03
LRP2	P98164						
IPHPFGVSL		3	3.84	2	0	6	75.00
LRRC20	Q8TCA0						
LVSFPIGIYK		3	3.54	11	0	4	26.67

Supplementary Table 6 (continued)

VSFPIGIYK		7	2.10	15	3	7	28.00
LRRC42	Q9Y546						
RYLVISEKL		5	2.04	10	4	7	33.33
LRRK2	Q5S007						
EEIVLHVL		3	4.37	1	0	3	75.00
FLDLNTEGY		8	3.32	2	4	15	71.43
NESGVLLHF		13	3.31	14	4	14	43.75
SLIGYLITK		4	3.12	5	0	6	54.55
SLIGYLITKK		4	3.82	7	2	7	43.75
MALT1	Q9UDY8						
LTDPIQGTEY		4	2.12	4	0	7	63.64
MAOB	P27338						
AIMGFILAH		6	2.27	7	1	10	55.56
MAP1B	P46821						
SESPIEKVL		5	2.75	3	4	8	53.33
MAP4	P27816						
SVPADLSRPK		4	2.60	2	1	4	57.14
TVKEVGLLK		3	3.07	0	1	2	66.67
MAPK1	P28482						
APFKFDMEL		3	2.44	17	2	8	29.63
MAT2A	P31153						
FPWEVPKKLKY		4	3.07	5	3	6	42.86
RRNGTLPWLR		3	6.17	9	1	4	28.57
MCM3	P25205						
ALKDFVASI		3	2.02	5	1	4	40.00
MCTP2	Q6DN12						
IFDLQKTSL		3	2.60	22	1	6	20.69
MDM2	Q00987						
DEVYQVTVY		3	3.06	1	1	4	66.67
YTMKEVLFY		4	3.40	13	0	11	45.83
MET	P08581						
TEGIIMKDF		3	3.42	1	0	5	83.33
MGEA5	O60502						
LPIDGANDLF		6	2.59	3	1	9	69.23
MGLL	Q99685						
KPTGTPKAL		3	2.75	6	1	4	36.36
MGMT	P16455						
HPVFQQESF		4	2.15	6	2	6	42.86
MITF	O75030						
LPVSGNLIDLY		4	2.86	4	2	6	50.00
MKL1	Q969V6						
GLAPAEVVVATV		4	2.27	6	1	5	41.67
MLF2	Q15773						
AEGPPRLAI		4	2.70	7	2	8	47.06
MMP24	Q9Y5R2						
LPARIDAAY		4	3.53	1	0	4	80.00
MOGS	Q13724						
FLWDEGFHQL		4	3.91	9	2	10	47.62

Supplementary Table 6 (continued)

MPI	P34949						
RPVEEIVTF		4	2.44	3	1	4	50.00
MSANTD4	Q8NCY6						
ERDPQSPEF		3	2.49	0	1	3	75.00
MSH6	P52701						
KISEVVELL		5	2.50	4	1	6	54.55
MTDH	Q86UE4						
WVDEERASL		5	2.05	12	4	7	30.43
MYH11	P35749						
KEIENLTQQY		3	3.11	4	2	6	50.00
SVLQLGNIVFK		7	3.01	28	4	8	20.00
TEFSIIHY		4	2.09	0	1	5	83.33
MYH9	P35579						
KTDLLLEPYNKY		11	2.04	21	7	14	33.33
MYO10	Q9HD67						
NSDVVEQIY		4	2.30	0	1	6	85.71
MYO1F	O00160						
FTDREIDLY		12	2.73	27	4	16	34.04
MYOF	Q9NZM1						
DDLLVVEKY		5	2.36	0	3	5	62.50
MPPLVIKV		4	2.41	2	3	6	54.55
NAA15	Q9BXJ9						
TPLEEAIKF		3	2.15	5	2	4	36.36
NAA20	P61599						
VYRTVIEYY		3	3.54	13	0	6	31.58
NAMPT	P43490						
VPVSVVSDSY		4	3.21	0	0	4	100.00
NAP1L1	P55209						
AVLYQPLFDK		8	2.47	46	5	9	15.00
NARS	O43776						
FPVEIKSFYM		5	3.66	9	0	7	43.75
NAT10	Q9H0A0						
KEIELPSGQL		3	3.15	2	0	4	66.67
NCEH1	Q6PIU2						
KYFLKPEVL		3	4.15	7	1	4	33.33
NCKAP1L	P55160						
HVYELLNTI		3	3.45	3	1	3	42.86
NCLN	Q969V3						
RLPAFTLSHL		3	3.31	7	0	4	36.36
NDRG1	Q92597						
AEMLPGVLQQF		10	2.78	20	8	12	30.00
KLDPTKTTL		16	2.11	12	15	23	46.00
MPSASMTRL		12	4.39	14	2	16	50.00
NDUFA3	O95167						
VILPPLSPYFK		4	2.83	5	1	4	40.00
NDUFA4L2	Q9NRX3						
DQYKFLAV		6	6.99	0	0	3	100.00
GASLGARFY		4	3.78	0	0	3	100.00
GSAALYLLR		7	5.94	0	0	9	100.00

Supplementary Table 6 (continued)

NDUFB4	O95168						
IENPALLRW		4	2.24	5	2	5	41.67
NEK6	Q9HC98						
SLADFQIEK		9	2.59	24	2	12	31.58
NFKBIE	O00221						
VLDIQNNLY		11	3.09	2	5	14	66.67
NHP2	Q9NX24						
EEVQSLPLPL		13	2.13	47	0	8	14.55
NIFK	Q9BYG3						
DETQIFSYF		4	2.76	5	1	5	45.45
NLRC5	Q86WI3						
ATLTNILEH		5	2.53	35	3	5	11.63
NMB	P08949						
RLLVQILQK		4	5.54	4	0	5	55.56
NMI	Q13287						
VSPYTEIHL		3	2.17	5	1	3	33.33
NNMT	P40261						
AESQILKHLL		3	2.63	0	0	4	100.00
DYLEKYYKF		3	4.00	17	2	6	24.00
WFEVISQSY		3	4.52	1	0	3	75.00
YYMIGEQKF		9	4.09	7	2	10	52.63
NOP56	O00567						
YPASTVQIL		4	2.14	3	1	4	50.00
NPM1	P06748						
TPPVVLRL		3	3.67	8	1	5	35.71
NPTX2	P47972						
LLAASVALA		3	3.18	0	0	5	100.00
NRIP1	P48552						
SVIESPSTNR		4	2.11	1	0	4	80.00
NRP1	O14786						
DTIKIESPGY		4	2.27	0	3	4	57.14
NUP153	P49790						
SPFYPGKTTY		5	2.55	8	2	5	33.33
NUP160	Q12769						
YVDAVLGKGHQY		3	2.63	2	0	5	71.43
NUSAP1	Q9BXS6						
SVASTPISQR		3	3.31	6	1	3	30.00
OASL	Q15646						
EEFLRQEHF		4	2.59	9	2	5	31.25
ODC1	P11926						
NIIAKKIVL		12	4.92	12	0	14	53.85
OGFOD3	Q6PK18						
GVTDVVITR		3	2.76	6	1	3	30.00
OGT	O15294						
EAIRISPTF		4	3.22	9	1	4	28.57
OPN3	Q9H1Y3						
VYNPVIYVF		4	2.83	22	1	7	23.33

Supplementary Table 6 (continued)

OR8G1	Q15617						
MYLQPSSISSM		4	4.30	0	0	3	100.00
ORC4	O43929						
SENVLQVHL		3	2.29	1	1	6	75.00
OS9	Q13438						
DVVIVSSKY		3	2.80	0	1	3	75.00
OSGIN2	Q9Y236						
TYITSVSRL		3	2.43	4	1	6	54.55
P3H4	Q92791						
FYPAIADLF		3	2.09	11	0	4	26.67
P4HA1	P13674						
AEIEIVKDL		5	2.46	4	1	7	58.33
P4HA2	O15460						
AEKELVQSL		3	3.90	0	0	5	100.00
PAICS	P22234						
FYPPKVELF		4	2.17	15	1	6	27.27
PAM	P19021						
YPVGHPVDVSF		3	3.26	1	0	5	83.33
PARD6B	Q9BYG5						
YPQQIEPSF		3	3.60	0	1	5	83.33
PARG	Q86W56						
YPDINFNRL		3	4.05	8	1	4	30.77
PARP12	Q9H0J9						
DEFGSWQEY		4	2.22	1	2	5	62.50
PARP14	Q460N5						
GVFGFPLGR		11	2.84	12	5	13	43.33
SPDSGVYEM		4	2.85	10	1	4	26.67
PARP4	Q9UKK3						
FIFSDTHEL		5	2.11	15	3	11	37.93
PATJ	Q8NI35						
SHADVVNLL		3	2.65	0	0	4	100.00
PATL1	Q86TB9						
YYQNYFEKL		4	2.63	21	4	9	26.47
PBK	Q96KB5						
SYQKVIELF		4	3.64	17	0	8	32.00
PCBP2	Q15366						
FPMTHGNTGF		8	2.21	23	5	9	24.32
PDCD11	Q14690						
KVFERAVQY		3	3.46	15	0	4	21.05
RLKDGVLAY		3	4.34	9	0	4	30.77
PDGFD	Q9GZP0						
HRLIFVYTL		8	2.41	4	4	8	50.00
PDIA3	P30101						
LALFPGVAL		3	2.35	10	0	5	33.33
PDK4	Q16654						
KEIDILPTQL		3	2.40	2	0	4	66.67
PDZK1IP1	Q13113						
IAFAVNHFW		3	3.73	3	2	5	50.00

Supplementary Table 6 (continued)

PER2	O15055						
EEQSFLQKF		3	2.18	8	2	5	33.33
VPVDLQHQF		4	3.45	0	1	5	83.33
PFDN5	Q99471						
FLSTSIAQL		4	2.03	5	1	9	60.00
KTAEDAKDFFK		4	2.55	18	1	5	20.83
PFKL	P17858						
TTEFLYNLY		5	2.86	6	0	11	64.71
PFKP	Q01813						
TTDFIYQLY		10	4.70	12	2	14	50.00
PGF	P49763						
YPSEVEHMF		4	4.98	0	0	5	100.00
PHKA2	P46019						
EIISKLQGR		4	3.61	4	1	4	44.44
PI4KAP1	Q8N8J0						
IYSTAFDYF		3	2.17	21	1	3	12.00
PIGP	P57054						
IPALRDISI		7	2.02	7	1	8	50.00
PIK3AP1	Q6ZUJ8						
NEPYIFKVF		3	3.87	11	1	5	29.41
PKM	P14618						
YPLEAVRM		3	3.98	0	0	3	100.00
PKP2	Q99959						
SQNIYIQNR		4	2.25	6	2	4	33.33
PLCB1	Q9NQ66						
RTDPQGFFFY		7	3.19	8	1	11	55.00
PLIN2	Q99541						
AEHIESRTL		8	2.17	5	1	12	66.67
DQYPYLKSV		5	3.77	1	3	7	63.64
GAVTGSVEK		4	2.85	0	0	5	100.00
HSTVHLIEF		4	4.78	1	0	4	80.00
IQDAQDKLYL		3	4.73	0	0	3	100.00
KSELLVEQY		12	3.88	2	1	15	83.33
LTSSKGQLQK		5	3.84	0	1	6	85.71
LVNNTPLNW		3	5.60	2	1	4	57.14
MAGDIYSVFR		3	3.31	15	2	3	15.00
MTSALPIIQK		8	4.30	8	3	9	45.00
RAYQQALSR		8	3.88	1	3	12	75.00
SELLVEQY		3	4.45	0	0	3	100.00
SINTVLGSR		3	3.58	0	0	5	100.00
SLLTSSKGQLQK		12	3.04	11	11	13	37.14
STQIVANAK		5	3.06	5	0	6	54.55
TLLSNIQGV		6	2.82	4	3	10	58.82
TSALPIIQK		16	3.18	68	13	19	19.00
TSSKGQLQK		4	2.58	0	0	4	100.00
VQKPSYYVR		4	5.21	1	2	4	57.14
VRLGSLSTK		3	6.22	2	0	4	66.67
PLOD2	O00469						
KIIAPLVTR		3	3.95	0	0	4	100.00

Supplementary Table 6 (continued)

KVFAGYYTK		5	3.52	9	1	7	41.18
PLOD3	O60568						
AVMNFVVRY		3	3.19	11	0	5	31.25
PLXNA2	O75051						
NKVFLLTFI		3	3.48	0	0	1	100.00
PLXNA3	P51805						
FPIDKPPSF		4	3.49	0	0	6	100.00
TQDPTVTRL		3	2.66	0	1	4	80.00
PLXNB2	O15031						
TYTDRVFFL		8	2.12	26	9	11	23.91
PLXNC1	O60486						
FLVTVIHTL		4	2.58	11	0	8	42.11
POLR1C	O15160						
DEILAHRL		3	2.15	2	0	3	60.00
TTDFPGNYSGY		3	2.88	2	0	6	75.00
POLR2H	P52434						
YPVDLGDKF		10	3.18	5	4	9	50.00
POP7	O75817						
SEIYIHGLGL		4	2.40	0	0	4	100.00
PPARGC1A	Q9UBK2						
LPVDEDGLPSF		4	3.66	2	0	7	77.78
PPM1G	O15355						
EVIKELAQI		4	2.00	13	2	6	28.57
PPP1R15A	O75807						
VPRGQGSQF		4	2.64	18	1	6	24.00
PPP1R3C	Q9UQK1						
GRMENLASYR		3	3.51	6	1	4	36.36
MPVDVAMRL		5	4.43	7	1	9	52.94
PPP1R7	Q15435						
NPLQKDPQY		4	2.14	3	1	4	50.00
PPP4R4	Q6NUP7						
VISSDQIYY		3	2.29	0	2	1	33.33
PQBP1	O60828						
LPVALQTRL		4	3.04	8	1	4	30.77
PRELID1	Q9Y255						
QRYPNPYSK		3	3.15	3	0	3	50.00
PRF1	P14222						
TSNVHVSV		3	2.15	1	1	3	60.00
PRKDC	P78527						
AEVLGLILRY		4	2.62	9	1	5	33.33
PRMT5	O14744						
FPVEVNTVL		3	3.50	1	0	5	83.33
PRMT7	Q9NVM4						
FPIHVQTSL		7	3.44	13	1	9	39.13
PROS1	P07225						
LPLNLDTKY		3	3.14	9	0	3	25.00
PRPF8	Q6P2Q9						
VYTTTVHWL		3	2.76	18	2	3	13.04

Supplementary Table 6 (continued)

PRRC2C	Q9Y520						
FYMDTSHLF		4	2.19	25	2	9	25.00
PRUNE2	Q8WUY3						
DEGKLSITL		4	3.42	0	0	4	100.00
DEINLHQL		3	2.95	0	0	4	100.00
SEINTTHNL		7	2.66	0	0	9	100.00
PSMA2	P25787						
RVASVMQEY		6	2.12	18	2	10	33.33
PSMA6	P60900						
AEIDAHLVAL		3	2.02	9	1	5	33.33
PSMB10	P40306						
GVDLTGPQLY		4	2.63	1	0	7	87.50
PSMB2	P49721						
RFILNLPTF		3	2.14	17	1	5	21.74
PSMB5	P28074						
GVMDRGYSY		3	2.79	1	3	3	42.86
PSMB8	P28062						
STDVSDLLHQY		11	2.75	9	2	14	56.00
PSMC6	P62333						
GEIDYEAIVKL		3	2.17	3	1	3	42.86
PSMD14	O00487						
AMLDTVVFK		5	2.18	18	3	9	30.00
VVVDPIQSVK		3	3.66	12	0	4	25.00
PSMD7	P51665						
KLLDIRSYL		4	2.44	6	2	9	52.94
LPINHQIIY		4	2.68	6	0	5	45.45
PSMD8	P48556						
RILFFNTPK		7	2.62	29	2	9	22.50
PSME2	Q9UL46						
KVLERVNAV		5	2.14	7	2	12	57.14
PSME4	Q14997						
FLQPELVKL		6	2.30	12	4	14	46.67
PTGS1	P23219						
EEAPVLMHY		5	2.36	9	6	5	25.00
HPTWGDEQL		4	5.20	5	1	5	45.45
PTP4A1	Q93096						
RPAPVEVTY		5	2.58	26	3	6	17.14
PTP4A3	O75365						
RPAPVEVSY		3	3.77	9	0	3	25.00
PTPN11	Q06124						
LPFDHTRVV		3	2.69	9	3	6	33.33
PTPRU	Q92729						
GLDDILLLSY		3	3.47	1	0	4	80.00
PTRF	Q6NZI2						
KSFTPDHVVYAR		9	3.82	2	1	11	78.57
SFTPDHVVY		3	4.27	0	0	3	100.00
PYGL	P06737						
WPVDLVEKL		6	2.79	1	3	11	73.33

Supplementary Table 6 (continued)

QPRT	Q15274						
VEAARGAGW		3	2.40	1	0	3	75.00
RAD50	Q92878						
EYVEKFYRI		4	2.85	22	1	6	20.69
RARRES2	Q99969						
FPAGIFVRL		6	3.30	7	0	8	53.33
RRLLIPLAL		3	3.07	2	0	5	71.43
RASSF2	P50749						
ATDYPLIAR		3	4.69	20	0	4	16.67
RBBP7	Q16576						
KDEIFQVHW		3	2.17	4	2	3	33.33
RBM47	A0AV96						
FPAAPAPKM		7	3.60	7	0	10	58.82
TEDTIKKSF		4	2.96	0	2	7	77.78
REXO4	Q9GZR2						
ARVSIVNQY		3	2.50	10	0	4	28.57
RFC4	P35249						
RIIEPLTSR		3	3.30	17	0	5	22.73
RGS5	O15539						
EIKIKLGI		4	5.55	0	0	7	100.00
GLASFKSFL		12	4.22	1	2	18	85.71
HALMEKDSL		4	4.80	0	0	5	100.00
ILLQKPDSV		4	3.42	0	0	5	100.00
KLLQNNYGL		4	4.06	0	0	5	100.00
KPAKTQKTSL		8	3.23	11	7	10	35.71
KTSLDEALQW		3	2.28	0	2	3	60.00
MAQKRIHAL		5	2.79	5	0	13	72.22
PAKTQKTSL		3	2.49	0	0	2	100.00
SSFDMAQKR		5	2.73	13	2	6	28.57
RHPN2	Q8IUC4						
HYAALAHYF		5	3.32	0	1	7	87.50
RIC1	Q4ADV7						
ETLLLSVFQ		5	2.12	1	0	1	50.00
RIOK2	Q9BVS4						
FPVPKPIDY		3	4.01	9	0	3	25.00
RIPK4	P57078						
QENIVRILL		6	3.02	0	0	8	100.00
RNF20	Q5VTR2						
HLAEVLERV		3	2.61	1	2	7	70.00
RNF213	Q63HN8						
EPLSQITAY		3	2.19	2	0	3	60.00
FPIPLINRL		8	2.13	11	2	9	40.91
IYPQVLHSL		3	3.29	8	0	7	46.67
NAFLSKSSV		3	2.01	5	4	5	35.71
RNFT1	Q5M7Z0						
DVHIQINSI		3	4.47	2	0	1	33.33
RNLS	Q5VYX0						
MPVPEILQL		4	2.58	2	0	5	71.43

Supplementary Table 6 (continued)

RPA1	P27694						
TEFPNFKY		4	2.79	2	1	5	62.50
RPF2	Q9H7B2						
RPFEDQTSL		6	3.59	9	2	7	38.89
RPL34	P49207						
RLSYNTASNK		3	2.24	6	0	4	40.00
RPL35	P42766						
QLDDLKVEL		8	3.02	12	1	11	45.83
RPL7A	P62424						
KVVNPLFEK		5	2.43	30	3	6	15.38
RPL9	P32969						
AHFPINVVI		3	2.12	2	1	3	50.00
IPENVDITL		3	2.32	0	1	4	80.00
RPN2	P04844						
ALSALTARL		7	2.22	3	3	11	64.71
RMLAQQAVK		7	2.14	12	2	10	41.67
RPS10	P46783						
YLTNEGIQYL		4	2.08	15	1	6	27.27
RPS19	P39019						
STARHLYLR		3	3.40	4	1	4	44.44
RRAD	P55042						
ALFEGVVRQI		3	3.93	0	0	5	100.00
MPVDERDLQA		3	4.84	0	0	4	100.00
RRAGA	Q7L523						
LLFERATFL		3	2.26	0	0	6	100.00
RRAGC	Q9HB90						
LENLLNIFI		3	2.93	1	0	3	75.00
RRBP1	Q9P2E9						
ATQKGDPVAILK		3	2.02	15	2	5	22.73
RRM1	P23921						
SPVSKGILQY		4	3.41	3	2	5	50.00
RRN3	Q9NYV6						
ITNKYQLVF		8	2.15	12	5	15	46.88
RRP12	Q5JTH9						
RPTDVAISF		3	4.58	6	0	4	40.00
RTKN	Q9BST9						
APRKPPQAL		3	2.27	9	2	6	35.29
RTN4	Q9NQC3						
ISEELVQKY		4	3.30	0	4	3	42.86
RUNX1	Q01196						
DVPDGTLVTVM		3	2.46	3	2	4	44.44
S100A10	P60903						
EHAMETMMF		3	2.00	0	1	3	75.00
S100A11	P31949						
FLSFMNTEL		8	2.34	4	6	17	62.96
S100A9	P06702						
LDTNADKQL		3	2.24	2	0	1	33.33

Supplementary Table 6 (continued)

SAP30	O75446						
IPVNEKDTL		4	5.07	0	0	5	100.00
SARAF	Q96BY9						
KGWDGYDVQW		3	3.61	1	1	4	66.67
YSEYPPFSHRY		14	2.70	22	10	18	36.00
SCD	O00767						
ITAPPSRVL		5	4.33	10	0	9	47.37
LPLRLFLII		5	2.52	0	3	8	72.73
SLLHLGALY		3	3.84	0	0	4	100.00
VFVATFLRY		4	2.51	3	4	4	36.36
SEC14L1	Q92503						
TRWPGFYIL		6	2.06	8	2	9	47.37
SEC16A	O15027						
GLWGHALLL		5	2.34	6	1	8	53.33
SEC23B	Q15437						
MPQFSTIEY		3	3.78	9	0	3	25.00
SEC24A	O95486						
FLLHIQQQV		13	3.07	22	8	17	36.17
SEC24B	O95487						
LPVVSSLADVY		4	2.32	11	1	5	29.41
SEC24C	P53992						
SVLPVLDNPLSK		5	3.39	9	0	5	35.71
SEC31A	O94979						
MPRVQTQQY		4	2.60	5	1	4	40.00
SEL1L3	Q68CR1						
SVSEIGGKIFEK		5	4.32	14	0	6	30.00
YYITGNLETF		5	2.96	16	0	7	30.43
SELL	P14151						
STQRDLWNIFK		3	3.99	15	0	5	25.00
SEMA5A	Q13591						
FTDLNNYDEY		3	2.47	2	0	3	60.00
SERINC2	Q96SA4						
SIAAVLPKV		4	4.11	0	0	6	100.00
SERPINA1	P01009						
SVLGQLGITK		6	2.35	22	2	7	22.58
SETD3	Q86TU7						
PSEYDTPLY		3	2.50	3	0	4	57.14
SF3B3	Q15393						
MVTEIRLKY		3	2.65	2	1	3	50.00
SF3B4	Q15427						
RPITVSYAF		3	3.11	13	0	4	23.53
SGPL1	O95470						
TELLVKAY		3	2.19	0	0	3	100.00
SH3BP1	Q9Y3L3						
YLADLYHFV		5	2.11	10	2	8	40.00
SHANK2	Q9UPX8						
KLWGDVTEI		7	2.18	1	2	11	78.57

Supplementary Table 6 (continued)

SHTN1	A0MZ66						
EVIEEVNKV		4	2.61	5	2	5	41.67
SLC11A1	P49279						
IIMPHNIYL		5	2.12	21	2	11	32.35
SLC15A4	Q8N697						
VSIKAIGW		3	2.88	1	1	3	60.00
SLC16A3	O15427						
KLLDATHVY		3	4.08	0	0	4	100.00
VPPVFVVSY		3	4.77	0	0	3	100.00
YAFPKAVSV		9	3.56	16	0	16	50.00
YAFPKAVSVF		6	3.44	7	1	8	50.00
SLC17A3	O00476						
ALIVSLPYL		6	2.57	0	0	8	100.00
SLC22A18	Q96BI1						
APEERPAAL		10	2.28	14	6	13	39.39
RSSVILLTY		3	3.45	3	1	3	42.86
SLC28A1	O00337						
SYILRPVAF		7	3.16	2	7	8	47.06
SLC2A1	P11166						
FHPLGADSQV		3	5.35	7	0	2	22.22
SLC35B3	Q9H1N7						
FICVAGVFVF		3	3.69	0	0	2	100.00
SLC38A1	Q9H2H9						
LPSSLYLKI		4	4.24	3	1	6	60.00
SLC3A1	Q07837						
EEIKEILRF		10	2.74	2	8	11	52.38
MPKEVLFQF		4	4.52	0	1	6	85.71
NELLLNRGW		8	2.03	0	2	8	80.00
QEADFPFNNY		3	3.11	0	0	4	100.00
TALNIKTVW		4	3.79	0	1	6	85.71
YHDFTTTQV		3	3.72	0	2	4	66.67
YRFMGTEAY		4	5.47	0	0	6	100.00
YSSVLNILY		4	4.63	0	1	10	90.91
SLC4A4	Q9Y6R1						
DEVFHDIAY		3	2.21	0	1	2	66.67
SLC6A17	Q9H1V8						
GFSVGLGNIW		3	3.73	0	0	1	100.00
SLC6A8	P48029						
IAYPRAVTL		3	3.80	0	0	7	100.00
SLC6A9	P48067						
AFVAYPEALTL		5	2.41	3	1	3	42.86
SLU7	O95391						
DPTKLELLY		3	2.35	5	0	3	37.50
SMAD2	Q15796						
LTELPPLDDY		6	2.01	7	2	9	50.00
SMPD4	Q9NXE4						
TQKPLPVSL		3	2.05	12	0	5	29.41
SMPDL3A	Q92484						
NPNLRIISL		4	3.98	2	0	9	81.82

Supplementary Table 6 (continued)

SNAPC1	Q16533						
RVGALYLLY		3	2.12	6	1	5	41.67
SND1	Q7KZF4						
ITDDLHFYV		5	3.09	2	0	7	77.78
NADAIVVKL		5	2.05	6	3	5	35.71
SNRNP200	O75643						
LYQDKFPFF		5	2.17	22	2	8	25.00
RPVPLEQTY		4	2.12	4	2	5	45.45
SYLKQLPHF		5	2.09	19	3	7	24.14
SOAT1	P35610						
DSYPRNPTV		5	3.53	6	1	6	46.15
SORBS1	Q9BX66						
IVNPTIVLL		4	2.40	11	0	4	26.67
SPATS2L	Q9NUQ6						
NVKEKIYAV		4	2.24	2	3	8	61.54
SPCS2	Q15005						
KYVENFGLI		4	2.38	3	1	6	60.00
SRC	P12931						
FYITSRTQF		4	2.88	12	1	5	27.78
STAMBPL1	Q96FJ0						
MPDHTDVSL		4	5.57	4	0	5	55.56
STAT1	P42224						
FLEQVHQLY		11	3.04	10	5	15	50.00
FPMEIRQY		5	3.03	4	2	5	45.45
FPMEIRQYL		5	2.22	19	2	8	27.59
IELLNVTEL		4	2.25	1	1	6	75.00
REGAITFTW		4	3.39	7	1	5	38.46
SEVLSWQF		5	2.84	3	3	6	50.00
VLWDRTFSLF		3	2.57	4	1	7	58.33
VTFPDIIRNYK		3	5.00	6	0	3	33.33
STAT2	P52630						
IELLLPKL		3	3.16	4	0	4	50.00
STAT3	P40763						
KFPELNYQL		5	4.00	13	0	6	31.58
SFAEIIMGY		4	2.31	0	1	4	80.00
STK39	Q9UEW8						
SEIPDEVKL		3	2.32	4	0	4	50.00
STMN3	Q9NZ72						
TQPHPNTVY		3	3.60	19	0	6	24.00
STOML1	Q9UBI4						
AEADLRALL		3	2.46	3	1	7	63.64
STXBP2	Q15833						
ILSGVIRSV		3	2.39	12	1	4	23.53
SWT1	Q5T5J6						
KLWGQSIQL		5	2.43	13	3	12	42.86
TAGLN	Q01995						
HVIGLQMGSNR		3	2.63	4	0	2	33.33
TAGLN2	P37802						
NVIGLQMGTNR		4	2.26	15	2	3	15.00

Supplementary Table 6 (continued)

TAP1	Q03518						
HPTAFVVSY		4	5.12	18	0	4	18.18
LLYESPERY		14	3.05	16	4	17	45.95
TALPRIFSL		3	2.20	5	1	5	45.45
VLLSIYPRV		4	2.94	4	0	5	55.56
VLRQETEFF		3	2.67	11	0	3	21.43
TAPBP	O15533						
MPAAQEGAVAF		5	4.53	8	1	5	35.71
SAFLLLGLFK		6	2.04	20	3	6	20.69
TAPT1	Q6NXT6						
TLLPLRVFL		7	2.01	10	5	13	46.43
TBC1D14	Q9P2M4						
EEFLFRTAL		7	2.01	12	3	8	34.78
TBL1XR1	Q9BZK7						
DEVNFLVY		4	2.35	1	1	4	66.67
TBL3	Q12788						
HPDPTRLLLF		3	3.27	1	1	4	66.67
TBX2	Q13207						
VEDDPKVTL		4	2.18	0	1	5	83.33
TBXAS1	P24557						
IPRPILVLL		4	2.24	17	3	7	25.93
TCEA3	O75764						
IEDHIYQEL		5	2.06	0	3	6	66.67
TCN2	P20062						
MRHLGAFLF		4	2.79	7	3	5	33.33
TCP1	P17987						
HPTSVISGY		3	2.79	12	1	3	18.75
TEP1	Q99973						
RYPSNLQLF		4	2.16	25	2	7	20.59
TFG	Q92734						
IPIHNEDITY		4	2.89	3	0	4	57.14
TFIP11	Q9UBB9						
APVNFISAGL		7	3.07	0	0	7	100.00
VYPLMKEYF		3	2.75	23	1	6	20.00
TFRC	P02786						
ELIERIPEL		3	3.46	1	1	4	66.67
TGFBI	Q15582						
ALFVRLLALA		10	2.66	3	8	13	54.17
LPAEVLDSL		5	4.30	2	0	7	77.78
THEMIS2	Q5TEJ8						
HPTDPLTSF		4	3.19	14	1	4	21.05
TIMP1	P01033						
APFEPLASGIL		6	2.90	17	3	9	31.03
DAADIRFVY		4	4.14	9	0	4	30.77
TIPARP	Q7Z3E1						
HYILHNSFF		4	2.68	16	2	6	25.00
TLN1	Q9Y490						
AVASAAAALVLK		6	2.30	11	4	6	28.57
RELETVRELL		4	3.09	3	0	5	62.50

Supplementary Table 6 (continued)

TLR3	O15455						
EYNNIQHLF		4	3.70	11	0	6	35.29
TLR7	Q9NYK1						
ILISKLLGA		4	2.63	2	3	11	68.75
TMED3	Q9Y3Q3						
TVIDSQTHY		3	2.66	13	0	6	31.58
TMED4	Q7Z7H5						
QLLDQVEQI		10	2.25	6	5	15	57.69
TMED9	Q9BVK6						
QLVEQVEQI		5	2.78	0	1	4	80.00
TMEM189	A5PLL7						
GSVELPIVGK		8	2.00	17	3	9	31.03
TMEM37	Q8WXS4						
AEDRLFGLW		5	3.02	4	0	6	60.00
TMEM38B	Q9NVV0						
FPFFDIAHY		5	2.29	11	3	10	41.67
TMEM86A	Q8N2M4						
VPYSRALIM		3	2.07	1	2	5	62.50
TMTC3	Q6ZXV5						
LSELKPMSY		3	3.58	10	0	7	41.18
TMX2	Q9Y320						
PLYMGPEYI		3	3.64	1	0	2	66.67
TNR	Q92752						
ITAKVATHL		3	5.20	2	0	4	66.67
TNS1	Q9HBL0						
HYPLNTVTF		8	2.22	3	4	10	58.82
ITIEPGLLLK		4	3.10	18	2	5	20.00
TNS3	Q68CZ2						
HTQGPVDGSLY		8	2.71	2	3	13	72.22
TOMM70	O94826						
NRAAAFEQL		3	2.62	4	2	4	40.00
TOP6BL	Q8N6T0						
VYTLLTTHL		4	2.78	4	0	5	55.56
TPMT	P51580						
TEIPGTKVF		6	2.13	5	1	8	57.14
TPX2	Q9ULW0						
KILEDVVGV		6	2.69	9	0	9	50.00
LPLPHFDTI		4	4.16	2	0	5	71.43
TRAFD1	O14545						
EEPDVIFQNF		3	4.71	8	1	5	35.71
TRAM1	Q15629						
IIHAVIQEY		4	2.31	8	2	5	33.33
TRAPPC2L	Q9UL33						
DVVDEKISAM		4	2.66	2	0	5	71.43
YPTEDYKVY		3	4.33	4	0	4	50.00
TRAPPC6A	O75865						
EELDVLKFL		4	2.47	11	3	6	30.00

Supplementary Table 6 (continued)

TRBC1	P01850						
YEILLGKATLY		3	2.77	6	0	3	33.33
TRIM23	P36406						
TEVADHIQL		4	3.23	1	0	5	83.33
TSC22D1	Q15714						
KELIEKNSQL		4	2.40	0	1	5	83.33
TSEN34	Q9BSV6						
SPQPDGKVVY		4	2.45	1	0	5	83.33
TTC17	Q96AE7						
AKVPLGDLDLY		6	2.81	2	0	1	33.33
HLDATKLLL		8	2.02	12	3	16	51.61
TTC39B	Q5VTQ0						
LPAPVKLIL		3	2.13	8	0	3	27.27
TTI1	O43156						
QYILFPLRF		3	2.70	18	1	4	17.39
TUBB	P07437						
QLDRISVYY		3	3.59	2	1	5	62.50
TUBGCP2	Q9BSJ2						
MPHDLITQL		5	3.34	3	2	7	58.33
TUFT1	Q9NNX1						
HEEIIKVYL		4	2.44	0	1	5	83.33
TUSC3	Q13454						
RPPNYSGTIAL		3	3.00	1	1	4	66.67
TXNDC11	Q6PKC3						
IPAKPPVSF		6	2.72	16	2	9	33.33
TYMS	P04818						
DAHIYLNHI		6	3.15	10	5	8	34.78
TYROBP	O43914						
YSDLNTQRPY		8	2.47	20	2	15	40.54
U2SURP	O15042						
YPEPFLIKL		4	2.55	2	0	5	71.43
UBA6	A0AVT1						
FPAAIEHTI		3	2.69	3	2	4	44.44
UBD	O15205						
DANPYDSVKKI		3	6.53	0	0	1	100.00
KMMADYGIRK		4	3.16	3	0	5	62.50
NPYDSVKKI		5	2.31	2	5	8	53.33
UBE2V2	Q15819						
LPQPPEGQTY		3	3.28	1	0	3	75.00
UBE2W	Q96B02						
YPFDSPQVMF		3	3.60	2	0	3	60.00
UBE2Z	Q9H832						
NPYHNEPGF		5	2.26	2	0	6	75.00
UBE3A	Q05086						
NESPLKYLF		3	2.39	6	1	5	41.67
UBL3	O95164						
SPNILRLIY		3	2.80	6	0	6	50.00

Supplementary Table 6 (continued)

UBR4	Q5T4S7						
MPIYEAADKAL		7	4.74	0	0	7	100.00
UBXN4	Q92575						
FPRREFTKEDY		4	4.96	2	0	4	66.67
UGP2	Q16851						
LPVAKDVSY		3	2.73	12	0	4	25.00
UGT2A3	Q6UWM9						
ATAIFLFTK		5	4.73	6	1	7	50.00
LAVPFVLTL		9	2.95	1	0	11	91.67
UHRF1	Q96T88						
TLFDYEVRL		10	3.92	13	2	18	54.55
UHRF1BP1L	A0JNW5						
YTDSSSILNY		4	2.65	12	0	8	40.00
USH1C	Q9Y6N9						
THEEVINLI		3	5.13	0	0	3	100.00
USP10	Q14694						
FPAEAGRDTL		4	2.53	1	1	5	71.43
USP7	Q93009						
VEGTIPKLF		3	2.37	6	1	5	41.67
USP8	P40818						
KYVTVYNLI		3	2.02	16	0	6	27.27
UXT	Q9UBK9						
VPDTSRIYV		4	3.76	5	1	6	50.00
VPDTSRIYVAL		6	2.77	21	2	8	25.81
VASN	Q6EMK4						
SRVPLLLPL		4	2.62	0	0	5	100.00
VAV1	P15498						
FLLDKALLI		4	2.10	21	2	13	36.11
VAV3	Q9UKW4						
GEVNGRVGW		3	2.40	2	2	4	50.00
VCAM1	P19320						
FPRDPEIEM		10	4.64	12	3	13	46.43
KSIDGAYTI		3	5.21	1	0	3	75.00
QIDSPLNGK		5	3.53	2	1	5	62.50
QIDSPLSGK		9	2.09	11	6	10	37.04
VCAN	P13611						
FPYSGDKILV		3	5.37	1	0	4	80.00
VEGFA	P15692						
HPIETLVDIF		6	4.40	0	0	9	100.00
VIM	P08670						
ALRPSTSRSLY		11	3.20	36	6	17	28.81
LEQQNKILL		7	2.62	5	5	7	41.18
LPLPNFSSL		12	2.98	26	5	16	34.04
QAKQESTEY		3	3.01	23	1	9	27.27
RISLPLPNF		11	2.02	40	10	14	21.88
SLPLVDTHSK		7	3.72	24	1	8	24.24
VN1R17P	Q8TDU5						
PIDMTISHL		3	4.13	0	1	2	66.67

Supplementary Table 6 (continued)

VPS13A	Q96RL7						
IPMAKSYVL		3	2.57	4	1	3	37.50
VPS13B	Q7Z7G8						
YPEPRVLTL		3	3.28	7	1	5	38.46
VPS25	Q9BRG1						
DEATLLRAL		4	2.02	1	4	5	50.00
VPS29	Q9UBQ0						
KTLAGDVHIVR		3	2.02	2	0	3	60.00
VPS35	Q96QK1						
DELHYLEVY		4	2.36	1	2	5	62.50
VWA5A	O00534						
KTFEDKVTF		3	2.23	13	2	3	16.67
VWF	P04275						
AVLSSPLSH		6	3.14	19	2	10	32.26
AYGFVARI		5	2.95	8	2	7	41.18
DALGFAVRY		6	3.88	10	2	8	40.00
EAYGFVARI		8	2.02	13	8	9	30.00
EVIASYAHL		6	3.79	6	3	4	30.77
IPARFAGVL		11	4.11	31	5	14	28.00
MPYASKGLYL		7	3.04	10	0	7	41.18
VTASVRLSY		6	4.18	11	1	8	40.00
WDFY4	Q6ZS81						
EEEGNLLRSW		3	3.59	6	0	3	33.33
WDR43	Q15061						
KLILLITQV		4	2.01	7	1	6	42.86
WDR72	Q3MJ13						
LSDVDSSSSFY		3	3.93	2	0	3	60.00
WDR81	Q562E7						
TLMDILPRI		9	2.12	11	2	16	55.17
WDR91	A4D1P6						
MPVPVILNF		7	2.45	4	1	10	66.67
WTAP	Q15007						
NELSAWKF		4	2.03	1	2	4	57.14
WWC2	Q6AWC2						
SLIENQILL		7	2.45	6	2	12	60.00
YBX3	P16989						
APAPAAHVA		3	2.07	9	1	5	33.33
YIPF3	Q9GZM5						
FPQKIAGELY		3	2.54	2	0	4	66.67
YTHDC2	Q9H6S0						
DEATIRAII		4	2.02	0	2	5	71.43
ZCRB1	Q8TBF4						
LPFSLTNNDLY		3	2.71	2	1	4	57.14
ZHX2	Q9Y6X8						
FPYPTQAEL		3	3.86	0	0	4	100.00
ZKSCAN1	P17029						
DGIVIVKV		5	2.53	9	2	6	35.29
ZWINT	O95229						
LPAKILVEF		7	2.39	10	3	8	38.10

Supplementary Table 7: Class II TUMAPs of selected target candidates. All TUMAPs found in at least 3 ccRCC patients are listed.

Gene TUMAP	Found on n ccRCC patients	Uniprot_ID
ADAM17	3	P78536
VRIIKPFPAPQTPG	3	
ADAMDEC1	3	O15204
KGNILNEKNSVAS	3	
AGRN	12	O00468
GAPVPAFEGRSFLAFPTL	3	
LEFRALEPQGLLL	3	
TGDTRIFFVNPAPPYLWPA	6	
ALAD	3	P13716
IQPITSLPGVARYG	3	
ALB	3	P02768
GERAFKAWAVARLS	3	
ALCAM	3	Q13740
TKKSVQYDDVPEYKDR	3	
ANG	3	P03950
PVHLDQSIFRRP	3	
ANPEP	4	P15144
STGTLSQEHFLLD	4	
ANXA4	10	P09525
IGRDLIDDLKSELSG	3	
ISQTYQQQYGRSLED	7	
ANXA5	3	P08758
IKQVYEEEYGSSLED	3	
APCS	8	P02743
SKVIEKFPAPVH	4	
TSKVIEKFPAPVH	4	
APOA1	14	P02647
RLAEYHAKATEHLST	7	
RLAEYHAKATEHLSTL	4	
RTHLAPYSDELRQR	3	
APOA4	13	P06727
GDLQKKLVPFATELH	3	
LQQRLEPYADQLRTQ	3	
QQRLEPYADQLR	4	
RQRLAPLAEDVRG	3	
B2M	3	P61769
FYLLYYTEFTPTEKDE	3	
BGN	5	P21810
VPKEISPDTTLLDLQ	5	
BTF3	3	P20290
AEALPKQSV	3	

Supplementary Table 7 (continued)

C1QA	3	P02745
VSSSRGQVR	3	
C1QC	3	P02747
APNSLIRFNAVLTNPQ	3	
C3	11	P01024
GISTKLMNIFLKDSIT	4	
KVTIKPAPETEKRPQ	3	
VYHHFISDGVRKS	4	
CAGE1	3	Q8TC20
ESMSESDTMNVSN	3	
CANX	8	P27824
DDWDEDAPAKIPDE	5	
KTDAPQPDVK	3	
CD3G	4	P09693
EDDQYSHLQGNQLR	4	
CD4	3	P01730
RVTQDPKLQMGKK	3	
CD74	3	P04233
GLGVTKQDLGPVPM	3	
CDV3	17	Q9UKY7
KTPQGPPEIYSDTQFPSLQ	8	
RKTPQGPPEIYSDTQFPSLQ	3	
TPQGPPEIYSDTQFPSLQ	6	
CECR1	3	Q9NZK5
HDEEWSVKTYQEVAQK	3	
CLU	3	P10909
VAEKALQEYRKKHRE	3	
CNN1	4	P51911
TNHTQVQSTL	4	
COL14A1	3	Q05707
APGNVEKYRVVYYPTRGGKPDE	3	
COL18A1	3	P39060
DPDKFQGVIAELKVR	3	
COL1A2	4	P08123
GKTIIEYKTNKPS	4	
COL4A2	6	P08572
AGIPQKIAVQPGTVGPQG	3	
IPQKIAVQPGTVGPQGR	3	
COL6A2	3	P12110
INRIIKVMKHEAYG	3	
CPE	3	P16870
APETKAVIHWIMDIPF	3	
CRP	3	P02741
TSYVSLKAPLT	3	

Supplementary Table 7 (continued)

CTSA	3	P10619
VARIVGNSGLNI	3	
CTSD	17	P07339
FIGRYYTVFDRDNN	3	
LVRIPLHKFTSIRR	3	
RIPLHKFTSIRR	3	
VFIGRYYTVFDRDN	4	
YPRISVNNVLPV	4	
CUBN	3	O60494
VIELKFSDFDVVPS	3	
CXCL14	4	O95715
KMVIITTKSVSRYR	4	
CYB5R3	3	P00387
SPDIKYPLR	3	
DNAH11	4	Q96DT5
LKKQDIPDSALAIFK	4	
DSC2	3	Q02487
TGSIKVFRSLDREA	3	
EDIL3	7	O43854
GVITQGAKRIGSPE	4	
VTGVITQGAKRIGSPE	3	
ENPEP	15	Q07075
DDAFALARAQLLDYK	3	
IDDAFALARAQLL	3	
IDDAFALARAQLLD	4	
IDDAFALARAQLLDY	5	
ENPP3	10	O14638
VPFYEPSHAEEVSK	5	
YNNEFRSMEAIFLAHGPS	5	
EZR	3	P15311
DRIQVWHAEHRG	3	
FAM162A	3	Q96A26
EEAAMKAKTE	3	
FGA	10	P02671
FPGFFSPMLG	3	
HPGIAEFPSRGK	4	
HPGIAEFPSRGKSSSY	3	
FGG	3	P02679
YLQEIYNSNNQKIVNLK	3	
FLT1	3	P17948
FPLDTLIPDGKRIIWD	3	
FN1	25	P02751
DDTSIVVRWSRPQAPI	3	
DEPQYLDLPSTATS	4	

Supplementary Table 7 (continued)

DEPQYLDLPSTATSV	3	
GDEPQYLDLPSTATSVN	3	
KTYHVGEQWQKEYLG	3	
SSPVVIDASTAIDAPS	6	
TPPESAVTGYRVDVIPVNLPG	3	
FTL	3	P02792
AAVNSLVNL	3	
GAA	4	P10253
SLPSQYITGLAEHLSPL	4	
GAPDH	5	P04406
AVGKVIPELNGKLTG	5	
GLRX	3	P35754
EIQDYLQQLTGARTVPR	3	
GPC4	3	O75487
LDRLVTDVKEKLKQAK	3	
GPNMB	6	Q14956
DVYVVTDQIPVFVTMFQKN	3	
VPIAQVKDVYVVTDQIPVFVTM	3	
GSN	3	P06396
KPMIIYKGGTSREG	3	
H2AFZ	3	P0C0S5
IGKKGQQKTV	3	
HLA-DRA	4	P01903
VDMAKKETVWRLEEF	4	
HMGB1	3	P09429
KDIAAYRAKGKPD	3	
HNRNPA3	3	P51991
GSGGYGSRRF	3	
HNRNPK	3	P61978
LQLPSPTATSQLPLESD	3	
HP	12	P00738
ATGILSFDKSCAVAE	3	
LPSKDYAEVGRVGYVS	3	
LPSKDYAEVGRVGYVSG	3	
YATGILSFDKSCAVAEYG	3	
HSP90AB1	3	P08238
AEEPNAAVPDEIPPLEGDEDASRME	3	
HSPD1	10	P10809
GIIDPTKVVR	4	
GSPKVTKDGVTVAK	3	
LKDKYKNIGAK	3	
HSPG2	25	P98160
APPIRIEPSSSRVA	4	
GGSLRYNVRYELAR	3	

Supplementary Table 7 (continued)

GPGYVGNPSVQGGQ	3	
STQLQIDPSLHE	6	
STQLQIDPSLHEFQL	6	
VTPTVRIESSSSQVAEG	3	
HTRA1	4	Q92743
KADIALIKIDHQGK	4	
IFI30	5	P13284
SPLQALDFFGNGPPVNYKTG	5	
IGF2	3	P01344
YPVGKFFQYDTWKQST	3	
IGFBP3	24	P17936
HSKIIIIKKG	4	
HSKIIIIKKGHA	3	
IIIIKKGHAK	5	
IIIIKKGHAKD	5	
IIIKKGHAK	3	
IIKKGHAKD	4	
IGFBP5	3	P24593
RPKHTRISELKAEAVKK	3	
IGHG1	6	P01857
APIEKTISKAKGQPREPQ	6	
ITGAX	3	P20702
RGAVYLFHGVLGPS	3	
ITGB2	3	P05107
SNQFQTEVGKQLISG	3	
ITIH2	3	P19823
LKKFYNQVSTPLLR	3	
ITIH4	6	Q14624
RPSLVPASAENVNKA	3	
WRPSLVPASAENVN	3	
KNG1	4	P01042
VHPISTQSPDLEP	4	
KRT2	3	P35908
SGGGKHSSGGGSRGG	3	
KRT9	3	P35527
GGGGLGSGGSIR	3	
LAMC1	4	P11047
FGDEVFNDPKVLKSY	4	
LCP1	7	P13796
IKIFHGLKSTDVAK	7	
LGALS1	3	P09382
VRGEVAPDAKSFVLNL	3	
LGALS3BP	5	Q08380
VPSELALLKAVDTWS	5	

Supplementary Table 7 (continued)

LRP1B	3	Q9NZR2
IPHCKDKSDEKLL	3	
LRP2	13	P98164
MPRHIVVDPKNRYLFW	3	
RRTVVQYLNNPR	3	
SSSVASDNAIRRIKPD	3	
VDREVIVNAAVHA	4	
MARCKS	3	P29966
TPKKKKKRF	3	
MDH2	3	P40926
LLKNSPLVSR	3	
NDUFA4L2	10	Q9NRX3
AGASLGARF	3	
AVSTDYKKLKKDRPDF	7	
NID1	9	P14543
LDGTQRRVLFETDLVNPR	3	
WESVAPYQGPSRDPD	3	
WESVAPYQGPSRDPDQ	3	
NPM1	6	P06748
RSAPGGGSKVPQK	6	
NPTX2	8	P47972
INDKVAQLPLFVSDG	4	
MPGNIIPWVDNNVDVF	4	
OLFML2B	3	Q68BL8
IRSALQRDAAAAYAHPE	3	
OR2A5	6	Q96R48
IQMLLSGLFSLL	6	
PCOLCE	3	Q15113
VIALTFEKFDLEPDT	3	
PCSK9	6	Q8NBP7
IEGRVMVTDFENVPEE	3	
VEVYLLDTSIQSDH	3	
PDGFD	3	Q9GZP0
DLYRRDETIQVKGN	3	
PEA15	3	Q15121
EEEIIKLAPPPKKA	3	
PLG	3	P00747
HSIFTPETNPRA	3	
PLIN2	3	Q99541
TKSELLVEQYLPLTEE	3	
PLXNC1	4	O60486
DEPVWRSEQAIGAIA	4	
POSTN	4	Q15063
IIHGNQIATNGVVHVIDR	4	

Supplementary Table 7 (continued)

PRSS23	15	O95084
LPVVLPQSTLNLAK	4	
LPVVLPQSTLNLAKP	4	
LPVVLPQSTLNLAKPD	7	
PSAP	23	P07602
APFMANIPLLLYP	4	
DPYQKQCDQFVAEYEPV	4	
EVVAPFMANIPLLLYPQ	6	
VAPFMANIPLLLYP	6	
VAPFMANIPLLLYPQDG	3	
PTMA	13	P06454
AAVDTSSEITTKDLKEKK	3	
AVDTSSEITTKDL	4	
AVDTSSEITTKDLKEKK	3	
ITTKDLKEK	3	
PXDN	11	Q92626
GKFHISPEGFLTINDV	11	
RPL13	3	P26373
PRKPSAPKKGDSSAEEL	3	
RPL7A	3	P62424
KVAPAPAVVK	3	
RPS11	4	P62280
YQKQPTIFQNK	4	
RPS13	3	P62277
RDSHGVAQVR	3	
RPS20	3	P60866
KTPVEPEVAIHRIR	3	
RPS6	3	P62753
IVKKGEKDIPGLTDTTVPR	3	
S100A9	3	P06702
LGHPDTLNQGEFKEL	3	
SDCBP	3	O00560
GKITSIVKDSSAARN	3	
SERPINF2	4	P08697
GPDLKLVPPMEEDYPQF	4	
SIRPA	3	P78324
LQVIQPDKSVLVAAG	3	
SLAMF7	9	Q9NQ25
DSIVWTFNTTPLVTIQP	3	
EDVIYTWKALGQA	3	
SIVWTFNTTPLVTIQPE	3	
SLIT3	3	O75094
KDSYVELASAKVRP	3	

Supplementary Table 7 (continued)

SPARC	3	P09486
YERDEDNNLLTEKQKLRVKKIHENE	3	
STAB1	3	Q9NY15
GHMIRNVEALASDLPN	3	
TEKT5	4	Q96M29
MEFLGTTQTA	4	
TF	7	P02787
IRAIAANEADAVT	4	
YEYVTAIRNLREGT	3	
TGFBI	9	Q15582
IDKVISTITNNIQ	3	
VNIELLNALRYHMVG	3	
VSGGIGALVRLKSLQ	3	
TGS1	3	Q96RS0
VTPEKIAEHIAG	3	
THBS1	7	P07996
SSPAFRIEDANLIPPV	3	
SSPAFRIEDANLIPPVPD	4	
THBS2	6	P35442
SRGTLLALEGPGLSQ	6	
TMEM57	3	Q8N5G2
QKDKQNISQLEKKL	3	
TMSB10	3	P63313
TQEKNTLPTKETIEQEKRSEIS	3	
TMSB4X	11	P62328
LKKTETQEKNPLPSK	4	
TETQEKNPLPSK	3	
TQEKNPLPSK	4	
TOB2	3	Q14106
FTTASFAATKFGS	3	
TTR	8	P02766
DAVRGSPAINVAVHVFRK	3	
VRGSPAINVAVHVFRK	5	
USP34	3	Q70CQ2
SRYIHDLFPSLIKN	3	
VCAM1	15	P19320
DRLEIELLKGETILE	3	
GETILENIEFLEDTDMK	4	
STLTLSPVSFENEHSYL	3	
TPESRYLAQIGDSVS	5	
VWA1	3	Q6PCB0
GPERIVISHARPRSL	3	
ZNF112	3	Q9UJU3
VMLENFRNLLLV	3	

8.2. SYFPEITHI matrices

The following tables display the SYFPEITHI matrices for each length variant established from monoallelic transfectants of C1R cells. The first lines constitute the amino acid position within the peptide. The first row represents the amino acid. Scores were distributed according to predefined standards. First, anchor and auxiliary anchor positions are defined depending on the frequency of one or a group of similar amino acids representing at least 75% or 50%, respectively, of all residues at a specific position. For anchor positions scores of 4-10 are assigned depending on the impact of the residue. The amino acid with the highest impact receives 10 points. Every other residue receives 10 points if not >3x less frequent than the amino acid with the highest impact, 8 points if >3x less frequent and 6 points if >5x less frequent. For residues representing less than 10%, 4 points are assigned if they have similar characteristics compared to the other anchor residues and if they are more frequent then their background frequency within the human proteome (residues appear on the positive axis of the sequence logos, see **Figure 25**). For auxiliary anchors scores of 4 or 6 are assigned. A percentage over 50% accounting for one residue is rewarded with 6 points. If auxiliary anchor definition is achieved by two (or more) residues, 4 points are distributed to each amino acid. An amino acid frequency of >30% in non-anchor and non-auxiliary anchor position is awarded with 3 points, a frequency of >20% with 2 points and a frequency of >10% with 1 point. Amino acids which are completely absent at a specific position may be also penalized with -1 point in non-anchor positions.

HLA-C*01:02, 8mers

	1	2	3	4	5	6	7	8
A	0	3	0	0	1	0	1	0
C	0	0	0	0	0	0	0	0
D	0	0	0	0	0	0	0	0
E	0	0	0	1	0	0	2	0
F	1	0	0	0	0	0	0	4
G	0	0	0	0	3	0	0	0
H	0	0	0	0	2	1	0	0
I	0	0	0	0	0	0	0	4
K	0	0	0	0	0	1	0	0
L	0	0	0	0	0	0	0	10
M	0	0	0	0	0	0	0	4
N	0	0	0	0	0	0	0	0
P	0	0	10	0	0	0	0	0
Q	0	0	0	0	0	0	0	0
R	0	0	0	0	0	1	0	0
S	1	3	0	0	1	1	1	0
T	0	0	0	1	0	0	1	0
V	1	1	0	1	0	0	1	4
W	0	0	0	0	0	0	0	0
Y	1	0	0	0	0	0	0	0

HLA-C*01:02, 9mers

	1	2	3	4	5	6	7	8	9
A	0	3	0	0	1	1	1	2	0
C	0	0	0	0	0	0	0	0	0
D	0	0	0	0	0	0	0	0	0
E	0	0	0	1	0	0	0	1	0
F	1	0	0	0	0	0	0	0	4
G	0	0	0	0	1	0	0	0	0
H	0	0	0	0	0	0	0	0	0
I	0	0	0	0	0	0	0	0	4
K	0	0	0	0	0	0	0	0	0
L	0	2	0	0	0	0	1	0	10
M	0	0	0	0	0	0	0	0	4
N	0	0	0	0	0	0	0	0	0
P	0	0	10	0	1	0	0	0	0
Q	0	0	0	0	0	0	0	0	0
R	0	0	0	0	0	0	1	0	0
S	1	2	0	1	1	0	1	2	0
T	0	0	0	0	0	1	0	0	0
V	1	0	0	0	0	0	0	0	4
W	0	0	0	0	0	0	0	0	0
Y	0	0	0	0	0	0	0	0	0

HLA-C*01:02, 10mers

	1	2	3	4	5	6	7	8	9	10
A	1	2	0	0	0	1	0	0	2	0
C	0	0	0	0	0	0	0	0	0	0
D	0	0	0	1	0	0	0	0	0	0
E	0	0	0	2	0	0	0	0	1	0
F	1	0	0	0	0	0	0	0	0	4
G	0	0	0	0	1	0	0	0	0	0
H	0	0	6	0	0	0	0	0	0	0
I	0	2	0	0	0	0	0	0	0	4
K	0	0	0	0	0	0	0	0	0	0
L	0	6	0	0	0	0	1	1	0	10
M	0	0	0	0	0	0	0	0	0	4
N	0	0	0	0	0	0	0	0	0	0
P	0	0	10	0	0	2	1	0	0	0
Q	0	0	0	0	0	0	0	0	0	0
R	0	0	0	0	0	0	0	0	0	0
S	1	0	6	0	1	0	0	2	2	0
T	0	0	0	0	0	0	0	1	1	0
V	0	0	0	0	0	0	0	0	0	4
W	0	0	0	0	0	0	0	0	0	0
Y	1	0	0	0	0	0	0	0	0	0

HLA-C*02:02, 8mers

	1	2	3	4	5	6	7	8
A	0	10	0	0	0	0	0	0
C	0	0	0	0	0	0	0	0
D	0	0	2	0	0	0	0	0
E	0	0	0	0	0	0	1	0
F	2	0	0	0	0	0	0	10
G	0	0	1	0	1	0	0	0
H	0	0	0	0	0	0	0	0
I	0	8	0	0	0	0	0	0
K	0	0	0	0	0	0	1	0
L	0	0	0	0	0	0	0	10
M	0	0	0	0	0	0	0	6
N	0	0	0	0	0	0	0	0
P	0	0	0	0	0	0	0	0
Q	0	6	0	0	0	0	0	0
R	0	0	0	0	0	1	0	0
S	0	8	0	0	0	0	0	0
T	0	8	0	0	0	0	0	0
V	0	8	0	1	0	1	0	6
W	0	0	0	0	0	0	0	0
Y	2	0	0	0	0	0	0	8

HLA-C*02:02, 9mers

	1	2	3	4	5	6	7	8	9
A	0	10	1	0	0	0	0	0	0
C	0	0	0	0	0	0	0	0	0
D	0	0	0	1	0	0	0	0	0
E	0	0	0	0	0	0	0	1	0
F	2	0	1	0	0	0	0	0	10
G	0	0	0	1	0	0	0	0	0
H	0	0	0	0	0	0	0	0	0
I	0	6	1	0	1	1	0	0	0
K	0	0	1	0	0	0	0	0	0
L	0	0	0	0	0	1	1	0	10
M	0	0	0	0	0	0	0	0	6
N	0	0	0	0	0	0	0	0	0
P	0	0	0	1	0	0	0	0	0
Q	0	6	0	0	0	0	0	0	0
R	0	0	0	0	0	0	0	0	0
S	1	6	0	1	0	0	1	0	0
T	0	6	0	0	0	0	0	1	0
V	0	6	0	0	0	1	1	0	8
W	0	0	0	0	0	0	0	0	0
Y	2	0	1	0	0	0	0	0	10

HLA-C*02:02, 10mers

	1	2	3	4	5	6	7	8	9	10
A	0	10	1	0	0	1	0	0	0	0
C	0	0	0	0	0	0	0	0	0	0
D	0	0	0	1	0	0	0	0	0	0
E	0	0	0	0	0	0	0	0	1	0
F	4	0	1	0	1	0	0	0	0	10
G	0	0	0	0	1	0	1	0	0	0
H	0	0	0	0	0	0	0	0	0	0
I	0	6	0	0	0	0	0	0	0	0
K	0	0	1	0	0	0	0	0	0	0
L	0	0	0	0	0	0	1	0	0	8
M	0	0	0	0	0	0	0	0	0	8
N	0	0	0	0	0	1	0	0	0	0
P	0	0	0	2	1	0	1	0	0	0
Q	0	6	0	0	0	0	0	0	0	0
R	0	0	0	0	0	0	0	0	0	0
S	0	8	0	0	0	1	0	1	1	0
T	0	6	0	0	0	0	0	1	0	0
V	0	8	0	0	0	0	0	0	0	6
W	0	0	0	0	0	0	0	0	0	0
Y	4	0	0	0	0	0	0	0	1	10

HLA-C*03:03, 8mers

	1	2	3	4	5	6	7	8
A	0	10	0	0	0	0	0	0
C	0	0	0	0	0	0	0	0
D	0	0	2	0	0	0	0	0
E	0	0	0	0	0	0	1	0
F	4	0	0	0	0	0	0	6
G	0	0	0	0	4	0	0	0
H	0	0	1	0	0	0	0	0
I	0	6	0	0	0	0	0	0
K	0	0	0	0	0	0	0	0
L	1	0	0	2	0	1	0	10
M	0	0	0	0	0	0	0	4
N	0	0	0	0	0	0	0	0
P	0	0	0	0	1	0	0	0
Q	0	0	0	0	0	0	0	0
R	0	0	0	0	0	2	1	0
S	0	10	0	0	0	0	0	0
T	0	8	0	0	0	0	0	0
V	0	6	0	1	0	0	0	0
W	0	0	0	0	0	0	0	0
Y	4	0	0	0	0	0	0	0

HLA-C*03:03, 9mers

	1	2	3	4	5	6	7	8	9
A	0	10	0	0	0	0	0	1	0
C	0	0	0	0	0	0	0	0	0
D	0	0	1	1	0	0	0	0	0
E	0	0	0	1	0	0	0	1	0
F	4	0	0	0	0	1	0	0	6
G	0	0	0	1	0	0	0	0	0
H	0	0	0	0	0	0	0	0	0
I	0	6	1	0	0	0	0	0	0
K	0	0	0	0	0	0	0	0	0
L	1	0	0	0	0	0	1	0	10
M	0	0	0	0	0	0	0	0	4
N	0	0	0	0	0	0	0	0	0
P	0	0	0	2	1	0	0	0	0
Q	0	0	0	0	0	0	0	0	0
R	0	0	0	0	0	0	1	0	0
S	0	8	0	0	0	0	0	1	0
T	0	6	0	0	0	0	0	1	0
V	0	6	1	0	0	0	0	1	0
W	0	0	0	0	0	0	0	0	0
Y	4	0	0	0	0	0	0	0	0

HLA-C*03:03, 10mers

	1	2	3	4	5	6	7	8	9	10
A	0	10	0	0	0	0	0	0	1	0
C	0	0	0	0	0	0	0	0	0	0
D	0	0	0	1	0	0	0	0	0	0
E	0	0	0	1	0	0	0	0	1	0
F	4	0	1	0	0	0	0	0	0	6
G	0	0	0	1	1	1	1	0	0	0
H	0	0	0	0	0	0	0	0	0	0
I	0	6	1	0	0	0	0	0	0	0
K	0	0	0	0	0	0	0	0	0	0
L	0	0	0	0	0	0	0	1	0	10
M	0	0	0	0	0	0	0	0	0	4
N	0	0	0	0	0	0	0	0	0	0
P	0	0	0	2	1	1	1	0	0	0
Q	0	0	0	0	0	0	0	0	0	0
R	0	0	0	0	0	0	0	0	0	0
S	0	8	0	0	0	1	0	0	1	0
T	0	6	0	0	0	0	0	0	0	0
V	0	6	1	0	0	0	0	0	1	0
W	0	0	0	0	0	0	0	0	0	0
Y	4	0	1	0	0	0	0	0	0	0

HLA-C*03:04, 8mers

	1	2	3	4	5	6	7	8
A	0	10	0	0	1	0	1	0
C	0	0	0	0	0	0	0	0
D	0	0	1	0	0	0	0	0
E	0	0	0	1	0	0	2	0
F	4	0	0	0	0	0	0	6
G	0	0	0	0	4	0	0	0
H	0	0	1	0	0	0	0	0
I	0	6	0	0	0	0	0	0
K	0	0	0	0	0	1	0	0
L	4	0	0	1	0	1	0	10
M	0	0	0	0	0	0	0	6
N	0	0	0	0	0	0	0	0
P	0	0	0	0	1	0	0	0
Q	0	0	0	0	0	0	0	0
R	0	0	0	0	0	1	0	0
S	0	10	0	0	0	0	0	0
T	0	10	0	0	0	0	0	0
V	0	6	0	1	0	0	0	0
W	0	0	0	0	0	0	0	0
Y	4	0	0	0	0	0	0	0

HLA-C*03:04, 9mers

	1	2	3	4	5	6	7	8	9
A	0	10	0	0	0	0	0	1	0
C	0	0	0	0	0	0	0	0	0
D	0	0	1	1	0	0	0	0	0
E	0	0	0	1	0	0	0	1	0
F	4	0	0	0	0	0	0	0	6
G	0	0	0	1	0	1	0	0	0
H	0	0	0	0	0	0	0	0	0
I	0	6	1	0	0	0	0	0	0
K	0	0	0	0	0	0	0	0	0
L	4	0	0	0	0	0	1	0	10
M	0	0	0	0	0	0	0	0	6
N	0	0	0	0	0	0	0	0	0
P	0	0	0	1	1	0	0	0	0
Q	0	0	0	0	0	0	0	0	0
R	0	0	0	0	0	0	1	0	0
S	0	8	0	0	0	1	0	1	0
T	0	6	0	0	0	0	0	1	0
V	1	6	1	0	0	0	0	1	0
W	0	0	0	0	0	0	0	0	0
Y	4	0	0	0	0	0	0	0	0

HLA-C*03:04, 10mers

	1	2	3	4	5	6	7	8	9	10
A	0	10	0	0	0	0	0	0	1	0
C	0	0	0	0	0	0	0	0	0	0
D	0	0	0	1	0	0	0	0	0	0
E	0	0	0	1	0	0	0	0	0	0
F	4	0	0	0	0	0	0	0	0	8
G	0	0	0	1	1	0	1	0	0	0
H	0	0	0	0	0	0	0	0	0	0
I	0	6	1	0	0	0	0	0	0	0
K	0	0	0	0	0	0	0	0	0	0
L	0	0	0	0	0	0	0	1	0	10
M	0	0	0	0	0	0	0	0	0	6
N	0	0	0	0	0	0	0	0	0	0
P	0	0	0	2	1	1	0	0	0	0
Q	0	0	0	0	0	0	0	0	0	0
R	0	0	0	0	0	0	0	0	0	0
S	0	6	0	0	0	1	0	0	1	0
T	0	6	0	0	0	1	0	0	1	0
V	1	6	1	0	0	0	0	0	1	0
W	0	0	0	0	0	0	0	0	0	0
Y	4	0	0	0	0	0	0	0	0	0

HLA-C*04:01, 8mers

	1	2	3	4	5	6	7	8
A	0	0	0	0	1	0	0	0
C	0	0	0	0	0	0	0	0
D	0	0	10	0	0	0	0	0
E	0	0	4	1	0	0	1	0
F	1	4	0	0	0	0	0	8
G	0	0	0	0	0	1	0	0
H	0	0	0	0	1	0	1	0
I	1	0	0	0	0	0	0	8
K	0	0	0	0	0	0	1	0
L	0	0	0	0	0	0	0	10
M	0	0	0	0	0	0	0	8
N	0	0	0	0	0	0	0	0
P	0	0	0	0	0	0	0	0
Q	0	0	0	0	0	0	0	0
R	0	0	0	0	0	0	1	0
S	0	0	0	0	0	0	0	0
T	0	1	0	0	0	0	0	0
V	1	0	0	1	0	2	0	8
W	0	0	0	0	0	0	0	0
Y	1	4	0	0	0	0	0	0

HLA-C*04:01, 9mers

	1	2	3	4	5	6	7	8	9
A	0	0	0	0	1	0	1	0	0
C	0	0	0	0	0	0	0	0	0
D	0	0	10	0	0	0	0	0	0
E	0	0	6	1	0	0	0	1	0
F	1	4	0	0	0	0	0	0	10
G	0	0	0	0	0	0	0	0	0
H	0	0	0	0	0	0	0	0	0
I	1	0	0	0	0	1	0	0	6
K	0	0	0	0	0	0	0	0	0
L	1	0	0	1	0	1	0	1	10
M	0	0	0	0	0	0	0	0	8
N	0	0	0	0	0	0	0	0	0
P	0	0	0	1	0	0	0	0	0
Q	0	0	0	0	0	0	0	0	0
R	0	0	0	0	0	0	0	0	0
S	0	0	0	0	0	0	0	0	0
T	0	0	0	0	0	0	0	0	0
V	1	0	0	0	0	1	1	0	8
W	0	4	0	0	0	0	0	0	0
Y	0	4	0	0	0	0	0	0	0

HLA-C*04:01, 10mers

	1	2	3	4	5	6	7	8	9	10
A	0	0	0	0	1	1	0	0	0	0
C	0	0	0	0	0	0	0	0	0	0
D	0	0	10	1	0	0	0	0	0	0
E	0	0	6	1	0	0	0	1	0	0
F	2	4	0	0	0	0	0	0	1	10
G	0	0	0	0	0	1	0	0	0	0
H	0	0	0	0	0	0	0	0	0	0
I	0	0	0	0	0	0	0	0	0	4
K	0	0	0	0	0	0	0	0	0	0
L	0	0	0	1	0	0	0	0	1	10
M	0	0	0	0	0	0	0	0	0	8
N	0	0	0	0	0	0	0	0	0	0
P	0	0	0	1	0	0	0	0	0	0
Q	0	0	0	0	0	0	0	0	0	0
R	0	0	0	0	0	0	0	0	0	0
S	0	0	0	0	1	0	0	0	0	0
T	0	0	0	0	1	0	0	1	0	0
V	2	0	0	1	0	0	0	1	1	8
W	0	4	0	0	0	0	0	0	0	0
Y	0	4	0	0	0	0	0	0	1	0

HLA-C*05:01, 8mers

	1	2	3	4	5	6	7	8
A	0	3	0	0	0	0	0	0
C	0	0	0	0	0	0	0	0
D	0	0	10	0	0	0	0	0
E	0	0	6	1	0	0	1	0
F	1	0	0	0	0	0	0	8
G	0	0	0	0	0	0	0	0
H	0	0	0	0	0	0	0	0
I	1	1	0	0	0	0	0	8
K	0	0	0	1	0	0	2	0
L	0	1	0	0	0	0	0	10
M	0	0	0	0	0	0	0	6
N	0	0	0	0	0	0	0	0
P	0	0	0	0	1	0	0	0
Q	0	0	0	0	0	1	0	0
R	0	0	0	0	0	0	1	0
S	1	1	0	0	0	1	0	0
T	0	0	0	0	0	1	0	0
V	1	1	0	0	0	2	0	8
W	0	0	0	0	0	0	0	0
Y	0	0	0	0	0	0	0	0

HLA-C*05:01, 9mers

	1	2	3	4	5	6	7	8	9
A	0	3	0	0	0	0	0	0	0
C	0	0	0	0	0	0	0	0	0
D	0	0	10	1	0	0	0	0	0
E	0	0	6	1	0	0	0	1	0
F	1	0	0	0	0	0	0	0	8
G	0	0	0	0	1	0	0	0	0
H	0	0	0	0	0	0	0	0	0
I	1	0	0	0	0	0	0	0	6
K	0	0	0	0	0	0	0	1	0
L	0	0	0	0	0	0	0	1	10
M	0	0	0	0	0	0	0	0	6
N	0	0	0	0	0	0	0	0	0
P	0	0	0	0	1	0	0	0	0
Q	0	0	0	0	0	0	0	0	0
R	0	0	0	0	0	0	0	0	0
S	1	1	0	0	0	0	1	0	0
T	0	0	0	0	0	0	1	0	0
V	1	1	0	0	0	1	2	0	8
W	0	0	0	0	0	0	0	0	0
Y	0	0	0	0	0	0	0	0	0

HLA-C*05:01, 10mers

	1	2	3	4	5	6	7	8	9	10
A	0	3	0	0	0	0	0	0	0	0
C	0	0	0	0	0	0	0	0	0	0
D	0	0	10	1	0	0	0	0	0	0
E	0	0	6	1	0	0	0	1	0	0
F	2	0	0	0	0	0	0	0	1	10
G	0	0	0	1	1	1	0	0	0	0
H	0	0	0	0	0	0	0	0	0	0
I	0	1	0	0	0	0	0	0	0	6
K	0	0	0	0	0	0	0	0	0	0
L	0	0	0	0	0	0	1	0	1	10
M	0	0	0	0	0	0	0	0	0	6
N	0	0	0	0	0	0	0	0	0	0
P	0	0	0	1	2	0	0	0	0	0
Q	0	0	0	0	0	0	0	0	0	0
R	0	0	0	0	0	0	0	0	0	0
S	0	1	0	0	0	1	0	0	1	0
T	0	0	0	0	0	0	0	1	1	0
V	1	1	0	0	0	0	0	1	0	8
W	0	0	0	0	0	0	0	0	0	0
Y	1	0	0	0	0	0	0	0	0	0

HLA-C*06:02, 8mers

	1	2	3	4	5	6	7	8
A	0	0	2	0	0	0	0	0
C	0	0	0	0	0	0	0	0
D	0	0	0	0	0	0	0	0
E	0	0	0	0	2	0	0	0
F	2	0	2	0	0	0	1	6
G	0	0	2	0	0	0	0	0
H	0	0	0	0	0	0	0	0
I	0	0	0	0	1	1	1	10
K	0	6	0	0	0	0	0	0
L	0	0	0	2	1	2	2	10
M	0	0	0	0	0	0	0	0
N	0	0	0	0	0	0	0	0
P	0	0	0	4	1	0	0	0
Q	0	0	0	0	0	2	0	0
R	0	10	0	0	0	0	0	0
S	1	0	0	0	0	0	0	0
T	0	0	0	0	0	0	0	0
V	0	0	0	0	0	0	0	8
W	1	0	0	0	0	0	0	0
Y	3	6	0	0	0	0	0	0

HLA-C*06:02, 9mers

	1	2	3	4	5	6	7	8	9
A	0	0	1	0	0	0	0	0	0
C	0	0	0	0	0	0	0	0	0
D	0	0	0	1	0	0	0	0	0
E	0	0	0	1	0	0	0	1	0
F	1	0	1	0	1	0	0	0	6
G	0	0	0	0	0	0	0	0	0
H	0	0	0	0	0	0	0	0	0
I	0	0	0	0	1	1	1	0	8
K	0	6	0	0	0	0	0	0	0
L	0	0	0	0	1	1	1	1	10
M	0	0	0	0	0	0	0	0	0
N	0	0	0	0	0	0	0	0	0
P	0	0	1	2	0	1	0	0	0
Q	0	0	0	0	0	0	1	0	0
R	0	10	0	0	0	0	1	0	0
S	1	0	0	0	0	0	0	0	0
T	0	0	0	0	0	0	0	0	0
V	0	0	0	0	0	1	1	0	10
W	0	0	0	0	0	0	0	0	0
Y	1	6	1	0	0	0	0	0	6

HLA-C*06:02, 10mers

	1	2	3	4	5	6	7	8	9	10
A	0	0	0	0	0	1	0	0	0	0
C	0	0	0	0	0	0	0	0	0	0
D	0	0	0	2	0	0	0	0	0	0
E	0	0	0	1	0	0	0	0	0	0
F	3	0	1	0	1	0	1	0	1	10
G	0	0	0	0	1	0	0	0	0	0
H	0	0	0	0	0	0	0	0	0	0
I	0	0	0	0	0	0	2	1	0	10
K	0	6	0	0	0	0	0	0	0	0
L	0	0	0	0	1	1	0	1	3	10
M	0	0	0	0	0	0	0	0	0	0
N	0	0	0	0	1	0	0	0	0	0
P	0	0	2	1	0	0	1	0	0	0
Q	0	0	0	0	0	0	0	2	0	0
R	0	10	0	0	0	0	0	0	0	0
S	0	0	1	0	0	0	0	0	0	0
T	0	0	0	0	0	0	0	0	0	0
V	0	0	0	0	0	1	0	0	0	8
W	0	0	0	0	0	0	0	0	0	0
Y	2	6	1	0	0	0	0	0	0	0

HLA-C*07:01, 8mers

	1	2	3	4	5	6	7	8
A	0	0	0	0	0	0	0	0
C	0	0	0	0	0	0	0	0
D	0	0	1	0	0	0	0	0
E	0	0	0	0	0	0	1	0
F	0	0	0	0	0	0	0	10
G	0	0	4	0	1	0	0	0
H	0	0	0	0	1	0	0	0
I	1	0	0	0	1	1	1	0
K	1	0	0	0	0	0	0	0
L	0	0	0	0	0	1	0	10
M	0	0	0	0	0	0	0	6
N	0	8	0	0	0	0	0	0
P	0	0	0	1	1	0	0	0
Q	0	0	0	0	0	0	0	0
R	1	10	0	0	0	0	0	0
S	0	0	0	0	0	0	1	0
T	0	10	0	0	0	0	0	0
V	0	0	0	2	1	0	1	0
W	0	0	0	0	0	0	0	0
Y	1	0	0	0	0	0	0	8

HLA-C*07:01, 9mers

	1	2	3	4	5	6	7	8	9
A	0	0	0	0	0	0	0	0	0
C	0	0	0	0	0	0	0	0	0
D	0	0	0	1	0	0	0	0	0
E	0	0	0	1	0	0	0	2	0
F	0	0	0	0	1	0	1	0	10
G	0	0	0	0	0	0	0	0	0
H	0	0	0	0	0	0	0	0	0
I	0	0	0	0	0	2	0	0	0
K	4	0	0	0	0	0	0	0	0
L	0	0	0	0	0	0	1	0	10
M	0	0	0	0	0	0	0	0	6
N	0	6	1	0	0	0	0	0	0
P	0	0	0	1	0	0	0	0	0
Q	0	0	0	0	0	0	0	0	0
R	4	10	0	0	0	0	1	0	0
S	1	0	0	0	0	0	0	0	0
T	0	8	0	0	0	0	0	0	0
V	0	0	0	0	1	1	1	2	0
W	0	0	0	0	0	0	0	0	0
Y	0	0	0	0	1	0	1	0	10

HLA-C*07:01, 10mers

	1	2	3	4	5	6	7	8	9	10
A	0	0	0	0	1	0	1	1	0	0
C	0	0	0	0	0	0	0	0	0	0
D	0	0	0	2	0	0	0	0	1	0
E	0	0	1	0	1	1	0	0	1	0
F	0	0	0	0	0	0	1	2	0	10
G	0	0	1	2	2	0	0	0	0	0
H	0	0	0	0	0	0	0	0	1	0
I	1	0	0	0	0	0	3	0	0	0
K	1	0	0	0	1	1	0	0	1	0
L	0	0	0	0	0	0	0	0	0	10
M	0	0	0	0	0	0	0	0	0	0
N	1	6	0	0	0	0	0	0	0	0
P	1	0	0	1	0	2	1	0	0	0
Q	0	0	0	0	0	0	0	0	0	0
R	1	10	0	0	0	0	0	0	0	0
S	1	0	0	0	0	1	1	1	0	0
T	0	6	0	0	1	0	0	1	2	0
V	0	0	0	0	0	0	0	0	0	0
W	0	0	0	0	0	0	0	1	0	0
Y	0	0	0	0	0	1	0	0	0	8

HLA-C*07:02, 8mers

	1	2	3	4	5	6	7	8
A	0	0	2	0	0	0	0	0
C	0	0	0	0	0	0	0	0
D	0	0	0	0	0	0	0	0
E	0	0	0	0	1	0	2	0
F	2	0	0	0	0	0	0	10
G	0	0	2	0	0	0	0	0
H	0	0	0	0	1	0	0	0
I	0	0	0	0	0	1	0	0
K	0	8	0	0	0	0	0	0
L	0	0	0	0	1	2	1	10
M	0	0	0	0	0	0	0	6
N	0	0	0	0	0	0	0	0
P	0	0	2	4	0	1	0	0
Q	0	0	0	0	0	1	1	0
R	0	10	0	0	0	0	0	0
S	1	0	0	0	0	0	0	0
T	0	0	0	0	0	0	0	0
V	0	0	0	1	1	0	1	0
W	0	0	0	0	0	0	0	0
Y	3	8	0	0	0	0	0	10

HLA-C*07:02, 9mers

	1	2	3	4	5	6	7	8	9
A	0	0	0	0	0	0	0	0	0
C	0	0	0	0	0	0	0	0	0
D	0	0	0	1	0	0	0	0	0
E	0	0	0	1	0	0	0	1	0
F	1	0	0	0	1	0	1	0	10
G	0	0	0	0	0	0	0	0	0
H	0	0	0	0	0	0	0	0	0
I	0	0	0	0	0	1	1	1	0
K	0	6	0	0	0	0	0	0	0
L	0	0	0	0	0	0	1	0	10
M	0	0	0	0	0	0	0	0	6
N	1	0	1	0	0	0	0	0	0
P	0	0	2	2	0	0	0	0	0
Q	0	0	0	0	0	0	0	0	0
R	0	10	0	0	0	0	0	0	0
S	1	0	0	0	0	0	0	1	0
T	0	0	0	0	0	1	0	1	0
V	0	0	0	0	1	2	1	1	0
W	0	0	0	0	0	0	0	0	0
Y	1	10	0	0	1	0	1	0	10

HLA-C*07:02, 10mers

	1	2	3	4	5	6	7	8	9	10
A	0	0	1	0	0	0	0	1	0	0
C	0	0	0	0	0	0	0	0	0	0
D	0	0	0	3	0	0	0	0	0	0
E	0	0	0	1	0	0	0	0	1	0
F	1	0	0	0	0	0	0	0	0	10
G	0	0	0	0	2	1	0	0	0	0
H	0	0	0	0	0	0	0	0	0	0
I	0	0	0	0	0	0	1	0	0	0
K	0	6	0	0	0	0	0	0	0	0
L	0	0	0	0	0	0	0	0	0	10
M	0	0	0	0	0	0	0	0	0	6
N	1	0	0	0	0	0	0	0	0	0
P	0	0	1	0	0	1	0	0	0	0
Q	0	0	0	0	1	0	0	2	0	0
R	0	10	0	0	0	0	0	0	0	0
S	1	0	0	0	0	0	0	0	0	0
T	0	0	0	0	0	1	0	0	0	0
V	0	0	1	0	1	0	1	0	3	0
W	0	0	0	0	0	0	0	0	0	0
Y	2	8	2	0	0	0	0	0	0	10

HLA-C*08:02, 8mers

	1	2	3	4	5	6	7	8
A	0	2	0	0	1	0	0	0
C	0	0	0	0	0	0	0	0
D	0	0	10	0	0	0	0	0
E	0	0	4	1	0	0	1	0
F	1	0	0	0	0	0	0	4
G	0	0	0	0	0	0	0	0
H	0	0	0	0	1	0	0	0
I	1	0	0	0	0	0	0	6
K	0	0	0	1	0	0	1	0
L	1	1	0	1	0	0	0	10
M	0	0	0	0	0	0	0	4
N	0	0	0	0	1	0	0	0
P	0	0	0	0	0	0	0	0
Q	0	0	0	0	0	0	0	0
R	0	0	0	0	0	0	0	0
S	0	1	0	0	1	1	0	0
T	0	0	0	0	0	1	0	0
V	1	0	0	0	0	0	0	6
W	0	0	0	0	0	0	0	0
Y	0	0	0	0	0	0	0	0

HLA-C*08:02, 9mers

	1	2	3	4	5	6	7	8	9
A	0	2	0	0	0	0	0	1	0
C	0	0	0	0	0	0	0	0	0
D	0	0	10	1	0	0	0	0	0
E	0	0	6	1	0	0	0	1	0
F	1	0	0	0	0	0	0	0	6
G	0	0	0	0	0	1	0	0	0
H	0	0	0	0	0	0	0	0	0
I	1	0	0	0	0	0	0	0	6
K	0	0	0	0	0	0	0	0	0
L	1	1	0	1	0	0	0	0	10
M	0	0	0	0	0	0	0	0	6
N	0	0	0	0	0	1	0	0	0
P	0	0	0	0	1	0	0	0	0
Q	0	0	0	0	0	0	0	0	0
R	0	0	0	0	0	0	0	0	0
S	1	1	0	0	1	1	1	1	0
T	0	0	0	0	0	0	0	1	0
V	1	1	0	0	0	0	0	0	6
W	0	0	0	0	0	0	0	0	0
Y	0	0	0	0	0	0	0	0	0

HLA-C*08:02, 10mers

	1	2	3	4	5	6	7	8	9	10
A	0	3	0	0	0	0	0	0	1	0
C	0	0	0	0	0	0	0	0	0	0
D	0	0	10	1	0	0	0	0	0	0
E	0	0	4	1	0	0	0	0	1	0
F	1	0	0	0	0	0	0	0	0	6
G	0	0	0	1	1	1	0	0	0	0
H	0	0	0	0	0	0	0	0	0	0
I	1	1	0	0	0	0	0	0	0	4
K	0	0	0	0	0	0	0	0	0	0
L	0	0	0	0	0	0	1	0	0	10
M	0	0	0	0	0	0	0	0	0	4
N	0	0	0	0	0	0	0	0	0	0
P	0	0	0	1	1	0	0	0	0	0
Q	0	0	0	0	0	0	0	0	0	0
R	0	0	0	0	0	0	0	0	0	0
S	0	1	0	0	1	1	0	1	2	0
T	0	0	0	0	0	0	0	1	1	0
V	1	1	0	0	0	0	0	0	0	4
W	0	0	0	0	0	0	0	0	0	0
Y	0	0	0	0	0	0	0	0	0	0

HLA-C*12:03, 8mers

	1	2	3	4	5	6	7	8
A	0	10	0	0	0	0	0	0
C	0	0	0	0	0	0	0	0
D	0	0	1	0	0	0	0	0
E	0	0	0	0	0	0	2	0
F	3	0	2	0	0	0	0	8
G	0	0	1	0	0	0	0	0
H	0	0	0	0	1	0	0	0
I	0	0	0	1	1	0	1	8
K	0	0	2	0	0	1	0	0
L	1	0	0	1	0	0	0	10
M	0	0	0	0	0	0	0	10
N	0	0	1	0	1	0	0	0
P	0	0	0	1	0	0	0	0
Q	0	0	0	0	0	0	0	0
R	0	0	0	0	0	1	0	0
S	0	8	0	0	0	1	0	0
T	0	8	0	0	0	0	0	0
V	1	0	0	1	0	0	1	10
W	0	0	0	0	0	0	0	0
Y	2	0	0	0	0	0	0	8

HLA-C*12:03, 9mers

	1	2	3	4	5	6	7	8	9
A	1	10	1	0	0	0	0	0	0
C	0	0	0	0	0	0	0	0	0
D	0	0	0	1	0	0	0	0	0
E	0	0	0	1	0	0	0	1	0
F	1	0	1	0	0	0	0	0	8
G	0	0	0	1	0	0	0	0	0
H	0	0	0	0	0	0	0	0	0
I	0	0	0	0	0	1	1	0	8
K	0	0	0	0	0	0	1	0	0
L	0	0	0	0	0	0	1	0	10
M	0	0	0	0	0	0	0	0	8
N	0	0	0	0	0	0	0	0	0
P	0	0	0	2	0	1	0	0	0
Q	0	0	0	0	0	0	0	0	0
R	0	0	0	0	0	0	1	0	0
S	0	8	1	1	0	0	0	0	0
T	0	8	0	0	0	0	0	1	0
V	1	0	0	0	0	1	1	1	10
W	0	0	0	0	0	0	0	0	0
Y	1	0	1	0	0	0	0	0	10

HLA-C*12:03, 10mers

	1	2	3	4	5	6	7	8	9	10
A	1	10	0	0	0	0	0	0	0	0
C	0	0	0	0	0	0	0	0	0	0
D	0	0	0	2	0	0	0	0	0	0
E	0	0	0	0	0	0	0	0	0	0
F	2	0	3	0	0	0	0	0	0	10
G	0	0	0	1	2	0	1	0	0	0
H	0	0	0	0	0	0	0	0	0	0
I	0	0	0	0	0	0	0	0	0	4
K	0	0	0	0	0	0	0	0	0	0
L	0	0	0	0	0	0	0	1	0	10
M	0	0	0	0	0	0	0	0	0	8
N	0	0	0	0	0	0	0	0	0	0
P	0	0	0	1	2	0	2	0	0	0
Q	0	0	0	0	0	0	0	1	0	0
R	0	0	0	0	0	0	0	1	0	0
S	0	8	0	0	0	0	0	0	1	0
T	0	6	0	0	0	1	0	0	0	0
V	0	0	0	0	0	0	0	0	2	8
W	0	0	0	0	0	0	0	0	0	0
Y	1	0	1	0	0	0	0	0	0	10

HLA-C*14:02, 8mers

	1	2	3	4	5	6	7	8
A	0	0	0	0	1	0	1	0
C	0	0	0	0	0	0	0	0
D	0	0	0	0	0	0	0	0
E	0	0	0	0	0	0	1	0
F	1	10	0	0	0	0	0	10
G	0	0	0	0	3	0	0	0
H	0	0	0	0	1	0	0	0
I	0	0	0	0	0	0	0	0
K	0	0	0	0	0	1	0	0
L	0	0	1	0	0	0	0	10
M	0	0	0	0	0	0	0	6
N	0	0	0	1	0	0	0	0
P	0	0	0	0	0	0	0	0
Q	0	0	1	0	0	0	0	0
R	0	0	0	0	1	1	0	0
S	0	0	0	0	0	1	1	0
T	0	0	0	1	0	0	0	0
V	1	0	0	1	0	0	1	0
W	0	0	0	0	0	0	0	0
Y	1	10	0	0	0	0	0	8

HLA-C*14:02, 9mers

	1	2	3	4	5	6	7	8	9
A	1	0	0	0	0	1	0	1	0
C	0	0	0	0	0	0	0	0	0
D	0	0	0	1	0	0	0	0	0
E	0	0	0	1	0	0	0	1	0
F	1	10	0	0	0	0	0	0	10
G	0	0	0	0	0	0	0	0	0
H	0	0	0	0	0	0	0	0	0
I	0	0	1	0	0	0	0	0	0
K	0	0	0	0	1	0	0	0	0
L	0	0	0	0	0	0	1	0	10
M	0	0	0	0	0	0	0	0	6
N	0	0	0	0	0	0	0	0	0
P	0	0	2	1	0	0	0	0	0
Q	0	0	1	0	0	0	0	0	0
R	0	0	0	0	0	0	0	0	0
S	1	0	0	0	1	0	1	1	0
T	0	0	0	0	0	0	0	0	0
V	1	0	0	0	0	1	0	0	0
W	0	0	0	0	0	0	0	0	0
Y	1	10	0	0	0	0	0	0	8

HLA-C*14:02, 10mers

	1	2	3	4	5	6	7	8	9	10
A	1	0	0	0	0	0	0	0	1	0
C	0	0	0	0	0	0	0	0	0	0
D	0	0	0	2	0	0	0	0	0	0
E	0	0	0	1	0	0	0	0	1	0
F	1	10	1	0	0	0	0	0	0	10
G	0	0	0	1	1	0	1	0	0	0
H	0	0	0	0	0	0	0	0	0	0
I	0	0	1	0	0	0	1	0	0	0
K	0	0	0	0	0	0	0	0	0	0
L	0	0	0	0	0	0	0	0	0	10
M	0	0	0	0	0	0	0	0	0	6
N	0	0	0	0	0	0	0	0	0	0
P	0	0	2	0	0	1	1	0	0	0
Q	0	0	0	0	0	0	0	0	0	0
R	0	0	0	0	0	0	0	0	0	0
S	1	0	0	0	0	0	0	1	2	0
T	0	0	0	0	0	0	1	1	1	0
V	0	0	0	0	0	0	1	0	0	0
W	0	0	0	0	0	0	0	0	0	0
Y	1	10	1	0	0	0	0	0	0	8

HLA-C*15:02, 8mers

	1	2	3	4	5	6	7	8
A	0	10	1	0	0	0	0	0
C	0	0	0	0	0	0	0	0
D	0	0	0	0	0	0	0	0
E	0	0	0	0	0	0	1	0
F	1	0	0	0	0	0	0	0
G	0	0	4	0	0	0	0	0
H	0	0	0	0	0	0	0	0
I	1	8	0	0	1	2	0	8
K	1	0	0	2	0	0	1	0
L	0	0	0	0	0	6	1	10
M	0	0	0	0	0	0	0	4
N	0	8	0	0	0	0	0	0
P	0	0	0	1	3	0	0	0
Q	0	0	0	0	0	0	0	0
R	1	0	0	1	0	0	0	0
S	0	10	2	0	0	0	0	0
T	0	10	0	0	0	0	0	0
V	1	8	0	0	0	2	0	10
W	0	0	0	0	0	0	0	0
Y	1	0	0	0	0	0	0	0

HLA-C*15:02, 9mers

	1	2	3	4	5	6	7	8	9
A	1	8	0	0	0	0	0	0	0
C	0	0	0	0	0	0	0	0	0
D	0	0	0	1	0	0	0	0	0
E	0	0	0	1	0	0	0	1	0
F	1	0	0	0	0	1	0	0	0
G	0	0	0	1	0	0	0	0	0
H	0	0	0	0	0	0	0	0	0
I	0	8	1	0	0	1	0	0	6
K	1	0	0	0	1	0	0	0	0
L	0	0	0	0	0	1	4	1	10
M	0	0	0	0	0	0	0	0	4
N	0	8	1	0	0	0	0	0	0
P	0	0	0	1	0	1	0	0	0
Q	0	0	0	0	0	0	0	0	0
R	1	0	0	0	0	0	0	0	0
S	0	10	0	1	0	0	0	0	0
T	0	10	0	0	0	0	0	0	0
V	0	8	0	0	1	1	0	0	10
W	0	0	0	0	0	0	0	0	0
Y	0	0	0	0	0	0	0	0	0

HLA-C*15:02, 10mers

	1	2	3	4	5	6	7	8	9	10
A	0	8	1	0	0	1	0	0	0	0
C	0	0	0	0	0	0	0	0	0	0
D	0	0	0	1	0	0	0	0	0	0
E	0	0	0	1	0	0	0	0	0	0
F	0	0	0	0	1	0	0	0	1	0
G	0	0	0	0	1	1	1	0	0	0
H	0	0	0	0	0	0	0	0	0	0
I	0	8	2	0	1	0	1	0	1	6
K	4	0	0	0	0	0	0	0	0	0
L	0	0	0	1	0	1	1	3	1	10
M	0	0	0	0	0	0	0	0	0	4
N	0	8	0	0	0	0	0	0	0	0
P	0	0	0	0	0	1	0	0	0	0
Q	0	0	0	0	0	0	0	0	0	0
R	4	0	0	0	0	0	0	0	0	0
S	0	10	0	0	0	0	0	0	0	0
T	0	10	0	0	0	0	0	0	0	0
V	0	8	0	0	0	0	0	0	1	10
W	0	0	0	0	0	0	0	0	0	0
Y	0	0	0	0	0	0	0	0	0	0

HLA-C*16:01, 8mers

	1	2	3	4	5	6	7	8
A	1	10	2	0	0	0	1	0
C	0	0	0	0	0	0	0	0
D	0	0	0	0	0	0	0	0
E	0	0	0	1	0	0	2	0
F	2	0	0	0	0	0	0	8
G	0	0	1	0	1	0	0	0
H	0	0	0	0	1	0	0	0
I	0	0	0	0	0	0	0	0
K	0	0	0	0	1	0	0	0
L	0	0	0	1	0	1	0	10
M	0	0	0	0	0	0	0	8
N	0	0	0	0	0	0	0	0
P	0	0	0	0	0	1	0	0
Q	0	0	0	0	0	0	0	0
R	0	0	0	0	3	2	0	0
S	0	10	2	0	0	0	0	0
T	0	8	1	0	0	0	0	0
V	1	0	0	1	0	0	1	6
W	0	0	0	0	0	0	0	0
Y	1	0	0	0	0	0	0	10

HLA-C*16:01, 9mers

	1	2	3	4	5	6	7	8	9
A	1	10	1	0	0	0	0	1	0
C	0	0	0	0	0	0	0	0	0
D	0	0	0	1	0	0	0	0	0
E	0	0	0	1	0	0	0	1	0
F	1	0	0	0	0	0	0	0	10
G	0	0	0	0	0	0	0	0	0
H	0	0	0	0	0	0	0	0	0
I	0	0	0	0	0	0	0	0	0
K	0	0	0	0	1	0	1	0	0
L	0	0	0	0	0	0	1	0	10
M	0	0	0	0	0	0	0	0	8
N	0	0	0	0	0	0	0	0	0
P	0	0	0	1	0	0	0	0	0
Q	0	0	0	0	0	0	0	0	0
R	0	0	0	0	2	1	2	0	0
S	0	10	2	0	0	0	0	1	0
T	0	8	1	0	0	0	0	1	0
V	1	0	0	0	0	0	0	1	8
W	0	0	0	0	0	0	0	0	0
Y	1	0	0	0	0	0	0	0	10

HLA-C*16:01, 10mers

	1	2	3	4	5	6	7	8	9	10
A	0	10	1	0	0	0	0	0	0	0
C	0	0	0	0	0	0	0	0	0	0
D	0	0	0	2	0	0	0	0	0	0
E	0	0	0	1	0	0	0	0	0	0
F	2	0	0	0	0	0	0	0	0	10
G	0	0	0	0	1	0	1	0	0	0
H	0	0	0	0	0	0	0	0	0	0
I	0	0	0	0	0	0	0	0	0	0
K	0	0	0	0	0	0	0	0	0	0
L	0	0	0	0	0	0	1	0	0	10
M	0	0	0	0	0	0	0	0	0	8
N	0	0	0	0	0	0	0	0	0	0
P	0	0	0	0	2	0	1	0	0	0
Q	0	0	0	0	0	0	0	0	0	0
R	0	0	0	0	0	0	1	3	0	0
S	0	8	1	0	0	0	0	0	0	0
T	0	8	1	0	1	0	0	0	1	0
V	1	0	0	0	0	0	0	0	1	6
W	0	0	0	0	0	0	0	0	0	0
Y	2	0	0	0	0	0	0	0	0	10

HLA-C*17:01, 8mers

	1	2	3	4	5	6	7	8
A	0	10	2	0	0	0	0	0
C	0	0	0	0	0	0	0	0
D	0	0	1	0	0	0	0	0
E	0	0	0	0	1	0	0	0
F	3	0	0	0	0	0	1	6
G	0	0	1	0	0	0	0	0
H	0	0	0	0	1	0	0	0
I	0	8	0	0	0	2	0	4
K	0	0	0	1	0	0	0	0
L	0	8	0	0	0	2	2	10
M	0	0	0	0	0	0	0	4
N	0	0	0	0	0	0	0	0
P	0	0	0	1	2	0	0	0
Q	0	0	0	0	0	0	0	0
R	0	0	0	0	0	0	0	0
S	0	8	1	0	0	0	0	0
T	0	0	0	0	0	0	0	0
V	0	8	0	0	0	2	0	0
W	0	0	0	0	0	0	0	0
Y	1	0	0	0	0	0	1	0

HLA-C*17:01, 9mers

	1	2	3	4	5	6	7	8	9
A	0	10	1	0	0	0	0	0	0
C	0	0	0	0	0	0	0	0	0
D	0	0	1	0	0	0	0	0	0
E	0	0	0	0	0	0	0	0	0
F	3	0	0	0	0	0	0	1	6
G	0	0	0	1	1	0	0	0	0
H	0	0	0	0	0	0	0	0	0
I	0	6	1	0	0	1	1	0	4
K	0	0	0	0	0	0	0	0	0
L	0	8	0	0	0	1	1	1	10
M	0	0	0	0	0	0	0	0	4
N	0	0	0	0	0	0	0	0	0
P	0	0	0	1	0	1	0	0	0
Q	0	0	0	0	0	0	0	0	0
R	0	0	0	0	0	0	0	0	0
S	1	8	0	1	0	0	0	0	0
T	0	0	0	0	0	0	1	0	0
V	0	8	1	0	0	1	1	0	0
W	0	0	0	0	0	0	0	0	0
Y	1	0	1	0	0	0	0	1	0

HLA-C*17:01, 10mers

	1	2	3	4	5	6	7	8	9	10
A	1	10	0	0	0	1	0	0	0	0
C	0	0	0	0	0	0	0	0	0	0
D	0	0	0	0	0	0	0	0	0	0
E	0	0	0	0	1	0	0	0	0	0
F	1	0	0	0	0	0	0	0	0	10
G	0	0	0	1	1	1	1	1	0	0
H	0	0	0	0	0	0	0	0	0	0
I	0	6	0	1	0	0	0	0	1	4
K	0	0	0	0	0	0	1	0	0	0
L	0	10	1	0	1	1	1	1	1	10
M	0	0	0	0	0	0	0	0	0	4
N	0	0	0	0	0	0	0	0	0	0
P	0	0	0	1	1	1	0	1	0	0
Q	0	0	0	0	0	0	0	0	0	0
R	0	0	0	0	0	0	0	0	1	0
S	0	10	0	0	0	0	1	0	0	0
T	0	0	0	0	1	0	0	0	0	0
V	1	10	0	0	0	0	1	0	0	0
W	0	0	0	0	0	0	0	0	0	0
Y	1	0	0	0	0	0	0	0	0	0

HLA-G*01:01, 8mers

	1	2	3	4	5	6	7	8
A	0	0	6	0	1	0	0	0
C	0	0	0	0	0	0	0	0
D	0	0	0	0	0	0	0	0
E	0	0	0	1	0	0	0	0
F	0	0	0	0	0	0	0	4
G	0	0	0	0	1	0	0	0
H	0	0	0	0	0	0	0	0
I	0	3	6	0	0	4	0	4
K	4	0	0	1	0	0	0	0
L	0	3	6	0	0	4	2	10
M	0	0	0	0	0	0	0	4
N	0	0	0	0	0	0	0	0
P	0	0	10	1	3	0	0	0
Q	0	0	0	0	0	0	0	0
R	4	0	0	0	0	0	0	0
S	0	0	0	0	0	0	0	0
T	0	0	0	0	0	0	0	0
V	0	0	6	0	0	4	0	0
W	0	0	0	0	0	0	0	0
Y	0	0	0	0	0	0	0	0

HLA-G*01:01, 9mers

	1	2	3	4	5	6	7	8	9
A	0	0	6	0	0	1	0	0	0
C	0	0	0	0	0	0	0	0	0
D	0	0	0	0	0	0	0	0	0
E	0	0	0	0	0	0	0	1	0
F	0	0	0	0	0	0	0	0	4
G	0	0	0	0	0	0	0	0	0
H	0	0	0	0	0	0	0	0	0
I	0	2	10	0	0	0	4	0	4
K	4	0	0	1	0	1	0	0	0
L	0	2	6	0	0	0	4	1	10
M	0	0	0	0	0	0	0	0	4
N	0	0	0	0	0	0	0	0	0
P	0	0	10	1	0	0	0	0	0
Q	0	0	0	0	0	0	0	0	0
R	4	0	0	0	0	0	0	0	0
S	0	0	0	0	0	0	0	0	0
T	0	0	0	0	0	0	0	0	0
V	0	1	8	0	0	0	4	1	0
W	0	0	0	0	0	0	0	0	0
Y	0	0	0	0	0	0	0	0	0

HLA-G*01:01, 10mers

	1	2	3	4	5	6	7	8	9	10
A	0	0	6	0	0	0	1	0	0	0
C	0	0	0	0	0	0	0	0	0	0
D	0	0	0	0	0	0	0	0	0	0
E	0	0	0	0	0	0	0	0	0	0
F	0	2	0	0	0	0	0	0	0	4
G	0	0	0	1	0	1	1	0	0	0
H	0	0	0	0	0	0	0	0	0	0
I	0	1	6	0	0	0	0	4	0	4
K	4	0	0	1	0	0	0	0	0	0
L	0	2	6	0	1	0	0	4	1	10
M	0	0	0	0	0	0	0	0	0	4
N	0	0	0	0	0	0	0	0	0	0
P	0	0	10	1	1	1	2	1	0	0
Q	0	0	0	0	0	0	0	0	0	0
R	4	0	0	0	0	0	0	0	0	0
S	0	0	0	1	0	0	0	0	0	0
T	0	0	0	0	0	0	0	0	0	0
V	0	0	8	0	0	0	0	4	1	0
W	0	0	0	0	0	0	0	0	0	0
Y	0	0	0	0	0	0	0	0	0	0

9. Publications

Di Marco M, Peper JK, Rammensee HG (2017): **Identification of Immunogenic Epitopes by MS/MS.** Cancer J., PMID: 28410297

Di Marco M, Schuster H, Backert L, Ghosh M, Rammensee HG, Stevanović S (2017): **Unveiling the peptide motifs of HLA-C, HLA-E and HLA-G from naturally presented peptides and generation of epitope prediction matrices.** Accepted for publication in the Journal of Immunology

Ebner P, Rinker J, Nguyen MT, Popella P, Nega M, Luqman A, Schittek B, **Di Marco M**, Stevanovic S, Götz F. (2016): **Excreted Cytoplasmic Proteins Contribute to Pathogenicity in Staphylococcus aureus**. Infect Immunol., PMID: 27001537

Klatt MG, Kowalewski DJ, Schuster H, **Di Marco M**, Hennenlotter J, Stenzl A, Rammensee HG, Stevanović S. (2016): **Carcinogenesis of renal cell carcinoma reflected in HLA ligands: A novel approach for synergistic peptide vaccination design**. Oncoimmunology, PMID: 27622074

Barth SM, Schreitmüller CM, Proehl F, Oehl K, Lumpp LM, Kowalewski DJ, **Di Marco M**, Sturm T, Backert L, Schuster H, Stevanović S, Rammensee HG, Planz O. (2016): **Characterization of the Canine MHC Class I DLA-88*50101 Peptide Binding Motif as a Prerequisite for Canine T Cell Immunotherapy**. PLoS One, PMID: 27893789